Universität Bremen

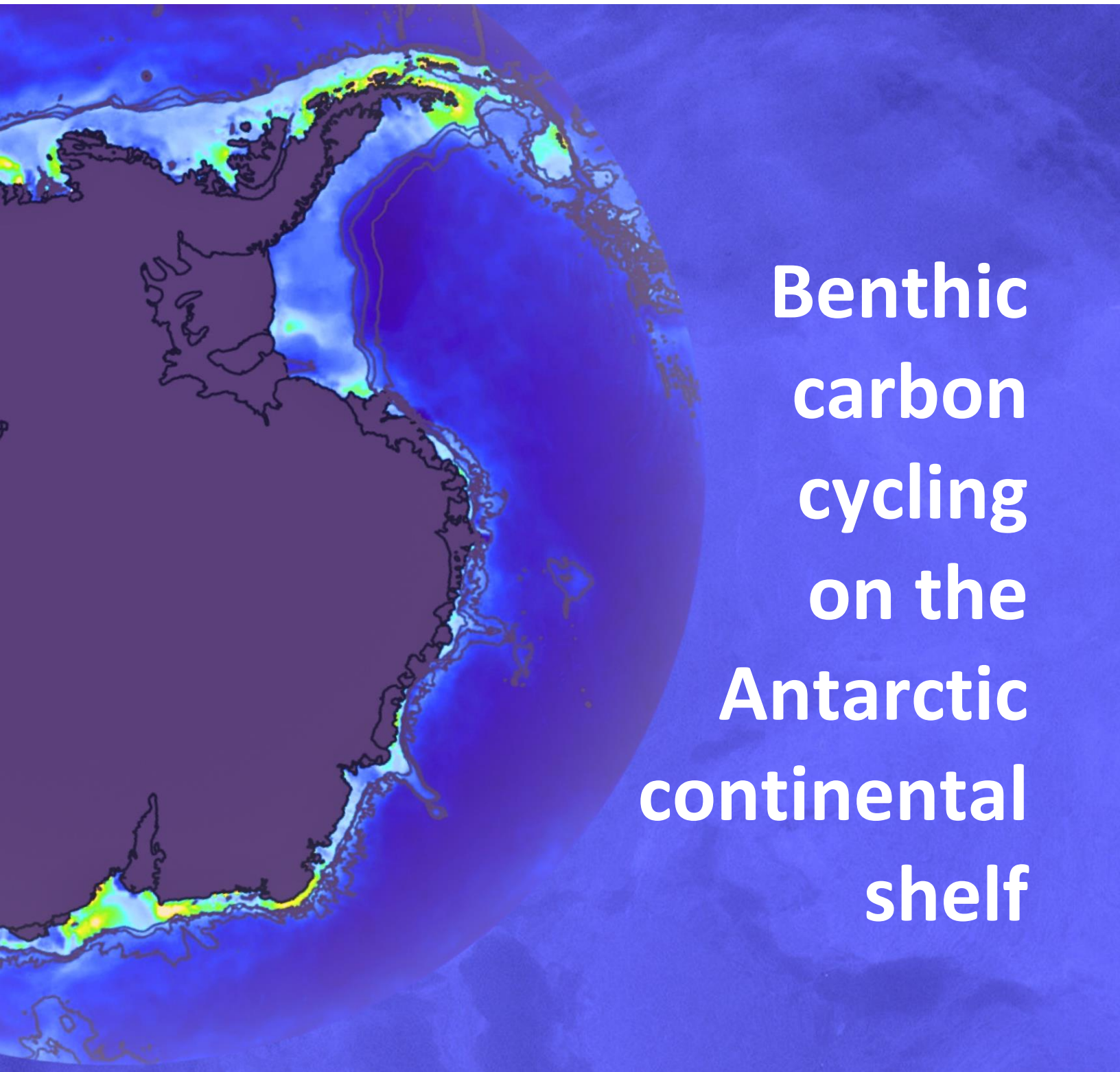

Benthic carbon cycling on the Antarctic continental shelf

Doctoral Dissertation

Marwa Baloza

Benthic carbon cycling on the Antarctic continental shelf

Dissertation

In partial fulfillment of the requirements for the degree of

Doctor of natural sciences

– Dr. rer. nat. –

Faculty of Biology/Chemistry

University of Bremen

Marwa Baloza

November 2023

The present study was carried out between December 2018 and November 2023 at the Alfred Wegener Institute Helmholtz Centre for Polar and Marine Research (AWI), Bremerhaven, Germany. Additional molecular analysis support was given by the Max Planck Institute for Marine Microbiology, Bremen, Germany. It was funded by the AWI Annex Funding.

Examination committee

1st examiner:	Dr. Massimiliano Molari Max Planck Institute for Marine Microbiology, Bremen, Germany
2nd examiner:	Dr. Jon Hawkings University of Pennsylvania, Philadelphia, USA
1st additional examiner:	Prof. Dr. Claudio Richter Alfred Wegener Institute Helmholtz Centre for Polar and Marine Research, Bremerhaven, Germany University of Bremen, Bremen, Germany
2nd additional examiner:	Prof. Dr. Tilmann Harder University of Bremen, Bremen, Germany
1st student member:	Gabriel Akoko Juma PhD candidate Alfred Wegener Institute Helmholtz Centre for Polar and Marine Research, Bremerhaven, Germany University of Bremen, Bremen, Germany
2nd student member:	Olivia Kohler MSc Biology student University of Bremen, Bremen, Germany
Advisor:	Dr. Moritz Holtappels Alfred Wegener Institute Helmholtz Centre for Polar and Marine Research, Bremerhaven, Germany

Date of doctoral colloquium: 08 February 2024

Table of Contents

Summary

The sedimentation of pelagic production makes continental shelf sediments important sites for organic matter (OM) remineralization and nutrient regeneration in the ocean. Consequently, shelf sediments play an important role in the bentho-pelagic coupling by providing essential nutrients for algal growth and maintaining the high primary production of shelf areas and the adjacent open ocean. In Antarctica, changes in sea ice cover have a major impact on surface primary production and the subsequent sinking of organic carbon to the seafloor. Recent observations indicate that global warming has led to substantial changes in sea ice cover, with a significant reduction of one million square kilometers in the annual maximum sea ice extent around Antarctica. These changes in sea ice conditions are expected to trigger significant changes in the pelagic ecosystem, with potentially profound effects on the benthic ecosystem. The imprint of climate-sensitive variables such as sea ice cover can be best studied in shelf sediments, where shallow water depths result in increased OM supply and tighter bentho-pelagic coupling. Therefore, a comprehensive understanding of the current carbon cycle on the Antarctic continental shelf is crucial for assessing the vulnerability of the ecosystem to climate change and for predicting the future trajectory of the carbon cycle in Antarctic waters. **This thesis aims** to quantify benthic carbon remineralization rates on the Antarctic continental shelf and the release of nutrients, particularly iron, that limit primary production in the Southern Ocean. In addition, the thesis aims to identify the main pathways of OM degradation and associated microbial communities, while contextualizing the above variables within the prevailing sea ice conditions.

For this purpose, I first studied the geochemistry of shelf sediments along a gradient of sea ice cover on the eastern shelf of the Antarctic Peninsula (AP) **(manuscript 1)**. The main focus was on carbon and iron fluxes within the sediment and between the water column and the sediment. The results were interpreted in the context of sea ice cover. An increase in carbon remineralization rates was observed as one moved from heavily ice-covered to moderately ice-covered stations where light availability and water column stratification increased. Conversely, the ice-free station displayed lower carbon remineralization rates and was subject to wind-driven

mixing of the water column, which can deepen the mixed layer depth below the critical depth, resulting in reduced surface production. In summary, a positive correlation was found between moderate sea ice cover and increased carbon fluxes to the sediment, which followed an exponential increase. The study also revealed significant iron cycling in sediments with increased carbon remineralization, resulting in high dissolved iron fluxes. This finding highlights the importance of sediments underlying the moderate ice cover as a source of limiting nutrients for primary production in this region.

A complementary study of benthic microbial communities along the AP transect was conducted using 16S ribosomal RNA (rRNA) gene sequencing **(manuscript 2)**. The results indicate that sea ice cover and its effect on organic carbon fluxes are the main drivers of changes in benthic microbial communities. As sea ice cover decreases, the benthic microbial community shifts towards anaerobic communities of iron and sulfate reducers. These communities were more abundant at low ice cover stations than at high ice cover stations. Furthermore, an increase in the relative abundance of Sva1033, a Desulfuromonadia clade, with dissolved iron concentration at low ice cover stations suggests a putative role for Sva1033 in dissimilatory iron reduction in surface sediments. In addition to Sva1033, this study successfully identified other taxa that could potentially contribute to dissimilatory iron reduction or have syntrophic partnerships and/or common metabolic preferences with iron reducers.

The focus was extended towards the southern shelf of the Weddell Sea, a region characterized by heavy sea ice cover **(manuscript 3)**. Benthic oxygen uptake rates were measured at stations with different water depths and sediment compositions. Benthic measurements also revealed a dependence of carbon fluxes on sediment grain size and water depth. In general, diffusive oxygen uptake (DOU) rates on the southern Weddell Sea shelf were low. DOU showed a positive correlation with preserved total organic carbon (TOC) at stations with fine-grained sediments, whereas stations with typical of coarse-grained sediments showed a markedly different correlation of DOU with TOC. Common to all stations is that dissolved iron and manganese concentrations in pore water were found only at greater depths, suggesting very limited release of these nutrients back into the water column.

The strong dependence of benthic carbon fluxes on sea ice cover and water depth was then combined to derive a simple empirical model, which was validated by all available DOU measurements reported in the literature for the Antarctic seasonal ice zone **(manuscript 4)**. The model allows extrapolation and budgeting of benthic carbon remineralization for the entire seasonal ice zone (16 million km²), yielding a total of 46 Tg C yr^{-1}. Notably, although the Antarctic continental shelf represents only 15% of the total area, it contributes a significant 71% (33 Tg C yr^{-1}) of the total benthic carbon remineralization. Furthermore, the total organic carbon supply to the sediments and the carbon burial in the sediments were estimated to amount to 52 Tg C yr^{-1} and 6 Tg C yr^{-1}, respectively.

Overall, the thesis highlights the pivotal role of sea ice cover in controlling the benthic carbon and iron cycling on the Antarctic continental shelf. Through extensive data correlation and empirical modeling, the thesis has provided, for the first time, a quantitative framework for the relationship between sea ice cover and benthic carbon fluxes. It also emphasizes the substantial contribution of Antarctic shelf sediments to the marine carbon remineralization, allowing a better assessment of the carbon cycling and related CO_2 sequestration across the Southern Ocean. Furthermore, it has improved our understanding of the main drivers of change in benthic microbial communities and, ultimately, nutrient fluxes across the sediment-water interface. These findings make a significant contribution to our understanding of the complex Antarctic ecosystem, which is necessary to assess the future trajectory of the Southern Ocean and its impact on the global carbon cycle.

Zusammenfassung

Die Sedimentation eines Teils der pelagischen Produktion macht die Sedimente des Kontinentalschelfs zu wichtigen Orten für die Remineralisierung organischer Stoffe und für die Regeneration von Nährstoffen im Ozean. Folglich spielen Schelfsedimente eine wichtige Rolle bei der bentho-pelagischen Kopplung, indem sie wichtige Nährstoffe für das Algenwachstum liefern und die hohe Primärproduktion der Schelfgebiete und des angrenzenden offenen Ozeans aufrechterhalten. In der Antarktis haben Veränderungen der Meereisbedeckung einen großen Einfluss auf die Primärproduktion an der Oberfläche und folglich auch auf das anschließende Absinken von organischem Kohlenstoff auf den Meeresboden. Jüngste Beobachtungen deuten darauf hin, dass die globale Erwärmung zu erheblichen Veränderungen der Meereisbedeckung geführt hat, mit einer jüngsten Verringerung der maximalen jährlichen Meereisausdehnung um die Antarktis um eine Million Quadratkilometer. Es wird erwartet, dass diese Veränderungen der Meereisbedeckung erhebliche Veränderungen im pelagischen Ökosystem auslösen werden, mit möglicherweise tiefgreifenden Auswirkungen auf das benthische Ökosystem. Die Auswirkungen von klimasensiblen Variablen wie der Meereisbedeckung lassen sich am besten in Schelfsedimenten untersuchen, wo geringe Wassertiefen zu einem erhöhten Angebot an organischen Stoffen und einer engeren bentho-pelagischen Kopplung führen. Daher ist ein umfassendes Verständnis des aktuellen Kohlenstoffkreislaufs auf dem antarktischen Kontinentalschelf von entscheidender Bedeutung für die Bewertung der Anfälligkeit des Ökosystems gegenüber dem Klimawandel und für die Vorhersage der zukünftigen Entwicklung des Kohlenstoffkreislaufs in antarktischen Gewässern. **Ziel dieser Arbeit** ist die Quantifizierung der benthischen Kohlenstoff-Remineralisierungsraten auf dem antarktischen Kontinentalschelf und die Freisetzung von Nährstoffen, insbesondere Eisen, welche die Primärproduktion im Südlichen Ozean begrenzen. Darüber hinaus sollen die Stoffwechselwege des Abbaus organischer Stoffe und die damit verbundenen mikrobiellen Gemeinschaften identifiziert werden, wobei die oben genannten Messgrößen in den Kontext der vorherrschenden Meereisbedingungen gestellt werden.

Zu diesem Zweck habe ich zunächst die Geochemie von Schelfsedimenten entlang eines Gradienten der Meereisbedeckung auf dem östlichen Schelf der Antarktischen Halbinsel untersucht **(Manuskript 1)**. Das Hauptaugenmerk lag dabei auf den Kohlenstoff- und Eisenflüssen innerhalb des Sediments und zwischen Wassersäule und Sediment. Die Ergebnisse wurden im Zusammenhang mit der Meereisbedeckung interpretiert. Es wurde ein Anstieg der Kohlenstoff-Remineralisierungsraten beobachtet, entlang von stark eisbedeckten zu mäßig eisbedeckten Stationen, wobei die Lichtverfügbarkeit und die Stratifizierung der Wassersäule zunahmen. Weiterhin wies die gänzlich eisfreie Station wiederum geringere Kohlenstoff-Remineralisierungsraten auf und war einer windbedingten Durchmischung der Wassersäule ausgesetzt, welches die Tiefe der oberen Mischschicht unter eine kritische Tiefe drücken kann, was zu einer geringeren Oberflächenproduktion führt. Zusammenfassend wurde eine positive Korrelation zwischen einer mäßigen Meereisbedeckung und erhöhten Kohlenstoffflüssen zum Sediment festgestellt, die einem exponentiellen Anstieg folgten. Die Studie zeigte auch, dass es in den Sedimenten zu einem erheblichen Eisenumsatz mit erhöhter Remineralisierung des Kohlenstoffs kommt, was zu hohen Flüssen von gelöstem Eisen führt. Dieses Ergebnis unterstreicht die Bedeutung der Sedimente unter Eisrandbedeckungen als Quelle von limitierenden Nährstoffen für die Primärproduktion in dieser Region.

Eine komplementäre Studie über benthische mikrobielle Gemeinschaften entlang des AP-Transekts wurde mit Hilfe der 16S ribosomalen RNA (rRNA)-Gensequenzierung durchgeführt **(Manuskript 2)**. Die Ergebnisse deuten darauf hin, dass die Meereisbedeckung und ihre Auswirkungen auf die organischen Kohlenstoffflüsse die Hauptursachen für Veränderungen in den benthischen mikrobiellen Gemeinschaften sind. Mit abnehmender Meereisbedeckung verschiebt sich die benthische mikrobielle Gemeinschaft hin zu anaeroben Gemeinschaften von Eisen- und Sulfatreduzierern. Diese Gemeinschaften waren an Stationen mit geringer Eisbedeckung häufiger anzutreffen als an Stationen mit hoher Eisbedeckung. Die Zunahme der relativen Häufigkeit von Sva1033, einer Desulfuromonadia-Gruppe, mit der Konzentration des gelösten Eisens an Stationen mit geringer Eisbedeckung deutet auf eine besondere Rolle von Sva1033 bei der dissimilatorischen Eisenreduktion in Oberflächensedimenten hin. Neben Sva1033 wurden in dieser Studie erfolgreich andere Taxa identifiziert, die möglicherweise zur

dissimilatorischen Eisenreduktion beitragen oder syntrophe Partnerschaften und/oder gemeinsame Stoffwechselpräferenzen mit Eisenreduzierern haben könnten.

Der Fokus wurde auf den südlichen Schelf des Weddellmeeres ausgedehnt, eine Region, die durch eine starke Meereisbedeckung gekennzeichnet ist **(Manuskript 3)**. Benthischen Sauerstoffaufnahmeraten wurden an Stationen mit unterschiedlichen Wassertiefen und Sedimentzusammensetzungen gemessen. Die benthischen Messungen zeigten auch eine Abhängigkeit der Kohlenstoffflüsse von der Sedimentkorngröße und der Wassertiefe. Im Allgemeinen waren die Raten der diffusen Sauerstoffaufnahme auf dem südlichen Weddellmeer-Schelf niedrig. Die Raten korrelierten positiv mit dem sedimentären organischen Kohlenstoff. Diese Korrelation war deutlich anders geartet an Stationen mit feinkörnigen Sedimenten im Vergleich mit Stationen, die grobkörnige Sedimente aufwiesen. Allen Stationen gemeinsam ist, dass gelöste Eisen- und Mangankonzentrationen im Porenwasser nur in größeren Tiefen gefunden wurden, was auf eine sehr begrenzte Flüsse dieser Nährstoffe zurück in die Wassersäule schließen lässt.

Die starke Korrelation der benthischen Kohlenstoffflüsse von der Meereisbedeckung und der Wassertiefe wurde dann genutzt, um ein einfaches empirisches Modell abzuleiten, welches durch alle benthische Ratenmessungen validiert wurde, die in der Literatur für die antarktische saisonale Eiszone zur Verfügung stehen **(Manuskript 4)**. Das Modell ermöglicht die Extrapolation und Budgetierung der benthischen Kohlenstoffremineralisierung für die gesamte saisonale Meereiszone (16 Mio. km²), was eine Gesamtmenge von 46 Tg C yr^{-1} ergibt. Obwohl der antarktische Kontinentalschelf nur 15 % der gesamten saisonalen Meereiszone ausmacht, trägt er mit 71 % besonders stark zur gesamten benthischen Kohlenstoffremineralisierung bei (33 Tg C yr^{-1}). Darüber hinaus wurde die geschätzte Gesamtzufuhr von organischem Kohlenstoff zum Meeresboden und die Einlagerung von Kohlenstoff im Sediment auf 52 Tg C pro Jahr bzw. 6 Tg C pro Jahr geschätzt.

Insgesamt unterstreicht die Arbeit die zentrale Rolle der Meereisbedeckung bei der Kontrolle des benthischen Kohlenstoff- und Eisenzyklus auf dem antarktischen Kontinentalschelf. Durch umfangreiche Messungen und empirische Modellierung hat die Arbeit zum ersten Mal einen

quantitativen Bezug zwischen Meereisbedeckung und benthischen Kohlenstoffflüssen geschaffen. Außerdem wird der wesentliche Beitrag der antarktischen Schelfsedimente zur marinen Kohlenstoffremineralisierung hervorgehoben, was eine bessere Bewertung des Kohlenstoffkreislaufs und der damit verbundenen CO_2-Sequestrierung im gesamten Südlichen Ozean ermöglicht. Darüber hinaus hat sich unser Verständnis der wichtigsten Treiber für Veränderungen der benthischen mikrobiellen Gemeinschaften und letztlich der Nährstoffflüsse an der Sediment-Wasser-Grenzfläche verbessert. Diese Ergebnisse tragen wesentlich zu unserem Verständnis des komplexen antarktischen Ökosystems bei, welches notwendig ist, um die künftige Entwicklung des antarktischen Ozeans und seine Auswirkungen auf den globalen Kohlenstoffkreislauf zu beurteilen.

ملخص الأطروحة

إن ترسيب الإنتاج السطحي يجعل رواسب الجرف القاري مواقع مهمة لإعادة تمعدن المواد العضوية وتجديد المغذيات في المحيط. وبالتالي، تلعب رواسب الجرف دورًا مهمًا في الاقتران القاعي بالسطحي من خلال توفير العناصر الغذائية الأساسية لنمو الطحالب والحفاظ على الإنتاج الأولي العالي لمناطق الجرف والمحيطات المفتوحة المجاورة. وفي القارة القطبية الجنوبية، يكون للتغيرات في الغطاء الجليدي البحري تأثير كبير على الإنتاج الأولي السطحي وما يتبع ذلك من غرق الكربون العضوي في قاع البحر. تشير الملاحظات الأخيرة إلى أن ظاهرة الاحتباس الحراري قد أدت إلى تغييرات كبيرة في الغطاء الجليدي البحري، مع انخفاض كبير قدره مليون كيلومتر مربع في الحد الأقصى السنوي لمساحة الجليد البحري حول القارة القطبية الجنوبية. ومن المتوقع أن تؤدي هذه التغيرات في ظروف الجليد البحري إلى تغييرات كبيرة في النظام البيئي السطحي، مع احتمال حدوث آثار عميقة على النظام البيئي القاعي. يمكن دراسة بصمة المتغيرات الحساسة للمناخ، مثل الغطاء الجليدي البحري، بشكل أفضل في رواسب الجرف، حيث تؤدي أعماق المياه الضحلة إلى زيادة إمدادات المواد العضوية وتشديد الاقتران بين القاع والسطح. ولذلك، فإن الفهم الشامل لدورة الكربون الحالية على الجرف القاري في القطب الجنوبي أمر بالغ الأهمية لتقييم مدى تعرض النظام البيئي لتغير المناخ والتنبؤ بالمسار المستقبلي لدورة الكربون في مياه القطب الجنوبي. تهدف هذه الأطروحة إلى قياس معدلات إعادة تمعدن الكربون القاعي على الجرف القاري في القطب الجنوبي وإطلاق العناصر الغذائية، وخاصة الحديد، التي تحد من الإنتاج الأولي في المحيط الجنوبي. بالإضافة إلى ذلك، تهدف الأطروحة إلى تحديد المسارات الرئيسية لتدهور المادة العضوية والمجتمعات الميكروبية المرتبطة بها، مع وضع المتغيرات المذكورة أعلاه في سياق ظروف الجليد البحري السائد.

ولهذا الغرض، قمت أولاً بدراسة الكيمياء الجيولوجية لرواسب الجرف على طول تدرج الغطاء الجليدي البحري على الجرف الشرقي لشبه جزيرة القطب الجنوبي (المخطوطة ١). كان التركيز الرئيسي على تدفقات الكربون والحديد داخل الرواسب وبين عمود الماء والرواسب. تم تفسير النتائج في سياق الغطاء الجليدي البحري. ولوحظت زيادة في معدلات إعادة تمعدن الكربون مع الانتقال من المحطات المغطاة بالجليد بكثافة إلى المحطات المغطاة بالجليد بشكل معتدل حيث زاد توافر الضوء وطبقات عمود الماء. على العكس من ذلك، أظهرت المحطة الخالية من الجليد معدلات إعادة تمعدن منخفضة للكربون وكانت عرضة لخلط عمود الماء بواسطة الرياح، مما قد يؤدي إلى تعميق الطبقة المختلطة تحت العمق الحرج، مما يؤدي إلى انخفاض الإنتاج السطحي. باختصار، تم العثور على علاقة إيجابية بين الغطاء الجليدي البحري المعتدل وزيادة تدفقات الكربون إلى الرواسب، والتي أعقبت زيادة هائلة. وكشفت الدراسة أيضًا عن وجود دورة كبيرة للحديد في الرواسب مع زيادة إعادة تمعدن الكربون، مما أدى إلى تدفقات عالية من الحديد الذائب. يسلط هذا الاكتشاف الضوء على أهمية الرواسب الكامنة وراء الغطاء الجليدي المعتدل كمصدر للحد من العناصر الغذائية للإنتاج الأولي في هذه المنطقة.

تم إجراء دراسة مكملة للمجتمعات الميكروبية القاعية على طول شبه الجزيرة القطبية الجنوبية باستخدام (16S rRNA) التسلسل الجيني للريبوسوم (المخطوطة ٢). تشير النتائج إلى أن الغطاء الجليدي البحري وتأثيره على تدفقات الكربون العضوي هما المحركان الرئيسيان للتغيرات في المجتمعات الميكروبية القاعية. مع انخفاض الغطاء الجليدي البحري، يتحول المجتمع الميكروبي القاعي نحو المجتمعات اللاهوائية التي تحتوي على مخفضات الحديد والكبريتات. كانت هذه المجتمعات أكثر وفرة في محطات الغطاء الجليدي المنخفض مقارنة بمحطات الغطاء الجليدي العالي. و علاوة على ذلك ، فإن الزيادة في الوفرة النسبية لفرع ديسولفورومونادیا، مع تركيز الحديد المذاب في محطات الغطاء الجليدي المنخفض ، تشير إلى دور مفترض في تقليل الحديد المتباين في الرواسب السطحية. بالإضافة إلى ذلك، نجحت هذه الدراسة في تحديد الأصناف الأخرى التي يمكن أن تساهم في تقليل الحديد المتباين أو لديها شراكات تركيبية و/أو تفضيلات أيضية مشتركة مع مع مخفضات الحديد.

امتد تركيز البحث نحو الجرف الجنوبي لبحر ويدل، وهي منطقة تتميز بغطاء جليدي بحري كثيف (المخطوطة ٣). تم قياس معدلات امتصاص الأكسجين القاعي في المحطات ذات أعماق المياه المختلفة وتركيبات الرواسب المختلفة. كشفت القياسات القاعية أيضًا عن اعتماد تدفقات الكربون على حجم حبيبات الرواسب وعمق المياه. بشكل عام، كانت معدلات امتصاص الأكسجين المنتشر على جرف بحر ويدل الجنوبي منخفضة. أظهر امتصاص الأكسجين المنتشر وجود علاقة إيجابية مع إجمالي الكربون العضوي المحفوظ في المحطات ذات الرواسب ذات الحبيبات الدقيقة، في حين أظهرت المحطات ذات الرواسب الخشنة الحبيبات ارتباطًا مختلفًا بشكل ملحوظ بين امتصاص الأكسجين المنتشر وإجمالي الكربون العضوي. من الشائع في جميع المحطات أن تركيزات الحديد والمنغنيز الذائبة في المياه المسامية تم العثور عليها فقط في أعماق أكبر، مما يشير إلى إطلاق محدود للغاية لهذه العناصر الغذائية مرة أخرى في عمود الماء.

تم بعد ذلك الجمع بين الاعتماد القوي لتدفقات الكربون القاعية على الغطاء الجليدي البحري وعمق المياه لاستخلاص نموذج تجريبي بسيط، والذي تم التحقق من صحته من خلال جميع قياسات امتصاص الأكسجين المنتشر المتاحة الواردة في الدراسات السابقة للمنطقة الجليدية الموسمية في القطب الجنوبي (المخطوطة ٤). يسمح النموذج باستقراء ووضع ميزانية لإعادة تمعدن الكربون القاعي لمنطقة الجليد الموسمية بأكملها (١٦ مليون كيلومتر مربع)، مما ينتج عنه إجمالي ٤٦ تيرا جرام كربون سنويًا. والجدير بالذكر أنه على الرغم من أن الجرف القاري في القطب الجنوبي لا يمثل سوى ١٥ % من المساحة الإجمالية، إلا أنه يساهم بنسبة كبيرة تبلغ ٧١ % (٣٣ تيرا جرام كربون سنويًا) من إجمالي إعادة تمعدن الكربون القاعي. علاوة على ذلك، تم تقدير إجمالي إمدادات الكربون العضوي في الرواسب ودفن الكربون في الرواسب بمقدار ٥٢ تيرا جرام كربون سنويًا و ٦ تيرا جرام كربون سنويًا ، على التوالى.

بشكل عام، تسلط الأطروحة الضوء على الدور المحوري للغطاء الجليدي البحري في التحكم في دورة الكربون والحديد القاعية على الجرف القاري في القطب الجنوبي. ومن خلال الارتباط المكثف للبيانات والنمذجة التجريبية، قدمت الأطروحة، لأول مرة، إطارًا كميًا للعلاقة بين الغطاء الجليدي البحري وتدفقات الكربون القاعية. ويؤكد أيضًا على المساهمة الكبيرة لرواسب

الجرف القطبي الجنوبي في إعادة تمعدن الكربون البحري، مما يسمح بإجراء تقييم أفضل لدورة الكربون وما يرتبط به من احتجاز ثاني أكسيد الكربون عبر المحيط الجنوبي. علاوة على ذلك، فقد أدى ذلك إلى تحسين فهمنا للمحركات الرئيسية للتغيير في المجتمعات الميكروبية القاعية، وفي نهاية المطاف، تدفقات المغذيات عبر واجهة الرواسب والمياه. وتساهم هذه النتائج بشكل كبير في فهمنا للنظام البيئي المعقد في القطب الجنوبي، وهو أمر ضروري لتقييم المسار المستقبلي للمحيط القطبي الجنوبي وتأثيره على دورة الكربون العالمية.

1

Introduction

The Antarctic Ocean in a warming world

Since the 1950s, about 93% of the energy imbalance has accumulated in the ocean as increased ocean heat content (Figure 1) (Cheng et al., 2019). The Southern Ocean (SO), also known as the Antarctic Ocean, alone has stored 35 – 43% of the global ocean heat content in the upper 2000 m of the water column from 1970 to 2017, and even more in recent years, with an estimated 45 – 62% of the global heat content from 2005 to 2017 (Meredith et al., 2019). The ongoing intensification of the westerly winds due to atmospheric warming over the SO increases the heat transport toward the south (Perren et al., 2020). The accelerated increase in near-surface air temperature in the SO and in the polar region in general, relative to the rest of the globe, is known as "polar amplification". In the Arctic, near-surface air temperatures have increased 2 to 3 times more than in the rest of the world in recent decades (Serreze & Barry, 2011) and similar amplification is reported for the Antarctic. For example, annual mean air temperatures on the Antarctic Peninsula (AP) have increased by 3.7 ± 1.6°C, which is six times higher than the global average of 0.6 ± 0.2°C (Smithson, 2002; Morris & Vaughan, 2003; Vaughan et al., 2003; Turner et al., 2005). The highest warming rates have been observed during the austral autumn and winter, with decadal mean air temperature increases of up to 1.09°C (King & Harangozo, 1998;

Turner et al., 2005; Ding & Steig, 2013). Due to its rapid warming, the AP is considered one of the fastest warming regions in the world, and therefore a model area for the study of climate change and its effects on marine ecosystems.

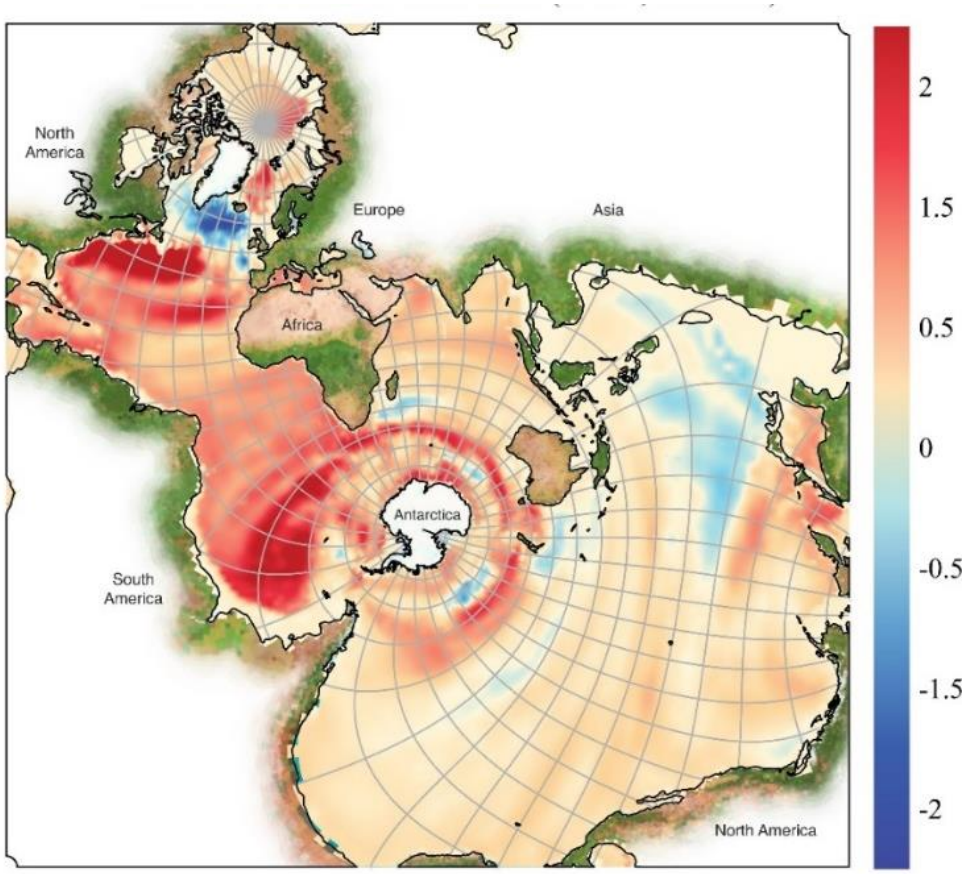

Figure 1. Change in ocean heat content in the upper 2000 m in W m^{-2} between 1958 and 2020 (Cheng et al., 2023).

The local warming trend in this polar region affects the marine realm through both changes in sea ice dynamics and changes in shelf ice dynamics. Significant decreases in the duration of sea ice extent have been recorded in the SO, particularly in the Ross, Amundsen, and Bellingshausen Seas and around the AP (Figure 2) (e.g. Thompson et al., 2011; Stammerjohn et al., 2012; Meehl et al., 2019; Eayrs et al., 2021). In 2023, the sea ice extent around Antarctica reached its lowest winter maximum extent of 17 million km², 1 million km² below the previous record low in 1986. This record low extent is a continuation of a downward trend in Antarctic sea ice that began after a record high in 2014. Prior to 2014, the sea ice surrounding the continent was slowly increasing

by about 1.5% per decade (Parkinson, 2019; Melsheimer et al., 2023). In addition, several authors have reported rapid retreat and disintegration of large ice shelves such as Larsen A, Larsen B, and Larsen C in the northwestern Weddell Sea (e.g. Rott et al., 1996; Rott et al., 2002; Vaughan et al., 2003; Rack & Rott, 2004; Scambos et al., 2017) and volume loss of ice shelves (Paolo et al., 2015; Scambos et al., 2017), leading to further destabilization and increased flow rates of outlet and valley glaciers on land (Rignot et al., 2004; Scambos et al., 2004). Such changes in the sea ice and shelf ice will clearly alter the pelagic ecosystem, which in turn will lead to changes in the benthic ecosystem (Smetacek & Nicol, 2005; Barnes, 2015; Deppeler & Davidson, 2017; Barnes et al., 2018).

Changes in ice shelf and sea ice dynamics are expected to significantly affect carbon fluxes throughout the food web as biological production shifts from sea ice-associated production to open water production, with severe consequences for secondary production, export production, benthic remineralization, and nutrient cycling (Smetacek & Nicol, 2005; Barnes, 2015; Barnes et al., 2018; Rogers et al., 2020). In coastal and shelf areas, ice shelf disintegration will provide new areas of increased light for surface primary producers, and the input of essential micronutrients from glacial runoff to surface waters may favor phytoplankton blooms (Gerringa et al., 2012). In the open ocean, longer ice-free growing seasons due to a reduction in the duration of ice cover will increase the availability of light to the surface water, which could promote the development of phytoplankton blooms that drive the biological carbon pump (Peck et al., 2010). However, it is also possible that sea ice loss will reduce regional productivity due to potential future changes in stratification. The increased westerly winds often associated with declining sea ice cover can lead to a deeper mixing layer (Leung et al., 2015). A deeper mixing layer can disperse macro- and micronutrients such as dissolved iron and reduce light availability by displacing phytoplankton away from the euphotic zone, resulting in reduced primary production and subsequent carbon flux (Vernet et al., 2008; Carvalho et al., 2016). How changes in ice shelf and sea ice dynamics will increase or decrease pelagic primary production and the associated carbon fluxes to the seafloor remains an open question.

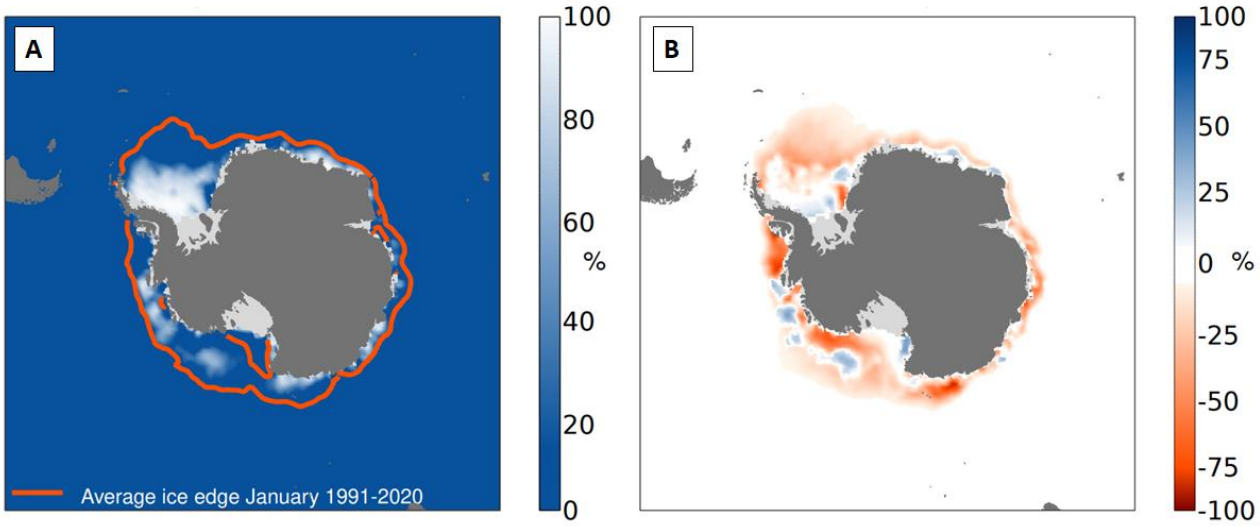

Figure 2. Antarctic sea ice for January 2023. A: Average sea ice cover for January 2023 relative to the 1991-2020. The thick orange line denotes the average ice edge for January for the period 1991-2020. B: Antarctic sea ice cover anomalies for January 2023 compared to the January average for the period 1991-2020. Data source: ERA5. Credit: Copernicus Climate Change Service/ECMWF.

The extent to which climate change will decrease or increase primary production and the subsequent cycling and sequestration of carbon in Antarctic sediments is related to the interplay of several variables that may affect coastal, shelf, and open ocean regions differently (Deppeler & Davidson, 2017). Because the bentho-pelagic coupling depends inversely on the water depth, early signs of change are expected to be found in shelf ecosystems where water depths are shallow and the imprint of climate sensitive variables such as sea ice cover can be studied best (Smith et al., 2006; Smith et al., 2012). Therefore, a comprehensive understanding of the present-day carbon cycle on the Antarctic continental shelf and its dependence on climate sensitive variables such as sea ice is crucial for assessing the ecosystem's susceptibility to climate change and for predicting the future trajectory of the carbon cycle in Antarctic waters. In the following, the characteristics of continental shelves in the carbon cycle, the role of sediments in organic matter degradation, and the microbial communities involved are presented before describing the specific conditions of the Southern Ocean and the Antarctic shelf region.

Biological production on the continental shelf

As part of the marine environment, the global continental shelf represents the link between the continents and the open ocean. Shelves usually form shallow (<200 m water depth) seas along the continents (Wollast, 2003). However, in the polar regions, shelf depths can reach up to 500 m (Anderson, 1991; Smith et al., 2006), and in some areas they can reach 800 – 1000 m (Smith et al., 2006). The global shelf covers an area of 27.1 million km^2, representing 7.5% of the world's ocean area (Menard & Smith, 1966; Wollast, 2003). The shelf ecosystems are biologically highly active. Despite its small size, the shelf contributes more than 30% of total oceanic primary production (Berger et al., 1989; Jahnke, 2010). For the global continental shelf, the estimated mean surface primary production is 200 – 230 g C m^{-2} yr^{-1} or 6 – 8 billion tons of carbon per year (Figure 3) (Gregg et al., 2003; Wollast, 2003). This high productivity within the shelf areas is essential for sustaining secondary production, with more than 90% of the world's fish catches taken from shelf seas (Pauly et al., 2002).

The basis for high productivity in shelf areas is the high nutrient availability due to the transfer of nutrient-rich deep ocean waters across the shelf break (Walsh, 1991; Wollast, 2003; Randelhoff & Sundfjord, 2018), as well as terrestrial inputs from rivers (Seitzinger et al., 2005; Beusen et al., 2016), surface runoff or submarine groundwater discharge that may additionally contain high anthropogenic nutrient loadings. Anthropogenic overuse of agricultural fertilizers that supply high levels of inorganic nutrients (i.e. nitrogen and phosphorus) are substantial nutrient source in many densely populated coastal regions (Seitzinger et al., 2005). Furthermore, the shallow depth along the continental shelf favors a strong bentho-pelagic coupling, where the rapid benthic remineralization of OM received from the water column enhances nutrient efflux from sediments and the availability for surface primary production (Smith et al., 2006).

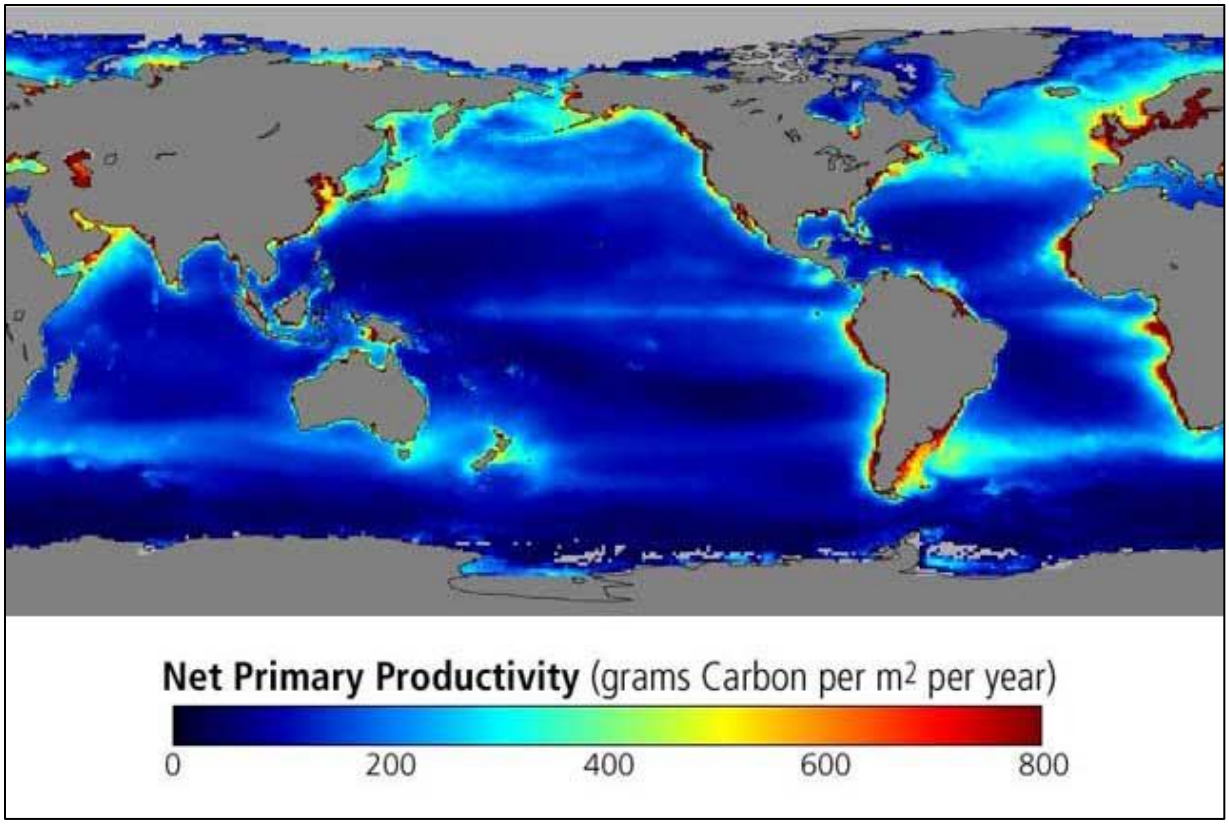

Figure 3. Ocean net primary productivity, averages from 1997 to 2002. Modified from Gregg et al. (2003).

In addition to the specific conditions on the continental shelves, the general patterns of marine primary production show a strong latitudinal and seasonal imprint (Pennington et al., 2006; Vernet et al., 2008; Lozier et al., 2011). This variability is mainly driven by changes in thermal stratification patterns, daylight length, and vertical mixing processes corresponding to the mixed layer depth (Siegel et al., 2002). In tropical regions, although sunlight is available throughout the year, productivity is low. In these regions, the surface water is always warm resulting in highly stratified water that prevents nutrient-rich bottom water from reaching the surface. As a result, productivity in tropical waters is always nutrient-limited and low throughout the year (Pennington et al., 2006; Lozier et al., 2011). In contrast, temperate regions show much greater seasonal variation in surface primary production. In spring, the abundant light and stratified nutrient-rich water lead to a spring bloom. In late summer, however, although light is still abundant, productivity is reduced by nutrient depletion in the mixed layer and the strengthening of the summer thermocline, which hinders nutrient replenishment from below. In winter, cooler

surface temperatures weaken the stratification, and increasing storms cause the erosion of the mixed layer, bringing nutrients back to the surface. However, limited light availability reduces surface primary production (Lozier et al., 2011).

In the polar regions, primary productivity is closely associated with variations in sea ice conditions and its effect on light availability and water column stratification. In winter, light is limited by day length and sea ice cover, reducing light penetration into the water column and drastically reducing primary production (Clarke, 1988). During the spring-summer season, the partial or complete retreat of the sea ice allows light to become available for photosynthesis. As the sea ice melts, heat and freshwater input cause stratification of the water column while the remaining ice sheets suppress wave mixing, both causing a shallow nutrient-rich euphotic zone (Rudels et al., 1996; Wassmann et al., 2006; Vernet et al., 2008), which supports the development of intensive phytoplankton blooms that follow the receding ice edge (Savidge et al., 1995). Therefore, elevated primary production is found along the marginal ice zone (MIZ) (Mitchell & Holm-Hansen, 1991; Sakshaug et al., 1991; Garibotti et al., 2005).

Deposition of organic carbon in marine sediments

The transfer of pelagic production to marine sediments is mainly regulated by the biological carbon pump (BCP). This process involves the sequestration of atmospheric CO_2 into organic carbon through photosynthesis, followed by its transport to the ocean interior and seafloor (Volk & Hoffert, 1985; Honjo et al., 2014). Organic matter (OM) produced by marine primary production is partially consumed and remineralized in the water column (Robinson et al., 2010; Herndl & Reinthaler, 2013). Yet, a significant fraction is exported and remineralized on the seafloor (Jahnke & Jackson, 1992). Continental shelves typically receive 25 – 50% of the OM produced in the surface ocean (Wollast, 1998; Jahnke, 2010), while deep-sea sediments receive only 1 – 10% (Klages et al., 2004; Jørgensen & Boetius, 2007) due to of the flux attenuation of OM with increasing water depth (Martin et al., 1987). Assuming that 30% of marine primary production takes place in shelf seas (Berger et al., 1989; Jahnke, 2010), 4% to 10% of the global fixed marine primary production reaches the surface sediments of the continental shelves

(Jahnke & Jackson, 1992; Wollast, 1998; Jahnke, 2010), which is equivalent to 2.16 – 6.21 Gt C yr^{-1}. These values are comparable to Jahnke's (2010) estimates of 1.9 – 4.8 Gt C yr^{-1}. Shelves are therefore potentially important sinks for atmospheric CO_2, accounting for the removal of nearly one-third of anthropogenic CO_2 emissions from the atmosphere (Chen & Borges, 2009; Laruelle et al., 2018).

The deposition of a relevant fraction of the surface primary production turn continental shelf sediments into important sites for OM remineralization and nutrient regeneration (Jahnke & Jackson, 1992). At the seafloor, OM is either remineralized and used for biosynthesis, or buried in the sediment (Canfield et al., 1993; Burdige, 2007). The vast majority of OM is remineralized into CO_2 and inorganic nutrients, which are subsequently released from the sediments into the water column, supporting again the growth of phytoplankton and maintaining the high primary production of the shelf areas and the adjacent open ocean (e.g. Graf, 1992; Smith et al., 2006; Griffiths et al., 2017). Ultimately, less than 10% of deposited OM escapes benthic remineralization and is buried and stored in the seafloor for thousands to millions of years, depending on the burial efficiency (Seiter et al., 2005; Burdige, 2007), which may exhibit significant spatial (e.g. Canfield, 1994; Blair & Aller, 2012) and temporal (e.g. Arthur et al., 1985) variations. These variations are influenced by factors such as OM deposition rate, macrobenthic activity, OM composition, electron acceptor availability, especially bottom water oxygen concentration, all of which determine whether OM is remineralized by microbial processes or buried and preserved in the sediment (Müller & Suess, 1979; Aller, 1982; Emerson, 1985; Canfield, 1994; Dauwe et al., 2001). Thus, shelf sediments play an important role in carbon storage and long-term CO_2-sequestration, as well as in enhanced nutrient cycling due to the tight bentho-pelagic.

The supply of OM to the seafloor plays a key role in shaping the size, composition, and functional traits of the benthic fauna (e.g. Pearson & Rosenberg, 1978, 1986; Herman et al., 1999; Smith et al., 2006). In Antarctica, where pronounced seasonal fluctuations in OM supply occur, this dynamic sustains a rich benthic fauna, composed mainly of endemic species that are well adapted to the cold bottom waters and the varying seasonal carbon input (Arntz et al., 1994). In addition, part of the OM remineralization proceeds through the suspension- and deposit-feeding benthic

mega-, macro-, and meiofauna (Kristensen, 2000), including sessile epi- and infauna, mobile forms roaming the sediment-water interface, as well as burrowing and interstitial infauna (Gutt & Starmans, 1998). They contribute to benthic-pelagic fluxes both directly through their metabolism and indirectly through bioturbation and bioirrigation (i.e. physical reworking of sediments and pore waters, and borrow ventilation; (Aller & Aller, 1992; Aller, 1994; Aller, 2001; Smith et al., 2006). Together, all these processes affect the physical and chemical conditions at the sediment-water interface and strongly influence OM remineralization (e.g. Aller, 1994; Glud, 2008).

Degradation of organic matter in marine sediments

The remineralization of OM is mainly driven by microbially-mediated metabolic reactions using sequences of terminal electron-accepting processes (TEAPs) known as the "redox cascade" (Froelich et al., 1979; Glud, 2008; Stumm & Morgan, 2012). According to the energy yield of the respective remineralization pathway, O_2 is the thermodynamically most favorable remineralization pathway, followed by the reduction of NO_3^-, Mn(IV), Fe(III), SO_4^{2-}, and CO_2 (Figure 4). The microbial degradation of OM by the TEAPs is the main driver of biogeochemical processes in marine sediments (D'Hondt et al., 2004; D'hondt et al., 2015). These processes take place in the pore space between the particles or on their surfaces and results in the release of dissolved inorganic carbon and inorganic nutrients such as NH_4^+ and PO_4^{3-} and the reduced products of the other electron-accepting processes (e.g. Mn^{2+}, Fe^{2+}, and HS^-) from anaerobic respiration into the sedimentary interstitial waters. The microbial remineralization of OM varies with sediment depth, forming a typical/distinct redox zonation (Figure 5) (e.g. Froelich et al., 1979; Jørgensen & Kasten, 2006). However, the spatial overlap between the redox zones where the respective oxidation-reduction processes occur is also facilitated by benthic faunal activities (e.g. Canfield et al., 1993; Glud, 2008). The extent of the different redox zones and the depth position of the redox boundaries are mainly controlled by sediment accumulation and bioturbation rates, the reactivity of the OM, and the availability of electron acceptors (e.g.

Froelich et al., 1979; Canfield, Jørgensen, et al., 1993; Jørgensen & Kasten, 2006). All together these factors determine the rate of OM remineralization.

Microbial communities inhabiting surface sediments react rapidly to the input of fresh OM by increasing carbon remineralization rates (Witte et al., 2003). This process involves the breakdown of large organic molecules such as structural carbohydrates, proteins, nucleic acids, and lipid complexes into smaller molecules that are reduced to CO_2 (e.g. Kappelmann et al., 2019), producing the energy to sustain microbial metabolism, and used for biosynthesis. Because bacterial membranes are generally unable to take up substrates with a molecular weight greater than 600 Daltons through their cell wall (Weiss et al., 1991), polymeric substances must first be degraded. This depolymerization process is mediated by extracellular enzymes that are either tethered to the cell wall or released into the environment. The resulting monomeric compounds are rapidly assimilated and metabolized. The full remineralization of OM usually requires the concerted action of a complex community of microbes (i.e. microbial food chain).

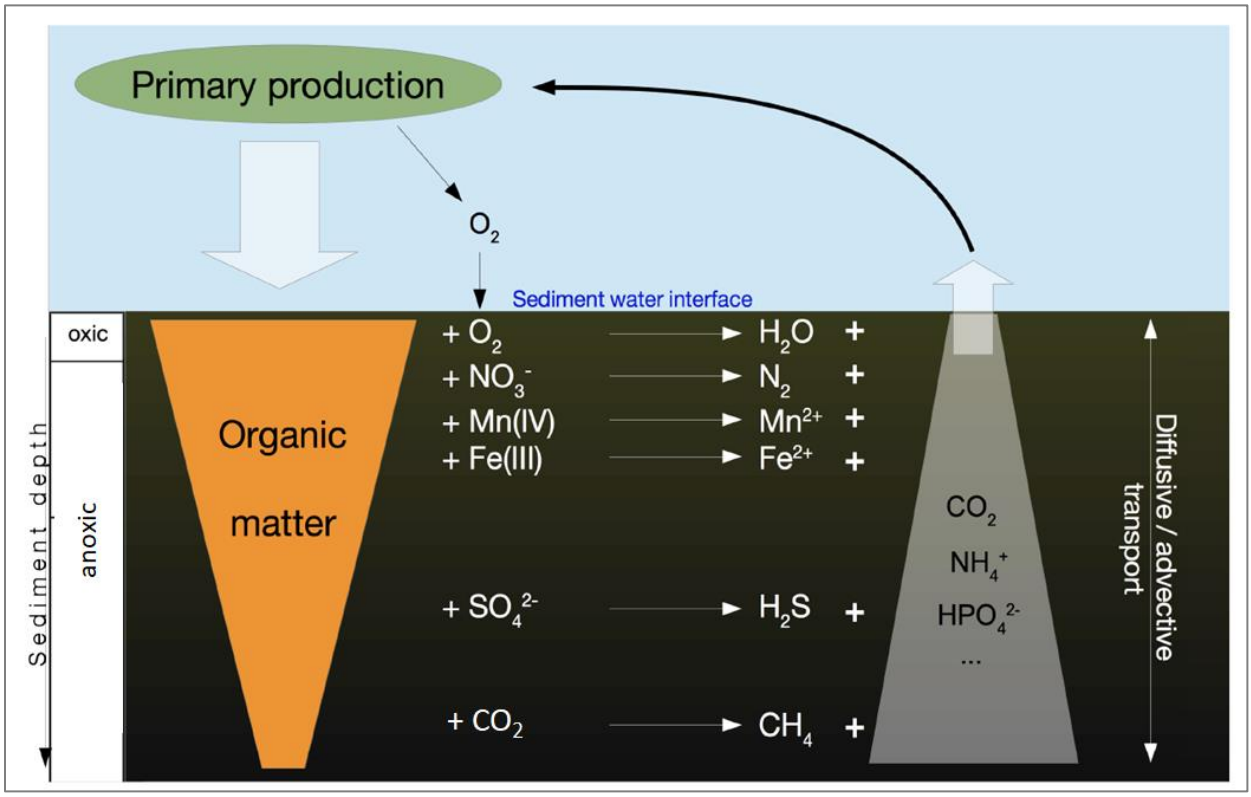

Figure 4. Typical steady-state zonation of organic matter remineralization pathways in marine sediments under mostly oxic bottom waters. Modified after Lipka (2017).

In the top layer of the sediment, O_2 is consumed by the aerobic respiration of fauna and bacteria, and by the re-oxidation of reduced inorganic products released during the anaerobic OM remineralization in the anoxic part of the sediment (Figure 5). Therefore, benthic O_2 uptake is commonly used as a proxy for the total benthic carbon remineralization rate, which is a composite of aerobic and anaerobic remineralization. An exception is denitrification, whose reduced product is N_2 gas, which is not further involved in sedimentary redox processes and therefore has no direct impact on the O_2 budget. The thickness of the oxic layer, i.e. the oxygen penetration depth, varies from millimeters in coastal areas to centimeters and decimeters in deeper oceanic areas (Jørgensen, 2000; Glud, 2008) and is mainly controlled by the O_2 concentration in the water column (source) and O_2 consumption in the sediment (sink).

Below the oxic zone, the anaerobic part of the microbial food chain begins to use alternative electron acceptors (Figure 5). Denitrification, the bacterial reduction of nitrate to N_2, is restricted to a thin anoxic layer below the oxic zone (Christensen et al., 1989). Denitrification causes massive losses of bioavailable nitrogen to N_2 in the ocean and therefore exerts a negative feedback on pelagic productivity, reducing the supply of fixed nitrogen from the coastal areas by about 40% (Seitzinger, 1988). Below the denitrification zone, microbial manganese reduction dominates in marine sediments that are rich in manganese oxides (Aller, 1990; Canfield et al., 1993). However, manganese oxides usually occur at lower concentrations than iron oxides, so that manganese reduction rates are often found lower than those of iron reduction (Thamdrup & Canfield, 1996; Kostka et al., 1999).

Because iron is the key limiting nutrient in most of the SO, a more comprehensive explanation of the benthic iron cycle is provided. In sediments rich with reactive iron oxides (ferruginous zones), iron reduction may play a dominant role in OM remineralization (Canfield et al., 1993; Vandieken et al., 2006; Canfield & Thamdrup, 2009). The relative contribution of iron reduction to OM remineralization is highly variable, ranging from below detection to 75%, with an average of 17% for a wide range of continental shelf sediments (Thamdrup, 2000; Mark Jensen et al., 2003; Dale et al., 2015; Henkel et al., 2018). The reduction of iron in sediments occurs directly by dissimilatory iron reduction mediated by microorganisms or indirectly by the process of

organoclastic sulfate reduction, followed by the oxidation of sulfide through iron reduction. In the ferruginous zone, iron reduction results in the accumulation of dissolved iron (DFe) in the pore waters, which can diffuse across the sediment-water interface, providing the water column with a micronutrient that can limit primary production, especially in the SO (Canfield & Thamdrup, 2009; Raiswell & Canfield, 2012). The release of DFe from the sediment to the water column is mainly controlled by the OM accumulation rate and the O_2 concentrations in the bottom waters (Elrod et al., 2004; Dale et al., 2015). The OM accumulation regulates the remineralization rate and the O_2 concentration determines the fraction of OM that is remineralized anaerobically. Together, these parameters affect both the rates of iron reduction and the position of the ferruginous zone.

The availability of OM on the seafloor also enhances the formation of organic ligands that are able to bind with DFe and serve to protect it from abiotic oxidation (Klar et al., 2017). However, only a small fraction of DFe is complexed by organic ligands, and most DFe is rapidly re-oxidized in oxic waters and lost to insoluble iron oxides which remain part of the solid phase of the sediment (Slomp et al., 1996; Raiswell & Canfield, 2012). Through processes such as resuspension, lateral transport by currents, and upwelling, these stable DFe ligands can be transported to the euphotic zone where they are rapidly taken up by phytoplankton (Nodwell & Price, 2001; Shaked et al., 2005).

In the sediment layers that contain reactive iron oxides such as ferrihydrite, lepidocrocite, goethite, and hematite, iron reduction will dominate over sulfate reduction. However, further below when this pool of reactive iron oxides is depleted, sulfate reduction becomes the dominant pathway of OM degradation. This is indicated by decreasing DFe concentrations and eventually by the appearance of free H_2S in the pore water, which is no longer precipitated via the formation of Fe-S minerals. Although sulfate reduction yields significantly less energy than the previously mentioned remineralization pathways, sulfate is abundant in seawater (28 mM), making it the primary oxidant in anoxic environments (Canfield et al., 1993). In shallow shelf sediments with high OM inputs, microbial sulfate reduction is reported to account for > 50% of OM remineralization (e.g. Canfield et al., 1993; Jørgensen & Kasten, 2006).

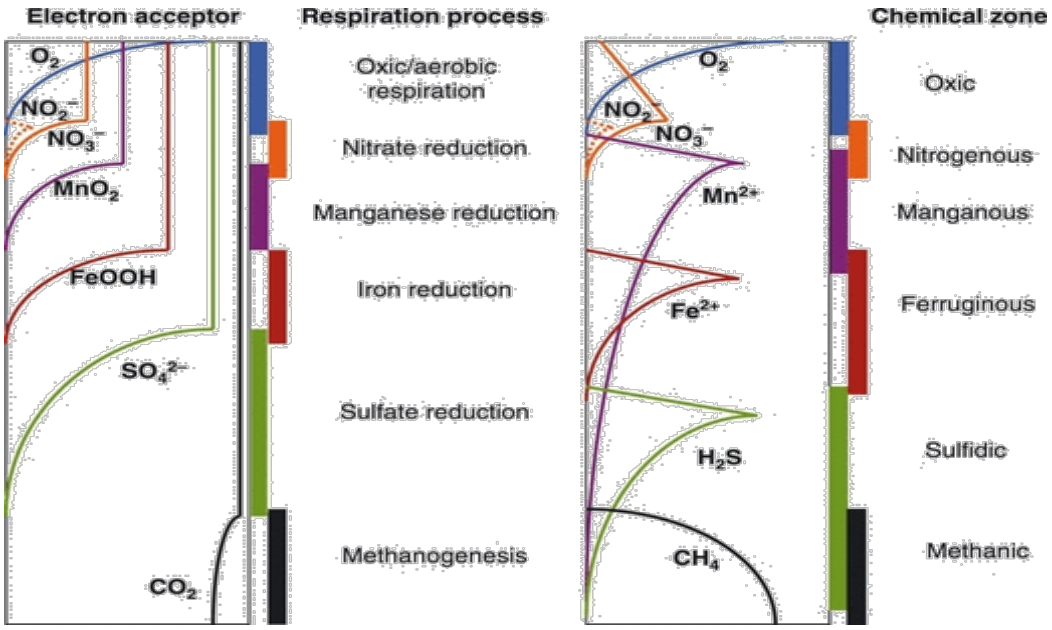

Figure 5. On the left is a diagram showing the depth distribution of common electron acceptors in marine sediments and the names used to represent the zones where these different electron acceptors are used. On the right is a diagram reflecting pore water solutes and the chemical zonation typically associated with respiration processes on the left (Canfield & Thamdrup, 2009).

Microbial communities in marine sediments

Microbial communities in marine sediments exceed any other environment in terms of the abundance of microbial cells (Whitman et al., 1998; Parkes et al., 2000). Microbial cell densities are usually orders of magnitude higher in marine sediments than in the water column (e.g. García-Moyano et al., 2012). Cell densities in coastal and shelf sediments are typically 10^8-10^9 cells/cm^3 in the uppermost sediment layers and decrease logarithmically with depth (Parkes et al., 2000). These microbial communities are composed of a wide variety of taxa, each with its own unique metabolic capabilities and ecological niches (e.g. Teske et al., 2011; Cardman et al., 2014). The complexity of these communities varies regionally across the global continental shelf (Kallmeyer et al., 2012; Sachithanandam et al., 2020) and it is mostly controlled by environmental factors (Bienhold et al., 2012; Jacob et al., 2013). Understanding community structure (i.e.

taxonomic diversity and abundance) is therefore crucial to anticipating the responses of marine ecosystems to environmental changes.

Key environmental factors such as the quantity and composition of OM, the availability and reactivity of electron acceptors, water depth, latitude, and sediment porosity and grain size have previously been shown to influence microbial community structure in marine sediments (Field et al., 1997; Bienhold et al., 2016; Varliero et al., 2019; Wunder et al., 2021; Lin et al., 2023). The hydrography of the overlying water masses, including salinity, temperature, and current velocity, significantly affects the dispersal of microorganisms (Hamdan et al., 2013). Some of these factors interact with each other, and usually, a complex set of interrelated parameters controls microbial diversity and distribution. The amount and composition of OM in the sediment can be shaped by several factors: the extent of primary production in the photic zone (Franco et al., 2007; Hoffmann et al., 2017), seasonal variations in sea ice cover that affect OM production and fluxes (Currie et al, 2021), proximity to land promoting lateral transport of terrigenous inputs (Michaud et al., 2020), water depth, namely the distance from sites of OM production (Varliero et al., 2019), and seafloor depth and topography affecting sediment physical properties and OM distribution (Bowman & McCuaig, 2003; Jorgensen et al., 2012; Liao et al., 2021).

Spatial distance has previously been identified as another important factor shaping the structure of benthic microbial communities (e.g. Schauer et al., 2010; Varliero et al., 2019). Distance-decay relationships (i.e., a decrease in taxonomic similarity with increasing geographic distance), together with a relatively high degree of endemism, have been documented at different scales, including local and regional (tens to hundreds of kilometers; Schauer et al., 2010; Bienhold et al., 2016; Varliero et al., 2019) as well as global scales (Ruff et al., 2015; Mino et al., 2017). Variations in microbial distance–decay relationships could be attributed to environmental conditions (e.g. temperature, pH, salinity, oxygen, and water content) (Fuhrman et al., 2006). If the species within a community are adapted to local conditions, communities are expected to become increasingly dissimilar as species are sorted according to their niche requirements. Marine sediments, for example, can have strong environmental gradients over distances ranging from a few meters (Lloyd et al., 2010) to the millimeter scale (Bowman & McCuaig, 2003), strengthening the correlation between distance and community dissimilarity. The presence of physical barriers (e.g.

mid-ocean ridges, seamounts, and ocean trenches) can also lead to distance–decay relationships by limiting the dispersal and connectivity between communities (Varliero et al., 2019). In well-connected systems where dispersal is more feasible due to ocean currents or migrating animals, distance–decay relationships should be weaker than in systems where dispersal is limited (Müller et al., 2014; Vašutová et al., 2019).

A wide range of microbial taxa dominates microbial communities in shelf sediments. Bacterial communities are by far the most abundant and diverse group of microorganisms in marine sediments, with thousands of different species identified (e.g. Hoshino et al., 2020). Previous studies have shown that bacterial communities in oxic sediments are very different from those in anoxic sediments (Bowman & McCuaig, 2003; Hoshino et al., 2020; Liao et al., 2021). Members of the Proteobacteria, including *Alphaproteobacteria* and *Gammaproteobacteria*, together with members of the *Firmicutes*, predominate in the upper oxic sediment layer (Bowman & McCuaig, 2003; Hoshino et al., 2020; Morono et al., 2020). In the anoxic sediment layer, members of *Alphaproteobacteria*, *Betaproteobacteria, Gammaproteobacteria*, *Planctomycetes*, and *Epsilonproteobacteria* (especially *Thiobacillus denitrificans* and *Sulfurimonas denitrificans*) have been suggested to play a major role in the denitrification zone of coastal marine sediments (Kuypers et al., 2003; Schmid et al., 2003; Shao et al., 2010; Lipsewers, 2017). Dissimilatory iron reducers such as members of the Desulfuromonadales (e.g. *Desulfuromusa*, *Desulfuromonas*, *Pelobacter*, *Geopsychrobacter*, *Geothermobacter*) are considered to be the major populations mediating iron reduction in marine sediments (Roden & Lovley, 1993; Kashefi et al., 2003; Holmes et al., 2004; Vandieken et al., 2006; Vandieken & Thamdrup, 2013; Oni et al., 2015; Aromokeye et al., 2018). In the sulfate reduction zone, *Deltaproteobacteria* and members of the *Desulfosarcina-Desulfococcus* group are usually the most abundant (Muyzer & Stams, 2008; Harrison et al., 2009; Knittel & Boetius, 2009), followed by sulfide-oxidizing *Gammaproteobacteria*, *Epsilonproteobacteria*, *Planctomycetes* and the metabolically diverse *Bacteroidetes* (Jørgensen & Nelson, 2004; Campbell et al., 2006; Lenk et al., 2011; Lipsewers, 2017). The vast majority of these groups vary substantially among locations (Bienhold et al., 2012; Kallmeyer et al., 2012; Jacob et al., 2013; Sachithanandam et al., 2020) and with sediment depths (Harrison et al., 2009; Oni et al., 2015).

Although archaeal communities are less abundant than bacterial communities in marine sediments, archaea play an important role in coastal and shelf sediment ecosystems (Oni et al., 2015; Buongiorno et al., 2019). They generally dominate the subsurface marine sediments deeper than 0.1 m below the seafloor (Biddle et al., 2006; Lipp et al., 2008). Members of the Deep Sea Archaeal Group (DSAG), Marine Group I (MG-I), the Miscellaneous Crenarchaeotic Group (MCG), and the South African Goldmine Euryarchaeotal Group (SAGMEG) (Teske & Sørensen, 2008; Fry et al., 2008; Orcutt et al., 2011) are commonly found in sediments where they are involved in methane, ammonia oxidation, and sulfur cycling.

In high-latitude environments, benthic microbial communities are highly diverse and well adapted to OM recycling at permanently cold temperatures (Arnosti et al., 1998; Arnosti et al., 2005; Kirchman et al., 2005; Bienhold et al., 2012; Wunder et al., 2021). High-latitude benthic microbial communities differ significantly from those of more temperate habitats, mainly due to the quantity and composition of OM (Miksch et al., 2021). This result is consistent with the findings of previous studies showing that the quality and quantity of OM is the main driver of microbial diversity and community composition, with certain taxonomic groups showing strong correlations with environmental parameters such as sediment algal pigment concentrations and total organic carbon (Bienhold et al., 2012; Learman et al., 2016; Cho et al., 2020). Furthermore, in an incubation experiment in Arctic deep-sea sediments in Fram Strait, Hoffmann et al. (2017) found that different substrate additions had a significant effect on microbial community composition. The addition of chitin led to an increase in microbial community activity without major compositional changes, whereas the addition of phytodetritus caused a strong change in microbial community composition. Comparable studies of benthic microbial communities are rare for the Antarctic shelf (Learman et al., 2016; Cho et al., 2020; Currie et al., 2021). Changes in the seasonal sea ice extent and duration are expected to influence phytoplankton productivity and species composition (Deppeler & Davidson, 2017; Heiden et al., 2019; Ferreira et al., 2020), and thus OM supply rates. Therefore, a baseline knowledge of the composition and function of benthic microbial communities along the Antarctic shelf is essential to predict the wider ecological and biogeochemical consequences and to assess the impact on ecosystem functioning.

The Southern Ocean and the Antarctic shelf

The Southern Ocean (SO) is a vast and diverse environment covering ~20% of the world's ocean surface area (Deppeler & Davidson, 2017). It is surrounded by the Antarctic Circumpolar Current (ACC), the largest water current in the ocean, which acts as a relatively cold geophysical barrier, resulting in a high degree of endemism of Antarctic marine species (e.g. Anderson, 1991; Ambroso et al., 2017). The ACC is a major driver of the global thermohaline circulation, controlling both global gas exchange and the heat flux between the sea surface and the atmosphere (Nowlin & Klinck, 1986; McNeil et al., 2001). As such, the SO contributes to global CO_2 removal (Rintoul & Bullister, 1999), where it is estimated to absorb ∼20 Gt of atmospheric CO_2 annually (Takahashi et al., 2002; Sabine et al., 2004). The biological carbon pump (BCP) is yet another important mechanism that leads to the uptake of atmospheric CO_2 by the SO, with the potential for negative feedback to climate change (e.g. Arrigo et al., 2008; Hauck et al., 2015). However, it is difficult to assess the potential for future CO_2 sequestration of this region as the response of primary production to future sea ice loss is currently not well constrained.

Changes in primary production due to seasonal variations in sea ice cover strongly influence OM sedimentation and long-term sequestration. The annual maximum of sea ice around Antarctica covers about 40% of the SO (Figure 6A). The presence of sea ice cover plays an important role in regulating the physical parameters of the ocean surface, in particular gas and heat exchange, light availability, and water column stratification, the latter of which is crucial for phytoplankton growth (Gupta et al., 2020). The pronounced seasonality of daylight and heat input between the winter and summer seasons results in a change in sea ice cover from 20×10^6 km^2 to 4×10^6 km^2, respectively (Figure 6A+B). This seasonal variation in sea ice cover makes the Seasonal Ice Zone (SIZ) one of the largest and most dynamic biogeochemical provinces on Earth (e.g. Arrigo et al., 2008; Michels et al., 2008). Seasonality in sea ice cover affects phytoplankton growth conditions, from light limitation under the dense ice cover to a more favorable light regime and shallow mixed layer in the MIZ, to a less favorable deep mixed layer in the ice-free waters (Sakshaug et al., 1991; Vernet et al., 2008).

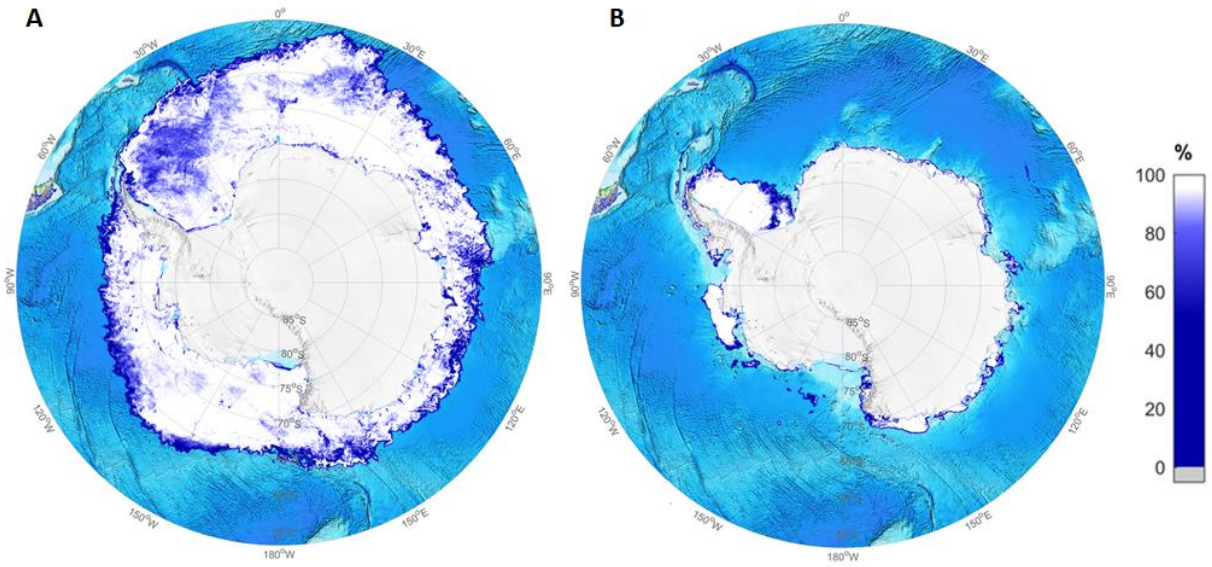

Figure 6. Examples of sea ice extension during (A) winter (September 2017) and (B) summer (February 2018) (Spreen et al., 2008).

The Antarctic shelf is the most productive region in the SO owing to the high surface concentrations of nutrients, on top of strong stratification and light availability (e.g. Arrigo et al., 2015; Deppeler & Davidson, 2017). In particular, the abundance of iron from basal ice melt and sediment inflow allows these regions to be highly productive compared to other SO regions (Boyd et al., 2012; Arrigo et al., 2015). In addition, Antarctic coastal polynyas, areas of reduced sea ice cover within the coastal sea ice zone, are formed by offshore winds and oceanic currents that advect ice away from the coast (Arrigo & van Dijken, 2003; Grebmeier & Barry, 2007). Because the polynya waters are already ice-free, the light availability compared to the nearby ice-covered areas stimulates intensive phytoplankton blooms (Arrigo & van Dijken, 2003). This results in high fluxes of sinking OC that support pelagic consumers and the benthic communities on the continental shelf (Smith et al., 2007; Barnes, 2015; Pineda-Metz et al., 2020). The Antarctic shelf is also an important site for dense water formation (Jacobs et al., 1970; Orsi et al., 1999), making this particular region of the SO a large CO_2 sink on an annual scale (Arrigo et al., 2008). The sinking of OM out of the euphotic layer feeds into dense water masses below, many of them are precursors of Antarctic bottom waters that are subducted from the shelf to the deep and efficiently sequester the associated organic and inorganic carbon pool (Arrigo et al., 2008). Thus,

the enhanced biological productivity of the Antarctic shelf region forms the basis of the food web in the SO (Smith et al., 2007; Karnovsky et al., 2007) and increases the efficiency of the local BCP (Arrigo et al., 2008).

The Antarctic continental shelf has considerable depth compared to other global continental shelves, with an average depth of 500 meters - five times deeper than the global average (Smith et al., 2006). This deep shelf is mainly due to isostatic depression caused by the grounded ice sheet (Anderson, 1991). It is also characterized by complex topography and ocean circulation (Hofmann & Klinck, 1998; Smith et al., 1999). In addition, the Antarctic shelf has comparatively low lithogenic sediment inputs compared to lower latitudes due to the absence of rivers and the presence of ice shelves (Anderson et al., 1980; Isla, 2016). How these distinctive characteristics of the Antarctic shelf, together with the seasonality of sea ice cover and surface primary production, affect the subsequent cycling and sequestration of carbon in Antarctic sediments is not yet fully understood. A thorough assessment of current benthic carbon cycling on the Antarctic continental shelf is needed to anticipate the effects of continued global warming and expected reductions in sea ice extent.

Another factor regulating surface primary production over large areas of the SO is the availability of iron, a limiting micronutrient for phytoplankton productivity (e.g. Martin et al., 1990; Boyd et al., 2007). Iron deficiency can limit phytoplankton growth rates, resulting in reduced fixation and sequestration of atmospheric CO_2 and reduced accumulation of OM at the seafloor. The abundance of iron in seawater is controlled by a balance between iron input, stabilization processes via organic complexation that keep iron in the dissolved phase, and by removal processes like (oxidative) precipitation and adsorptive scavenging (e.g. Gledhill & van den Berg, 1994; Boye et al., 2001; Cullen et al., 2006; Monien, 2014; Raiswell et al., 2016). Iron enters the SO from various sources, with considerable uncertainty in their estimated contribution. Some of the most prominent sources of bioavailable iron include iceberg-rafted debris to the shelf, which contributes approximately 180-1,400 Gg a^{-1} (Raiswell et al., 2016). According to Monien et al. (2014), Antarctic shelf sediments contribute up to 790 Gg a^{-1} of bioavailable iron. This is followed by aeolian input from dust, which accounts for an input of less than 1.12 Gg a^{-1} (Lancelot et al., 2009; Raiswell et al., 2016). In addition, a substantial release of dissolved iron from anoxic

subglacial meltwater is estimated to be between 8.9 and 11,000 Gg a^{-1}, but only a small fraction (0.03-5.9 Gg a^{-1}) of this can reach the shelf waters due to the rapid oxidation of dissolved Fe(II) to Fe(III) (Wadham et al., 2013).

The anoxic shelf sediments have recently been considered a potential source of bioavailable iron to Antarctic coastal waters and beyond (Nielsdóttir et al., 2012; Wadham et al., 2013; Measures et al., 2013; Hatta et al., 2013; Monien et al., 2014; Borrione et al., 2014; Henkel et al., 2018; Burdige & Christensen, 2022). The availability of shelf-derived micronutrients is likely to be facilitated by the upwelling of iron-enriched bottom waters caused by the seasonal occurrence of a well-mixed water column, as shown in the Ross Sea (Collier et al., 2000; Sedwick et al., 2000). In addition, significant iron fluxes from the shelves of the Antarctic Peninsula and sub-Antarctic islands into the iron-poor ACC have been reported by Venables & Meredith (2009), Nielsdóttir et al. (2012), Hatta et al. (2013), Measures et al. (2013) and Borrione et al. (2014). They argue that this shelf-derived iron is rapidly transported by the ACC and is likely responsible for extensive phytoplankton blooms downstream in the Drake Passage. Thus, the regeneration of micronutrients (especially iron) in shelf sediments of Antarctica and sub-Antarctic islands may significantly influence phytoplankton production in the SO and the Antarctic region. Although considered to be of high relevance, there are only few studies on the contribution of Antarctic shelf sediments to the iron pool of the SO so far.

Research questions and objectives

The aim of this thesis is to quantify benthic carbon remineralization rates and the release of nutrients, particularly iron, that limit primary production in the Southern Ocean. In addition, the thesis aims to identify the main pathways of OM degradation and associated microbial communities, while contextualizing the above variables within the prevailing sea ice conditions.

I hypothesize that *sea ice cover controls the production and flux of organic matter to the seafloor, affecting benthic microbial communities driving changes in redox zonation, and promoting nutrient (iron) release across the Antarctic shelf*. To test this hypothesis and to fill the existing

knowledge gaps, the thesis outlines a series of research questions aimed at shedding light on the pivotal role of sea ice cover in driving the benthic carbon cycling along the Antarctic shelf:

1) How are benthic remineralization rates affected by long-term sea ice cover?
2) What are the major degradation pathways of organic matter in Antarctic shelf sediments under varying sea ice conditions?
3) What is the contribution of Antarctic shelf sediments to benthic remineralization in the Southern Ocean?
4) How is iron cycling affected by organic carbon accumulation and how much iron is recycled back into the water column?
5) What is the impact of sea ice cover on the benthic microbial communities?
6) How do microbial communities change in the ferruginous zone?

The following objectives were derived from these questions:

- Investigate the impact of long-term sea ice cover on benthic carbon and iron cycling.
- Determine the contribution of the Antarctic shelf sediments to benthic remineralization in the Southern Ocean.
- Examine the effects of sea ice cover on the benthic microbial communities.

Manuscripts within the context of the research questions

This section describes how the four manuscripts of this thesis will address the questions mentioned in the previous section:

Manuscript 1: Benthic Carbon Remineralization and Iron Cycling in Relation to Sea ice Cover Along the Eastern Continental Shelf of the Antarctic Peninsula

Marwa Baloza, Susann Henkel, Walter Geibert, Sabine Kasten, and Moritz Holtappels

Manuscript published 2022 in *Journal of Geophysical Research: Oceans, 127*(7). doi.org/10.1029/2021JC018401

The study aimed to fill knowledge gaps regarding the influence of sea ice cover and water column stratification on carbon supply, remineralization and burial rates, as well as metal cycling in Antarctic shelf sediments. Sediment samples were collected from five stations along a gradient of cryopelagic productivity on the eastern shelf of the Antarctic Peninsula. Samples were collected at comparable water depths (350-450 meters) to avoid the effect of water depth on sinking OM fluxes. The study includes a range of data, including oxygen profiles and fluxes, and pore water profiles of dissolved metals (Mn, Fe), nutrients (NO_3^-, PO_4^{3-}), sulfate, and metabolites (NH_4^+, H_2S, DIC). The data obtained were coupled with solid phase analyses, including total organic carbon, Mn, Fe, P, and the radioisotope ^{210}Pb, to provide a detailed picture of the geochemical conditions and the biogeochemical processes under different sea ice cover conditions. This includes the estimation of the total carbon remineralization rate and the dissolved iron fluxes.

Authors' contributions: M.B. and M.H. collected the samples , M.B. and M.H. worked on the field measurements, M.B. carried out the laboratory analysis, M.B., M.H., S.H., S.K. and W.G. analyzed and interpreted the data, M.B. and M.H. prepared the figures, M.B. and M.H. wrote the first draft and S.H., S.K. and W.G. contributed to the manuscript.

Manuscript 2: The Impact of Sea ice Cover on Microbial Communities in Antarctic Shelf Sediments

Marwa Baloza, Susann Henkel, Sabine Kasten, Moritz Holtappels, and Massimiliano Molari

Manuscript published 2023 in *Microorganisms, 11*(6), 1572. doi.org/10.3390/microorganisms11061572

This manuscript is complementary to the geochemical findings presented in manuscript 1 and is based on the same set of sediment samples. It is intended as a baseline study to assess how changes in sea ice conditions affect benthic microbial communities and ultimately nutrient fluxes across the sediment– water interface. The following hypotheses were tested: (I) the impacts of sea ice cover on OM fluxes are responsible for changes in benthic microbial communities, (II) the strong changes in redox zonation, induced by intense microbial OM remineralization rates, are coupled with an increment of iron-reducers at stations with increased OM fluxes. To address these hypotheses, sediment samples from five stations along the AP with contrasting sea ice conditions were investigated by 16S ribosomal RNA (rRNA) gene sequencing. Correlation, multivariate regression, and differential taxa abundance analyses were performed to identify the key drivers of the microbial community composition. In addition, the key microbial taxa dominating the ferruginous zone at each station were identified and studied in detail to understand their role in the benthic iron cycle.

Authors' contributions: M.B. and M.H. collected the sediment samples, M.B., M.M. and M.H. designed the sample collections, M.B. carried out the laboratory analysis, M.B., M.M. and M.H. analyzed and interpreted the data, M.B. prepared the figures, M.B. and M.M. wrote the first draft and M.H., S.H. and S.K. contributed to the manuscript.

Manuscript 3: Benthic Carbon Cycling on the Southern Weddell Sea Shelf

Marwa Baloza, Sandra Maier, Claudia Hanfland, Susann Henkel, Sabine Kasten, Claudio Richter, Moritz Holtappels

Manuscript ready for submission to *Biogeosciences*

This manuscript builds on the previous findings and extends the investigation of the impact of sea ice cover on the carbon cycle towards the southern Weddell Sea shelf. Benthic oxygen uptake rates were measured at 15 stations on the southern Weddell Sea shelf characterized by heterogeneous sea ice conditions and water depths, covering the Filchner Trough (794 - 932 m depth), the eastern (387 - 663 m) and the western shelf regions (332 - 660 m). Sampling stations included two coastal polynyas, the Halley Bay polynya on the eastern shelf and the Ronne polynya on the western shelf, as well as stations outside the polynyas that were mostly covered by ice (Filchner Trough). The study also included measurements of pore water concentrations of various compounds such as NO_3^-, PO_4^{3-}, NH_4^+, Mn, Fe, and SO_4^{2-}, as well as total organic carbon content to estimate the total carbon remineralization rate and to gain insight into the redox conditions along the southern Weddell Sea sediments and their implications for iron cycling. Furthermore, benthic oxygen uptake rates, water depth, and other geochemical variables from this study, and other regions of the Antarctic shelf were compiled and investigated in detail to identify the key factors controlling the spatial variation in benthic carbon remineralization rates across the Antarctic shelf seas.

Authors' contributions: S.M., C.H. and C.R. collected the sediment samples, S.M. and C.R. worked on the field measurements, M.B. and S.H. carried out the laboratory analysis, M.B., M.H., and S.H. analyzed and interpreted the data, M.B. prepared the figures, M.B. and M.H. wrote the first draft and S.H., S.M., C.H., S.K. and C.R. contributed to the manuscript.

Manuscript 4: The Imprint of Sea ice on the Biological Carbon Pump in the Southern Ocean

Moritz Holtappels and **Marwa Baloza**

Manuscript ready for submission to *Nature Geoscience*

The last manuscript is an attempt to upscale benthic rate measurements to the entire seasonal ice zone of the Southern Ocean. For this, an empirical model of benthic carbon remineralization rates has been established based on only two input variables: the long-term occurrence of moderate sea ice cover and water depth. The model was calibrated with measured benthic carbon remineralization rates from manuscripts 1 and 3 and from reviewed literature. Maps of moderate sea ice cover and water depth are employed to construct maps of benthic carbon turnover and calculate budgets for the entire seasonal ice zone of the Southern Ocean.

Authors' contributions: M.H. and M.B. analyzed and interpreted the data, M.H. and M.B. prepared the figures, M.H. and M.B. wrote the first draft.

References

Aller, R. (1990). Bioturbation and manganese cycling in hemipelagic sediments. *Philosophical Transactions of the Royal Society of London. Series A, Mathematical and Physical Sciences, 331*(1616), 51-68.

Aller, R. C. (1982). Carbonate dissolution in nearshore terrigenous muds: the role of physical and biological reworking. *The Journal of geology, 90*(1), 79-95.

Aller, R. C. (1994). Bioturbation and remineralization of sedimentary organic matter: effects of redox oscillation. *Chemical Geology, 114*(3), 331-345. doi:https://doi.org/10.1016/0009-2541(94)90062-0

Aller, R. C. (2001). 11 TRANSPORT AND REACTIONS IN THE BIOIRRIGATED ZONE. *The benthic boundary layer: transport processes and biogeochemistry*, 269.

Aller, R. C., & Aller, J. Y. (1992). Meiofauna and solute transport in marine muds. *Limnology and Oceanography, 37*(5), 1018-1033.

Ambroso, S., Salazar, J., Zapata-Guardiola, R., Federwisch, L., Richter, C., Gili, J. M., et al. (2017). Pristine populations of habitat-forming gorgonian species on the Antarctic continental shelf. *Scientific Reports, 7*(1), 12251.

Anderson, J. B. (1991). The Antarctic continental shelf: Results from marine geological and geophysical investigations. In R. J. Tingey (Ed.), The Geology of Antarctica (pp. 285–334). Clarendon Press, Oxford.

Anderson, J. B., Kurtz, D. D., Domack, E. W., & Balshaw, K. M. (1980). Glacial and Glacial Marine Sediments of the Antarctic Continental Shelf. *The Journal of Geology, 88*(4), 399-414. doi:10.1086/628524

Arnosti, C., Finke, N., Larsen, O., & Ghobrial, S. (2005). Anoxic carbon degradation in Arctic sediments: microbial transformations of complex substrates. *Geochimica et Cosmochimica Acta, 69*(9), 2309-2320.

Arnosti, C., Jørgensen, B. B., Sagemann, J., & Thamdrup, B. (1998). Temperature dependence of microbial degradation of organic matter in marine sediments: polysaccharide hydrolysis, oxygen consumption, and sulfate reduction. *Marine Ecology Progress Series, 165*, 59-70.

Arntz, W., Brey, T., & Gallardo, V. (1994). Antarctic zoobenthos. *Oceanography and marine biology, 32*, 241-304.

Aromokeye, D. A., Richter-Heitmann, T., Oni, O. E., Kulkarni, A., Yin, X., Kasten, S., et al. (2018). Temperature controls crystalline iron oxide utilization by microbial communities in methanic ferruginous marine sediment incubations. *Frontiers in Microbiology, 9*, 2574.

Arrigo, K. R., & van Dijken, G. L. (2003). Phytoplankton dynamics within 37 Antarctic coastal polynya systems. *Journal of Geophysical Research: Oceans, 108*(C8).

Arrigo, K. R., van Dijken, G. L., & Bushinsky, S. (2008). Primary production in the Southern Ocean, 1997–2006. *Journal of Geophysical Research: Oceans, 113*(C8). doi:https://doi.org/10.1029/2007JC004551

Arrigo, K. R., Van Dijken, G. L., & Strong, A. L. (2015). Environmental controls of marine productivity hot spots around Antarctica. *Journal of Geophysical Research: Oceans, 120*(8), 5545-5565. doi:10.1002/2015JC010888

Arthur, M., Dean, W., Pollastro, R., Scholle, P., & Claypool, G. (1985). A comparative geochemical study of two transgressive pelagic limestone units, Cretaceous Western Interior basin, US. In *Fine-Grained Deposits and Biofacies of the Cretaceous Western Interior Seaway: Evidence of Cyclic Sedimentary Processes* (Vol. 4, pp. 16-27): SEPM, Field Trip Guidebook.

Barnes, D. (2015). Antarctic sea ice losses drive gains in benthic carbon drawdown. *Current Biology, 25*(18), R789-R790.

Barnes, D. K., Fleming, A., Sands, C. J., Quartino, M. L., & Deregibus, D. (2018). Icebergs, sea ice, blue carbon and Antarctic climate feedbacks. *Philosophical Transactions of the Royal Society A: Mathematical, Physical and Engineering Sciences, 376*(2122), 20170176.

Berger, W., Smetacek, V., & Wefer, G. (1989). Ocean productivity and paleoproductivity—an overview. *Productivity of the ocean: present and past, 44*, 1-34.

Beusen, A. H. W., Bouwman, A. F., Van Beek, L. P. H., Mogollón, J. M., & Middelburg, J. J. (2016). Global riverine N and P transport to ocean increased during the 20th century despite increased retention along the aquatic continuum. *Biogeosciences, 13*(8), 2441-2451. doi:10.5194/bg-13-2441-2016

Biddle, J. F., Lipp, J. S., Lever, M. A., Lloyd, K. G., Sørensen, K. B., Anderson, R., et al. (2006). Heterotrophic Archaea dominate sedimentary subsurface ecosystems off Peru. *Proceedings of the National Academy of Sciences, 103*(10), 3846-3851. doi:doi:10.1073/pnas.0600035103

Bienhold, C., Boetius, A., & Ramette, A. (2012). The energy–diversity relationship of complex bacterial communities in Arctic deep-sea sediments. *The ISME journal, 6*(4), 724-732.

Bienhold, C., Zinger, L., Boetius, A., & Ramette, A. (2016). Diversity and Biogeography of Bathyal and Abyssal Seafloor Bacteria. *PLoS One, 11*(1), e0148016. doi:10.1371/journal.pone.0148016

Blair, N. E., & Aller, R. C. (2012). The fate of terrestrial organic carbon in the marine environment. *Annual Review of Marine Science, 4*, 401-423.

Borrione, I., Aumont, O., Nielsdóttir, M., & Schlitzer, R. (2014). Sedimentary and atmospheric sources of iron around South Georgia, Southern Ocean: a modelling perspective. *Biogeosciences, 11*(7), 1981-2001.

Bowman, J. P., & McCuaig, R. D. (2003). Biodiversity, community structural shifts, and biogeography of prokaryotes within Antarctic continental shelf sediment. *Applied and Environmental Microbiology, 69*(5), 2463-2483.

Boyd, P. W., Arrigo, K. R., Strzepek, R., & Van Dijken, G. L. (2012). Mapping phytoplankton iron utilization: Insights into Southern Ocean supply mechanisms. *Journal of Geophysical Research: Oceans, 117*(6). doi:10.1029/2011JC007726

Boyd, P. W., Jickells, T., Law, C., Blain, S., Boyle, E., Buesseler, K., et al. (2007). Mesoscale iron enrichment experiments 1993-2005: synthesis and future directions. *Science, 315*(5812), 612-617.

Boye, M., van den Berg, C. M., de Jong, J. T., Leach, H., Croot, P., & De Baar, H. J. (2001). Organic complexation of iron in the Southern Ocean. *Deep Sea Research Part I: Oceanographic Research Papers, 48*(6), 1477-1497.

Buongiorno, J., Herbert, L. C., Wehrmann, L. M., Michaud, A. B., Laufer, K., Røy, H., et al. (2019). Complex Microbial Communities Drive Iron and Sulfur Cycling in Arctic Fjord Sediments.

Applied and Environmental Microbiology, 85(14), e00949-00919. doi:doi:10.1128/AEM.00949-19

Burdige, D. J. (2007). Preservation of organic matter in marine sediments: controls, mechanisms, and an imbalance in sediment organic carbon budgets? *Chemical reviews, 107*(2), 467-485.

Burdige, D. J., & Christensen, J. P. (2022). Iron biogeochemistry in sediments on the western continental shelf of the Antarctic Peninsula. *Geochimica et Cosmochimica Acta, 326*, 288-312. doi:https://doi.org/10.1016/j.gca.2022.03.013

Campbell, B. J., Engel, A. S., Porter, M. L., & Takai, K. (2006). The versatile ε-proteobacteria: key players in sulphidic habitats. *Nature reviews microbiology, 4*(6), 458-468.

Canfield, D. E. (1994). Factors influencing organic carbon preservation in marine sediments. *Chemical geology, 114*(3-4), 315-329.

Canfield, D. E., Jørgensen, B. B., Fossing, H., Glud, R., Gundersen, J., Ramsing, N. B., et al. (1993). Pathways of organic carbon oxidation in three continental margin sediments. *Marine geology, 113*(1-2), 27-40.

Canfield, D. E., & Thamdrup, B. (2009). Towards a consistent classification scheme for geochemical environments, or, why we wish the term 'suboxic'would go away. In (Vol. 7, pp. 385-392): Wiley Online Library.

Canfield, D. E., Thamdrup, B., & Hansen, J. W. (1993). The anaerobic degradation of organic matter in Danish coastal sediments: iron reduction, manganese reduction, and sulfate reduction. *Geochimica et Cosmochimica Acta, 57*(16), 3867-3883.

Cardman, Z., Arnosti, C., Durbin, A., Ziervogel, K., Cox, C., Steen, A., et al. (2014). Verrucomicrobia are candidates for polysaccharide-degrading bacterioplankton in an arctic fjord of Svalbard. *Applied and Environmental Microbiology, 80*(12), 3749-3756.

Carvalho, F., Kohut, J., Oliver, M. J., Sherrell, R. M., & Schofield, O. (2016). Mixing and phytoplankton dynamics in a submarine canyon in the West Antarctic Peninsula. *Journal of Geophysical Research: Oceans, 121*(7), 5069-5083. doi:https://doi.org/10.1002/2016JC011650

Chen, C.-T. A., & Borges, A. V. (2009). Reconciling opposing views on carbon cycling in the coastal ocean: Continental shelves as sinks and near-shore ecosystems as sources of atmospheric CO2. *Deep Sea Research Part II: Topical Studies in Oceanography, 56*(8-10), 578-590.

Cheng, L., Abraham, J., Hausfather, Z., & Trenberth, K. E. (2019). How fast are the oceans warming? *Science, 363*(6423), 128-129.

Cheng, L., Abraham, J., Trenberth, K. E., Fasullo, J., Boyer, T., Mann, M. E., et al. (2023). Another Year of Record Heat for the Oceans. *Advances in Atmospheric Sciences, 40*(6), 963-974. doi:10.1007/s00376-023-2385-2

Cho, H., Hwang, C. Y., Kim, J.-G., Kang, S., Knittel, K., Choi, A., et al. (2020). A unique benthic microbial community underlying the Phaeocystis antarctica-dominated Amundsen Sea polynya, Antarctica: a proxy for assessing the impact of global changes. *Frontiers in Marine Science, 6*, 797.

Christensen, P. B., Nielsen, L. P., & Revsbech, N. P. (1989). Microzonation of denitrification activity in stream sediments as studied with a combined oxygen and nitrous oxide microsensor. *Applied and Environmental Microbiology, 55*(5), 1234-1241.

Clarke, A. (1988). Seasonality in the Antarctic marine environment. *Comparative Biochemistry and Physiology Part B: Comparative Biochemistry, 90*(3), 461-473.

Collier, R., Dymond, J., Honjo, S., Manganini, S., Francois, R., & Dunbar, R. (2000). The vertical flux of biogenic and lithogenic material in the Ross Sea: moored sediment trap observations 1996–1998. *Deep Sea Research Part II: Topical Studies in Oceanography, 47*(15-16), 3491-3520.

Cullen, J. T., Bergquist, B. A., & Moffett, J. W. (2006). Thermodynamic characterization of the partitioning of iron between soluble and colloidal species in the Atlantic Ocean. *Marine Chemistry, 98*(2-4), 295-303.

Currie, A. A., Marshall, A. J., Lohrer, A. M., Cummings, V. J., Seabrook, S., & Cary, S. C. (2021). Sea ice dynamics drive benthic microbial communities in McMurdo Sound, Antarctica. *Frontiers in Microbiology*, 3189.

D'Hondt, S., Jørgensen, B. B., Miller, D. J., Batzke, A., Blake, R., Cragg, B. A., et al. (2004). Distributions of microbial activities in deep subseafloor sediments. *Science, 306*(5705), 2216-2221.

D'hondt, S., Inagaki, F., Zarikian, C. A., Abrams, L. J., Dubois, N., Engelhardt, T., et al. (2015). Presence of oxygen and aerobic communities from sea floor to basement in deep-sea sediments. *Nature Geoscience, 8*(4), 299-304.

Dale, A. W., Nickelsen, L., Scholz, F., Hensen, C., Oschlies, A., & Wallmann, K. (2015). A revised global estimate of dissolved iron fluxes from marine sediments. *Global Biogeochemical Cycles, 29*(5), 691-707. doi:https://doi.org/10.1002/2014GB005017

Dauwe, B., Middelburg, J. J., & Herman, P. M. (2001). Effect of oxygen on the degradability of organic matter in subtidal and intertidal sediments of the North Sea area. *Marine Ecology Progress Series, 215*, 13-22.

Deppeler, S. L., & Davidson, A. T. (2017). Southern Ocean phytoplankton in a changing climate. *Frontiers in Marine Science, 4*, 40.

Ding, Q., & Steig, E. J. (2013). Temperature change on the Antarctic Peninsula linked to the tropical Pacific. *Journal of Climate, 26*(19), 7570-7585.

Eayrs, C., Li, X., Raphael, M. N., & Holland, D. M. (2021). Rapid decline in Antarctic sea ice in recent years hints at future change. *Nature Geoscience, 14*(7), 460-464.

Elrod, V. A., Berelson, W. M., Coale, K. H., & Johnson, K. S. (2004). The flux of iron from continental shelf sediments: A missing source for global budgets. *Geophysical Research Letters, 31*(12).

Emerson, S. (1985). Organic carbon preservation in marine sediments. *The carbon cycle and atmospheric CO2: natural variations Archean to present, 32*, 78-87.

Ferreira, A., Costa, R. R., Dotto, T. S., Kerr, R., Tavano, V. M., Brito, A. C., et al. (2020). Changes in Phytoplankton Communities Along the Northern Antarctic Peninsula: Causes, Impacts and Research Priorities. *Frontiers in Marine Science, 7*, 576254. doi:10.3389/fmars.2020.576254

Field, K., Gordon, D., Wright, T., Rappé, M., Urback, E., Vergin, K., et al. (1997). Diversity and depth-specific distribution of SAR11 cluster rRNA genes from marine planktonic bacteria. *Applied and Environmental Microbiology, 63*(1), 63-70.

Franco, M. A., Mesel, I. D., Diallo, M. D., Gucht, K. V. d., Gansbeke, D. V., Rijswijk, P. v., et al. (2007). Effect of phytoplankton bloom deposition on benthic bacterial communities in two contrasting sediments in the southern North Sea. *Aquatic Microbial Ecology, 48*(3), 241-254. Retrieved from https://www.int-res.com/abstracts/ame/v48/n3/p241-254/

Froelich, P. N., Klinkhammer, G., Bender, M. L., Luedtke, N., Heath, G. R., Cullen, D., et al. (1979). Early oxidation of organic matter in pelagic sediments of the eastern equatorial Atlantic: suboxic diagenesis. *Geochimica et Cosmochimica Acta, 43*(7), 1075-1090.

Fry, J. C., Parkes, R. J., Cragg, B. A., Weightman, A. J., & Webster, G. (2008). Prokaryotic biodiversity and activity in the deep subseafloor biosphere. *FEMS Microbiology Ecology, 66*(2), 181-196.

Fuhrman, J. A., Hewson, I., Schwalbach, M. S., Steele, J. A., Brown, M. V., & Naeem, S. (2006). Annually reoccurring bacterial communities are predictable from ocean conditions. *Proceedings of the National Academy of Sciences, 103*(35), 13104-13109. doi:doi:10.1073/pnas.0602399103

García-Moyano, A., González-Toril, E., Aguilera, Á., & Amils, R. (2012). Comparative microbial ecology study of the sediments and the water column of the Río Tinto, an extreme acidic environment. *FEMS Microbiology Ecology, 81*(2), 303-314. doi:10.1111/j.1574-6941.2012.01346.x

Garibotti, I. A., Vernet, M., Smith, R. C., & Ferrario, M. E. (2005). Interannual variability in the distribution of the phytoplankton standing stock across the seasonal sea ice zone west of the Antarctic Peninsula. *Journal of Plankton Research, 27*(8), 825-843.

Gerringa, L. J. A., Alderkamp, A.-C., Laan, P., Thuróczy, C.-E., De Baar, H. J. W., Mills, M. M., et al. (2012). Iron from melting glaciers fuels the phytoplankton blooms in Amundsen Sea (Southern Ocean): Iron biogeochemistry. *Deep Sea Research Part II: Topical Studies in Oceanography, 71*, 16-31. doi:https://doi.org/10.1016/j.dsr2.2012.03.007

Gledhill, M., & van den Berg, C. M. (1994). Determination of complexation of iron (III) with natural organic complexing ligands in seawater using cathodic stripping voltammetry. *Marine Chemistry, 47*(1), 41-54.

Glud, R. N. (2008). Oxygen dynamics of marine sediments. *Marine Biology Research, 4*(4), 243-289.

Graf, G. (1992). Benthic-pelagic coupling: a benthic view. *Oceanography and marine biology: an annual review*.

Grebmeier, J., & Barry, J. (2007). Benthic processes in polynyas. *Elsevier oceanography series, 74*, 363-390.

Gregg, W. W., Conkright, M. E., Ginoux, P., O'Reilly, J. E., & Casey, N. W. (2003). Ocean primary production and climate: Global decadal changes. *Geophysical Research Letters, 30*(15).

Griffiths, J. R., Kadin, M., Nascimento, F. J., Tamelander, T., Törnroos, A., Bonaglia, S., et al. (2017). The importance of benthic–pelagic coupling for marine ecosystem functioning in a changing world. *Global Change Biology, 23*(6), 2179-2196.

Gupta, M., Follows, M. J., & Lauderdale, J. M. (2020). The effect of Antarctic sea ice on Southern Ocean carbon outgassing: Capping versus light attenuation. *Global Biogeochemical Cycles, 34*(8), e2019GB006489.

Gutt, J., & Starmans, A. (1998). Structure and biodiversity of megabenthos in the Weddell and Lazarev Seas (Antarctica): ecological role of physical parameters and biological interactions. *Polar Biology, 20*, 229-247.

Hamdan, L. J., Coffin, R. B., Sikaroodi, M., Greinert, J., Treude, T., & Gillevet, P. M. (2013). Ocean currents shape the microbiome of Arctic marine sediments. *The ISME journal, 7*(4), 685-696. doi:10.1038/ismej.2012.143

Harrison, B. K., Zhang, H., Berelson, W., & Orphan, V. J. (2009). Variations in archaeal and bacterial diversity associated with the sulfate-methane transition zone in continental margin sediments (Santa Barbara Basin, California). *Applied and Environmental Microbiology, 75*(6), 1487-1499.

Hatta, M., Measures, C., Selph, K., Zhou, M., & Hiscock, W. (2013). Iron fluxes from the shelf regions near the South Shetland Islands in the Drake Passage during the austral-winter 2006. *Deep Sea Research Part II: Topical Studies in Oceanography, 90*, 89-101.

Hauck, J., Völker, C., Wolf-Gladrow, D. A., Laufkötter, C., Vogt, M., Aumont, O., et al. (2015). On the Southern Ocean CO_2 uptake and the role of the biological carbon pump in the 21st century. *Global Biogeochemical Cycles, 29*(9), 1451-1470.

Heiden, J. P., Völkner, C., Jones, E. M., van de Poll, W. H., Buma, A. G., Meredith, M. P., et al. (2019). Impact of ocean acidification and high solar radiation on productivity and species composition of a late summer phytoplankton community of the coastal Western Antarctic Peninsula. *Limnology and Oceanography, 64*(4), 1716-1736.

Henkel, S., Kasten, S., Hartmann, J. F., Silva-Busso, A., & Staubwasser, M. (2018). Iron cycling and stable Fe isotope fractionation in Antarctic shelf sediments, King George Island. *Geochimica et Cosmochimica Acta, 237*, 320-338.

Herman, P., Middelburg, J., Van de Koppel, J., & Heip, C. (1999). Ecology of estuarine macrobenthos. *Advances in ecological research, 29*(780), 195-240.

Herndl, G. J., & Reinthaler, T. (2013). Microbial control of the dark end of the biological pump. *Nature Geoscience, 6*(9), 718-724.

Hoffmann, K., Hassenrück, C., Salman-Carvalho, V., Holtappels, M., & Bienhold, C. (2017). Response of Bacterial Communities to Different Detritus Compositions in Arctic Deep-Sea Sediments. *Frontiers in Microbiology, 8*, 266. doi:10.3389/fmicb.2017.00266

Hofmann, E., & Klinck, J. (1998). Hydrography and circulation of the Antarctic continental shelf: 150 E eastward to the Greenwich Meridian. *The Sea, The Global Coastal Ocean, Regional Studies and Synthesis, 11*, 997-1042.

Holmes, D. E., Nicoll, J. S., Bond, D. R., & Lovley, D. R. (2004). Potential role of a novel psychrotolerant member of the family Geobacteraceae, Geopsychrobacter electrodiphilus gen. nov., sp. nov., in electricity production by a marine sediment fuel cell. *Applied and Environmental Microbiology, 70*(10), 6023-6030.

Honjo, S., Eglinton, T. I., Taylor, C. D., Ulmer, K. M., Sievert, S. M., Bracher, A., et al. (2014). Understanding the role of the biological pump in the global carbon cycle: an imperative for ocean science. *Oceanography, 27*(3), 10-16.

Hoshino, T., Doi, H., Uramoto, G.-I., Wörmer, L., Adhikari, R. R., Xiao, N., et al. (2020). Global diversity of microbial communities in marine sediment. *Proceedings of the National Academy of Sciences, 117*(44), 27587-27597.

Isla, E. (2016). Environmental controls on sediment composition and particle fluxes over the Antarctic continental shelf. In A. Beylich, J. Dixon, & Z. Zwoliński (Eds.), Source-to-sink fluxes in undisturbed cold environments (pp. 199–212). Cambridge University Press, Cambridge. https://doi.org/10.1017/CBO9781107705791.017

Jacob, M., Soltwedel, T., Boetius, A., & Ramette, A. (2013). Biogeography of deep-sea benthic bacteria at regional scale (LTER HAUSGARTEN, Fram Strait, Arctic). *PLoS One, 8*(9), e72779.

Jacobs, S. S., Amos, A. F., & Bruchhausen, P. M. (1970). *Ross Sea oceanography and Antarctic bottom water formation.* Paper presented at the Deep Sea Research and Oceanographic Abstracts.

Jahnke, R. A. (2010). Global synthesis. *Carbon and Nutrient Fluxes in Continental Margins: A Global Synthesis*, 597-615.

Jahnke, R. A., & Jackson, G. A. (1992). The Spatial Distribution of Sea Floor Oxygen Consumption in The Atlantic and Pacific Oceans. In G. T. Rowe & V. Pariente (eds.), *Deep-Sea Food Chains and the Global Carbon Cycle* (pp. 295-307). Dordrecht: Springer Netherlands.

Jørgensen, B. B. (2000). Bacteria and marine biogeochemistry. *Marine geochemistry*, 173-207.

Jørgensen, B. B., & Boetius, A. (2007). Feast and famine — microbial life in the deep-sea bed. *Nature reviews microbiology, 5*(10), 770-781. doi:10.1038/nrmicro1745

Jørgensen, B. B., & Kasten, S. (2006). Sulfur cycling and methane oxidation. *Marine geochemistry*, 271-309.

Jørgensen, B. B., & Nelson, D. C. (2004). Sulfide oxidation in marine sediments: Geochemistry meets microbiology. In J. P. Amend, K. J. Edwards, & T. W. Lyons (Eds.), Sulfur Biogeochemistry: Past and Present (Vol. 379). Geological Society of America.

Jorgensen, S. L., Hannisdal, B., Lanzén, A., Baumberger, T., Flesland, K., Fonseca, R., et al. (2012). Correlating microbial community profiles with geochemical data in highly stratified sediments from the Arctic Mid-Ocean Ridge. *Proc Natl Acad Sci U S A, 109*(42), E2846-2855. doi:10.1073/pnas.1207574109

Kallmeyer, J., Pockalny, R., Adhikari, R. R., Smith, D. C., & D'Hondt, S. (2012). Global distribution of microbial abundance and biomass in subseafloor sediment. *Proceedings of the National Academy of Sciences, 109*(40), 16213-16216.

Kappelmann, L., Krüger, K., Hehemann, J.-H., Harder, J., Markert, S., Unfried, F., et al. (2019). Polysaccharide utilization loci of North Sea Flavobacteriia as basis for using SusC/D-protein expression for predicting major phytoplankton glycans. *The ISME journal, 13*(1), 76-91.

Karnovsky, N., Ainley, D., & Lee, P. (2007). The impact and importance of production in polynyas to top-trophic predators: three case histories. *Elsevier oceanography series, 74*, 391-410.

Kashefi, K., Holmes, D. E., Baross, J. A., & Lovley, D. R. (2003). Thermophily in the Geobacteraceae: Geothermobacter ehrlichii gen. nov., sp. nov., a novel thermophilic member of the Geobacteraceae from the "Bag City" hydrothermal vent. *Applied and Environmental Microbiology, 69*(5), 2985-2993.

King, J., & Harangozo, S. (1998). Climate change in the western Antarctic Peninsula since 1945: observations and possible causes. *Annals of Glaciology, 27*, 571-575.

Kirchman, D. L., Malmstrom, R. R., & Cottrell, M. T. (2005). Control of bacterial growth by temperature and organic matter in the Western Arctic. *Deep Sea Research Part II: Topical Studies in Oceanography, 52*(24-26), 3386-3395.

Klages, M., Boetius, A., Christensen, J. P., Deubel, H., Piepenburg, D., Schewe, I., et al. (2004). The Benthos of Arctic Seas and its Role for the Organic Carbon Cycle at the Seafloor. In R. Stein & R. W. MacDonald (Eds.), *The Organic Carbon Cycle in the Arctic Ocean (pp. 139-167)*. Berlin, Heidelberg: Springer Berlin Heidelberg.

Klar, J. K., Homoky, W. B., Statham, P. J., Birchill, A. J., Harris, E. L., Woodward, E. M. S., et al. (2017). Stability of dissolved and soluble Fe (II) in shelf sediment pore waters and release to an oxic water column. *Biogeochemistry, 135*, 49-67.

Knittel, K., & Boetius, A. (2009). Anaerobic oxidation of methane: progress with an unknown process. *Annual review of microbiology, 63*, 311-334.

Kostka, J. E., Thamdrup, B., Glud, R. N., & Canfield, D. E. (1999). Rates and pathways of carbon oxidation in permanently cold Arctic sediments. *Marine Ecology Progress Series, 180*, 7-21.

Kristensen, E. (2000). Organic matter diagenesis at the oxic/anoxic interface in coastal marine sediments, with emphasis on the role of burrowing animals. *Hydrobiologia, 426*, 1-24.

Kuypers, M. M. M., Sliekers, A. O., Lavik, G., Schmid, M., Jørgensen, B. B., Kuenen, J. G., et al. (2003). Anaerobic ammonium oxidation by anammox bacteria in the Black Sea. *Nature, 422*(6932), 608-611. doi:10.1038/nature01472

Lancelot, C., de Montety, A., Goosse, H., Becquevort, S., Schoemann, V., Pasquer, B., et al. (2009). Spatial distribution of the iron supply to phytoplankton in the Southern Ocean: a model study. *Biogeosciences, 6*(12), 2861-2878.

Laruelle, G. G., Cai, W.-J., Hu, X., Gruber, N., Mackenzie, F. T., & Regnier, P. (2018). Continental shelves as a variable but increasing global sink for atmospheric carbon dioxide. *Nature Communications, 9*(1), 454. doi:10.1038/s41467-017-02738-z

Learman, D. R., Henson, M. W., Thrash, J. C., Temperton, B., Brannock, P. M., Santos, S. R., et al. (2016). Biogeochemical and microbial variation across 5500 km of Antarctic surface sediment implicates organic matter as a driver of benthic community structure. *Frontiers in Microbiology, 7*, 284.

Lenk, S., Arnds, J., Zerjatke, K., Musat, N., Amann, R., & Mußmann, M. (2011). Novel groups of Gammaproteobacteria catalyse sulfur oxidation and carbon fixation in a coastal, intertidal sediment. *Environmental Microbiology, 13*(3), 758-774.

Leung, S., Cabré, A., & Marinov, I. (2015). A latitudinally banded phytoplankton response to 21st century climate change in the Southern Ocean across the CMIP5 model suite. *Biogeosciences, 12*(19), 5715-5734. doi:10.5194/bg-12-5715-2015

Liao, W., Tong, D., Li, Z., Nie, X., Liu, Y., Ran, F., et al. (2021). Characteristics of microbial community composition and its relationship with carbon, nitrogen and sulfur in

sediments. *Science of The Total Environment, 795*, 148848. doi:https://doi.org/10.1016/j.scitotenv.2021.148848

Lin, J., Zhou, X., Lu, X., Xu, Y., Wei, Z., & Ruan, A. (2023). Grain size distribution drives microbial communities vertically assemble in nascent lake sediments. *Environmental Research, 227*, 115828. doi:https://doi.org/10.1016/j.envres.2023.115828

Lipka, M. (2017). Current Biogeochemical Processes and Element Fluxes in Surface Sediments of Temperate Marginal Seas (Baltic Sea and Black Sea). Universität Greifswald.

Lipp, J. S., Morono, Y., Inagaki, F., & Hinrichs, K.-U. (2008). Significant contribution of Archaea to extant biomass in marine subsurface sediments. *Nature, 454*(7207), 991-994.

Lipsewers, Y. A. (2017). *Role of chemolithoautotrophic microorganisms involved in nitrogen and sulfur cycling in coastal marine sediments.* Utrecht University,

Lloyd, K. G., Albert, D. B., Biddle, J. F., Chanton, J. P., Pizarro, O., & Teske, A. (2010). Spatial structure and activity of sedimentary microbial communities underlying a Beggiatoa spp. mat in a Gulf of Mexico hydrocarbon seep. *PLoS One, 5*(1), e8738.

Lozier, M. S., Dave, A. C., Palter, J. B., Gerber, L. M., & Barber, R. T. (2011). On the relationship between stratification and primary productivity in the North Atlantic. *Geophysical Research Letters, 38*(18). doi:https://doi.org/10.1029/2011GL049414

Mark Jensen, M., Thamdrup, B., Rysgaard, S., Holmer, M., & Fossing, H. (2003). Rates and regulation of microbial iron reduction in sediments of the Baltic-North Sea transition. *Biogeochemistry, 65*, 295-317.

Martin, J. H., Gordon, R. M., & Fitzwater, S. E. (1990). Iron in Antarctic waters. *Nature, 345*(6271), 156-158. doi:10.1038/345156a0

Martin, J. H., Knauer, G. A., Karl, D. M., & Broenkow, W. W. (1987). VERTEX: carbon cycling in the northeast Pacific. *Deep Sea Research Part A. Oceanographic Research Papers, 34*(2), 267-285.

McNeil, B. I., Tilbrook, B., & Matear, R. J. (2001). Accumulation and uptake of anthropogenic CO_2 in the Southern Ocean, south of Australia between 1968 and 1996. *Journal of Geophysical Research: Oceans, 106*(C12), 31431-31445. doi:https://doi.org/10.1029/2000JC000331

Measures, C., Brown, M., Selph, K., Apprill, A., Zhou, M., Hatta, M., et al. (2013). The influence of shelf processes in delivering dissolved iron to the HNLC waters of the Drake Passage, Antarctica. *Deep Sea Research Part II: Topical Studies in Oceanography, 90*, 77-88.

Meehl, G. A., Arblaster, J. M., Chung, C. T., Holland, M. M., DuVivier, A., Thompson, L., et al. (2019). Sustained ocean changes contributed to sudden Antarctic sea ice retreat in late 2016. *Nature Communications, 10*(1), 14.

Melsheimer, C., Spreen, G., Ye, Y., & Shokr, M. (2023). First results of Antarctic sea ice type retrieval from active and passive microwave remote sensing data. *The Cryosphere, 17*(1), 105-126. doi:10.5194/tc-17-105-2023

Menard, H. W., & Smith, S. M. (1966). Hypsometry of ocean basin provinces. *Journal of Geophysical Research, 71*(18), 4305-4325.

Meredith, M., Sommerkorn, M., Cassotta, S., Derksen, C., Ekaykin, A., Hollowed, A., et al. (2019). Polar Regions. Chapter 3, IPCC Special Report on the Ocean and Cryosphere in a Changing Climate.

Michaud, A. B., Laufer, K., Findlay, A., Pellerin, A., Antler, G., Turchyn, A. V., et al. (2020). Glacial influence on the iron and sulfur cycles in Arctic fjord sediments (Svalbard). *Geochimica et Cosmochimica Acta, 280*, 423-440. doi:https://doi.org/10.1016/j.gca.2019.12.033

Michels, J., Dieckmann, G. S., Thomas, D. N., Schnack-Schiel, S. B., Krell, A., Assmy, P., et al. (2008). Short-term biogenic particle flux under late spring sea ice in the western Weddell Sea. *Deep Sea Research Part II: Topical Studies in Oceanography, 55*(8), 1024-1039. doi:https://doi.org/10.1016/j.dsr2.2007.12.019

Miksch, S., Meiners, M., Meyerdierks, A., Probandt, D., Wegener, G., Titschack, J., et al. (2021). Bacterial communities in temperate and polar coastal sands are seasonally stable. *ISME Communications, 1*(1), 29.

Mino, S., Nakagawa, S., Makita, H., Toki, T., Miyazaki, J., Sievert, S. M., et al. (2017). Endemicity of the cosmopolitan mesophilic chemolithoautotroph Sulfurimonas at deep-sea hydrothermal vents. *The ISME Journal, 11*(4), 909-919.

Mitchell, B. G., & Holm-Hansen, O. (1991). Observations of modeling of the Antartic phytoplankton crop in relation to mixing depth. *Deep Sea Research Part A. Oceanographic Research Papers, 38*(8-9), 981-1007. doi:https://doi.org/10.1016/0198-0149(91)90093-U

Monien, P. (2014). *The geochemical response of sedimentary archives to rapid recent glacier retreat at the western Antarctic Peninsula (WAP): from source to sink.* Universität Oldenburg.

Monien, P., Lettmann, K. A., Monien, D., Asendorf, S., Wölfl, A.-C., Lim, C. H., et al. (2014). Redox conditions and trace metal cycling in coastal sediments from the maritime Antarctic. *Geochimica et Cosmochimica Acta, 141*, 26-44.

Morono, Y., Ito, M., Hoshino, T., Terada, T., Hori, T., Ikehara, M., et al. (2020). Aerobic microbial life persists in oxic marine sediment as old as 101.5 million years. *Nature Communications, 11*(1), 3626. doi:10.1038/s41467-020-17330-1

Morris, E. M., & Vaughan, D. G. (2003). Spatial and temporal variation of surface temperature on the Antarctic Peninsula and the limit of viability of ice shelves. *Antarctic Research Series, 79*(10.1029).

Müller, A. L., De Rezende, J. R., Hubert, C. R., Kjeldsen, K. U., Lagkouvardos, I., Berry, D., et al. (2014). Endospores of thermophilic bacteria as tracers of microbial dispersal by ocean currents. *The ISME Journal, 8*(6), 1153-1165.

Müller, P. J., & Suess, E. (1979). Productivity, sedimentation rate, and sedimentary organic matter in the oceans—I. Organic carbon preservation. *Deep Sea Research Part A. Oceanographic Research Papers, 26*(12), 1347-1362.

Muyzer, G., & Stams, A. J. (2008). The ecology and biotechnology of sulphate-reducing bacteria. *Nature reviews microbiology, 6*(6), 441-454.

Nielsdóttir, M. C., Bibby, T. S., Moore, C. M., Hinz, D. J., Sanders, R., Whitehouse, M., et al. (2012). Seasonal and spatial dynamics of iron availability in the Scotia Sea. *Marine Chemistry, 130*, 62-72.

Nodwell, L. M., & Price, N. M. (2001). Direct use of inorganic colloidal iron by marine mixotrophic phytoplankton. *Limnology and Oceanography, 46*(4), 765-777.

Nowlin, W. D., & Klinck, J. M. (1986). The physics of the Antarctic Circumpolar Current. *Reviews of Geophysics, 24*(3), 469-491. doi:https://doi.org/10.1029/RG024i003p00469

Oni, O., Miyatake, T., Kasten, S., Richter-Heitmann, T., Fischer, D., Wagenknecht, L., et al. (2015). Distinct microbial populations are tightly linked to the profile of dissolved iron in the methanic sediments of the Helgoland mud area, North Sea. *Frontiers in Microbiology, 6,* 365. doi:10.3389/fmicb.2015.00365

Orcutt, B. N., Sylvan, J. B., Knab, N. J., & Edwards, K. J. (2011). Microbial ecology of the dark ocean above, at, and below the seafloor. *Microbiology and molecular biology reviews, 75*(2), 361-422.

Orsi, A. H., Johnson, G. C., & Bullister, J. L. (1999). Circulation, mixing, and production of Antarctic Bottom Water. *Progress in Oceanography, 43*(1), 55-109.

Paolo, F. S., Fricker, H. A., & Padman, L. (2015). Volume loss from Antarctic ice shelves is accelerating. *Science, 348*(6232), 327-331.

Parkes, R. J., Cragg, B. A., & Wellsbury, P. (2000). Recent studies on bacterial populations and processes in subseafloor sediments: a review. *Hydrogeology Journal, 8*, 11-28.

Parkinson, C. L. (2019). A 40-y record reveals gradual Antarctic sea ice increases followed by decreases at rates far exceeding the rates seen in the Arctic. *Proceedings of the National Academy of Sciences, 116*(29), 14414-14423.

Pauly, D., Christensen, V., Guénette, S., Pitcher, T. J., Sumaila, U. R., Walters, C. J., et al. (2002). Towards sustainability in world fisheries. *Nature, 418*(6898), 689-695. doi:10.1038/nature01017

Pearson, T., & Rosenberg, R. (1978). Macrobenthic succession in relation to organic enrichment and pollution of the marine environment. *Oceanography and marine biology: an annual review, 16*, 229-311.

Pearson, T. H., & Rosenberg, R. (1987). Feast and famine: Structuring factors in marine benthic communities. In J. H. R. Gee & P. S. Giller (Eds.), Organization of Communities, Past and Present (pp. 373-395). Blackwell Scientific Publications, Oxford.

Peck, L. S., Barnes, D. K., Cook, A. J., Fleming, A. H., & Clarke, A. (2010). Negative feedback in the cold: ice retreat produces new carbon sinks in Antarctica. *Global Change Biology, 16*(9), 2614-2623.

Pennington, J. T., Mahoney, K. L., Kuwahara, V. S., Kolber, D. D., Calienes, R., & Chavez, F. P. (2006). Primary production in the eastern tropical Pacific: A review. *Progress in Oceanography, 69*(2), 285-317. doi:https://doi.org/10.1016/j.pocean.2006.03.012

Perren, B. B., Hodgson, D. A., Roberts, S. J., Sime, L., Van Nieuwenhuyze, W., Verleyen, E., et al. (2020). Southward migration of the Southern Hemisphere westerly winds corresponds with warming climate over centennial timescales. *Communications Earth & Environment, 1*(1), 58.

Pineda-Metz, S. E. A. (2020). Benthos-pelagos interconnectivity: Antarctic shelf examples. In S. Jungblut, V. Liebich, & M. Bode-Dalby (Eds.), YOUMARES 9 – The Oceans: Our Research, Our Future. Proceedings of the 2018 Conference for YOUng MArine RESearchers in Oldenburg, Germany (pp. 211-223). Springer, Cham. https://doi.org/10.1007/978-3-030-20389-4_11

Pineda-Metz, S. E., Gerdes, D., & Richter, C. (2020). Benthic fauna declined on a whitening Antarctic continental shelf. *Nature Communications, 11*(1), 2226.

Rack, W., & Rott, H. (2004). Pattern of retreat and disintegration of the Larsen B ice shelf, Antarctic Peninsula. *Annals of Glaciology, 39*, 505-510.

Raiswell, R., & Canfield, D. E. (2012). The iron biogeochemical cycle past and present. *Geochemical perspectives, 1*(1), 1-2.

Raiswell, R., Hawkings, J. R., Benning, L. G., Baker, A. R., Death, R., Albani, S., et al. (2016). Potentially bioavailable iron delivery by iceberg-hosted sediments and atmospheric dust to the polar oceans. *Biogeosciences, 13*(13), 3887-3900.

Randelhoff, A., & Sundfjord, A. (2018). Short commentary on marine productivity at Arctic shelf breaks: upwelling, advection and vertical mixing. *Ocean Sci., 14*(2), 293-300. doi:10.5194/os-14-293-2018

Rignot, E., Casassa, G., Gogineni, P., Krabill, W., Rivera, A., & Thomas, R. (2004). Accelerated ice discharge from the Antarctic Peninsula following the collapse of Larsen B ice shelf. *Geophysical Research Letters, 31*(18).

Rintoul, S. R., & Bullister, J. L. (1999). A late winter hydrographic section from Tasmania to Antarctica. *Deep Sea Research Part I: Oceanographic Research Papers, 46*(8), 1417-1454.

Robinson, C., Steinberg, D. K., Anderson, T. R., Arístegui, J., Carlson, C. A., Frost, J. R., et al. (2010). Mesopelagic zone ecology and biogeochemistry–a synthesis. *Deep Sea Research Part II: Topical Studies in Oceanography, 57*(16), 1504-1518.

Roden, E. E., & Lovley, D. R. (1993). Dissimilatory Fe (III) reduction by the marine microorganism Desulfuromonas acetoxidans. *Applied and Environmental Microbiology, 59*(3), 734-742.

Rogers, A., Frinault, B., Barnes, D., Bindoff, N., Downie, R., Ducklow, H., et al. (2020). Antarctic futures: an assessment of climate-driven changes in ecosystem structure, function, and service provisioning in the Southern Ocean. *Annual Review of Marine Science, 12*, 87-120.

Rott, H., Rack, W., Skvarca, P., & De Angelis, H. (2002). Northern Larsen ice shelf, Antarctica: Further retreat after collapse. *Annals of Glaciology, 34*, 277-282.

Rott, H., Skvarca, P., & Nagler, T. (1996). Rapid collapse of northern Larsen ice shelf, Antarctica. *Science, 271*(5250), 788-792.

Rudels, B., Anderson, L. G., & Jones, E. P. (1996). Formation and evolution of the surface mixed layer and halocline of the Arctic Ocean. *Journal of Geophysical Research: Oceans, 101*(C4), 8807-8821. doi:https://doi.org/10.1029/96JC00143

Ruff, S. E., Biddle, J. F., Teske, A. P., Knittel, K., Boetius, A., & Ramette, A. (2015). Global dispersion and local diversification of the methane seep microbiome. *Proceedings of the National Academy of Sciences, 112*(13), 4015-4020.

Sabine, C. L., Feely, R. A., Gruber, N., Key, R. M., Lee, K., Bullister, J. L., et al. (2004). The oceanic sink for anthropogenic CO_2. *Science, 305*(5682), 367-371.

Sachithanandam, V., Saravanane, N., Chandrasekar, K., Karthick, P., Lalitha, P., Sai Elangovan, S., et al. (2020). Microbial diversity from the continental shelf regions of the Eastern Arabian Sea: A metagenomic approach. *Saudi J Biol Sci, 27*(8), 2065-2075. doi:10.1016/j.sjbs.2020.06.011

Sachs, O. (2008). Benthic organic carbon fluxes in the Southern Ocean: Regional differences and links to surface primary production and carbon export. Berichte zur Polar- und Meeresforschung (Reports on Polar and Marine Research), *578,* 158. Alfred Wegener Institute for Polar and Marine Research, Bremerhaven. https://doi.org/10.2312/BzPM_0578_2008

Sakshaug, E., Slagstad, D., & Holm-Hansen, O. (1991). Factors controlling the development of phytoplankton blooms in the Antarctic Ocean—a mathematical model. *Marine Chemistry, 35*(1-4), 259-271.

Savidge, G., Harbour, D., Gilpin, L. C., & Boyd, P. W. (1995). Phytoplankton distributions and production in the Bellingshausen sea, Austral spring 1992. *Deep Sea Research Part II: Topical Studies in Oceanography, 42*(4), 1201-1224. doi:https://doi.org/10.1016/0967-0645(95)00062-U

Scambos, T. A., Bell, R. E., Alley, R. B., Anandakrishnan, S., Bromwich, D. H., Brunt, K., et al. (2017). How much, how fast?: A science review and outlook for research on the instability of Antarctica's Thwaites Glacier in the 21st century. *Global and Planetary Change, 153*, 16-34. doi:https://doi.org/10.1016/j.gloplacha.2017.04.008

Scambos, T. A., Bohlander, J., Shuman, C. A., & Skvarca, P. (2004). Glacier acceleration and thinning after ice shelf collapse in the Larsen B embayment, Antarctica. *Geophysical Research Letters, 31*(18).

Schauer, R., Bienhold, C., Ramette, A., & Harder, J. (2010). Bacterial diversity and biogeography in deep-sea surface sediments of the South Atlantic Ocean. *The ISME journal, 4*(2), 159-170. doi:10.1038/ismej.2009.106

Schmid, M., Walsh, K., Webb, R., Rijpstra, W. I., van de Pas-Schoonen, K., Verbruggen, M. J., et al. (2003). Candidatus “Scalindua brodae”, sp. nov., Candidatus “Scalindua wagneri”, sp. nov., two new species of anaerobic ammonium oxidizing bacteria. *Systematic and applied microbiology, 26*(4), 529-538.

Sedwick, P. N., DiTullio, G. R., & Mackey, D. J. (2000). Iron and manganese in the Ross Sea, Antarctica: Seasonal iron limitation in Antarctic shelf waters. *Journal of Geophysical Research: Oceans, 105*(C5), 11321-11336.

Seiter, K., Hensen, C., & Zabel, M. (2005). Benthic carbon mineralization on a global scale. *Global Biogeochemical Cycles, 19*(1). doi:https://doi.org/10.1029/2004GB002225

Seitzinger, S. P. (1988). Denitrification in freshwater and coastal marine ecosystems: ecological and geochemical significance. *Limnology and Oceanography, 33*(2), 702-724.

Seitzinger, S. P., Harrison, J. A., Dumont, E., Beusen, A. H. W., & Bouwman, A. F. (2005). Sources and delivery of carbon, nitrogen, and phosphorus to the coastal zone: An overview of Global Nutrient Export from Watersheds (NEWS) models and their application. *Global Biogeochemical Cycles, 19*(4). doi:https://doi.org/10.1029/2005GB002606

Serreze, M. C., & Barry, R. G. (2011). Processes and impacts of Arctic amplification: A research synthesis. *Global and planetary change, 77*(1-2), 85-96.

Shaked, Y., Kustka, A. B., & Morel, F. M. (2005). A general kinetic model for iron acquisition by eukaryotic phytoplankton. *Limnology and Oceanography, 50*(3), 872-882.

Shao, M.-F., Zhang, T., & Fang, H. H.-P. (2010). Sulfur-driven autotrophic denitrification: diversity, biochemistry, and engineering applications. *Applied microbiology and biotechnology, 88*, 1027-1042.

Siegel, D., Doney, S., & Yoder, J. (2002). The North Atlantic spring phytoplankton bloom and Sverdrup's critical depth hypothesis. *Science, 296*(5568), 730-733.

Slomp, C. P., Van der Gaast, S. J., & Van Raaphorst, W. (1996). Phosphorus binding by poorly crystalline iron oxides in North Sea sediments. *Marine Chemistry, 52*(1), 55-73. doi:https://doi.org/10.1016/0304-4203(95)00078-X

Smetacek, V., & Nicol, S. (2005). Polar ocean ecosystems in a changing world. *Nature, 437*(7057), 362-368.

Smith, C. R., Mincks, S., & DeMaster, D. J. (2006). A synthesis of bentho-pelagic coupling on the Antarctic shelf: food banks, ecosystem inertia and global climate change. *Deep Sea Research Part II: Topical Studies in Oceanography, 53*(8-10), 875-894.

Smith, C. R., DeMaster, D. J., Thomas, C., Sršen, P., Grange, L., Evrard, V., et al. (2012). Pelagic-benthic coupling, food banks, and climate change on the West Antarctic Peninsula Shelf. Oceanography, 25(3), 188-201.

Smith, D. A., Hofmann, E. E., Klinck, J. M., & Lascara, C. M. (1999). Hydrography and circulation of the west Antarctic Peninsula continental shelf. *Deep Sea Research Part I: Oceanographic Research Papers, 46*(6), 925-949.

Smith, W. O., Ainley, D. G., & Cattaneo-Vietti, R. (2007). Trophic interactions within the Ross Sea continental shelf ecosystem. *Philosophical Transactions of the Royal Society B: Biological Sciences, 362*(1477), 95-111.

Smithson, P. A. (2002). IPCC, 2001: Climate Change 2001: The Scientific Basis. Contribution of Working Group 1 to the Third Assessment Report of the Intergovernmental Panel on Climate Change, edited by J. T. Houghton, Y. Ding, D. J. Griggs, M. Noguer, P. J. van der Linden, X. Dai, K. Maskell and C. A. Johnson (Eds). Cambridge University Press, Cambridge, UK, and New York, USA, 2001. International Journal of Climatology, 22(9), 1144-1144. https://doi.org/10.1002/joc.763

Spreen, G., Kaleschke, L., & Heygster, G. (2008). Sea ice remote sensing using AMSR-E 89-GHz channels. *Journal of Geophysical Research: Oceans, 113*(C2).

Stammerjohn, S., Massom, R., Rind, D., & Martinson, D. (2012). Regions of rapid sea ice change: An inter-hemispheric seasonal comparison. *Geophysical Research Letters, 39*(6).

Stumm, W., & Morgan, J. J. (2012). *Aquatic Chemistrtry*, Chemical Equilibria and Rates in Natural Waters. John Wiley & Sons, Inc., New York.

Takahashi, T., Sutherland, S. C., Sweeney, C., Poisson, A., Metzl, N., Tilbrook, B., et al. (2002). Global sea–air CO_2 flux based on climatological surface ocean pCO_2, and seasonal biological and temperature effects. *Deep Sea Research Part II: Topical Studies in Oceanography, 49*(9-10), 1601-1622.

Teske, A., Durbin, A., Ziervogel, K., Cox, C., & Arnosti, C. (2011). Microbial Community Composition and Function in Permanently Cold Seawater and Sediments from an Arctic Fjord of Svalbard. *Applied and Environmental Microbiology, 77*(6), 2008-2018. doi:doi:10.1128/AEM.01507-10

Teske, A., & Sørensen, K. B. (2008). Uncultured archaea in deep marine subsurface sediments: have we caught them all? *The ISME journal, 2*(1), 3-18.

Thamdrup, B. (2000). Bacterial manganese and iron reduction in aquatic sediments. *Advances in microbial ecology*, 41-84.

Thamdrup, B., & Canfield, D. E. (1996). Pathways of carbon oxidation in continental margin sediments off central Chile. *Limnology and Oceanography, 41*(8), 1629-1650.

Thompson, D. W., Solomon, S., Kushner, P. J., England, M. H., Grise, K. M., & Karoly, D. J. (2011). Signatures of the Antarctic ozone hole in Southern Hemisphere surface climate change. *Nature Geoscience, 4*(11), 741-749.

Turner, J., Colwell, S. R., Marshall, G. J., Lachlan-Cope, T. A., Carleton, A. M., Jones, P. D., et al. (2005). Antarctic climate change during the last 50 years. *International journal of Climatology, 25*(3), 279-294.

Vandieken, V., Mußmann, M., Niemann, H., & Jørgensen, B. B. (2006). Desulfuromonas svalbardensis sp. nov. and Desulfuromusa ferrireducens sp. nov., psychrophilic, Fe (III)-reducing bacteria isolated from Arctic sediments, Svalbard. *International Journal of Systematic and Evolutionary Microbiology, 56*(5), 1133-1139.

Vandieken, V., & Thamdrup, B. (2013). Identification of acetate-oxidizing bacteria in a coastal marine surface sediment by RNA-stable isotope probing in anoxic slurries and intact cores. *FEMS Microbiology Ecology, 84*(2), 373-386.

Varliero, G., Bienhold, C., Schmid, F., Boetius, A., & Molari, M. (2019). Microbial diversity and connectivity in deep-sea sediments of the South Atlantic Polar Front. *Frontiers in Microbiology, 10*, 665.

Vašutová, M., Mleczko, P., López-García, A., Maček, I., Boros, G., Ševčík, J., et al. (2019). Taxi drivers: the role of animals in transporting mycorrhizal fungi. *Mycorrhiza, 29*(5), 413-434. doi:10.1007/s00572-019-00906-1

Vaughan, D. G., Marshall, G. J., Connolley, W. M., Parkinson, C., Mulvaney, R., Hodgson, D. A., et al. (2003). Recent rapid regional climate warming on the Antarctic Peninsula. *Climatic change, 60*, 243-274.

Venables, H. J., & Meredith, M. P. (2009). Theory and observations of Ekman flux in the chlorophyll distribution downstream of South Georgia. *Geophysical Research Letters, 36*(23).

Vernet, M., Martinson, D., Iannuzzi, R., Stammerjohn, S., Kozlowski, W., Sines, K., et al. (2008). Primary production within the sea ice zone west of the Antarctic Peninsula: I—Sea ice, summer mixed layer, and irradiance. *Deep Sea Research Part II: Topical Studies in Oceanography, 55*(18), 2068-2085. doi:https://doi.org/10.1016/j.dsr2.2008.05.021

Volk, T., & Hoffert, M. I. (1985). Ocean carbon pumps: Analysis of relative strengths and efficiencies in ocean-driven atmospheric CO_2 changes. In E. T. Sundquist & W. S. Broecker (Eds.), The Carbon Cycle and Atmospheric CO_2: Natural Variations Archean to Present. Chapman Conference Papers, 1984 (pp. 99-110). American Geophysical Union; Geophysical Monograph 32.

Wadham, J. L., De'Ath, R., Monteiro, F., Tranter, M., Ridgwell, A., Raiswell, R., et al. (2013). The potential role of the Antarctic Ice Sheet in global biogeochemical cycles. *Earth and Environmental Science Transactions of the Royal Society of Edinburgh, 104*(1), 55-67.

Walsh, J. J. (1991). Importance of continental margins in the marine biogeochemical cycling of carbon and nitrogen. *Nature, 350*(6313), 53-55.

Wassmann, P., Slagstad, D., Riser, C. W., & Reigstad, M. (2006). Modelling the ecosystem dynamics of the Barents Sea including the marginal ice zone: II. Carbon flux and interannual variability. *Journal of Marine Systems, 59*(1-2), 1-24.

Weiss, M., Abele, U., Weckesser, J., Welte, W., Schiltz, E., & Schulz, G. (1991). Molecular architecture and electrostatic properties of a bacterial porin. *Science, 254*(5038), 1627-1630.

Whitman, W. B., Coleman, D. C., & Wiebe, W. J. (1998). Prokaryotes: the unseen majority. *Proceedings of the National Academy of Sciences, 95*(12), 6578-6583.

Witte, U., Aberle, N., Sand, M., & Wenzhöfer, F. (2003). Rapid response of a deep-sea benthic community to POM enrichment: an in situ experimental study. *Marine Ecology Progress Series, 251*, 27-36.

Wollast, R. (1998). Evaluation and comparison of the global carbon cycle in the coastal zone and in the open ocean. In K. H. Brink & A. R. Robinson (Eds.), The Sea — Vol 10: The Global Coastal Ocean: Processes and Methods (pp. 213–252). John Wiley & Sons, Chichester.

Wollast, R. (2003). Continental margins—review of geochemical settings. *Ocean margin systems*, 15-31.

Wunder, L. C., Aromokeye, D. A., Yin, X., Richter-Heitmann, T., Willis-Poratti, G., Schnakenberg, A., et al. (2021). Iron and sulfate reduction structure microbial communities in (sub-) Antarctic sediments. *The ISME journal, 15*(12), 3587-3604. doi:10.1038/s41396-021-01014-9

2

Manuscript 1

Benthic carbon remineralization and iron cycling in relation to sea ice cover along the eastern continental shelf of the Antarctic Peninsula

Marwa Baloza[1,2], Susann Henkel[1], Walter Geibert[1], Sabine Kasten[1,3], Moritz Holtappels[1,4]

[1]Alfred Wegener Institute Helmholtz Centre for Polar and Marine Research, Bremerhaven, Germany
[2]Faculty 2 Biology /Chemistry, University Bremen, Bremen, Germany
[3]Faculty of Geosciences, University Bremen, Bremen, Germany
[4]MARUM - Center for Marine Environmental Sciences, University of Bremen, Bremen, Germany

Manuscript published 2022 in Journal of Geophysical Research: Oceans, *127*(7).
doi.org/10.1029/2021JC018401

Abstract

Rapid and profound climatic and environmental changes have been predicted for the Antarctic Peninsula with so far unknown impact on the biogeochemistry of the continental shelves. In this study, we investigate benthic carbon sedimentation, remineralization and iron cycling using sediment cores retrieved on a 400 mile transect with contrasting sea ice conditions along the eastern shelf of the Antarctic Peninsula. Sediments at comparable water depths of 330-450 m showed sedimentation and remineralization rates of organic carbon, ranging from 2.5-13 and 1.8-7.2 mmol C m^{-2} d^{-1}, respectively. Both rates were positively correlated with the occurrence of marginal sea ice conditions (5-35% ice cover) along the transect, suggesting a favorable influence of the corresponding light regime and water column stratification on algae growth and sedimentation rates. From south to north, the burial efficiency of organic carbon decreased from 58% to 27%, while bottom water temperatures increased from -1.9 to -0.1 °C. Net iron reduction rates, as estimated from pore-water profiles of dissolved iron, were significantly correlated with carbon degradation rates and contributed 0.7-1.2% to the total organic carbon remineralization. Tightly coupled phosphate-iron recycling was indicated by significant covariation of dissolved iron and phosphate concentrations, which almost consistently exhibited P/Fe flux ratios of 0.26. Iron efflux into bottom waters of 0.6-4.5 µmol Fe m^{-2} d^{-1} was estimated from an empirical model. Despite the deep shelf waters, a clear bentho-pelagic coupling is indicated, shaped by the extent and duration of marginal sea ice conditions during summer, and likely to be affected by future climate change.

Key points:

- Antarctic shelf sediments underlying marginal sea ice cover exhibit high sedimentation and remineralization rates of organic carbon.
- A high degree of sedimentary Fe-recycling is found which scales with organic carbon remineralization rates.
- Coupling between P and Fe recycling is observed with a constant P/Fe flux ratio of 0.26 for sediments with high Fe and P recycling rates.

1 Introduction

The biogeochemical properties of shelf sediments, such as organic matter (OM) content and degradation rates, serve as a reference point for the time-integrated organic carbon export from surface waters to the seafloor (Seiter et al., 2005; Smith et al., 2006). In the Antarctic, the amount of organic matter originating from surface primary production is highly variable – both temporally and spatially - due to seasonal sea ice cover and buoyancy production (i.e. stratification) and their effect on light regime and mixed layer depth (Savidge et al., 1995). The partial or complete retreat of sea ice cover in the spring–summer season allows light to become available for photosynthesis. When part of the ice melts, a stratified water column with nutrient-rich surface waters develops due to the input of sea ice meltwater and suppressed wind mixing (Vernet et al., 2008). This strong stratification forms a shallow summer mixed layer depth (5–25 m) (Garibotti et al., 2005; Vernet et al., 2008), which supports the growth of intensive phytoplankton blooms that usually follow the receding ice edge with a maximum production at the marginal ice zone (Savidge et al., 1995). A low production is observed in open waters of the Southern Ocean (SO), where a deepening of the summer mixed layer by wind forcing disperses macro- and micronutrients, such as Fe, and a deep mixing depth limits light availability (Vernet et al., 2008). On the other hand, the occurrence of sea ice cover reduces the light availability and thereby suppresses primary production. Thus, in Antarctic areas variations in sea ice cover and water column stability affect phytoplankton growth conditions and, ultimately, the carbon flux to the sea floor.

The deposition of pelagic production causes continental shelf sediments to be major sites of OM remineralization and nutrient regeneration in the ocean (Jahnke & Jackson, 1992). After OM reaches the seafloor, some of it is degraded and remineralized by microbes to form dissolved inorganic carbon, ammonium, silicate and phosphate, while the reduction of metal oxides releases adsorbed phosphate and micronutrients such as dissolved Fe, which are then potentially transported back to the water column (Billen, 1982; Wehrmann et al., 2014) and may fuel extensive phytoplankton blooms (Venables & Meredith, 2009; Nielsdóttir et al., 2012; Hatta et al., 2013; Measures et al., 2013; Borrione et al., 2014). Thus, shelf sediments play an important role in the bentho-pelagic coupling by providing essential nutrients for algae growth and maintaining the high primary production of shelf areas and the adjacent open ocean.

In the SO, which is known to be a high nutrient-low chlorophyll (HNLC) region, primary production is limited by low abundance of bioavailable iron (Martin et al., 1990; Boyd et al., 2007). The recycling of trace metals in Antarctic shelf sediments and their subsequent release into the water column could possibly represent an important source of bioavailable iron to the SO. According to Monien et al. (2014), Antarctic shelf sediments contribute up to 790 Gg a^{-1} of bioavailable Fe, comparable to the contribution of iceberg–hosted material, which is assumed to contribute 180-1400 Gg a^{-1} of bioavailable Fe (Raiswell et al., 2016), whereas aeolian transport accounts for an input of less than 1.12 Gg a^{-1} (Lancelot et al., 2009; Raiswell et al., 2016). In addition, a substantial release of dissolved Fe by anoxic subglacial meltwaters is estimated to range between 8.9 and 11,000 Gg a^{-1}, but only 0.03–5.9 Gg a^{-1} of this bioavailable iron can reach oxic shelf waters when taking into account the rapid oxidation of dissolved Fe to Fe(III) (Wadham et al., 2013). The availability of shelf-derived micronutrients, in turn, is likely to be facilitated by the seasonal occurrence of a well-mixed water column promoting the upwelling of iron-enriched bottom waters, as shown for the Ross Sea (Collier et al., 2000; Sedwick et al., 2000). Further, significant lateral fluxes of Fe from the shelf of the Antarctic Peninsula and of sub-Antarctic islands to the Fe-poor Antarctic Circumpolar Current (ACC) have been reported by (Venables & Meredith, 2009; Nielsdóttir et al., 2012; de Jong et al., 2012; Hatta et al., 2013; Measures et al., 2013; Borrione et al., 2014). They argue that large quantities of this shelf-derived Fe were rapidly transported by the ACC and likely responsible for the extensive phytoplankton blooms in areas downstream of the Drake Passage. Thus, phytoplankton production in the circum-Antarctic and Southern Ocean may be substantially influenced by micronutrient regeneration (especially of iron) in shelf sediments of Antarctica and sub-Antarctic islands.

The Antarctic Peninsula is projected to undergo profound climatic and environmental changes (Vaughan et al., 2003) affecting seasonal sea ice cover, water column stratification, terrestrial melt water run-off and related nutrient input, and thus the conditions for primary production, organic carbon export and benthic remineralization. Our study serves two purposes, first to investigate and compare the present-day sediment biogeochemistry of the eastern continental shelf of the Antarctic Peninsula, especially OM remineralization and iron cycling, along a gradient of above-mentioned boundary conditions (sea ice cover, stratification), and second to provide a

baseline of comprehensive geochemical data along a sea ice gradient from southern to northern stations that can be compared to future studies by revisiting the same sites.

Here, we report for the first time oxygen profiles and respective fluxes in combination with pore-water profiles of redox sensitive trace metals (Mn, Fe), nutrients (NO_3^-, PO_4^{3-}), sulfate and metabolic products (NH_4^+, H_2S, DIC) from 7 different locations along the eastern coast of the AP. These results are paired with solid-phase contents of total organic carbon (TOC), Mn, Fe, P and radioisotope ^{210}Pb data to provide a detailed picture of carbon fluxes, mineralization and burial as well as trace metal cycling under various environmental conditions. This includes the estimation of the total carbon re-mineralization rate as well as the contribution of the various electron acceptors to the overall OM degradation. The established fluxes are discussed in light of the boundary conditions for primary production, such as sea ice cover and stratification. Moreover, we discuss geochemical conditions and biogeochemical processes affecting the iron efflux from Antarctic shelf sediments as a potential source of bioavailable iron for the Southern Ocean.

2 Materials and Methods

2.1 Sample collection

During the research cruise PS118 with the German research vessel RV POLARSTERN (Feb 2019-April 2019, Dorschel 2019) sediments were collected from 7 stations along a 400 mile transect from the eastern shelf of the Antarctic Peninsula to the West of the South Orkney Islands (Figure 1, Table 1). At five stations, sediment samples were collected on the shelf at similar depths, ranging between 350 – 450 m, to allow cross-comparison of sediment properties independent from water depth. Another two stations were situated in the Powell Basin at 3300 m and 2900 m, serving as deep sea reference. Prior to the sediment sampling, the water column was sampled by means of a conductivity-temperature-depth-probe (CTD, Seabird 911plus), equipped with an additional O_2 sensor (Sea-Bird SBE43) and a Rosette water sampler with 24 Niskin bottles of 12 liter capacity.

At each station, a total of 9 sediment cores with intact surface sediments and overlying water were collected from multiple deployments of a multicorer (Oktopus GmbH, Kiel, Germany).

Immediately upon retrieval, sediment cores were transferred to the ship's cool laboratory and placed in a water bath at 0°C. Three cores were used for oxygen micro-profiles and whole core oxygen consumption measurements and three cores each were used for pore-water and solid phase analyses, respectively. Finally, 3-5 cores per station (usually cores used for pore-water sampling and oxygen measurements) were size-fractioned through 1,000 µm, 500 µm and 300 µm sieves and the macrofauna (plus larger grains/stones) fixed in borax-buffered formaline (4% final concentration). For this study, the macrofauna was only visually inspected while a thorough determination of species abundance and diversity was not performed.

The pore-water was sampled with rhizon samplers (pore size 0.1 µm; Rhizosphere Research Products, Netherlands) within 1-2 hours after core retrieval (Seeberg-Elverfeldt et al., 2005). Samples were taken at depth resolutions of 1 cm from 0-10 cm and below 10 cm with a resolution of 2 cm down to a maximum depth of 30 cm. Subsamples for trace element analyses of dissolved iron (DFe) and manganese (DMn), for dissolved inorganic carbon (DIC), hydrogen sulfide (H_2S) and for nutrients such as ammonium (NH_4^+), phosphate (PO_4^{3-}), nitrate (NO_3^-), nitrite (NO_2^-) and silicate (SiO_3^{2-}) were taken. For trace elements, the first 1 ml of extracted pore-water was discarded to ensure that the samples had not been in contact with air. Then, 1 ml of pore-water was taken and filled into 2 mL polypropylene (PP) tubes prefilled with 25 µl of 2% v/v of HCl and stored at 4°C. For DIC, 2.2 ml of pore-water was preserved with 10 µL of 10 % $HgCl_2$ in brown glass vials without headspace and stored at 4°C. For nutrient, sulfate (SO_4^{2-}) and chloride analyses, 4 ml of pore-water were filled into 15 ml plastic tubes and stored at -20 °C. For H_2S analyses, 1.5 mL of pore-water was directly transferred into a 2 mL PP tube (Eppendorf, Germany) already filled with 0.6 ml of a 50 mM Zn acetate solution and stored at 4°C. Sediments of parallel cores were sampled for solid phase analyses at the same depth resolution and stored at -20 °C. At 6 stations, additional seawater samples 5 m above the seafloor were obtained by using the CTD-rosette system.

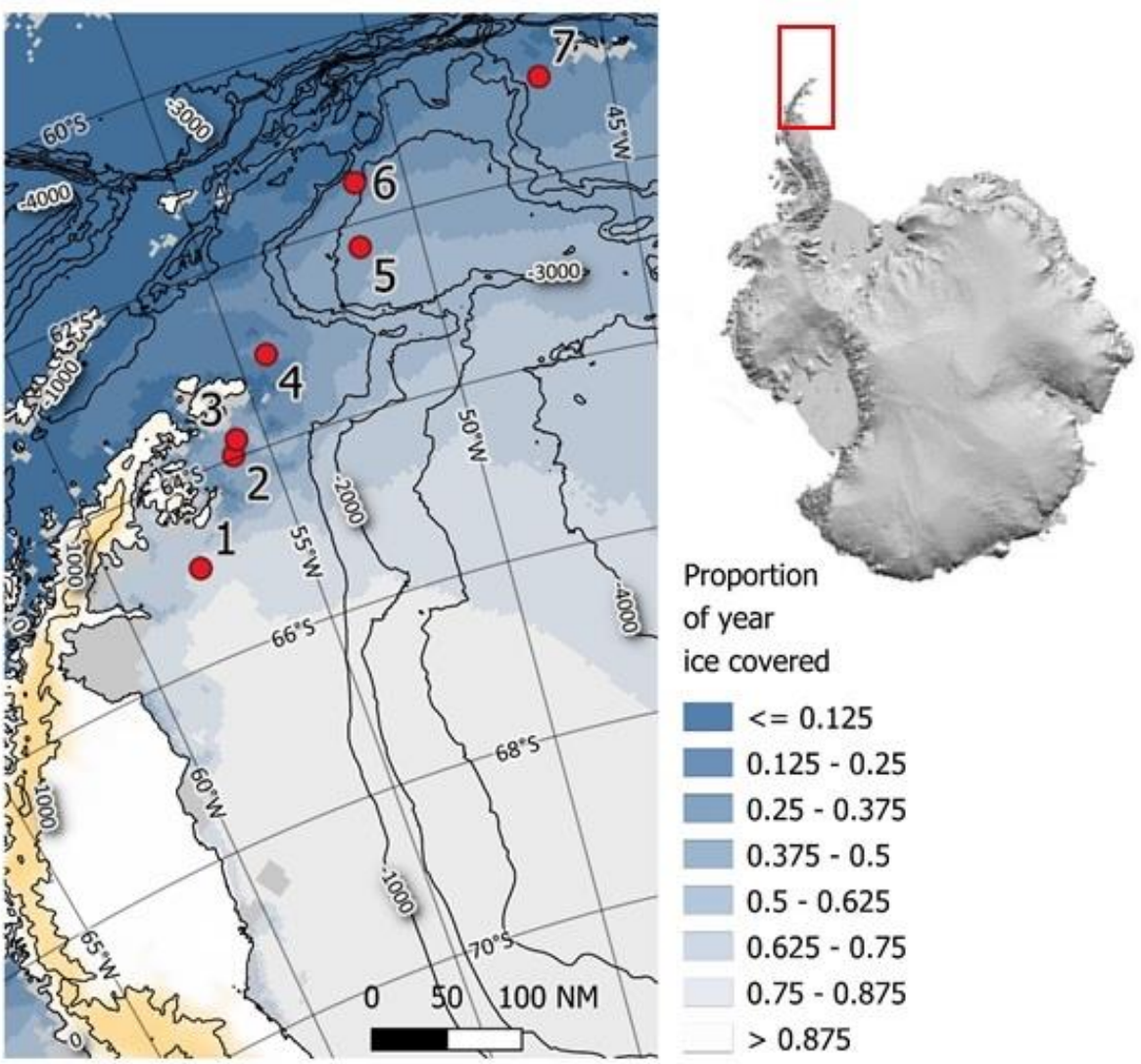

Figure 1. Map showing the Antarctic Peninsula with the locations of the sampled stations (red circles with station numbers) during PS118 expedition. Colors denote the proportion of time the ocean is covered by sea ice of concentration 85% or higher as calculated from AMSR-E satellite estimates of daily sea ice cover at 6.25 km resolution (Spreen et al. 2008). Water depth is indicated by isolines

Table 1. Characteristics of sea surface, bottom water (BW) and sediment at the sampled stations. Ice cover (30 year average of daily sea ice cover), marginal sea ice index (occurrence of 5-35% cover), upper water column stratification as density difference (Δρ) between 5 m and 50 m depth. Total organic carbon (TOC) from the upper 5 cm depth. Oxygen penetration depth (OPD), diffusive oxygen uptake (DOU), and total oxygen uptake (TOU) data are presented as average ± SD with the number of measurements in parentheses. n.a.: not analyzed. At station 5, O_2 penetration was below the max. possible O_2 profiling depth of 15 cm, so that the OPD was estimated by fitting to a model from Sachs et al. 2009.

	Lon °E	Lat °N	Date	Water depth	Ice cover	Marg. sea ice index	WC-strat. Δρ (50-5m)	BW salinity	BW temperature	BW O_2 conc.	BW NO^{3-} Conc.	TOC	OPD	DOU	TOU
			DD/MM/YYYY	m	%		Kg m^{-3}	‰	˚C	$\mu molL^{-1}$	$\mu molL^{-1}$	wt%	cm	mmol m^{-2} d^{-1}	mmol m^{-2} d^{-1}
Station 1	-57.75	-64.98	04/03/2019	428	81	0.038	1.00	34.57	-1.9	308.60	32.921	0.71	6.31 ± 0.71 (7)	1.40 ± 0.27 (7)	2.15 (1)
Station 2	-55.90	-63.97	11/03/2019	415	49	0.127	0.27	34.54	-1.5	304.13	32.483	1.02	0.65 ± 0.08 (7)	3.54 ± 0.70 (8)	4.14 ± 1.16 (2)
Station 3	-55.74	-63.80	14/03/2019	455	47	0.084	0.19	34.54	-1.2	296.09	31.685	0.19	0.85 ± 0.18 (7)	1.75 ± 0.34 (9)	4.01 ±1.10 (2)
Station 4	-54.33	-63.05	17/03/2019	447	33	0.174	0.16	34.56	-0.9	276.89	35.581	1.26	0.52 ± 0.07 (16)	6.87 ± 0.83 (16)	7.19 ± 0.44 (2)
Station 5	-51.42	-62.25	20/03/2019	3295	46	0.122	0.28	34.63	-0.7	263.49	33.846	0.37	64.25 ± 0.58 (7)	0.18 ± 0.04 (7)	0.84 ± 0.25 (2)
Station 6	-51.13	-61.57	26/03/2019	2908	34	0.121	0.10	34.64	-0.5	253.85	n. a.	0.30	8.65 ± 0.26 (12)	0.24 ± 0.09 (10)	0.87 (1)
Station 7	-46.55	-60.93	28/032019	329	28	0.092	0.03	34.56	-0.1	250.09	34.651	0.60	1.87 ± 0021 (15)	1.98 ± 0.84 (16)	1.77 ± 0.14 (2)

2.2 Oxygen uptake measurements

High-resolution O_2 profiles were measured in the upper sediment layer using optical microsensors (Optodes, Pyroscience) in order to determine oxygen penetration depths and diffusive oxygen uptake (Table 1). For deep oxygen penetration depths (>5 cm), we used 430 µm bare fiber optodes glued into 20 cm long needles, while 50 µm thin retractable needle optodes were used for shallow oxygen penetration depths to increase the spatial resolution. Oxygen sensors were calibrated with 100% air saturation (air-bubbled sea water) and 0% air saturation (by adding sodium dithionite) at -1.0 ± 0.3 °C and mounted on a motor-driven micromanipulator (MU1, Pyroscience). Temperature of the sediment core was recorded by a thermistor (Pyroscience) submersed into the overlying water. A minimum of 3 profiles per core at randomly chosen positions were carried out in 100 – 500 µm vertical resolution from 4 mm above the sediment water interface down to 10 – 160 mm into the sediment. Profile data (depth, oxygen concentration, temperature) were recorded using a 4-channel FireSting oxygen meter (FSO2-4, Pyroscience) and processed using the "Profix" software from Pyroscience.

Volumetric oxygen consumption rates and diffusive oxygen uptake (DOU) was determined by inversely fitting the transport-reaction model PROFILE (Berg et al., 1998) to the measured oxygen concentration profiles. Oxygen diffusion coefficient in sediments was calculated according to Berg et al. (1998) as $D_s = \varphi^2 D$ where *D* is the diffusion coefficient of O_2 in seawater at 35 PSU and 0°C, and φ is the porosity of the sediment in the specific depth layer.

Two intact cores with undisturbed overlying water were used for whole core incubations to determine the total oxygen uptake (TOU). A plastic stopper was introduced into the core liner and pushed down to leave approximately 8 - 12 cm of water height above the sediment surface. The stopper was perforated with a hole to allow introducing a mini-optode (Pyroscience) from above. The overlying water in the cores was stirred by small magnetic bars mounted in the core liners and driven by a rotating magnet outside the cores. The cores were incubated in the water bath at controlled temperatures for at least 12 hours. Oxygen concentration was measured every 5 seconds using the 4-channel FireSting oxygen meter (FSO2-4, Pyroscience) and the software

Pyro Oxygen Logger. Sediment total oxygen uptake rates were computed using linear regression of the O_2 concentration over time.

2.3 Pore-water analyses

All pore-water analyses were performed at the Alfred Wegener Institute, Helmholtz Centre for Polar and Marine Research (AWI) in Bremerhaven. NH_4^+, NO_3^-, NO_2^-, PO_4^{3-}, and DIC were measured on a QuAAtro four-channel flow injection analyzer (Seal Analytical). DFe, DMn were determined after a 10-fold dilution using Inductively Coupled Plasma Optical Emission Spectrometry (ICP-OES, Thermo iCAP7000) and yttrium internal standard solution used for calibration. The quantification limits of DFe and DMn were 0.143 $\pm$ 0.143 µM and 0.036 µM, respectively. Recoveries for DFe and DMn added in known concentrations to IAPSO Standard Seawater were 97.8 ± 7.1% and 100.7 ± 7.6%, respectively. H_2S was analysed using methylene blue method as described by Cline (1969). Sulfate (SO_4^{2-}) and chloride samples (1:100 dilutions with ultrapure water) were analyzed by ion chromatography (Metrohm IC Net 2.3).

2.4 Solid phase analyses

About 50 mg of freeze-dried and ground sediment was used for total nitrogen (TN), total carbon (TC) and TOC analyses in an Elemental analyzer (Vario EL III, Germany) equipped with a heat conductivity detector. For TOC contents, freeze-dried and homogenized sediment samples were decalcified using 0.5 mL of 37 % HCl at 250 °C for 2 h and then measured by an Eltra CS-800 element analyzer. A soil calibration sample for CHNS (part no. 502-062, Leco, USA) and other internal standards were used for calibration. For the shelf stations (i.e. stations 1-4 and 7), a full acid digestion of freeze-dried and homogenized sediments was performed. Samples were treated with a mixture of 3 ml HCl, 2 ml HNO_3 and 0.5 ml HF and were heated and dissolved in a CEM Mars Xpress microwave system (e.g., Volz et al., 2020). Elemental contents were determined by ICP-OES, Thermo iCAP7000 analyses using an yttrium internal standard for correction of different ionic strengths. Recoveries for a total of nine processed sediment standards (MESS4) were 93.1 ± 3% for Al, 97.7 ± 3% for Fe (Fe total), 97 ± 3% for Mn, and 82 ± 11% for S. Sediment porosity was determined from water content, measured as weight loss after freeze drying and assuming a solid density of 2.6 g cm^{-3} as described by Burdige (2006).

2.5 Sedimentation rate from ^{210}Pb

In order to determine and compare the sedimentation rates at all shelf stations (1-4 and 7), excess ^{210}Pb ($^{210}Pb_{ex}$) was measured in freeze-dried and homogenized sediments. The sample amounts used here ranged from 1-20 g, with most samples in the range of 4-10 g. The analyses was conducted on a planar HPGe gamma detector (Canberra/mirion). Sediment samples were weighed and sealed with hot glue in gas-tight petri dishes to prevent loss of ^{222}Rn ingrowing from ^{226}Ra. Samples were stored for >3 weeks to allow the relevant daughters of ^{226}Ra to grow into secular equilibrium before measurement. ^{226}Ra (for supported ^{210}Pb) was monitored via its daughters ^{214}Bi and ^{214}Pb at lines 295 keV, 351 keV, and 609 keV. ^{210}Pb was measured at 46 keV, 241Am at 59 keV, and 137Cs at 661 keV. We do not report ^{241}Am and ^{137}Cs data because the peaks were only detected in a few instances, and were not sufficiently above background for a quantification. In profiles station 1 to 4, supported ^{210}Pb was set as the mean measured ^{226}Ra value because the scatter of the individual values due to analytical uncertainty was larger than the uncertainty in mean ^{226}Ra, which would have affected $^{210}Pb_{ex}$ in the older samples. For station 7, scatter in ^{226}Ra was small enough to subtract each individual ^{226}Ra value as supported ^{210}Pb. Samples were typically counted until approximately 1000 net counts of ^{210}Pb were reached, or for maximum of three days if this number was not reached within this time period. Variable sample masses may affect detector efficiencies via self-absorption, especially at the low energy range of ^{210}Pb. This was addressed by determining mass-dependent efficiencies using IAEA-385 Irish Sea reference material for ^{210}Pb. No correction of the specific activities for salt was performed, as the cumulated dry mass is also determined including the salt component. Therefore, the inventory of ^{210}Pb, which is used for our preferred age model, is unaffected by salt in the samples.

The measurements were evaluated using the ScientissiMe software, determining the age of samples according to the constant flux constant sedimentation model (CFCS) (Goldberg, 1963), the constant initial concentration model (CIC), and the constant rate of supply model (CRS) (Appleby & Oldfield, 1978; Appleby, 2002). The CRS model is insensitive to dilution, but sensitive to variations in sediment redistribution and to residual inventories below the sampling depth. Quite contrary, CIC is sensitive to dilution, but not to variable sediment redistribution or residual

inventories. CFCS is not allowing for variations in lead flux or sedimentation rate. None of the approaches used here would correctly consider mixing due to bioturbation, with CFCS being probably the least affected. In general, we use in this study the CRS-age, taking the information from the other models into account for our interpretation.

2.6 Calculation of sulfate depletion

Sulfate depletion ($SO_4^{2-}{}_{dep}$) in pore-water reflects the net amount of sulfate consumption via microbial SO_4^{2-} reduction in the sediments and was calculated according to Weston et al (2006):

$$SO_4^{2-}{}_{Dep} = \left(\frac{Cl^-{}_{PW}}{R_{SW}}\right) - SO_4^{2-}{}_{PW} \quad (1)$$

where $Cl^-{}_{PW}$ and $SO_4^{2-}{}_{PW}$ are the measured concentrations of chloride and sulfate in the pore-water in mmol/L and R_{SW} is the molar ratio of Cl^- and SO_4^{2-} of seawater (R_{SW} = 19.33). Since the ratio of $Cl^-{}_{PW}$ to R_{SW} reflects the expected SO_4^{2-} concentration in the pore-water at a given salinity, the difference between this concentration and $SO_4^{2-}{}_{PW}$ provides an estimate for the amount of sulfate reduction.

2.7 Calculation of pore-water diffusive flux and carbon remineralization rates

Besides oxygen uptake, fluxes of DFe, DMn, and NH_4^+ were estimated from the respective pore-water concentration gradients using Fick's first law of diffusion:

$$J = -\varphi D_s \frac{dC\,(z)}{dz} \quad (2)$$

in which *J* represents the flux of the specific solute and $dC(z)/dz$ represents the concentration gradient of the solute in a specific depth interval calculated by linear regression. Aerobic and anaerobic carbon remineralization rates (R_{aero} and R_{ana} in mmol C m^{-2} d^{-2}) were calculated from diffusive fluxes of O_2, NH_4^+, DFe and DMn considering the respective stoichiometric factors of the redox reactions (Froelich et al., 1979). Aerobic carbon remineralization (Eq. 3) is calculated from the measured diffusive oxygen uptake subtracted by the re-oxidation of reduced reaction products (DFe, DMn, and S^{2-}) diffusing upward towards the oxic sediment layer. The total

anaerobic remineralization was calculated from the upward flux of NH_4^+ (J_{NH4+}, Eq. 4) multiplied by the C/N ratio of the organic matter. We used the NH_4^+ gradients below the NO_3^- penetration depth to exclude biases from anammox and/or bioturbation. The NH_4^+ gradients of 3 cores were used to calculate the average flux of NH_4^+. Total remineralization rates of organic carbon (R_{tot} in mmol C m^{-2} d^{-1}) are calculated as the sum of aerobic and anaerobic rates (Eq. 5).

$$R_{aero} = \frac{106}{138} J_{O2} - \frac{1}{4} J_{DFe} - \frac{1}{2} J_{dMn} - 2 J_{H_2S} \quad (3)$$

$$R_{ana} = \frac{C}{N} J_{NH_4^+} \quad (4)$$

$$R_{tot} = R_{aero} + R_{ana} \quad (5)$$

From the DFe profile we calculated the upward flux using the DFe gradients above the DFe concentration peak. This needs to be distinguished from the total DFe flux which reflects the total net release of DFe and includes also the downward flux below the DFe peak. For comparison of concurrent PO_4^{3-} and DFe fluxes in the pore water, we calculate the flux ratio (J_P/J_{DFe}) from the respective pore-water gradients (dP/dz and $dDFe/dz$) and respective diffusion coefficients (D_P and D_{DFe} = 2.46 and 3.15 x 10^{-10} m^2 s^{-1}) in seawater at 0°C, (Boudreau, 1997):

$$\frac{J_P}{J_{Fe}} = \frac{-\varphi\ D_P \frac{dP}{dz}}{-\varphi\ D_{Fe} \frac{dDFe}{dz}} = \frac{D_P}{D_{Fe}} \frac{dP}{dDFe} = 0.78 \frac{dP}{dDFe} \quad (6)$$

where the ratio $dP/dDFe$ represents the slope of the linear regression between pore-water concentrations of PO_4^{3-} and DFe.

2.8 Calculation of organic carbon supply rate and burial efficiency

From the sedimentation rate (see above) the solid accumulation rate of the upper 2 cm is used in combination with the TOC content of the same layer to derive a TOC-accumulation rate for each station. In order to derive the total supply of organic carbon received by the sediments, the TOC removed in the upper layer due to aerobic C-remineralization is added to the TOC accumulation rate.

$$C_{supply} = TOC_{accumulation} + R_{aero} \quad (7)$$

The burial efficiency was also calculated for the individual station from the respective ratio of C-remineralization (R_{tot}) over C-supply as:

$$Burial = 1 - \frac{R_{tot}}{C_{supply}} \quad (8)$$

2.9 Calculation of water column stratification and sea ice cover

The conditions in the upper water column at time of sampling were characterized in terms of sea ice cover and water column stratification. Stratification was calculated from the density difference between 5 m and 50 m water depth, $\Delta\rho = \rho_{50} - \rho_5$, measured on site with the CTD. In order to investigate how the measured water column stratification relates to the sea ice conditions encountered, the recent sea ice cover was calculated from satellite derived daily sea ice cover (0-100%) at the stations, averaging a two-month interval prior the sampling date (Sea ice Index, version 3, (Fetterer et al., 2017).

From historic satellite data (Sea ice Index, version 3, (Fetterer et al., 2017), daily sea ice cover for the respective stations were extracted for the last 30 years (1990-2019) to calculate the long term mean sea ice cover (Table 1). To further characterize for each station the different degrees of sea ice cover over the season, each day of the 30 years of sea ice cover was classified as either no sea ice (<5%), marginal sea ice (5-35%), dominant sea ice (35-85%) and full sea ice (>85%), and their relative occurrence, weighted by the length of daylight (sunrise to sunset) was calculated to derive indices for the respective sea ice conditions.

3 Results

3.1 Sea ice conditions and water column stratification

Long-term sea ice cover (Table 1) were found to decrease towards the North, from 81% (station 1) and ~47% (stations 2, 3, 5) to ~34% (stations 4, 6) and 28% (station 7). The stratification of the upper water column was strongest at station 1 with a density difference between 5 and 50 m of Δρ=1 kg m^{-3} and decreased towards station 7 down to Δρ=0.03 kg m^{-3} (Table 1). The density differences were dominated by changes in salinity, which were likely maintained by a combination of high fresh water inflow from ice melt and reduced wave mixing due to the sea

ice cover. The water column stratification was therefore significantly correlated with the recent sea ice cover (R^2=0.88, p<0.001), but also with long-term sea ice cover (R^2=0.94, p<0.001).

Bottom-water salinity was between 34.54 and 34.64 PSU at all stations (Table 1). Bottom-water temperatures ranged from -1.9 °C at station 1 to -0.1 °C at station 7. All bottom waters were well-oxygenated with concentrations decreasing from 310 µmol L^{-1} (82% air saturation) at station 1 to 250 µmol L^{-1} (70% air saturation) at station 7. Concentrations of bottom-water nitrate were between 33 and 35 µmol L^{-1}.

3.2 General characteristics of sediments

Sediments consisted of silty clays to clayey silts across all stations, except for station 3, which contained a high fraction of fine sand (median grain size 116 µm) and thus exhibited a low porosity of 0.42-0.48. Porosities of the other shelf stations ranged between 0.83-0.89 at the surface and 0.68-0.78 at 30 cm depth, whereas porosity of deep-sea sediments (stations 5 and 6) were between 0.55-0.75. Sediments of stations 1, 3, 5, 6, and 7 had a distinct brown color throughout the cored interval, whereas station 2 exhibited a 6 cm thick brown surface layer, below which the sediment color changed to gray. Sediment of station 4 was characterized by a blackish color and a sulfidic odor below 10 cm depth.

The mean TOC content in the upper 5 cm depth (Table 1) was lowest at the sandy station 3 (0.19 wt%) and at the deep stations 5 and 6 (0.37 wt% and 0.30 wt%). On the shelf, TOC increased from 0.71 wt% at the ice-covered station 1 to 1.02 wt% at the dominant sea ice station 2 and 1.26 wt% at the marginal sea ice station 4, and decreased thereafter to 0.60 wt% at the poorly ice-covered station 7. Except for station 3, which showed no trend with sediment depth, TOC content at 25-30 cm depth was significantly lower compared to the upper 5 cm, with values lowered by 15% (stations 5 and 6), 25% (stations 1, 4 and 7) and 45% (station 2). Molar C/N ratios at the sediment surface (0-5 cm) were between 8 and 9 for all stations, except for station 1, where values were above 10. At this station, C/N ratio decreased downward to 8 at 25-30 cm depth, while at all other stations the values slightly increased by 5-15%.

Benthic macrofauna, when present, consisted mainly of polychaetes, bivalves, brittle stars, and few isopods. Considering the fraction larger than 1000 µm, station 1 showed the lowest fauna

diversity and abundance compared to other stations. Stations 2 and 3 showed the highest density of benthic species with communities dominated by polychaetes and bivalves. Further, station 4 had a relatively high faunal density, dominated by small bivalves and brittle stars. On contrary, we found lots of empty polychaete tubes at station 7.

3.3 Dissolved oxygen flux and C-remineralization rates

Oxygen penetration depths (OPD) were 6.3 cm at station 1 and 8.7 to 64.2 cm at stations 6 and 5 (deep sea), reflecting low oxygen consumption in these sediments (Table 1, Figure 2). Stations 2, 3 and 4 were characterized by similar penetrations depths ranging between 0.85 and 0.52 cm. At station 7, the OPD slightly increased again to 1.9 cm. Repeated oxygen profiles were highly reproducible for each station and showed no signs of fauna burrows. High volumetric oxygen consumption rates were found either close to the sediment-water interface or near the OPD, indicating aerobic remineralization of fresh organic matter at the surface and re-oxidation of reduced solutes at the OPD. In general, the calculated diffusive oxygen uptake (DOU) corresponds to the OPD, showing low values of 1.4 mmol O_2 m^{-2} d^{-1} at station 1 and 0.2 mmol O_2 m^{-2} d^{-1} at stations 5 and 6, while increasing to 3.5 and 6.9 mmol O_2 m^{-2} d^{-1} at stations 2 and 4. Due to the low porosity (0.48) of the sandy sediment at station 3, the DOU was as low as 1.8 mmol O_2 m^{-2} d^{-1}, despite the shallow OPD. At station 7, the DOU was found to be 2.0 mmol O_2 m^{-2} d^{-1}. The total oxygen uptake (TOU) corresponds to DOU and there was no significant difference between DOU and TOU, except for the sandy station 3 where total uptake was approximately twice the diffusive uptake.

From pore-water profiles of NH_4^+, DFe, DMn and H_2S (Figure 3) respective fluxes were calculated and balanced with the DOU to derive aerobic, anaerobic and total C-remineralization rates (Table 2) according to equations 3-5. Total C-remineralization was reduced to 0.14-0.18 mmol C m^{-2} d^{-1} in the deep sea. On the shelf, the rates ranged from 1.2 to 7.4 mmol C m^{-2} d^{-1} and are distributed similarly across the stations as for DOU. At stations 4 and 7, a high contribution of anaerobic C-remineralization came from increased sulfate reduction rates as inferred from H_2S gradients (see below).

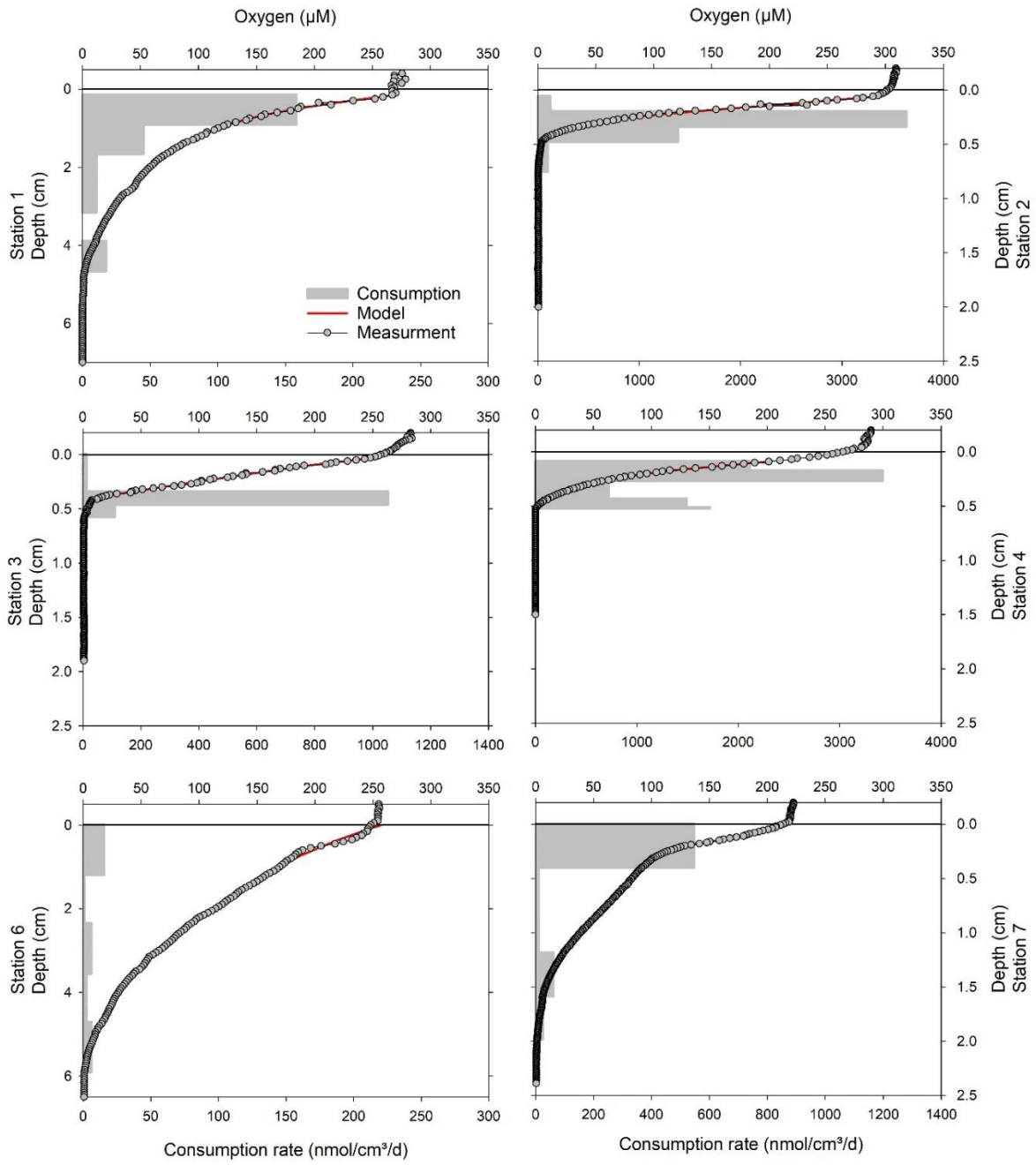

Figure 2. Representative O_2 profiles measured with optical microsensors for stations 1, 2, 3, 4, 6 and 7. The horizontal lines indicate the sediment surface. Grey circles mark measured O_2 profiles. Red lines are the modeled oxygen profiles and grey shaded boxes show the modeled consumption rate for specific depth intervals, both calculated using the transport-reaction model PROFILE (Berg et al., 1998). Note the different scales for the consumption rates and sediment depths.

Table 2. The rates of aerobic, anaerobic and total carbon remineralization were calculated via equations 2, 3, and 4. Average fluxes of NH_4^+, DFe, and upward DFe were estimated from pore water gradients and presented as average ± SD with the number of the total profiles in parentheses. Modelled benthic DFe flux to water column was calculated from bottom water oxygen concentrations (µM), and carbon remineralization rates using the equation from Dale et al. (2015).

	C equivalents total aerobic remineralization rate	C equivalents total anaerobic remineralization rate	C equivalents total remineralization rate	Anaerobic C remineralization of total C remineralization	Fe reduction of anaerobic C remineralization	Net NH_4^+ flux	Net DFe flux	Upward DFe flux	Modelled DFe flux
	mmol m^{-2} d^{-1}	mmol m^{-2} d^{-1}	mmol m^{-2} d^{-1}	%	%	mmol m^{-2} d^{-1}	mmol m^{-2} d^{-1}	µmol m^{-2} d^{-1}	µmol m^{-2} d^{-1}
Station 1	1.067	0.067	1.134	5.924	11.933	0.008 ± 0.004 (3)	0.032 ± 0.037 (3)	17.74 ± 0.018 (3)	0.62
Station 2	2.699	0.409	3.108	13.145	3.871	0.043 ± 0.003(3)	0.063 ± 0.003 (3)	51.90 ± 0.008 (3)	1.74
Station 3	1.330	0.122	1.452	8.389	14.573	0.014 ± 0.008 (3)	0.071 ± 0.073 (3)	58.00 ± 0.074 (3)	0.83
Station 4	4.699	2.697	7.396	36.465	2.926	0.310 ± 0.223 (2)	0.316 ± 0.248 (2)	170.63 ± 0.140 (2)	4.54
Station 5	0.136	-	0.136	-	-	-	-	-	0.09
Station 6	0.183	0.016	0.199	8.165	2.081	0.002 (1)	0.001 (1)	0.00	-
Station 7	1.314	0.519	1.833	28.301	3.277	0.057 ± 0.005(3)	0.068 ± 0.015 (2)	56.43 ± 0.051 (3)	1.25

3.4 Pore-water chemistry

Pore-water profiles obtained at station 1 (81% sea ice cover) and station 6 (deep sea) show similar patterns (Figure 3), although station 1 has higher TOC contents (0.7%) compared to station 6 (0.3%). Nitrate concentrations gradually decrease from bottom water concentrations (37 µM) to zero within the uppermost 10 cm indicating denitrification under reducing conditions, just below the oxygen penetration depth. The relatively deep location of the nitrate reduction zone is in accordance with the moderate OM content. Concurrently, a steady downward increase of DMn concentrations (10 µM) caused by Mn(IV) reduction at a depth of 11 cm (and below) documents the metal reduction zone of these sediments. Furthermore, the downward increase of DFe concentration at a depth of 25-30 cm indicates the position of the Fe(III)-reduction layer. The deep and rather moderate increase of DFe is in line with a rather slow increase in nutrient concentration with depth (below 10 cm: <15 µM NH_4^+, <10 µM PO_4^{3-} and <2.5 mM DIC) reflecting low microbial activity and nutrient recycling in these sediments. Furthermore, no clear evidence for a significant depletion in sulfate is found.

Pore-waters of station 2, which has an increased content of OM in the upper 5 cm (1.0% TOC, Table 1, Figure 4), show a more condensed redox zonation compared to station 1 and 6. We found complete nitrate consumption within 1-2 cm below the sediment surface. The nitrate reduction zone is followed by enhanced concentrations of DFe reaching a maximum of 133 µM in the first 5 cm. In contrast to station 1 and 6, the phosphate concentration (Figure 3) increases in the upper layer to a maximum of 50 µM at 5 cm depth. In this layer, phosphate concentrations significantly correlate with dissolved Fe concentrations, indicating co-precipitation and co-dissolution of phosphate and iron phases. The gradual increase in DIC to 4 mM and NH_4^+ to 400 µM indicates increased degradation of organic matter and nutrient release under progressively reducing conditions.

Station 3 has the lowest organic matter content (0.2% TOC) in the solid phase due to the high fraction of fine sand which also results in a low porosity. Nevertheless, reactivity in the pore space of the upper layer (0-5 cm) is comparable to station 2 with similar pore-water profiles of O_2, NO_3^-, DFe and PO_4^{3-} concentrations. Further below the decreased gradients of DIC and NH_4^+ suggest

that remineralization rates are limited by the organic matter content. The removal of dissolved Fe from the liquid phase in deeper sediment layers at station 2 and 3 strongly suggests sequestration of iron into sulfide minerals in these depths (>10 cm). This is confirmed by the sulfate depletion profiles showing increasing values with depth (station 2), whereas H_2S was not detected.

Pore-water profiles at station 4 show the characteristic sequence of typical redox zones, including the accumulation of H_2S in pore waters, as expected for sediment with high content of organic matter (1.3% TOC, Table 1). Nitrate is consumed within the first cm followed by a sharply bounded zone of dissolved Fe concentration peaking at 3-7 cm. This pattern is to some extent paralleled by dissolved Mn, however at 40-fold lower concentrations. Station 4 exhibits the highest concentrations of DFe (670 µM) found in all sampled sediments and, correspondingly, high phosphate concentrations of up to 125 µM significantly correlate with DFe concentrations. Further below, the removal of iron from the pore-water in deeper, more blackish sediments (>10 cm) marks the beginning of the sulfidic zone, where dissolved iron precipitates as iron sulfides. The upper part of the H_2S concentration profile was concave up, but further down the concentration showed an overall decrease with depth. At the base of the core, this is accompanied by a steady increase in $SO_4^{2-}{}_{dep}$ (1.5 mM), DIC (4.5 mM), and NH_4^+ (443 µM) which suggest increased organic matter degradation at depth compared to the other sites. However, across the entire core the latter profiles show discontinuities, such as local maxima at 5 cm depth and minima at 20 cm depth, which coincide with local maxima (1.7 wt%) and minima (0.8 wt%) of the organic carbon content (Figure 4).

At station 7, the redox zonation is less condensed, showing NO_3^- penetration to 3 cm depth. Only low concentrations of dissolved Mn (max. 2.2 µM) are detected in the upper core, while DFe peaks at 5 cm depth with 150 µM, again well correlated with phosphate concentrations. Below the DFe peak, a gradual increase in $SO_4^{2-}{}_{dep}$ (1.2 mM) and the steep increase of H_2S concentration mark high sulfate reduction rates. Across the entire core, continuously increasing concentrations of DIC (max. 4.2 mM) and NH_4^+ (max. 285 µM) are similar to those of station 2 and correspond to continuously decreasing TOC contents (Figure 4).

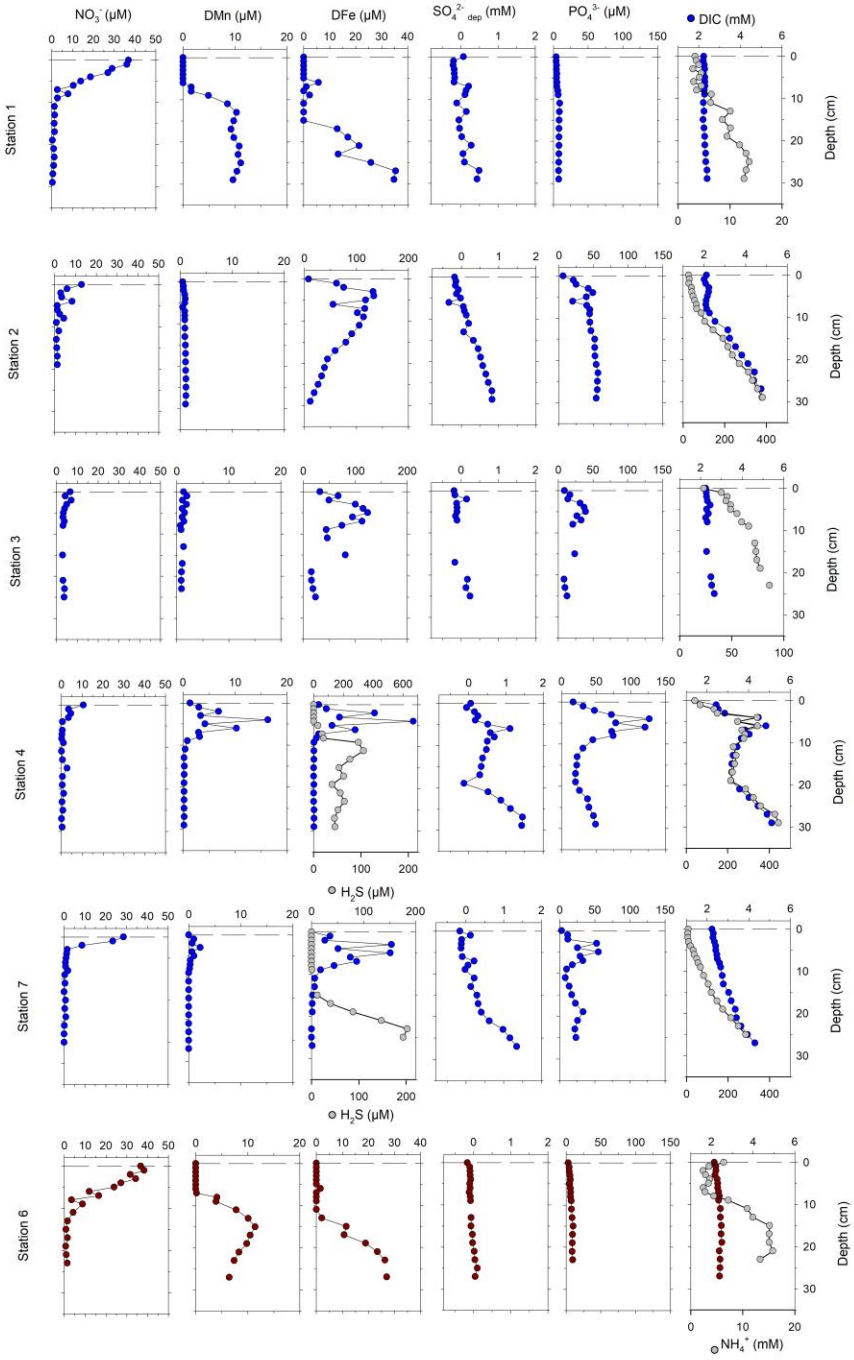

Figure 3. Representative profiles of reactive pore water compounds at the 5 shelf stations (blue) and 1 deep station (in red). SO_4^{2-} depletion profiles calculated based on the molar ratio of Cl^- and SO_4^{2-} of seawater (equation 1). Note that the scale for DFe and NH_4^+ concentrations changes between stations. Free H_2S was present only at stations 4 and 7.

3.5 Bulk sedimentary geochemistry

For shelf sediments (stations 1-4 and 7), the elemental composition of the solid phase was analyzed (Figure 4). Across stations and depths, Al/Ti ratios are relatively constant (14.8 ±0.1 to 15.5 ±0.1) confirming that both elements behave conservatively and are not affected by early diagenetic alterations. At all stations, Mn contents range from 0.02 wt% to 0.07 wt%, with Mn/Al ratios between 0.004 and 0.01. The Mn/Al ratio is stable at 0.005 at stations 2 and 4, while the coarse sandy sediment of station 3 results in lower Mn/Al ratio of 0.004. Station 7 exhibits elevated values of around 0.009. Variations with sediment depth are only found at station 1 where Mn content decreases downward from 0.010 to 0.005 within the uppermost 5 cm, just above the DMn increase in the pore-water (Figure 3), indicating Mn dissolution and re-precipitation.

The Fe contents range from 1.2 wt% to 4.5% with Fe/Al ratios of 0.3 to 0.62. Station 1 exhibits the highest Fe content (3.5-4.5 wt%) while station 3 shows low Fe contents (1.2-1.6 wt%). All other stations have values between 2.5 wt% and 3.5 wt%. The variation of Fe with sediment depth shows no clear trend, with the exception of stations 2 and 7, where an upward increase of Fe/Al is visible in the surface layer (0-5 cm). The P content ranges from 0.03 wt% to 0.12 wt%. Station 3 shows lowest values (0.03-0.04 wt%), while values between 0.06 wt% and 0.08 wt% are found at all other stations below 10 cm. Elevated P contents of up to 0.12 wt% are found at the surface of stations 2, 4 and 7. Normalization of Mn, Fe and P contents to the conservative Al contents emphasizes the depth dependent trends in elemental composition, showing the correlating trends of Fe/Al and P/Al in the surface sediments (0-5 cm) for station 2 and 4. An exception is found at station 4 in 10 cm depth, where a 3-fold higher TOC content indicates a change in sediment composition. At the same depth, Fe/Al, P/Al and S/Al (not shown) are elevated, indicating increased precipitation of Fe, S and P. This corresponds with the pore water profiles at the same depth where a sink for DFe from above and H_2S from below suggests the formation of iron sulfides (Figure 3).

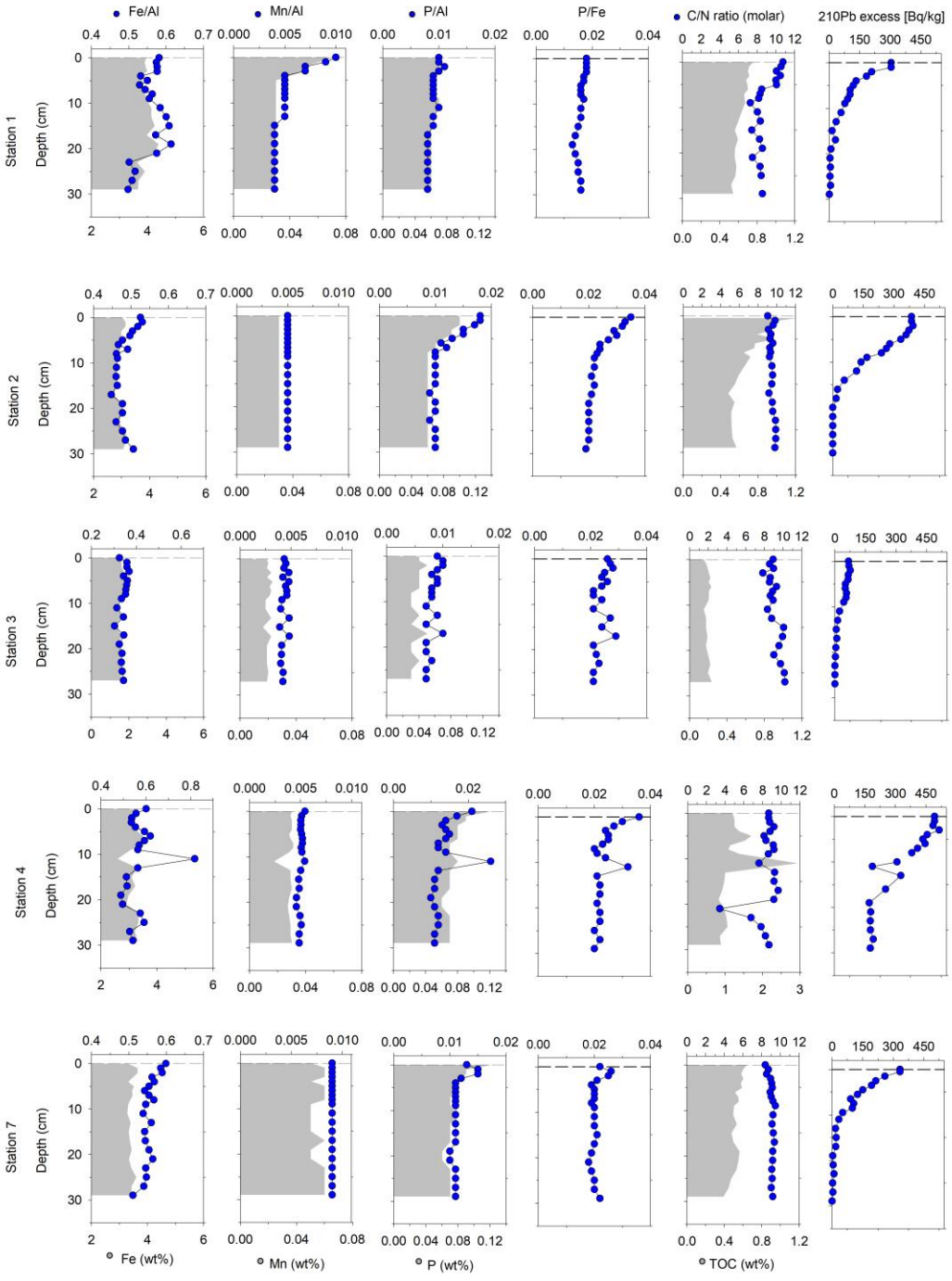

Figure 4. Detailed analysis of the solid phase for shelf stations. The total content of Fe, Mn and P is depicted as weight fraction (wt%) and normalized to aluminum. Further, the TOC and TN contents and excess activity of ^{210}Pb are shown.

3.6 Iron-phosphate cycling

In pore waters of all shelf stations, concentrations of DFe and PO_4^{3-} were significantly correlated in the surface layers at and above the DFe peak concentrations (Figure 5). The linear regression of the correlating values for stations 2, 3, 4 and 7 reveals a striking similarity with almost identical slopes between 0.33 and 0.35 µM PO_4^{-3} per µM DFe. Only the correlation at station 1 showed a lower slope of 0.18 µM PO_4^{-3} per µM DFe (Figure 5). The slopes of the linear regressions are used to calculate flux-ratios of PO_4^{-3} over DFe (see equation 6) of 0.14 for station 1 and between 0.26 and 0.28 for all other stations (Table 3).

The results of solid-phase contents of P and Fe are analyzed in a similar way (Figure 6). Despite the high background of Fe, the variations of P and Fe are nevertheless correlated with slopes between 0.18 and 0.37 mmol g^{-1} P per mmol g^{-1} Fe for stations 2, 4 and 7, showing a molar ratio similar to the flux ratios of PO_4^{3-} and DFe in the pore water. However, at stations 1 and 3, the slopes are 7-fold and 3-fold lower, respectively, at around 0.03 and 0.07 mmol g^{-1} P per mmol g^{-1} Fe (Figure 6, Table 3).

The range of variable Fe content for which the P-Fe correlation is detected (see example of drop lines in Figure 6) is between 1.4 and 4.1 mg Fe per gram solid and can be conservatively interpreted as the dynamic Fe fraction, which is accessible to Fe(III) reduction. When normalized by the total Fe content for each station, we can estimate that 9.0 ± 3.3% of total Fe content is accessible for Fe(III) reduction and takes part in the concurrent recycling of P and Fe (Table 3). The variable P content is calculated the same way and is estimated to make up 33 ± 20.6% of the total P content.

Table 3. Detailed analysis of shelf sediments. The molar Fe:P pore water concentration ratios (calculated from the DFe peak position). P-Fe variability ratio in solids and pore water (flux ratio) and calculated fraction of accessible Fe and P in solids. Sedimentation rates (whole core averages, CFC model) from ^{210}Pb analysis and accumulation rates of solids, TOC, particulate Fe, and the total carbon supply rate (=TOC accumulation + C-remineralization). Burial efficiency = 1- (C-remineralization/ total carbon supply rate).

	Porewater Fe-P Conc. ratio	Porewater P-Fe flux ratio	Solid P-Fe variability ratio	Solid-Fe recycled (accessible Fe)	Solid-P recycled (accessible P)	Sedimentation rate	Solid acc. rate	TOC acc. rate	Total C supply rate	Total Fe acc. rate	Burial efficiency
				%	%	mm yr^{-1}	g m^{-2} d^{-1}	mmol m^{-2} d^{-1}	mmol m^{-2} d^{-1}	mmol m^{-2} d^{-1}	
Station 1	4.81	0.139	0.028	10.7	10.1	1.9	2.71	1.60	2.67	1.92	0.57
Station 2	2.65	0.264	0.237	13.1	58.8	2.2	4.82	4.08	6.78	2.60	0.54
Station 3	3.45	0.264	0.074	7.7	14.3	2.3	12.05	1.87	3.20	3.10	0.54
Station 4	2.15	0.276	0.367	4.3	43.1	7.6	7.91	8.27	12.97	4.67	0.43
Station 7	2.46	0.261	0.175	9.4	40.0	1.7	2.38	1.18	2.50	1.40	0.26

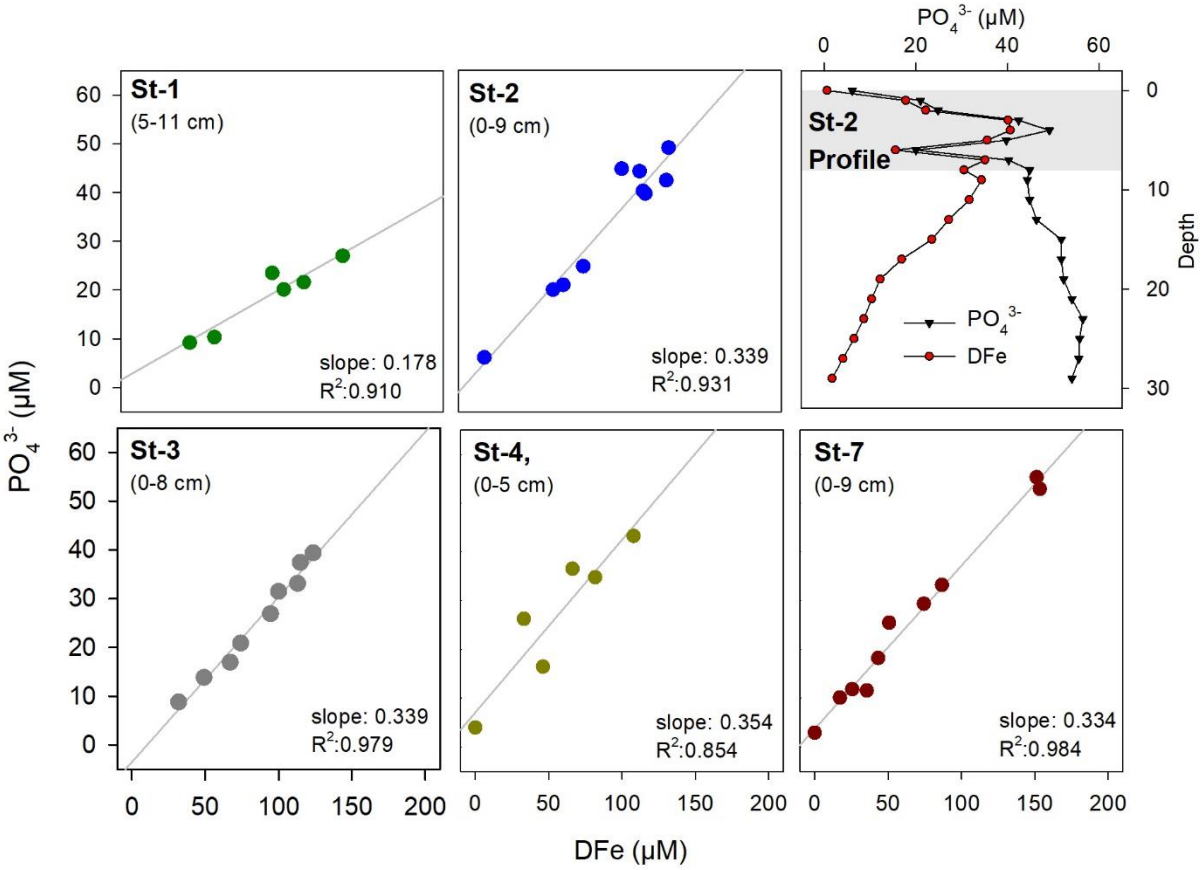

Figure 5. Correlation of PO_4^{3-} and DFe concentrations in the pore water of shelf stations. The relative standard error (RSE) of the slope is less than 10% ($p<0.001$), except for station 4 (RSE~20%, $p<0.01$). Upper right: example of correlating concentration profiles of DFe and PO_4^{3-} at station 2. The grey area marks the depth range of significant correlation.

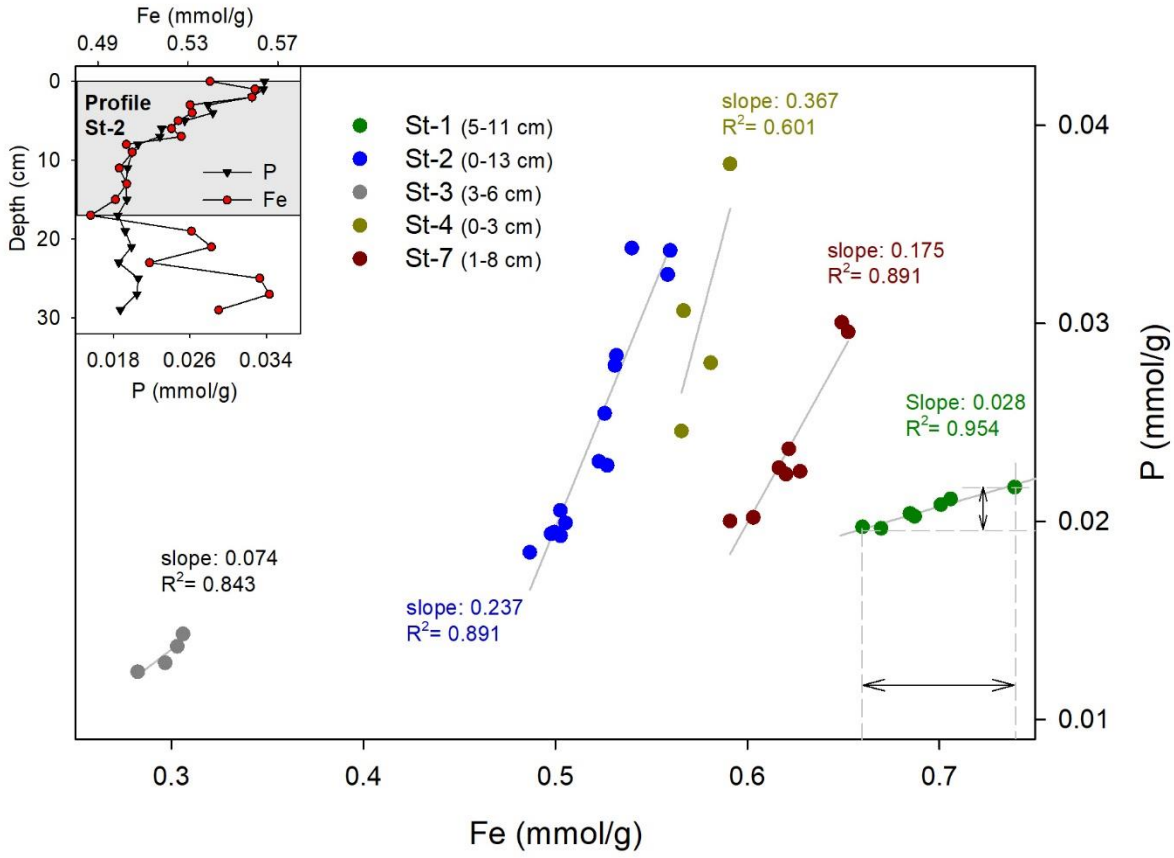

Figure 6. Correlation of P and Fe content in the solid phase of shelf stations. For stations 1, 2 and 7, the correlation was significant with a relative standard error (RSE) of the slope of 19% or less ($p<0.005$). For station 3 (RSE=30%, $p=0.082$) and station 4, (RSE=58%, $p=0.22$) the correlation was not significant. The range of variable Fe and P content is indicated for station 1 by arrows between dashed drop-lines. The range was calculated for each station and used to estimate the percentage of Fe and P involved in the P-Fe recycling as presented in Table 3. Insert: example of correlating Fe and P content at station 2. The grey area marks the depth range of significant correlation.

3.7 ^{210}Pb and sedimentation rates of OM and iron

Profiles of excess activity of ^{210}Pb (Figure 4) indicate no bioturbation for station 1 and 7, whereas slight mixing of the upper 3-4 cm is indicated for stations 2, 3, and 4. Mean sedimentation rates, calculated from $^{210}Pb_{ex}$, range from 1.9 mm y^{-1} at station 1 to 7.6 mm y^{-1} at station 4 (Table 3). The TOC accumulation ranges from 1.6 mmol C m^{-2} d^{-1} at station 1 to 8.3 mmol C m^{-2} d^{-1} at station 4. Across all shelf stations these values are significantly correlated with the respective C-remineralization rate, independently derived from pore-water profiles (Figure 7A).

The supply rate of organic carbon ranges from 2.7 mmol C m^{-2} d^{-1} at station 1 to 13.0 mmol C m^{-2} d^{-1} at station 4. Across all shelf stations, a linear regression model relating the C-supply rate with the C-remineralization rate can be established (Figure 7A). The regression model can be fitted through the origin, as would be expected for a benthic C-remineralization that depends entirely on the C-supply rate. The slope of 0.54 implies that, on average, 54% of the organic carbon supplied to sediments on the shelf is mineralized, while 46% is preserved. Moreover, the burial efficiency, when calculated for each station according to equation 8, decreased from station 1 (0.58) to station 7 (0.27) as bottom water temperatures increased from -1.9 to -0.1°C (linear correlation R^2=0.92).

Further, a significant linear relation (through the origin) is established between the total flux of DFe and the C-remineralization with a slope of 0.04 (Figure 7C). Considering a stoichiometry of 4 mole DFe released per mole C mineralized, we estimate that about 1% of the C-remineralization is coupled to Fe-reduction.

The solid accumulation rate is multiplied with the Fe content in the upper layer to derive the Fe-accumulation rate for each station (Table 3). The Fe accumulation ranges from 1.4 mmol Fe m^{-2} d^{-1} at station 7 to 4.7 mmol Fe m^{-2} d^{-1} at station 4. Across all shelf stations these values are neither correlated with upward flux nor total DFe flux (Figure 7D), suggesting that either the fraction of the Fe pool available for reduction varies between stations, or that Fe-reduction is not limited by Fe-sedimentation but mainly controlled by C-supply.

3.8 Carbon fluxes under variable sea ice conditions

In order to relate the rates of C-remineralization and C-supply to conditions in the productive water layers above, we calculated sea ice indices for each station reflecting the relative frequency of different degrees of sea ice cover over the past 30 years, classified as no sea ice (<5% cover), marginal sea ice (5-35%), dominant sea ice (35-85%) and full sea ice (>85%). Only the occurrence of marginal sea ice cover (Table 1) was significantly correlated with the distribution of C-remineralization and C-supply rates of the shelf stations (Figure 7B). Marginal sea ice conditions combine both, favorable light conditions due to reduced sea ice cover and sufficient buoyancy production by melt waters to establish a favorable stratification. Intriguingly, the relation between the marginal sea ice index and C-supply (and C-remineralization) is best described by an exponential growth function, indicating that increasing periods of favorable sea ice conditions lead to over-proportional rates of primary production and, subsequently, benthic carbon supply.

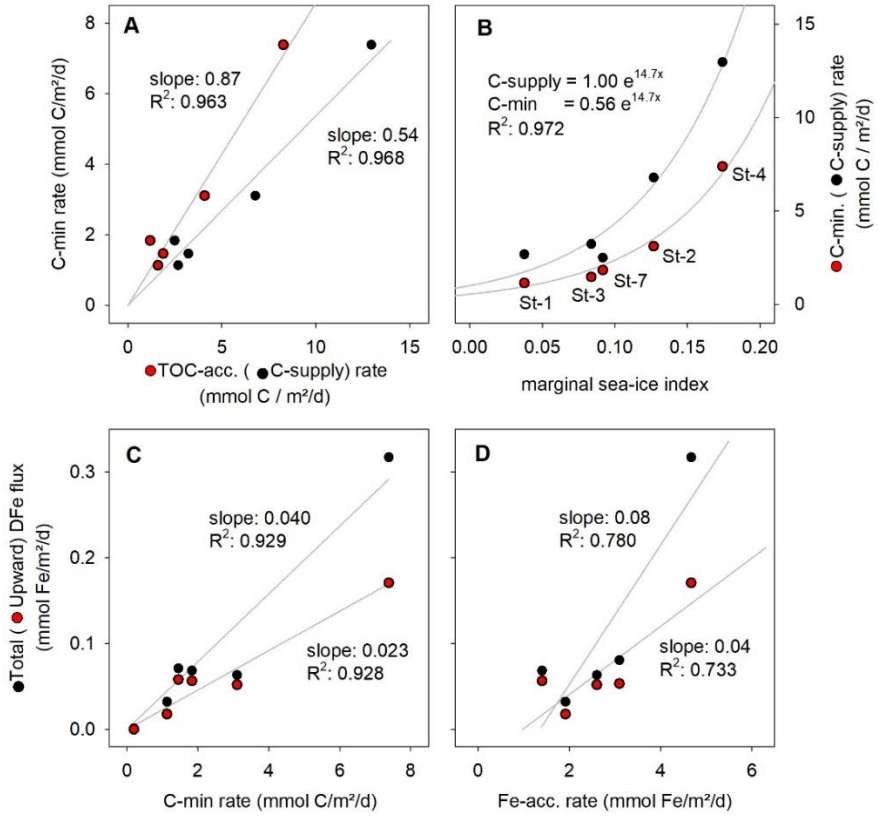

Figure 7. Relation between characteristic variables of shelf stations: **(a)** significant linear relationship between the independently measured values of C-remineralization and TOC-accumulation (red). Consequently, the C-supply rate (black) correlates as well (see equation 7). The linear fit is forced through the origin, assuming that a constant proportion of 54% (see slope) of the C-supply is remineralized (RSE of slopes < 6%, p<0.0001). **(b)** The C-remineralization and C-supply rate as function of the marginal sea ice index (see text). The relationship is best explained by an exponential growth function with a global growth constant of 14.7 (RSE < 9%, p<0.0001). The assumption for applying a growth function is that increasing periods of favorable sea ice conditions lead to over-proportional primary production and, subsequently, over-proportional organic carbon supply of the sediments. **(c)** Significant increase of both, upward and total DFe flux as function of C-remineralization rates. The linear fit is forced through the origin, assuming that a constant proportion of 1% (see text) of C-remineralization is due to Fe-reduction (RSE of slopes < 11% (p≤0.0001). **(d)** The correlation between both upward and total DFe flux with the Fe accumulation rate in solids is not significant (RSE of slopes < 30%).

4 Discussion

4.1 Benthic carbon supply and remineralization

We found low C-supply rates at stations that, on average, have either little light availability and strong summer stratification (heavy sea ice cover) or high light availability and little stratification (low sea ice cover). In contrast, intermediate stations with marginal sea ice cover (Figure 8) show a high C-supply rate. This suggests that primary production and export production is enhanced when both, light availability and stratification are sufficient to support a shallow critical mixing depth. Accordingly, a positive correlation between the measured C-supply rates with the marginal sea ice index (Figure 7B) was found, indicating that the shallow mixed layer depth at the marginal sea ice stations 2, 3 and 4 sustains primary production, yielding high C-supply rates of 7.6 mmol $m^{-2}d^{-1}$ on average. An elevated primary production is reported for the marginal ice zone (MIZ) where ice melting also increases the supply of nutrients, iron in particular (Schloss et al., 2002), which further promotes surface primary production. In the coastal waters of the West Antarctic Peninsula, previous studies have attributed high biomass (i.e. chl a) accumulation to light availability and shallow mixed-layer depths (Mitchell & Holm-Hansen, 1991; Sakshaug et al., 1991; Schloss et al., 2002), of usually < 25 m (Garibotti et al., 2005), supporting our findings of high C- supply rates at the marginal sea ice stations. In fact, when our marginal sea ice index is calculated for a larger region (Figure 8), highest values of >0.2 coincide with elevated phytoplankton concentrations measured by Garibotti et al. (2005). In contrast, the ice-free station 7 (C-supply rate 2.5 mmol $m^{-2}d^{-1}$) is exposed to wind-driven water-column mixing, which can deepen the mixed layer depth below the critical depth and thus reduce surface production, as found by Savidge et al. (1995). The occurrence of heavy sea ice cover at station 1 (C-supply rate to 2.6 mmol $m^{-2}d^{-1}$) ultimately reduces the light availability and thereby suppresses primary production as found by Arrigo et al. (2008) and Bourgeois et al. (2017). As a consequence, the expected future changes in the sea ice cover will influence the pelagic primary production, likely leading to a regional shift of marginal sea ice conditions and related high export of particulate organic carbon to shelf sediments.

The marginal ice-covered stations show an elevated TOC content (1.02 -1.21 wt %) (Table 1) and high remineralization rates (3.1 – 7.3 mmol m^{-2} d^{-1}) (Table 2), supported by high C-supply rates. The C-supply to shelf sediments correlates with TOC content and carbon remineralization rates (Figure 7A), indicating that on average 54% of the received organic carbon is remineralized while 46% is preserved and buried to greater sediment depth. The positive correlation between C-supply rate and benthic carbon remineralization rate is consistent with many previous studies (e.g. Wenzhöfer & Glud, 2002) and thus a basic assumption for several models predicting benthic carbon mineralization in the ocean (e.g. Middelburg et al., 1993; Zonneveld et al., 2010; Freitas et al., 2021). The fraction of organic carbon that is buried/preserved in the uppermost sediments is high (27-58%) but still in the range of reported burial efficiencies for marine sediments with comparable sedimentation rates (Canfield, 1994; Katsev & Crowe, 2015; Freitas et al., 2021). However, we cannot exclude the effects of lateral sediment transport from areas adjacent to the sampled stations, which could have shifted the composition of the accumulated organic matter towards a higher refractory percentage. Lateral transport is indeed indicated by the ^{210}Pb inventories which were above the inventories expected for the region and water depths. However, a detailed analysis of this mismatch is out of the scope of this study and will be investigated elsewhere.

The organic carbon supply to the sediments is one of the major controls on sedimentary redox processes (Seiter et al., 2005; Freitas et al., 2021). The high organic carbon content determined at station 4 increases the relative importance of sulfate reduction (Jørgensen & Kasten, 2006), while the approximate net contribution of Fe reduction to anaerobic carbon remineralization is 3% at most. Thus, sulfate reduction is by far the major anaerobic carbon remineralization pathway contributing > 30% to the total carbon remineralization. The dominance of sulfate reduction in anaerobic carbon remineralization agrees with the results of Nickel et al. (2008) who found that ice-free conditions along the northern Barents Sea support higher rates of sulfate reduction than found at the more permanently ice-covered stations which are characterized by lower carbon export to the sediment. In line with this, Wehrmann et al. (2014) found that in Arctic fjord sediments, high contents of reducible iron oxides combined with low contents of fresh organic matter lead to a dominance of dissimilatory iron reduction (DIR). We suggest that

this is also the case at our stations 1, 2 and 3 with intermediate organic carbon contents of 0.71, 1.02 and 0.19 wt%. At these sites DIR could contribute about 4 to 14% to the anaerobic carbon oxidation. It should be noted that we might overestimate the contribution of DIR since DFe can also derive from sulfide oxidation via Fe(III) reduction (e.g. Poulton et al., 2004, Wehrmann et al., 2017). Organoclastic sulfate reduction, which produces sulfide, might occur without being visible in the sulfate profile as diffusion pathways are short and the sulfate pool is quickly replenished in the uppermost centimeters of the sediment (Jørgensen et al., 2001). This pathway of DFe release increases with increasing TOC contents and the respective promotion of OM degradation via sulfate reduction. In the end, however, the Fe liberation into pore water is always driven by OM degradation, either directly via DIR or indirectly via sulfide oxidation.

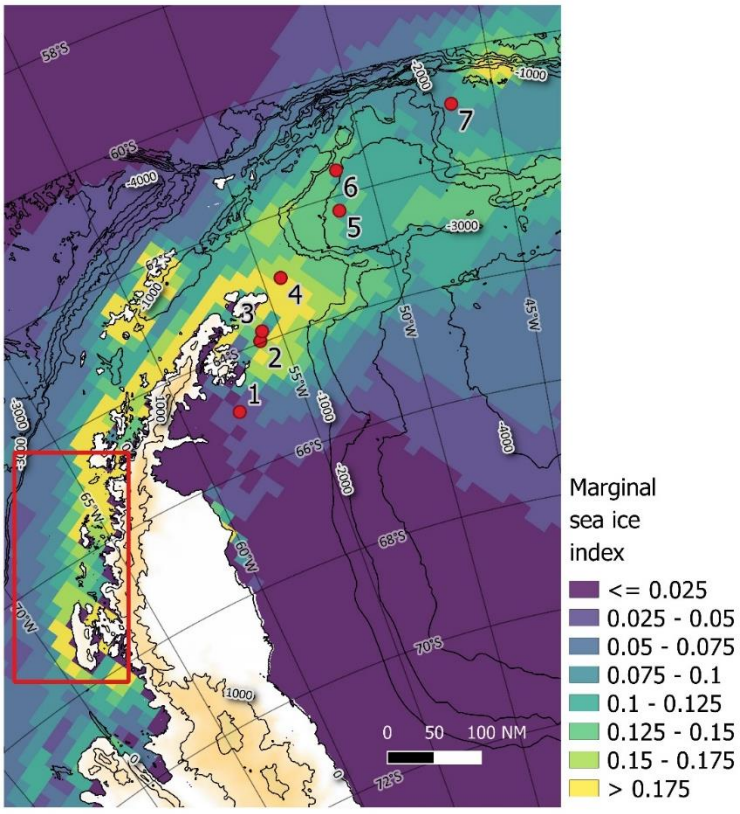

Figure 8. Map of marginal sea ice index, defined as relative occurrence of marginal sea ice cover (5-35%), weighted by the length of daylight (sunrise to sunset). Values were derived from satellite data of daily sea ice cover from 1990 to 2019 at 25 km resolution (Fetterer et al. 2017). Sampling stations of this study are shown (red dots) as well as the study area of Garibotti et al. (2005) along the western shelf of the Antarctic Peninsula (red square). Isolines denote water depths.

4.2 Controls on benthic iron release

Primary production in many regions in the Southern Ocean is iron-limited (e.g., Martin et al., 1990; Boyd et al., 2007). The input of Fe into the surface waters of the Southern Ocean can enhance primary production resulting in a higher uptake of atmospheric CO_2 and enhanced organic matter deposition to the seafloor, i.e. enhanced CO_2 sequestration (Boyd, 2002, 2007; Raiswell et al., 2008; Death et al., 2014). Therefore, knowledge about the sources and the recycling of iron is of utmost importance. Recently, research studies have found that the Fe fluxes from coastal sediments are at least as significant as the input of iceberg–hosted material (Venables & Meredith, 2009; Nielsdóttir et al., 2012; Hatta et al., 2013; Measures et al., 2013; Monien et al., 2014; Borrione et al., 2014). Furthermore, Klunder et al. (2014) found that the elevated concentration of DFe in the WAP bottom water is mainly derived from shelf sediments. However, the contribution of benthic DFe efflux from deep shelf sediments to the bioavailable iron pool in the water column has not yet been sufficiently explored.

In the following, we discuss the DFe flux within the sediments as derived from pore-water profiles. This is not equivalent to the DFe efflux across the sediment-water interface, which is discussed thereafter. Our results show that upward and total DFe fluxes are significantly correlated with carbon remineralization rates (Figure 7C), explaining most of the variability in DFe fluxes, whereas the correlation of upward and total DFe fluxes with Fe-accumulation is not significant (Figure 7D). This finding agrees with Elrod et al. (2004) who found that benthic carbon remineralization rate is an important factor for predicting DFe fluxes. As mentioned above, the DFe liberation is driven by OM degradation – either directly via DIR or indirectly through organoclastic sulfate reduction and subsequent sulfide oxidation by Fe(III) reduction.

Measurements of DFe pore-water fluxes from polar continental shelf sediments are only available from a very limited number of studies (Monien et al., 2014; Wehrmann et al., 2014; Henkel et al., 2018; Laufer-Meiser et al., 2021; Schnakenberg et al., 2021). Comparison with existing data reveals that our estimated total DFe fluxes along the eastern coast of the Antarctic Peninsula are within the same range of the total DFe fluxes calculated for sediments from Potter Cove, King George Island, western Antarctic Peninsula (Monien et al., 2014). Including all stations of this study (Table 2), the resulting total DFe fluxes ranged between 0.032 to 0.316 mmol DFe

m^{-2} d^{-1}, which is comparable to the range of 0.011 to 0.424 mmol DFe m^{-2} d^{-1} estimated for Potter Cove sediments (Monien et al., 2014).

Both upward and total fluxes of DFe in the sediment were elevated at the marginal sea ice stations while moderate fluxes were observed at ice-free and ice-covered stations, respectively. At the marginal sea ice stations, the steep concentration gradients of DFe close to the sediment surface indicate that more DFe might escape from shelf sediments into the water column. Further, the high availability of easily reducible Fe oxides at the marginal sea ice stations favor Fe-reduction over organoclastic sulfate reduction as found in other continental shelf environments (Oni et al., 2015; Henkel et al., 2018; Herbert et al., 2021; Schnakenberg et al., 2021; Wunder et al., 2021). We assume that the majority of easily reducible Fe is derived from re-oxidation/precipitation of upward diffusing DFe at the Fe(II)/Fe(III) redox boundary. A similar pattern of easily reducible Fe through benthic iron cycling was found in Arctic fjord sediments (Laufer-Meiser et al., 2021). Furthermore, high accumulation rates of detrital inputs from rock weathering and erosion may represent additional sources of easily reducible Fe (Laufer-Meiser et al., 2021). How much of the Fe-reduction is fueled by recycled iron oxides depends on the spatial distance of the DFe source (i.e. location of Fe-reduction) to the DFe sinks above (re-oxidation) and below (FeS formation) as they shape respective gradients and fluxes. Similar upward and downward gradients of DFe as observed at station 4 (Figure 3) suggest that only about half of the reduced Fe is recycled, while at station 2 more than 80% of the reduced Fe is diffusing upwards towards the oxic layer. This corresponds to the solid phase analyses (Table 3) where we calculated a significantly higher percentage of recycled solid-Fe for station 2 (10.1%) compared to station 4 (4.3%).

Quantifying the DFe-efflux into the water column from DFe profiles is compromised by the re-oxidation/precipitation of DFe in the thin oxic layer. This oxidative trap prevents the transfer of most of the sediment sourced DFe to oxic bottom waters. The resolution of pore-water profiles is too coarse to resolve the partition between DFe-efflux and DFe-recycling, so that we employ a model from Dale et al. (2015) to calculate the DFe efflux across the sediment-water interface using carbon remineralization rates (C_{min} in mmol m^{2-} d^{-1}) and O_2 concentrations (O_2 in µM) in bottom water:

$$\text{DFe efflux} = \gamma \tanh\left(\frac{C_{min}}{O_2}\right) \quad (9)$$

where γ (= 170 µmol m^{2-} d^{-1}) is the maximum DFe efflux for sediments at steady state located away from river mouths (Dale et al. 2015). The estimated benthic DFe efflux on the shelf ranges from 13-93 mg Fe m^{-2} yr^{-1} (or 0.62 µmol m^{2-} d^{-1} to 4.54 µmol m^{2-} d^{-1}, Table 2), which is 30-70 times lower than the upward DFe fluxes derived from DFe concentration gradients. The modeled DFe efflux scales primarily with the C-mineralization as it is the most variable model input (DFe efflux = $6.1 \cdot 10^{-4}$ C-mineralization, R^2 = 0.99). Together with the previously described correlation of carbon remineralization rate and marginal sea ice index, we can now link sea ice conditions and organic matter export to the potential release of DFe from the seafloor.

4.3 Coupled iron-phosphate cycling

The presence of phosphate can have pronounced effects on the formation and types of Fe minerals and thus on the rate of microbial Fe-reduction (O'Loughlin et al., 2021). As organic matter is remineralized, phosphate is released into adjacent pore waters and diffuses upward where it may be released to bottom waters or is sequestered via sorption on primary and secondary Fe-oxide minerals (e.g. Paytan & McLaughlin, 2007). During sediment accumulation, reactive Fe-oxides and adsorbed (or co-precipitated) PO_4^{3-} are gradually buried until they reach the Fe reduction zone where Fe oxides are reductively dissolved releasing both DFe and PO_4^{3-} into the pore-water (Canfield et al., 1993; Niewöhner et al., 1998; Küster-Heins et al., 2010a, 2010b; Holmkvist et al., 2010; März et al., 2018). This redox Fe-cycling between oxidized and reduced Fe mainly controls the PO_4^{3-} flux and can promote the formation of secondary, poorly crystalline Fe (oxyhydr-) oxide minerals at the Fe redox boundary (Slomp et al., 1996), which are characterized by a high surface area and high reactivity (Canfield et al., 2006) that can adsorb significant amounts of PO_4^{3-}. In deeper sediments, the reductive release of DFe and PO_4^{3-} can be directly linked to the formation of fluorapatite and vivianite (März et al. 2008, 2018).

The significant correlation of phosphate and DFe concentration profiles at all shelf stations indicates a tight coupling of P and Fe cycles (Figure 5). The molar DFe:PO_4^{3-} concentration ratios calculated from pore-water profiles at the DFe peak position ranged between 2.1 to 4.8 (Table 3), a ratio which was reported to indicate that the majority of PO_4^{3-} release is closely associated

with the reduction of iron (oxyhydr-) oxides (Slomp et al., 1996; Küster-Heins et al. 2010a, 2010b; Noffke et al., 2012; Voegelin et al., 2013; Kraal et al., 2019; 2020). Below the iron reduction zone, lower DFe:PO_4^{3-} ratios were observed suggesting the presence of a DFe sink (FeS formation) and the continuing release of PO_4^{3-} from organic matter remineralization (Schulz et al., 1994; Niewöhner et al., 1998; Wunder et al., 2021) and/or desorption from Fe-minerals. Similar trends of pore-water profiles of PO_4^{3-} and DFe have previously been observed in the Arctic marginal sea ice zone (Tessin et al., 2020), in the Peruvian oxygen minimum zone (Noffke et al., 2012), in sediments off Namibia (Küster-Heins et al., 2010a, 2010b) and in shelf sediments of the sub-Antarctic island of South Georgia (Wunder et al., 2021).

Intriguingly, the relative fluxes of PO_4^{3-} and DFe in the upper sediment of the sites investigated in this study, as calculated from the respective pore-water concentration (Figure 5, equation 6), were almost identical at four of the five shelf stations with PO_4^{3-}/DFe flux ratios ranging between 0.261 and 0.276 (Table 3). Further, similar P/Fe ratios were detected in the sedimentary solid phase, although impaired by larger relative standard errors (Figure 6). The measurements indicate that the Fe-oxides carry a fixed proportion of phosphate, which is liberated upon Fe reduction. The proportion of ~0.26 may represent the upper phosphate incorporation capacity of the respective Fe-oxides. Voegelin et al. (2013) measured the dynamic phosphate incorporation into Fe(III)-precipitates during continuing Fe(II) oxidation and described the formation of phosphate-rich hydrous ferric oxide (HFO-P) with a similar maximum P/Fe ratio of 0.25. A high degree of Fe-recycling in our sediments may support the buildup of a large pool of such HFO-P which then imprints a P/Fe ratio of 0.25 onto the pore-water fluxes. To our knowledge it is quite unique for field measurements to provide such consistent evidence for the experimentally derived P sorption capacity. Only at station 1, the P/Fe ratio of 0.17 deviates from all other shelf stations. We speculate that the pool of HFO-P at station 1 is reduced because the Fe reduction rate is low (Table 2) compared to the Fe-accumulation rate (Table 3), which also explains that the Fe content is 25% higher compared to the other shelf stations (~4 wt%, Figure 4). Further investigations on the formation/dissolution of P-Fe co-precipitates in surface sediments are important, especially for the Southern Ocean, to assess their impact on the P and Fe efflux into the water column.

5 Conclusions and Outlook

This study provides insight into benthic biogeochemical cycles and benthic carbon remineralization rates along a 400 mile transect from the eastern shelf of the Antarctic Peninsula to the West of the South Orkney Islands with different sea ice cover. Based on our estimates, carbon remineralization rates increased gradually from the heavy ice-covered station to the marginal sea ice stations from 1.1 to 7.3 mmol C m^{-2} d^{-1}, respectively. The rates decreased again to 1.8 mmol C m^{-2} d^{-1} at the ice-free station, likely driven by a deeper water column mixed layer depth, which decreases primary production and thus organic carbon export to the sediment. Iron cycling in the sediment was highest at the marginal sea ice stations where Fe-reduction led to total DFe fluxes in the pore-water of up to 0.316 mmol DFe m^{-2} d^{-1}, while moderate fluxes were observed at ice-free and ice-covered stations, respectively. In pore waters, concentrations of DFe and PO_4^{3-} were significantly correlated with almost identical flux ratios of 0.26 mol PO_4^{3-} per mol DFe for most of the stations, indicating a strong control of iron redox cycling on the phosphate release to the water column. The high benthic fluxes of DFe and PO_4^{3-} highlight the importance of sediments underlying the marginal ice zone as source for limiting nutrients to the shelf waters.

We propose that the extent and duration of sea ice cover are important in maintaining a preferential water column stratification and light regime for primary production and organic carbon export to the seafloor. As the iron, carbon and phosphate cycles are tightly linked, not only by primary production but also by carbon remineralization and sedimentary Fe redox cycling, changes in sea ice cover may affect both the biological carbon pump and the function of sediments as a potential source of iron and phosphate to the water column.

Recently, the Antarctic sea ice cover showed a drastic decline after 2015 hinting towards increased interannual variability (Eayrs et al. 2021) and eventually a continuous decline in the near future. Although a (southward) shift of areas with marginal sea ice cover can be expected, the impact on benthic processes depends on the site-specific seasonal dynamics of sea ice cover. For regions in which the MIZ is rapidly changing position with seasonal sea ice growth and retreat, favorable conditions for primary production pass quickly and the impact of climatological

changes on the sediments might be low compared to our study area where the seasonal position of the MIZ is relatively stable, sufficient to leave a clear imprint on the benthic turnover.

Acknowledgments

We acknowledge the help and effort made by the captain and crew members of RV POLARSTERN during Expedition PS118. We further thank Henning Schröder and Axel Nordhausen for preparing the multicorer and executing the deployment and recovery during the expedition. Special thanks go to Juliane Müller (AWI Bremerhaven) for carbon and nitrogen analyses of the sediments. Moreover, we gratefully acknowledge the help of Ingrid Stimac and Ingrid Dohrmann (AWI Bremerhaven) in the laboratory analyses. We also would like to thank Claudio Richter for his guidance while collecting macrofauna samples. We thank Peter Kraal, Alexander Michaud and another anonymous reviewer for their supportive and valuable comments. This study was funded by the AWI Grant-No. AWI_PS118_05.

Data Availability Statement

Data presented in this study are deposited at Pangaea (Baloza et al. 2022), accessible under doi: https://doi.org/10.1594/PANGAEA.942455.

References

Appleby, P. G. (2002). Chronostratigraphic techniques in recent sediments. In *Tracking environmental change using lake sediments* (pp. 171-203): Springer.

Appleby, P. G., & Oldfield, F. (1978). The calculation of lead-210 dates assuming a constant rate of supply of unsupported 210Pb to the sediment. *Catena, 5*(1), 1-8.

Arrigo, K. R., van Dijken, G., & Pabi, S. (2008). Impact of a shrinking Arctic ice cover on marine primary production. *Geophysical Research Letters, 35*(19). doi:https://doi.org/10.1029/2008GL035028

Baloza, M., Henkel, S., Geibert, W., Kasten, S.& Holtappels, M. (2022). Oxygen profiles, pore-water geochemistry and solid phase data of surface sediments retrieved from the eastern continental shelf of the Antarctic Peninsula. *PANGAEA*. doi:https://doi.org/10.1594/PANGAEA.942455

Berg, P., Risgaard-Petersen, N., & Rysgaard, S. (1998). Interpretation of measured concentration profiles in sediment pore water. *Limnology and Oceanography, 43*(7), 1500-1510. doi:https://doi.org/ 10.4319/lo.1998.43.7.1500

Billen, G. (1982). Modelling the processes of organic matter degradation and nutrients recycling in sedimentary systems. *American Journal of Science, 282*(4), 512-541. doi:https://doi.org/10.2475/ajs.282.4.512

Borrione, I., Aumont, O., Nielsdóttir, M. C., & Schlitzer, R. (2014). Sedimentary and atmospheric sources of iron around South Georgia, Southern Ocean: a modelling perspective. *Biogeosciences, 11*(7), 1981-2001. doi:https://doi.org/10.5194/bg-11-1981-2014

Boudreau, B. P. (1997). *Diagenetic models and their implementation* (Vol. 410): Springer, Berlin.

Bourgeois, S., Archambault, P., & Witte, U. (2017). Organic matter remineralization in marine sediments: A Pan-Arctic synthesis. *Global Biogeochemical Cycles, 31*(1), 190-213. doi:https://doi.org/10.1002/2016GB005378

Boyd, P. W. (2002). Environmental factors controlling phytoplankton processes in the Southern Ocean. *Journal of Phycology, 38*(5), 844-861. doi:https://doi.org/10.1046/j.1529-8817.2002.t01-1-01203.x

Boyd, P. W., Jickells, T., Law, C. S., Blain, S., Boyle, E. A., Buesseler, K. O., et al. (2007). Mesoscale iron enrichment experiments 1993-2005: synthesis and future directions. *Science, 315*(5812), 612-617. doi:DOI: 10.1126/science.1131669

Burdige, D. J. (2006). *Geochemistry of marine sediments*: Princeton University Press.

Canfield, D. E. (1994). Factors influencing organic carbon preservation in marine sediments. *Chemical geology, 114*(3-4), 315-329. doi:https://doi.org/10.1016/0009-2541(94)90061-2

Canfield, D. E., Rosing, M. T., & Bjerrum, C. (2006). Early anaerobic metabolisms. *Philosophical Transactions of the Royal Society B: Biological Sciences, 361*(1474), 1819-1836. doi:https://doi.org/10.1098/rstb.2006.1906

Canfield, D. E., Thamdrup, B., & Hansen, J. W. (1993). The anaerobic degradation of organic matter in Danish coastal sediments: iron reduction, manganese reduction, and sulfate reduction. *Geochimica et Cosmochimica Acta, 57*(16), 3867-3883. doi:https://doi.org/10.1016/0016-7037(93)90340-3

Cline, J. D. (1969). Spectrophotometric determination of hydrogen sulfide in natural waters *Limnology and Oceanography, 14*(3), 454-458. doi: https://doi.org/10.4319/lo.1969.14.3.0454

Collier, R., Dymond, J., Honjo, S., Manganini, S., Francois, R., & Dunbar, R. (2000). The vertical flux of biogenic and lithogenic material in the Ross Sea: moored sediment trap observations 1996–1998. *Deep Sea Research Part II: Topical Studies in Oceanography, 47*(15-16), 3491-3520. doi:https://doi.org/10.1016/S0967-0645(00)00076-X

Dale, A. W., Nickelsen, L., Scholz, F., Hensen, C., Oschlies, A., & Wallmann, K. (2015). A revised global estimate of dissolved iron fluxes from marine sediments. *Global Biogeochemical Cycles, 29*(5), 691-707. doi: https://doi.org/10.1002/2014GB005017

de Jong, J., Schoemann, V., Lannuzel, D., Croot, P., de Baar, H., & Tison, J.-L. (2012). Natural iron fertilization of the Atlantic sector of the Southern Ocean by continental shelf sources of the Antarctic Peninsula. *Journal of Geophysical Research: Biogeosciences, 117*(G1). doi:https://doi.org/10.1029/2011JG001679

Death, R., Wadham, J. L., Monteiro, F., Le Brocq, A. M., Tranter, M., Ridgwell, A., et al. (2014). Antarctic ice sheet fertilises the Southern Ocean. *Biogeosciences, 11*(10), 2635-2643. doi:https://doi.org/10.5194/bg-11-2635-2014

Dorschel, B. (2019). The Expedition PS118 of the Research Vessel POLARSTERN to the Weddell Sea in 2019. In Berichte zur Polar- und Meeresforschung = Reports on Polar and Marine Research (Vol. 735, pp. 1-149). Alfred-Wegener-Institut, Helmholtz-Zentrum für Polar- und Meeresforschung. doi:https://doi.org/10.2312/BzPM_0735_2019

Eayrs, C., Li, X., Raphael, M.N. et al. Rapid decline in Antarctic sea ice in recent years hints at future change. Nat. Geosci. 14, 460–464 (2021). doi:https://doi.org/10.1038/s41561-021-00768-3

Elrod, V. A., Berelson, W. M., Coale, K. H., & Johnson, K. S. (2004). The flux of iron from continental shelf sediments: A missing source for global budgets. *Geophysical Research Letters, 31*(12), n/a-n/a. doi: https://doi.org/10.1029/2004gl020216

Fetterer, F., Knowles, K., Meier, W. N., Savoie, M., & Windnagel, A. K. (2017). *Sea ice Index, Version 3. [Years 1978-2019]. Boulder, Colorado USA. NSIDC: National Snow and Ice Data Center. doi: https://doi.org/10.7265/N5K072F8. [last access April 2021].*

Freitas, F. S., Pika, P. A., Kasten, S., Jørgensen, B. B., Rassmann, J., Rabouille, C., et al. (2021). New insights into large-scale trends of apparent organic matter reactivity in marine sediments and patterns of benthic carbon transformation. *Biogeosciences, 18*(15), 4651-4679. doi:https://doi.org/10.5194/bg-18-4651-2021

Froelich, P. N., Klinkhammer, G., Bender, M. L., Luedtke, N., Heath, G. R., Cullen, D., et al. (1979). Early oxidation of organic matter in pelagic sediments of the eastern equatorial Atlantic: suboxic diagenesis. *Geochimica et Cosmochimica Acta, 43*(7), 1075-1090. doi:https://doi.org/10.1016/0016-7037(79)90095-4

Garibotti, I. A., Vernet, M., Smith, R. C., & Ferrario, M. E. (2005). Interannual variability in the distribution of the phytoplankton standing stock across the seasonal sea ice zone west of the Antarctic Peninsula. *Journal of Plankton Research, 27*(8), 825-843.

Goldberg, E. D. (1963). *Geochronology with 210Pb*. Paper presented at the Symposium on radioactive dating 1962, Athens.

Hatta, M., Measures, C. I., Selph, K. E., Zhou, M., & Hiscock, W. T. (2013). Iron fluxes from the shelf regions near the South Shetland Islands in the Drake Passage during the austral-winter 2006. *Deep Sea Research Part II: Topical Studies in Oceanography, 90*, 89-101. doi:https://doi.org/10.1016/j.dsr2.2012.11.003

Henkel, S., Kasten, S., Hartmann, J. F., Silva-Busso, A., & Staubwasser, M. (2018). Iron cycling and stable Fe isotope fractionation in Antarctic shelf sediments, King George Island. *Geochimica et Cosmochimica Acta, 237*, 320-338. doi:https://doi.org/10.1016/j.gca.2018.06.042

Herbert, L. C., Zhu, Q., Michaud, A. B., Laufer-Meiser, K., Jones, C. K., Riedinger, N., et al. (2021). Benthic iron flux influenced by climate-sensitive interplay between organic carbon availability and sedimentation rate in Arctic fjords. Limnology and Oceanography, 66(9), 3374-3392. doi: https://doi.org/10.1002/lno.11885

Holmkvist, L., Arning, E. T., Küster-Heins, K., Vandieken, V., Peckmann, J., Zabel, M., et al. (2010). Phosphate geochemistry, mineralization processes, and Thioploca distribution in shelf sediments off central Chile. *Marine Geology, 277*(1-4), 61-72. doi:https://doi.org/10.1016/j.margeo.2010.08.011

Jahnke, R. A., & Jackson, G. A. (1992). The spatial distribution of sea floor oxygen consumption in the Atlantic and Pacific Oceans. In *Deep-sea food chains and the global carbon cycle* (pp. 295-307): Springer.

Jørgensen, B. B., Weber, A., & Zopfi, J. (2001). Sulfate reduction and anaerobic methane oxidation in Black Sea sediments. *Deep-Sea Research I*, 48, 2097-2120. doi: https://doi.org/10.1016/S0967-0637(01)00007-3

Jørgensen, B. B., & Kasten, S. (2006). Sulfur Cycling and Methane Oxidation. In H. D. Schulz & M. Zabel (Eds.), *Marine Geochemistry* (pp. 271-309). Berlin, Heidelberg: Springer Berlin Heidelberg. doi:https://doi.org/10.1007/3-540-32144-6_8

Katsev, S., & Crowe, S. A. (2015). Organic carbon burial efficiencies in sediments: The power law of mineralization revisited. *Geology, 43*(7), 607-610. doi:https://doi.org/10.1130/G36626.1

Klunder, M., Laan, P., De Baar, H., Middag, R., Neven, I., & Van Ooijen, J. (2014). Dissolved Fe across the Weddell Sea and Drake Passage: impact of DFe on nutrient uptake. *Biogeosciences, 11*(3), 651-669. doi:https://doi.org/10.5194/bg-11-651-2014

Küster-Heins, K., de Lange, G. J., & Zabel, M. (2010a). Benthic phosphorus and iron budgets for three NW African slope sediments: a balance approach. *Biogeosciences, 7*(2), 469-480. doi:https://doi.org/10.5194/bg-7-469-2010

Küster-Heins, K., Steinmetz, E., De Lange, G. J., & Zabel, M. (2010b). Phosphorus cycling in marine sediments from the continental margin off Namibia. *Marine Geology, 274*(1), 95-106. doi:https://doi.org/10.1016/j.margeo.2010.03.008

Kraal, P., van Genuchten, C. M., Behrends, T., & Rose, A. L. (2019). Sorption of phosphate and silicate alters dissolution kinetics of poorly crystalline iron (oxyhydr) oxide. Chemosphere, 234, 690-701.doi: https://doi.org/10.1016/j.chemosphere.2019.06.071

Kraal, P., van Genuchten, C. M., Lenstra, W. K., & Behrends, T. (2020). Coprecipitation of phosphate and silicate affects environmental iron (oxyhydr) oxide transformations: A gel-based diffusive sampler approach. Environmental Science & Technology, 54(19), 12795-12802. doi: https://doi.org/10.1021/acs.est.0c02352

Lancelot C., De Montety A., Goosse H., Becquevort S., Schoemann V., Pasquer B. and Vancoppenolle M. (2009) Spatial distribution of the iron supply to phytoplankton in the Southern Ocean: a model study. Biogeosciences 6, 2861–2878.

Laufer-Meiser, K., Michaud, A. B., Maisch, M., Byrne, J. M., Kappler, A., Patterson, M. O., et al. (2021). Potentially bioavailable iron produced through benthic cycling in glaciated Arctic fjords of Svalbard. *Nat Commun, 12*(1), 1349. doi:https://doi.org/10.1038/s41467-021-21558-w

Martin, J. H., Gordon, R. M., & Fitzwater, S. E. (1990). Iron in Antarctic waters. *Nature, 345*(6271), 156-158. doi:https://doi.org/10.1038/345156a0

März, C., Hoffmann, J., Bleil, U., de Lange, G. J., & Kasten, S. (2008). Diagenetic changes of magnetic and geochemical signals by anaerobic methane oxidation in sediments of the Zambezi deep-sea fan (SW Indian Ocean). *Marine Geology, 255*(3-4), 118-130. doi:https://doi.org/10.1016/j.margeo.2008.05.013

März, C., Riedinger, N., Sena, C., & Kasten, S. (2018). Phosphorus dynamics around the sulphate-methane transition in continental margin sediments: Authigenic apatite and Fe (II) phosphates. *Marine Geology, 404*, 84-96. doi:https://doi.org/10.1016/j.margeo.2018.07.010

Measures, C. I., Brown, M. T., Selph, K. E., Apprill, A., Zhou, M., Hatta, M., et al. (2013). The influence of shelf processes in delivering dissolved iron to the HNLC waters of the Drake Passage, Antarctica. *Deep Sea Research Part II: Topical Studies in Oceanography, 90*, 77-88. doi:https://doi.org/10.1016/j.dsr2.2012.11.004

Middelburg, J. J., Vlug, T., Jaco, F., & Van der Nat, W. (1993). Organic matter mineralization in marine systems. *Global and Planetary change, 8*(1-2), 47-58. doi:https://doi.org/10.1016/0921-8181(93)90062-S

Mitchell, B. G., & Holm-Hansen, O. (1991). Observations of modeling of the Antartic phytoplankton crop in relation to mixing depth. *Deep Sea Research Part A. Oceanographic Research Papers, 38*(8-9), 981-1007. doi:https://doi.org/10.1016/0198-0149(91)90093-U

Monien, P., Lettmann, K. A., Monien, D., Asendorf, S., Wölfl, A.-C., Lim, C. H., et al. (2014). Redox conditions and trace metal cycling in coastal sediments from the maritime Antarctic. *Geochimica et Cosmochimica Acta, 141*, 26-44. doi:https://doi.org/10.1016/j.gca.2014.06.003

Nickel, M., Vandieken, V., Brüchert, V., & Jørgensen, B. B. (2008). Microbial Mn(IV) and Fe(III) reduction in northern Barents Sea sediments under different conditions of ice cover and organic carbon deposition. *Deep Sea Research Part II: Topical Studies in Oceanography, 55*(20), 2390-2398. doi:https://doi.org/10.1016/j.dsr2.2008.05.003

Nielsdóttir, M. C., Bibby, T. S., Moore, C. M., Hinz, D. J., Sanders, R., Whitehouse, M., et al. (2012). Seasonal and spatial dynamics of iron availability in the Scotia Sea. *Marine Chemistry, 130*, 62-72. doi:https://doi.org/10.1016/j.marchem.2011.12.004

Niewöhner, C., Hensen, C., Kasten, S., Zabel, M., & Schulz, H. (1998). Deep sulfate reduction completely mediated by anaerobic methane oxidation in sediments of the upwelling area off Namibia. *Geochimica et Cosmochimica Acta, 62*(3), 455-464. doi:https://doi.org/10.1016/S0016-7037(98)00055-6

Noffke, A., Hensen, C., Sommer, S., Scholz, F., Bohlen, L., Mosch, T., et al. (2012). Benthic iron and phosphorus fluxes across the Peruvian oxygen minimum zone. *Limnology and Oceanography, 57*(3), 851-867. doi: https://doi.org/10.4319/lo.2012.57.3.0851

O'Loughlin, E. J., Boyanov, M. I., Gorski, C. A., Scherer, M. M., & Kemner, K. M. (2021). Effects of Fe(III) Oxide Mineralogy and Phosphate on Fe(II) Secondary Mineral Formation during Microbial Iron Reduction. *Minerals, 11*(2). doi: https://doi.org/10.3390/min11020149

Oni, O., Miyatake, T., Kasten, S., Richter-Heitmann, T., Fischer, D., Wagenknecht, L., et al. (2015). Distinct microbial populations are tightly linked to the profile of dissolved iron in the methanic sediments of the Helgoland mud area, North Sea. *Frontiers in microbiology, 6*(365). doi:https://doi.org/10.3389/fmicb.2015.00365

Paytan, A., & McLaughlin, K. (2007). The oceanic phosphorus cycle. *Chemical reviews, 107*(2), 563-576. doi:https://doi.org/10.1021/cr0503613

Poulton, S. W., Krom, M. D., and Raiswell, R. (2004). A revised scheme for the reactivity of iron (oxyhydr)oxide minerals towards dissolved sulfide. Geochimica et Cosmochimica Acta, 68(18), 3703–3715, doi:https://doi.org/10.1016/j.gca.2004.03.012

Raiswell, R., Benning, L. G., Tranter, M., & Tulaczyk, S. (2008). Bioavailable iron in the Southern Ocean: the significance of the iceberg conveyor belt. *Geochemical Transactions, 9*(1), 7. doi:https://doi.org/10.1186/1467-4866-9-7

Raiswell, R., Hawkings, J. R., Benning, L. G., Baker, A. R., Death, R., Albani, S., et al. (2016). Potentially bioavailable iron delivery by iceberg-hosted sediments and atmospheric dust to the polar oceans. *Biogeosciences, 13*(13), 3887-3900. doi:https://doi.org/10.5194/bg-13-3887-2016

Sachs, O., Sauter, E. J., Schlüter, M., van der Loeff, M. M. R., Jerosch, K., & Holby, O. (2009). Benthic organic carbon flux and oxygen penetration reflect different plankton provinces in the Southern Ocean. Deep sea research part I: Oceanographic research papers, 56(8), 1319-1335. Doi: https://doi.org/10.1016/j.dsr.2009.02.003

Sakshaug, E., Slagstad, D., & Holm-Hansen, O. (1991). Factors controlling the development of phytoplankton blooms in the Antarctic Ocean—a mathematical model. *Marine Chemistry, 35*(1-4), 259-271. doi:https://doi.org/10.1016/S0304-4203(09)90021-4

Savidge, G., Harbour, D., Gilpin, L., & Boyd, P. (1995). Phytoplankton distributions and production in the Bellingshausen Sea, Austral spring 1992. *Deep Sea Research Part II: Topical Studies in Oceanography, 42*(4-5), 1201-1224. doi:https://doi.org/10.1016/0967-0645(95)00062-U

Schloss, I. R., Ferreyra, G. A., & Ruiz-Pino, D. (2002). Phytoplankton biomass in Antarctic shelf zones: a conceptual model based on Potter Cove, King George Island. *Journal of Marine Systems, 36*(3-4), 129-143. doi:https://doi.org/10.1016/S0924-7963(02)00183-5

Schnakenberg, A., Aromokeye, D. A., Kulkarni, A., Maier, L., Wunder, L. C., Richter-Heitmann, T., et al. (2021). Electron acceptor availability shapes anaerobically methane oxidizing archaea (ANME) communities in South Georgia sediments. *Frontiers in microbiology, 12*. doi:https://doi.org/10.3389/fmicb.2021.617280

Schulz, H. D., Dahmke, A., Schinzel, U., Wallmann, K., & Zabel, M. (1994). Early diagenetic processes, fluxes, and reaction rates in sediments of the South Atlantic. *Geochimica et Cosmochimica Acta, 58*(9), 2041-2060. doi:https://doi.org/10.1016/0016-7037(94)90284-4

Sedwick, P. N., DiTullio, G. R., & Mackey, D. J. (2000). Iron and manganese in the Ross Sea, Antarctica: Seasonal iron limitation in Antarctic shelf waters. *Journal of Geophysical Research: Oceans, 105*(C5), 11321-11336. doi:https://doi.org/10.1029/2000JC000256

Seeberg-Elverfeldt, J., Schlüter, M., Feseker, T., & Kölling, M. (2005). Rhizon sampling of porewaters near the sediment-water interface of aquatic systems. *Limnology and oceanography: Methods, 3*(8), 361-371. doi: https://doi.org/10.4319/lom.2005.3.361

Seiter, K., Hensen, C., & Zabel, M. (2005). Benthic carbon mineralization on a global scale. *Global Biogeochemical Cycles, 19*(1). doi:https://doi.org/10.1029/2004GB002225

Slomp, C., Van der Gaast, S., & Van Raaphorst, W. (1996). Phosphorus binding by poorly crystalline iron oxides in North Sea sediments. *Marine Chemistry, 52*(1), 55-73. doi:https://doi.org/10.1016/0304-4203(95)00078-X

Smith, C. R., Mincks, S., & DeMaster, D. J. (2006). A synthesis of bentho-pelagic coupling on the Antarctic shelf: Food banks, ecosystem inertia and global climate change. *Deep Sea*

Research Part II: Topical Studies in Oceanography, 53(8-10), 875-894. doi:https://doi.org/10.1016/j.dsr2.2006.02.001

Spreen G, Kaleschke L, Heygster G (2008), Sea ice remote sensing using AMSR-E 89 GHz channels, J. Geophys. Res., doi:10.1029/2005JC003384

Tessin, A., März, C., Kędra, M., Matthiessen, J., Morata, N., Nairn, M., et al. (2020). Benthic phosphorus cycling within the Eurasian marginal sea ice zone. *Philosophical Transactions of the Royal Society A, 378*(2181), 20190358. doi:https://doi.org/10.1098/rsta.2019.0358

Vaughan, D. G., Marshall, G. J., Connolley, W. M., Parkinson, C., Mulvaney, R., Hodgson, D. A., et al. (2003). Recent rapid regional climate warming on the Antarctic Peninsula. *Climatic change, 60*(3), 243-274. doi:https://doi.org/10.1023/A:1026021217991

Venables, H. J., & Meredith, M. P. (2009). Theory and observations of Ekman flux in the chlorophyll distribution downstream of South Georgia. *Geophysical Research Letters, 36*(23). doi:https://doi.org/10.1029/2009GL041371

Vernet, M., Martinson, D., Iannuzzi, R., Stammerjohn, S., Kozlowski, W., Sines, K., et al. (2008). Primary production within the sea ice zone west of the Antarctic Peninsula: I—Sea ice, summer mixed layer, and irradiance. *Deep Sea Research Part II: Topical Studies in Oceanography, 55*(18), 2068-2085. doi:https://doi.org/10.1016/j.dsr2.2008.05.021

Voegelin, A., Senn, A.-C., Kaegi, R., Hug, S. J., & Mangold, S. (2013). Dynamic Fe-precipitate formation induced by Fe (II) oxidation in aerated phosphate-containing water. *Geochimica et Cosmochimica Acta, 117*, 216-231. doi:https://doi.org/10.1016/j.gca.2013.04.022

Volz, J. B., Liu, B., Köster, M., Henkel, S., Koschinsky, A., & Kasten, S. (2020). Post-depositional manganese mobilization during the last glacial period in sediments of the eastern Clarion-Clipperton Zone, Pacific Ocean. *Earth and Planetary Science Letters, 532*. doi:https://doi.org/10.1016/j.epsl.2019.116012

Wadham, J. L., De'Ath, R., Monteiro, F., Tranter, M., Ridgwell, A., Raiswell, R., et al. (2013). The potential role of the Antarctic Ice Sheet in global biogeochemical cycles. *Earth and Environmental Science Transactions of the Royal Society of Edinburgh, 104*(1), 55-67. doi:https://doi.org/10.1017/S1755691013000108

Wehrmann, L. M., Formolo, M. J., Owens, J. D., Raiswell, R., Ferdelman, T. G., Riedinger, N., et al. (2014). Iron and manganese speciation and cycling in glacially influenced high-latitude fjord sediments (West Spitsbergen, Svalbard): Evidence for a benthic recycling-transport mechanism. *Geochimica et Cosmochimica Acta, 141*, 628-655. doi:https://doi.org/10.1016/j.gca.2014.06.007

Wehrmann, L. M., Riedinger, N., Brunner, B., Kamyshny, A., Hubert, C. R. J., Herbert, L. C., et al. (2017). Iron-controlled oxidative sulfur cycling recorded in the distribution and isotopic composition of sulfur species in glacially influenced fjord sediments of west Svalbard. Chemical geology, 466, 678-695. doi:https://doi.org/10.1016/j.chemgeo.2017.06.013

Wenzhöfer, F., & Glud, R. N. (2002). Benthic carbon mineralization in the Atlantic: a synthesis based on in situ data from the last decade. *Deep Sea Research Part I: Oceanographic Research Papers, 49*(7), 1255-1279. doi:https://doi.org/10.1016/S0967-0637(02)00025-0

Weston, N. B., Porubsky, W. P., Samarkin, V. A., Erickson, M., Macavoy, S. E., & Joye, S. B. (2006). Porewater stoichiometry of terminal metabolic products, sulfate, and dissolved organic carbon and nitrogen in estuarine intertidal creek-bank sediments. *Biogeochemistry, 77*(3), 375-408. doi:https://doi.org/10.1007/s10533-005-1640-1

Wunder, L. C., Aromokeye, D. A., Yin, X., Richter-Heitmann, T., Willis-Poratti, G., Schnakenberg, A., et al. (2021). Iron and sulfate reduction structure microbial communities in (sub-)Antarctic sediments. *The ISME Journal*. doi:https://doi.org/10.1038/s41396-021-01014-9

Zonneveld, K. A., Versteegh, G. J., Kasten, S., Eglinton, T. I., Emeis, K.-C., Huguet, C., et al. (2010). Selective preservation of organic matter in marine environments; processes and impact on the sedimentary record. *Biogeosciences, 7*(2), 483-511. doi:https://doi.org/10.5194/bg-7-483-2010

3

Manuscript 2

The impact of sea ice cover on microbial communities in Antarctic shelf sediments

Marwa Baloza[1,2], Susann Henkel[1], Sabine Kasten[1,3], Moritz Holtappels[1,4], Massimiliano Molari[5]

[1]Alfred Wegener Institute Helmholtz Centre for Polar and Marine Research, Bremerhaven, Germany
[2]Faculty 2 Biology /Chemistry, University Bremen, Bremen, Germany
[3]Faculty of Geosciences, University Bremen, Bremen, Germany
[4]MARUM - Center for Marine Environmental Sciences, University of Bremen, Bremen, Germany
[5]HGF-MPG Joint Research Group for Deep-Sea Ecology and Technology, Max Planck Institute for Marine Microbiology, Bremen, Germany

Manuscript published 2023 in Microorganisms, *11*(6), 1572. doi.org/10.3390/microorganisms11061572

Abstract

The area around the Antarctic Peninsula (AP) is facing rapid climatic and environmental changes, with so far unknown impacts on the benthic microbial communities of the continental shelves. In this study, we investigated the impact of contrasting sea ice cover on microbial community compositions in surface sediments from five stations along the eastern shelf of the AP using 16S ribosomal RNA (rRNA) gene sequencing. Redox conditions in sediments with long ice-free periods are characterized by a prevailing ferruginous zone, whereas a comparatively broad upper oxic zone is present at the heavily ice-covered station. Low ice cover stations were highly dominated by microbial communities of *Desulfobacterota* (mostly *Sva1033*, *Desulfobacteria*, and *Desulfobulbia*), *Myxococcota*, and *Sva0485*, whereas *Gammaproteobacteria*, *Alphaproteobacteria*, *Bacteroidota*, and *NB1-j* prevail at the heavy ice cover station. In the ferruginous zone, *Sva1033* was the dominant member of Desulfuromonadales for all stations and, along with eleven other taxa, showed significant positive correlations with dissolved Fe concentrations, suggesting a significant role in iron reduction or an ecological relationship with iron reducers. Our results indicate that sea ice cover and its effect on organic carbon fluxes are the major drivers for changes in benthic microbial communities, favoring potential iron reducers at stations with increased organic matter fluxes.

Keywords: benthic microbial communities; iron reducers; dissolved iron; pore-water profiles; redox zones; Sva1033

1 Introduction

Shelf sediments play a significant role in the remineralization of organic matter (OM) and the recycling of nutrients and trace metals (e.g. Elderfield, 1985; Shaw et al., 1990; Jørgensen & Kasten, 2006; Monien et al., 2014). In shelf regions, photosynthetic primary production accounts for 30–40% of organic matter supplied to the sea floor (de Haas et al., 2002). The majority of OM deposited at the seabed is remineralized while part of it is buried permanently (e.g., Canfield, 1993; Burdige, 2007). The remineralization of OM is mainly driven through microbially-mediated metabolic reactions using sequences of terminal electron accepting processes (TEAPs) with electron acceptors such as O_2 for aerobic respiration followed by NO_3^-, Mn(IV), Fe(III), SO_4^{2-}, and CO_2 for anaerobic respiration (e.g., Froelich et al., 1979; Berner, 1980; Canfield & Thamdrup, 2009; Stumm & Morgan, 2012; Monien et al., 2014). The microbial remineralization of OM through the TEAPs is the main driver for biogeochemical processes in marine sediments (D'Hondt et al., 2002; D'Hondt et al., 2004; Azam & Malfatti, 2007; Falkowski et al., 2008) and is responsible for the formation of a typical/distinct sedimentary redox zonation (e.g., Froelich et al., 1979; Berner, 1980; Kasten et al., 2003). The extent of the different redox zones and the depth position of redox boundaries are mainly controlled by the reactivity and availability of terminal electron acceptors and OM accumulation rates (e.g., Froelich et al., 1979; Canfield et al., 1993; Kasten et al., 2003; Zonneveld et al., 2010), suggesting that each of these zones is shaped by microbes with specific metabolic traits (Ravenschlag et al., 2000; Jørgensen et al., 2012). Therefore, differences in microbial community composition have been successfully used to decipher the redox state and biogeochemical processes in a wide range of coastal marine and deep-sea sediments (Sogin et al., 2006; Bienhold et al., 2012; Ruff et al., 2014; Oni et al., 2015; Buongiorno et al., 2019; Molari et al., 2020; Wunder et al., 2021; Schnakenberg et al., 2021).

In the area of the Antarctic Peninsula (AP), the amount of organic matter originating from surface-water primary production is highly variable—both temporally and spatially—and depends mainly on the availability of light, which is regulated by season and sea ice cover (Savidge et al., 1995; Smith et al., 2001; 2006). During the spring-summer season, the melting of sea ice provides light for surface-water primary production with maximum production at the marginal

ice zone (Savidge et al., 1995). On the other hand, the growth of sea ice cover during winter reduces light penetration, thereby limiting primary production. Sea ice cover thus controls the flux of OM to the seafloor. Baloza et al. (2022) found that moderate sea ice cover (5–35%), which combines both favorable light conditions and water column stratification for algal growth, correlates with a high OM supply rate to the seabed. Previous studies have demonstrated that the quantity and quality of OM determine the microbial community composition, with certain taxonomic groups showing strong correlations with sedimentary parameters such as chlorophyll a concentration (Bienhold et al., 2012; Currie et al., 2021) and total organic carbon content (Abell & Bowman, 2005; Learman et al., 2016; Cho et al., 2020).

Another factor regulating the production and subsequent deposition of OM over large parts of the Southern Ocean is the availability of dissolved iron (DFe), a limiting micronutrient for phytoplankton productivity (e.g. Martin et al., 1990; Boyd et al., 2007). Iron supply can enhance phytoplankton growth resulting in higher sequestration of atmospheric CO_2 and enhanced accumulation of phytodetritus on the sea floor, a process known as the biological carbon pump (Martin, 1990; Raiswell et al., 2008). Iron enters the Southern Ocean from various sources, with considerable variability in their estimated contribution. This includes iceberg-rafted debris (IRD) to sub-ice shelf, which contributes about 180–1400 Gg a^{-1} of bioavailable Fe (Raiswell et al., 2016), followed by anoxic shelf sediments (7–790 Gg a^{-1}) (Monien et al., 2014), aeolian input (1.12 Gg a^{-1}) (Lancelot et al., 2009; Raiswell et al., 2016), and anoxic subglacial meltwaters (0.03–5.9 Gg a^{-1}) (Wadham et al., 2013). The importance of anoxic shelf sediments as a potential source of dissolved iron to the water column has recently been reported for Antarctic shelf sediments (Measures et al., 2013; Monien et al., 2014; Henkel et al., 2018; Baloza et al., 2022), and this source appears to be at least as significant as the input of iceberg–hosted material (Nielsdóttir et al., 2012; Hatta et al., 2013; Measures et al., 2013; Monien et al., 2014; Borrione et al., 2014). Therefore, identifying microbial key players involved in the iron cycle is essential, especially for the Southern Ocean, to better understand the factors that control iron bioavailability and efflux into the water column. At the moment, however, baseline knowledge about iron-reducing microbial taxa in Antarctic sediment is very limited (Wunder et al., 2021; Aromokeye et al., 2021).

In shelf sediments, dissimilatory microbial iron reduction (DIR) plays a key role in the remineralization of organic matter (Thamdrup et al., 2000; Monien et al., 2014; Oni et al., 2015; Henkel et al., 2016; Henkel et al., 2018; Wunder et al., 2021; Schnakenberg et al., 2021; Baloza et al., 2022). Predominantly, the microbial communities identified in performing DIR include bacterial taxa belonging to the order *Desulfuromonadales* (mostly those of the genera *Desulfuromonas*, *Desulfuromusa*, *Pelobacter*, *Geopsychrobacter*, and *Geothermobacter*) (Kashefi et al., 2003; Holmes et al., 2004; Vandieken et al., 2006a; 2006b; Vandieken & Thamdrup, 2013; Aromokeye et al., 2018). Furthermore, *Sva1033*, a clade of *Desulfuromonadales*, was identified by Ravenschlag et al. (1999) and Wunder et al. (2021) using RNA stable isotope probing experiments with permanently cold marine sediments from the Arctic and Sub-Antarctic, respectively. Both studies showed that the clade *Sva1033* has iron-reducing capabilities.

Sedimentary redox conditions along the eastern shelf of the AP have recently been investigated by Baloza et al. (2022), who found that the supply of OM to the seafloor is mainly controlled by a sea ice cover. In areas of heavy ice cover, the low carbon supply coincides with low rates of benthic carbon remineralization. There, the surface sediments were characterized by a comparatively broad upper oxic zone of up to 4 cm with an underlying comparatively narrow ferruginous zone. With decreasing sea ice cover, an increase in carbon supply and benthic carbon remineralization rates was observed. At these sites, high dissolved iron concentrations of up to 400 µM were found at very shallow depths and below the ferruginous zones. A gradual decrease in sulfate concentrations and a steep increase in H_2S concentrations marked the beginning of the sulfidic zone (Baloza et al., 2022).

The present work on the microbial communities is complementary to the geochemical findings of Baloza et al. (2022) and is based on the same set of sediment samples. The study is intended as a base study to evaluate the impact of changing sea ice conditions on benthic microbial communities and—ultimately—nutrient fluxes across the sediment–water interface. We hypothesize that (i) the impacts of sea ice cover on organic matter fluxes are responsible for changes in benthic microbial communities, and (ii) the strong changes in redox zonation, induced by intense microbial organic matter remineralization rates, are coupled with an increment of

iron-reducers at stations with increased organic matter fluxes. In order to test the two hypotheses, sediment samples from five stations along a 400 nautical mile transect with contrasting sea ice conditions were investigated by 16S ribosomal RNA (rRNA) gene sequencing. Correlation, multivariate regression, and differential taxa abundance analyses were performed to identify the main factors shaping the microbial community composition.

2 Materials and Methods

2.1 Sample Collection

During research cruise PS118 with the German research vessel RV POLARSTERN (February–April 2019), sediments were collected from five stations along a 400-nautical mile transect from the eastern Antarctic Peninsula to the West of the South Orkney Islands (Figure 1; Table 1). In this study, we used sediments collected from five shelf stations at water depths ranging between 329 and 455 m to allow cross-comparison of sediment properties and OM turnover rates independent from water depth. The two deep stations (St5 and St6) were excluded from this study. At each station, a total of nine sediment cores with intact sediments and overlying water were collected from multiple deployments of a multi-corer (Oktopus GmbH, Kiel, Germany). Immediately upon retrieval, sediment cores were transferred to the ship's cool laboratory and placed in a water bath at 0 °C. Three cores were sliced on board to 0–1, 1–2, 2–3, 3–5, 5–7, and 14–16 cm layers and stored at −20 °C for DNA analysis. For pore-water and solid-phase analysis, six different cores were used and analyzed, as described previously by Baloza et al. (2022).

2.2 DNA Extraction and Sequencing

The DNA was extracted from 0.25 g of wet sediment using the DNeasy PowerSoil Kit (Q-BIOgene, Heidelberg, Germany) following the protocol provided by the manufacturer. Amplicon sequencing was conducted on an Illumina MiSeq machine at AWI laboratory. For the 16S rRNA gene amplicon library preparation, we used the bacterial primers 341F (5'-CCTACGGGNGGCWGCAG-3') and 785R (50-GACTACHVGGGTATC TAATCC-30), which amplify the 16S rRNA gene hypervariable region V3–V4 in Bacteria (400–425 bp fragment length). The amplicon library was sequenced with MiSeq v3 chemistry in a 2 × 300 bp paired-end run with >

50,000 reads per library, following the standard instructions of the 16S Metagenomic Sequencing Library Preparation protocol (Illumina, Inc., San Diego, CA, USA).

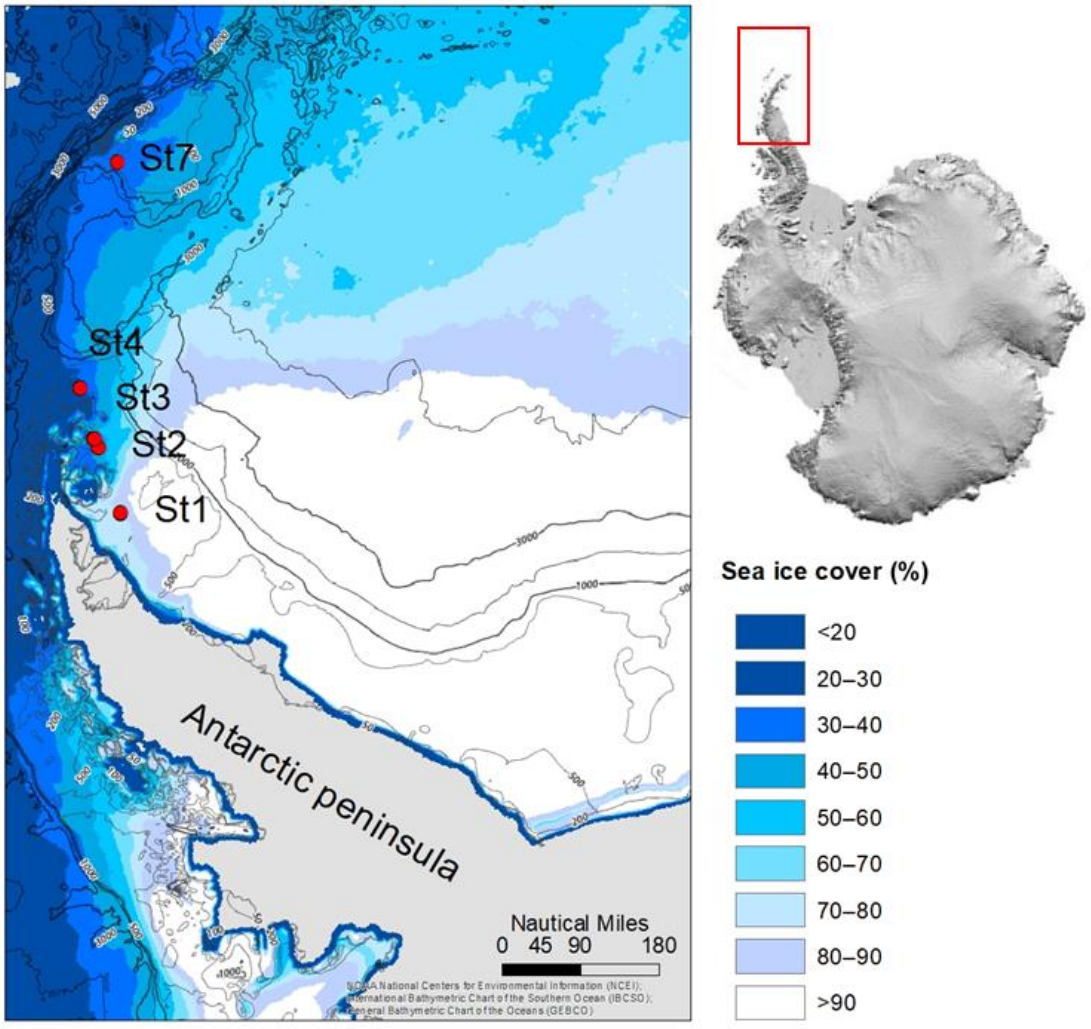

Figure 1. Map showing the Antarctic Peninsula with the locations of the sampled stations (red circles with station numbers) during the PS118 expedition modified after Baloza et al. (2022). Colors denote the proportion of time the ocean is covered by sea ice of concentration 85% or higher as calculated from AMSR-E satellite estimates of daily sea ice cover at 3.37 nautical mile resolution (Spreen et al., 2008). Water depth is indicated by isolines.

Table 1. Description of investigated stations, including water depth, ice cover, moderate sea ice index, and bottom water temperature. The ice cover (30-year average of daily sea ice concentration) was calculated from historical satellite data of the Sea ice Index, version 3 (Fetterer et al., 2017). The moderate sea ice index is the relative occurrence of moderate ice cover (defined as 5–35% ice cover), weighted by the length of daylight (sunrise to sunset), as described by Baloza et al. (2022). Total organic carbon (TOC) from the upper five cm depth. The Total Carbon Remineralization Rate was calculated from diffusive fluxes of O_2, NH_4^+, DFe, DMn, and S^{2-} using the equation from Baloza et al. (2022). The Total Carbon Supply Rate was calculated from the TOC removed in the upper layer due to aerobic C-remineralization added to the TOC accumulation rate.

	Longitude	Latitude	Date	Water Depth	Ice Cover	Mod. Sea ice Index	Bottom Water Temperature	TOC	Total Carbon Remineralization Rate	Total Carbon Supply Rate
	°W	°S	DD/MM/YYYY	m	%		°C	wt%	mmol m^{-2} d^{-1}	mmol m^{-2} d^{-1}
Shelf St1	57.75	64.98	04/03/2019	428	81	0.038	−1.9	0.71	1.134	2.67
Shelf St2	55.90	63.97	11/03/2019	415	49	0.127	−1.5	1.02	3.108	6.78
Shelf St3	55.74	63.80	14/03/2019	455	47	0.084	−1.2	0.19	1.452	3.20
Shelf St4	54.33	63.05	17/03/2019	447	33	0.174	−0.9	1.26	7.396	12.97
Shelf St7	46.55	60.93	28/03/2019	329	28	0.092	−0.1	0.60	1.833	2.50

2.3 Amplicon Data Analysis

The quality cleaning of the sequences was performed using several software tools. The first tool was Cutadapt (Martin, 2011), which was used to remove the attached primers from the data. Then, DADA2 packages in R (Callahan et al., 2016) were used for filtering and trimming low-quality sequences. Further, sequences with more than two expected errors were removed depending on their quality profiles. DADA2 was also used to merge the filtered forward and reverse reads and remove Chimeras from the denoised output. For the taxonomic classification, the SILVA 138 database (Quast et al., 2012) was used, and sequences with less than 90% of similarity with SILVA sequences were removed from the dataset. Absolute singletons (i.e., which refer to ASV sequence occurring only once in the full dataset) (Gobet et al., 2014), contaminant sequences (as observed in the negative control), and unspecific sequences (i.e., unclassified sequences at the domain level, chloroplast, and mitochondrial sequences) were removed from amplicon datasets before the statistical analysis. The total number of reads per sample was summarized in an amplicon sequence variants (ASVs) table (Table S1).

All statistical analyses were conducted using RStudio (v4.0.2; R Core Team, 2020). Sample data matrices and alpha diversity indices were generated using the R package 'phyloseq' (v1.32.0; McMurdie & Holmes, 2013). The rarefaction curves for each sample were generated based on 50 equally spaced rarefied sample sizes with 100 iterations. Non-metric multidimensional scaling (NMDS) analysis was conducted on Euclidean distance matrix based on ASV abundances that have undergone centered log-ratio (CLR) transformation using R package 'vegan' v2.5.7 (v2.5.7; Oksanen et al., 2013) and 'Composition' (v2.0.4; Van den Boogaart & Tolosana-Delgado, 2013), respectively. Differences in bacterial communities between groups of stations, defined based on sea ice cover, were tested with analysis of similarities (ANOSIM) in the R package 'vegan' (v2.5.7; Oksanen et al., 2013). Furthermore, the significance of the relationship between the frequency of moderate sea ice conditions, sediment depth, and community composition was tested using permanova tests (9999 unrestricted permutations; p-values < 0.05) with 'vegan' (v2.5.7; Oksanen et al., 2013). Geochemical parameters that shape microbial community compositions were standardized (z-scoring) and tested for predictor variable collinearity, then investigated to

determine the correlations between geochemical parameters and bacterial community compositions by distance-based redundancy analysis (dbRDA) in the R package 'vegan' (v2.5.7; Oksanen et al., 2013). The significance of the relationship between explanatory variables and community composition was tested using Monte Carlo permutation tests (9999 unrestricted permutations; with *p*-value < 0.05).

In order to identify taxonomical associations with iron cycling of all shelf stations, the Metastats-test-based differential abundance analysis of taxa was performed using the ALDEx2 package (v1.20.0; Fernandes et al., 2013) at a significance threshold of < 0.01 for the parametric test (glm.eBH) and non-parametric test (kw.ep). This analysis was done to examine the different bacterial taxa between the upper 3 cm of sediment of Shelf St4 dominated by ferruginous conditions against the upper 3 cm of Shelf St1 in which oxic respiration is the dominant process for OM degradation. Linear regression between centered log-ratio values of the ASV highly abundant in the ferruginous zone and dissolved iron (DFe) concentrations (in µmol/L) for the five shelf stations was performed using Pearson's correlations at $p < 0.05$. Furthermore, the environment coverage for the most closely related sequences (>99% similarity) to ASV highly abundant in the ferruginous zone was identified with BLASTn (GeneBank nucleotide database, 11 March 2022) and reported for each ASV.

3 Results

3.1 Bacterial Diversity and Sequencing Data Normalization

Using Illumina 16S rRNA amplicon sequencing of the V3–V4 hypervariable region, we obtained a final dataset of 4,252,065 reads (amplicons) in 90 samples, which were assigned to 38,655 ASVs belonging to bacterial taxonomies of 64 phyla, 162 classes, 378 orders, 536 families, and 786 genera. Rarefaction profiles of 16S rRNA gene sequences reached a plateau for most of the samples (Figure S1). Sediments hosted from hundreds to thousands of ASVs in each station were investigated. The highest bacterial richness (measured as the number of ASVs per sample) was observed in the uppermost sediments from all stations. However, bacterial diversity (measured with the observed richness, Shannon index and the inverse Simpson index) decreased northward

in the AP surface sediments and differed among sediment depths (Table S1, Figure S1). Overall, the heavy ice-covered station (St1) had the highest species richness and diversity of all stations.

Sample read counts ranged from 942 to 250,824 per sample (Table S1), the median sequencing depth was 30,167, and the 75th percentile and the 25th percentile were 55,749 and 18,651, respectively (Table S1). To check whether the uneven sequencing depth could introduce bias in the analysis of microbial communities between stations/layers, we tested if there is a significant correlation between the original dataset and the dataset that is normalized by a fixed number of reads. We normalized the dataset to the median sequencing depth (30,000) and to the smallest number of reads (942). Our results showed high correlations between the original dataset and the dataset that is normalized to the median sequencing depth (Mantel statistic r: 0.99, Significance: 1×10^{-4}). In contrast, the original dataset and the normalized dataset to the smallest number of reads did not significantly correlate (Mantel statistic r = 0.047, Significance: 0.2035). Based on this result, the original dataset was used for further analysis.

3.2 Effect of Sea ice Cover and Geochemistry on Bacterial Community Structure

Non-metric multidimensional scaling of ASVs did not show any clear pattern between stations (Figure 2A). However, when similarity in bacterial community structure was investigated between the stations grouped according to sea ice cover, the ANOSIM showed that bacterial communities between heavy ice cover and low ice cover stations are significantly different (ANOSIM, $r > 0.53$, $p < 0.001$). This result suggests that sea ice cover is a variable affecting the microbial community composition in the AP shelf sediments. To further test the contribution of sea ice cover in explaining differences in the microbial community, a permanova test was carried out, also including sediment depth as an explanatory factor, which is an important environmental constraint for microbes (Table S2). The permanova test showed that the frequency of moderate sea ice conditions (here defined as 5–35% sea ice cover) is significantly different between stations ($p < 0.0001$) and can explain 4% (when testing all sediment depths) to 13% (when testing the surface layers only) of the variation between microbial communities. Sediment depth was also tested as another factor affecting the microbial community structure. The results showed a significant difference between sediment depths ($p < 0.0001$), explaining 9% of the variance.

In order to identify the potential geochemical parameters that correlate with the microbial communities across all sites, a dbRDA was performed (Figure 2B, F = 2.90, $p < 0.001$, Df: 7, 81). The factors of O_2, DFe, DIC, SO_4^{2-}, Fe(III)/Al, S/Al, and the C/N ratio were included as explanatory variables in the model and together explained 20% of the total variation in the bacterial community. The variance inflation factor between these variables was below five (VIF = 4.3), indicating independence between variables. The total organic carbon content (TOC) was not used as an explanatory variable due to collinearity to other variables such as DIC, SO_4^{2-}, Fe (III)/Al and S/Al. NH_4^+. H_2S was also removed from this data analysis as it correlated with DIC and SO_4^{2-}, respectively. However, we used the sulfur content in the solid phase (S/Al) instead of H_2S as an indication of sulfate reduction and accumulation of pyrite.

Community composition between high ice cover and low ice cover stations was described mainly by the increase of O_2 (F = 3.754, $p = 0.003$) and DFe concentrations (F = 3.703, $p = 0.003$), followed by S/Al (F = 2.190, $p = 0.005$), Fe/Al (F = 2.009, $p = 0.005$), then C/N ratio (F = 1.868, $p = 0.011$), DIC (F = 1.636, $p = 0.025$), and SO_4^{2-} (F = 0.954, $p = 0.476$). In accordance with the NMDS ordination (Figure 2A,B), oxic layers at the heavy ice cover station exhibited a strong separation of bacterial communities from the low ice cover stations. However, anoxic layers at the heavy ice cover station tend to cluster together with the low ice cover stations. The model strongly attributed this distinction to O_2 and DFe differences between groups.

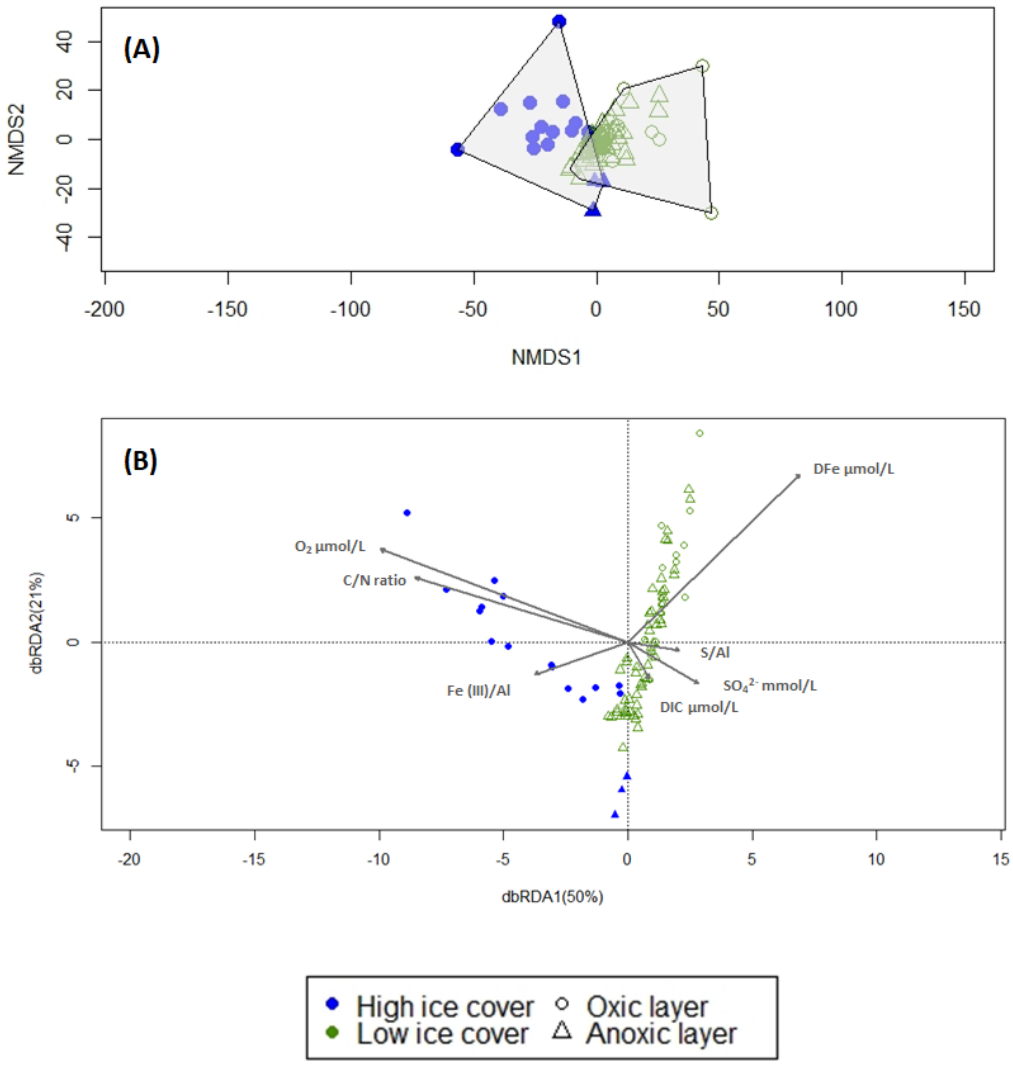

Figure 2. Microbial community composition of all five shelf stations. (**A**) Non-metric Multidimensional Scaling (NMDS) ordination of microbial community composition based on Euclidean distance after transforming the data using CLR for stations under high ice cover (Shelf St1) and low ice cover (Shelf St2, St3, St4, St7) (stress value = 0.152, R^2 = 0.98). (**B**) Distance-based redundancy analysis (dbRDA) ordination plot of bacterial communities. Sample points in panels A and B are distinguished by site and sediment depth (oxic and anoxic layer) and by color and shape, respectively. dbRDA1 (variation 50%) and dbRDA2 (variation 21%) axes are displayed, which constrain the Euclidean distance matrix with geochemical parameters O_2, DFe, DIC, SO_4^{2-}, Fe(III)/Al, S/Al, C/N ratio. The total model (F = 2.90, $p < 0.001$, Df: 7, 81) and each individual parameter ($p < 0.05$) were significant except for SO_4^{2-}.

3.3 Patterns in Bacterial Community Composition

Figure 3 shows the relative abundance of the 30 most abundant taxa (> 0.1%) across all five shelf stations. Across all stations, similarities in the distribution of benthic microbial communities have been observed. Dominant taxa belonged mostly to Gammaproteobacteria and Woeseia, Bacteroidota (mostly Bacteroidia), and NB1-j were present in all sediment depths and represented > 15% of the total microbial community (Figure 3). Distinct differences in the benthic microbial communities between heavy ice cover (Shelf St1) and low ice cover stations (Shelf St2, St3, St4 and St7) were also evident. Surface sediments of the low ice cover stations were dominated by anaerobic bacterial groups belonging to Proteobacteria (i.e., Halioglobus, order_B2M28, OM60(NOR5) clade, family_Rhodobacteraceae, and order_BD7-8) (>13%), Desulfobacterota (i.e., order_Sva1033, family_Desulfocapsaceae, order_Desulfobulbales, phylum_Desulfobacterota, family_Desulfosarcinaceae, Sva0081 sediment group) (> 16%) Sva0485 (3%), and Bacteroidota (i.e., Lutibacter, Lutimonas, family_Bacteroidetes BD2-2, class_Bacteroidia, family_Flavobacteriaceae) (10%) within the upper 3 cm of sediment. However, unlike the low ice cover stations, abundances of Desulfobacterota (order_Desulfobulbales, phylum_Desulfobacterota, family_Desulfosarcinaceae, Sva0081 sediment group) Sva0485, and Bacteroidota (i.e., Lutibacter, Lutimonas, family_Bacteroidetes BD2-2) were very low (< 0.1%) in the top 3 cm of the heavy ice cover station (Shelf St1) where oxic respiration dominated OM degradation. At the same site, the relative abundance of Proteobacteria (i.e., order_BD7-8, class_Alphaproteobacteria, order_AT-s2-59) (> 5%), Desulfobacterota (i.e., order_Sva1033, family_Desulfocapsaceae, phylum_Desulfobacterota) (> 7%), Sva0485 (1.4%) and Bacteroidota (i.e., Lutibacter, Lutimonas, family_Bacteroidetes BD2-2, class_Bacteroidia) (8.5%) increased with depth (in the ferruginous zone). Importantly, Sva1033, a clade of Desulfuromonadia, was highly abundant within the top 3 cm of the sediment at the low ice cover stations (> 7%) and at the sulfate reduction zones at 14 cm depth (> 4%). Except for the high ice cover station, the highest abundance of Sva1033 occurred below 3 cm sediment at the ferruginous zone (> 4%). In addition, sequences related to known sulfate reducers, such as Desulfobacterota (mostly Desulfobacteria and Desulfobulbia), Myxococcota (mostly Polyangia), and Sva0485 were highly abundant at 14

cm layer at low ice cover stations (14%) compare to the heavy ice cover station (< 3%; at 14 cm layer).

3.4 Potential Iron-Reducing Bacteria

The results of the differential abundance analysis between the ferruginous zone at Shelf St4 against the oxic zone at Shelf St1 revealed that 791 ASVs were significantly different between the two stations (Shelf St1 + Shelf St4) ($p < 0.05$; Table S3). Among these taxa, 12 ASVs contributed individually to more than 1% of the total community at the ferruginous zone, contributing together up to 14–20% at low ice cover stations in contrast to only < 6% at the high ice cover station of bacteria community in the ferruginous zone. The major groups of bacteria present were identified as members of Sva1033 (class Desulfuromonadia), SEEP-SRB4 (class Desulfobulbia), Persicirhabdus (class Verrucomicrobiae), Halioglobus, order_B2M28 and OM60 (NOR5) clade (class Gammaproteobacteria), Maribacter and Lutimonas (class Bacteroidia) and class Polyangia.

Across all stations, the relative abundance of 12 putative Fe-reducing bacterial taxa show similar patterns along sediment profiles mirroring dissolved iron profiles (Figure 4). Sva1033 was the most abundant taxon in the ferruginous sediments, with a peak in the relative abundance at the same depth as the highest dissolved Fe concentrations (Figure 4). The relative abundance of Sva1033 was highest (> 5%) near the sediment surface at low ice cover stations (Shelf St2, St3, St4, and St7) compared to the high ice cover station where the iron reduction zone is deeper (below 4 cm depth). There, its relative abundance was < 2% at the surface and 0.3% below 5 cm depth (Figure 4).

Furthermore, significant positive correlations between centered log-ratio values of putative Fe-reducing bacteria and dissolved Fe concentrations were observed for all potential iron-reducers ($p < 0.05$), except for order_B2M28, where $p = 0.08$ (Figure 5). The class_Gammaproteobacteria (asv4) showed the highest correlation with DFe concentrations, followed by Lutimonas (asv26), while order_B2M28 (asv6) had the weakest correlation (Figure 5).

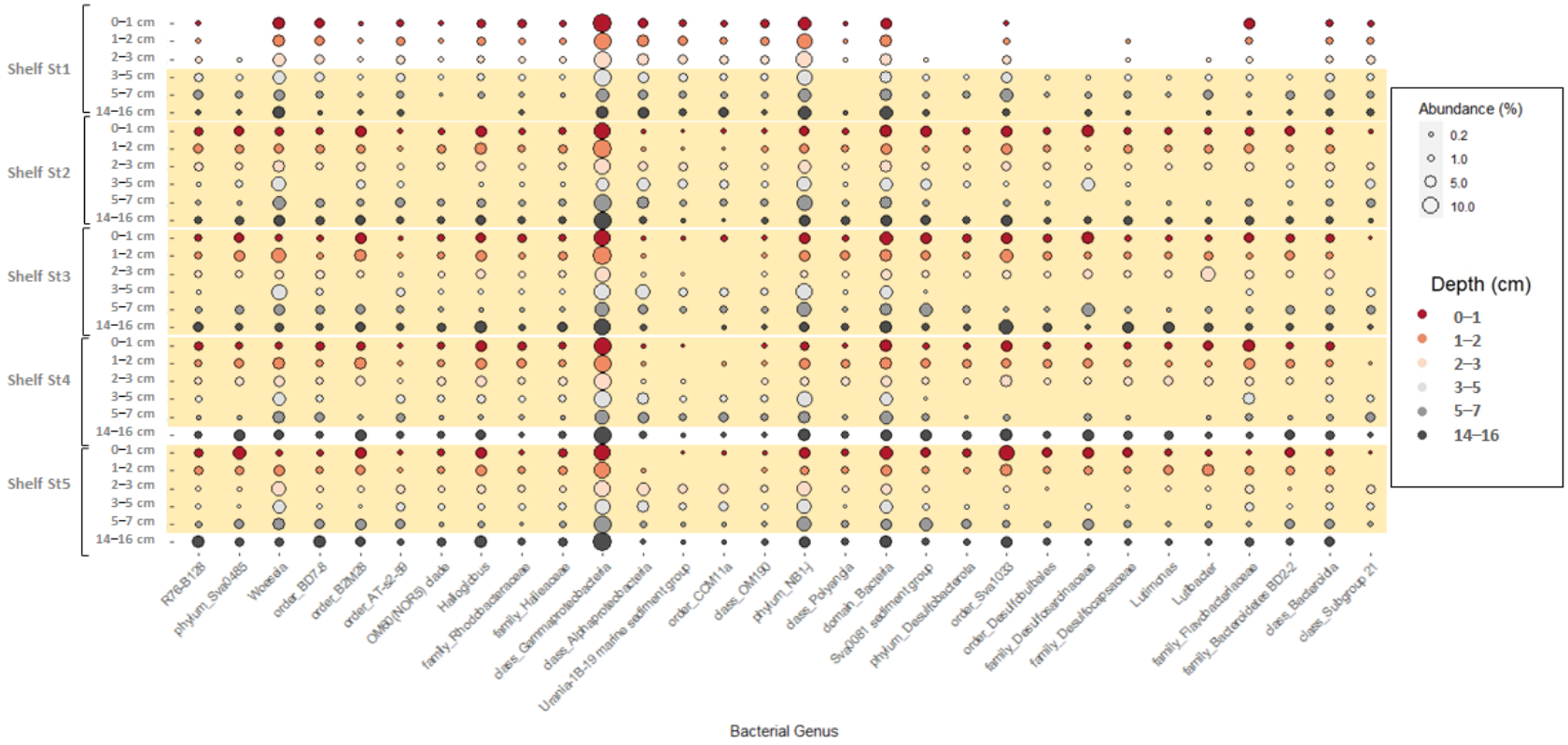

Figure 3. Microbial community composition in five shelf stations across the eastern coast of the Antarctic Peninsula. The relative abundance of bacterial 16S rRNA genes (cut-off > 0.1%) at genus-level resolution is shown for six sediment layers. For those taxa unclassified at genus, the higher taxonomic level is reported. Orange shadings represent the ferruginous zone in each station.

For the 12 putative Fe-reducing bacterial taxa, sequence homology searches within GenBank with the highest similarity (e.g., 100% or > 99%) were performed using BLASTn (NCBI website) (Table S4). The most closely related sequences were retrieved from the permanently cold marine sediment (e.g., Arctic and Antarctic; 31%) (Ravenschlag et al., 1999; Bowman et al., 2003; Purdy et al., 2003; Li et al., 2009; Hubert et al., 2009; Park et al., 2011; Teske et al., 2011; Cardman et al., 2014), from suboxic sediment (23%) (Vandieken & Thamdrup, 2013; Ruff et al., 2013), from methane seep sediment (17%) (Lösekann et al., 2007; Beal et al., 2009; Nunoura et al., 2010; Pischedda et al., 2011; Ruff et al., 2013), from tidal flat sediment (17%), and from hydrothermal or mud volcanos sediments and deposits (9%) (Figure 6 and Table S4).

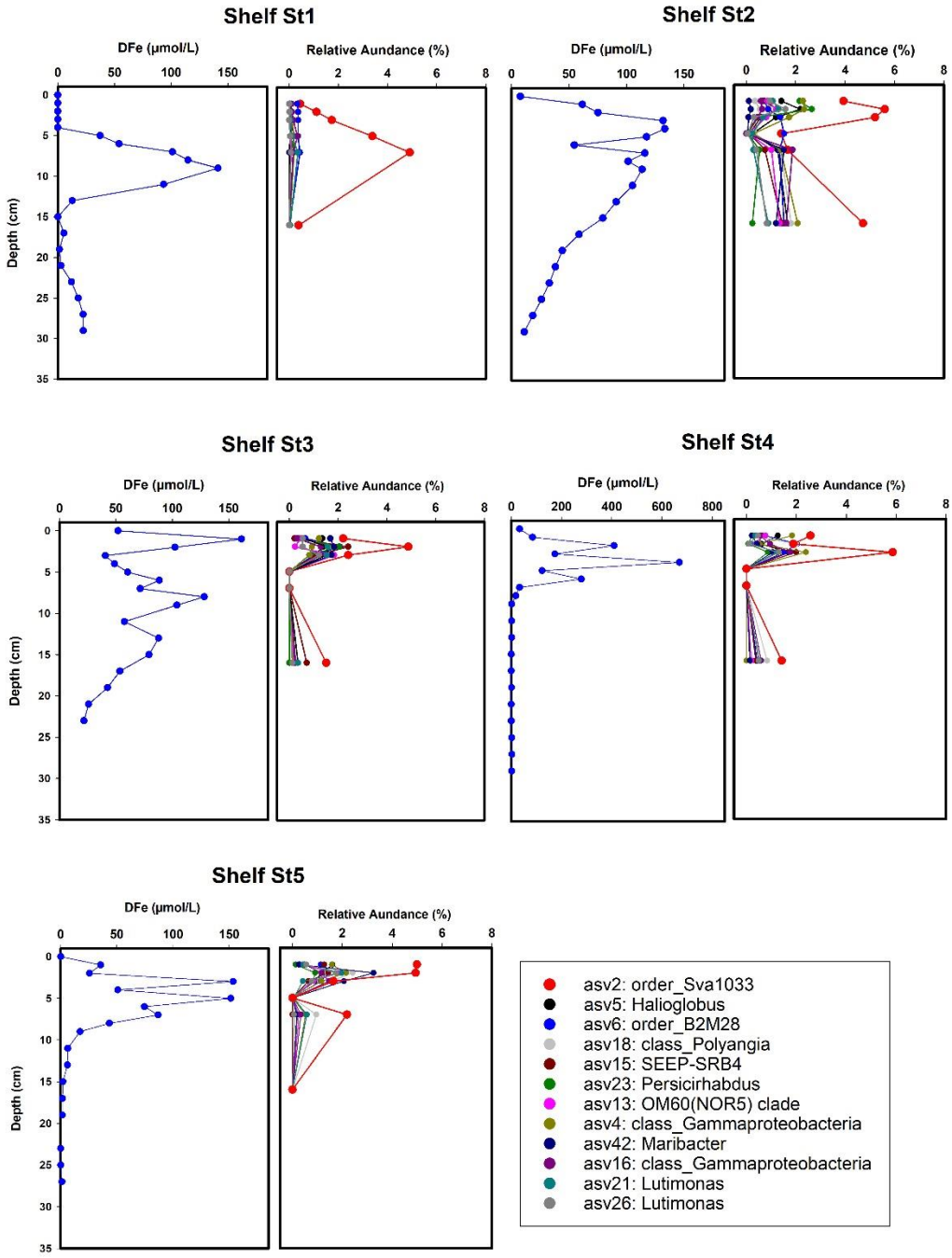

Figure 4. Representative profiles of the depth distribution of abundances of putative Fe-reducing bacteria in relation to dissolved iron (DFe) concentrations. Twelve different taxa were identified by applying differential abundance analysis. The relative abundance for each taxon was estimated from one sediment core. DFe concentrations were measured in a core near (<1 m) the collected microbial samples.

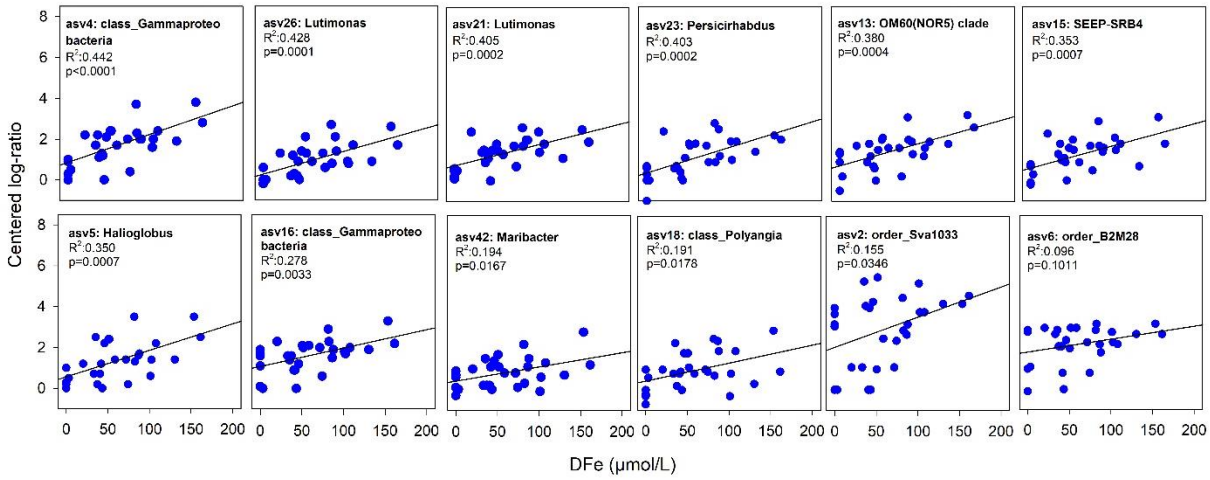

Figure 5. Linear regression between centered log-ratio values of putative Fe-reducing bacteria and DFe concentrations (in µmol/L) for five shelf stations. Linear models' R^2, Pearson's correlations, and their *p*-value are reported in each panel. The centered log ratio of putative Fe-reducing bacteria used in the correlations is the average of two sediment cores. At Shelf St4, only five depths were used in the correlations. The last depth was excluded as it is below the ferruginous zone.

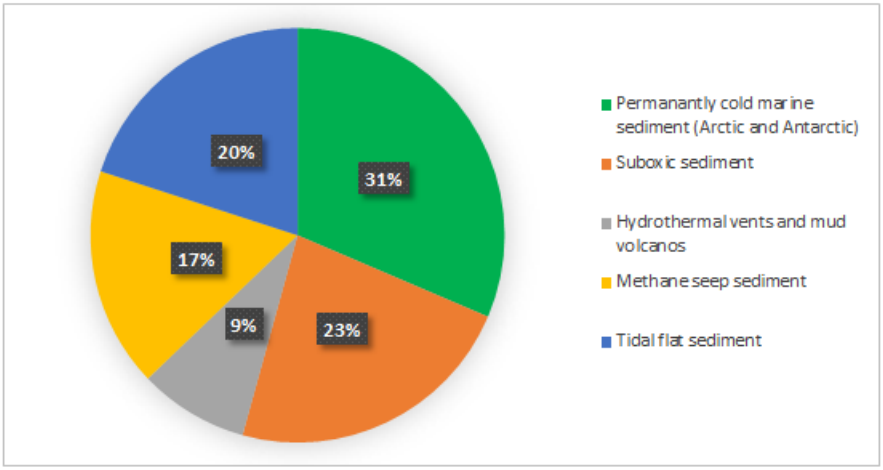

Figure 6. Environmental distribution for the most closely related sequences (> 99% similarity) to ASV highly abundant in the ferruginous zone. For details, see Table S2.

4 Discussion

The Antarctic Peninsula is projected to undergo profound climatic and environmental changes affecting seasonal sea ice cover, water column stratification, terrestrial meltwater run-off, and related nutrient input, and thus the conditions for primary production, organic carbon (OC) export, and benthic remineralization (Vaughan et al., 2003; Eayrs et al., 2021; Baloza et al., 2022). The impact of sea ice cover on microbial communities in underlying sediments is currently understudied. We hypothesize that (i) the impact of sea ice cover on organic matter fluxes are responsible for changes in benthic microbial communities, (ii) the strong changes in redox zonation, induced by intense microbial organic matter remineralization rates, are coupled with an increment of iron-reducers at stations with increased organic matter fluxes. In order to test the two hypotheses, microbial community composition at different sites with contrasting sea ice conditions along the eastern shelf of the AP was analyzed using 16S ribosomal RNA (rRNA) gene sequencing in surface (top 16 cm) sediments. Our findings, as discussed below, confirmed our hypotheses, showing that the effect of sea ice cover on organic carbon fluxes is the major driver for the variability in benthic microbial communities and redox zonation in the sediments of the eastern coast of the AP. Importantly, at low ice cover stations, characterized by high carbon supply and remineralization rates, we identified the dominance of potential iron-reducing bacteria (up to 20% of total sequences; Figure 4).

In this study, we observed that benthic microbial communities are significantly different between sites with high and low ice cover. Recently, a biogeochemical study of sediments from the exact same stations (Baloza et al., 2022) described sea ice conditions as the main factor controlling rates of organic carbon supply and benthic remineralization. A low carbon supply rate of 2.7 mmol C m^{-2} d^{-1} was measured for the station with heavy ice cover, explained by limited light availability and thus low surface-water primary production. In contrast, the locations with low sea ice cover showed high carbon supply rates of up to 13.0 mmol C m^{-2} d^{-1}, indicating that primary and export production are both enhanced when both light and water column stratification is sufficient to support phytoplankton growth. This scenario is supported by known large phytoplankton blooms and high primary production during spring/summer seasons on the

marginal ice zone along the AP (Mitchell & Holm-Hansen, 1991; Sakshaug et al., 1991; Schloss et al., 2002; Garibotti et al., 2005). Our results are in agreement with the previous studies on bacterial communities in marine Antarctic surface sediments (Learman et al., 2016; Currie et al., 2021). Currier et al. (2021) also found that the structure and composition of benthic microbial communities reflect the condition of sea ice cover. Microbial communities underlying first-year sea ice cover are highly dominated by heterotrophic algal polysaccharide degrading taxa and sulfate-reducing bacteria and correlate with higher chlorophyll a and total organic carbon content, reflecting increased surface-water productivity and high OC fluxes to the seafloor (Currie et al., 2021). Conversely, in sediments underlying multi-year sea ice cover, an enrichment of known archaeal and bacterial chemoautotrophs was found with considerably lower chlorophyll a and TOC contents, reflecting low surface-water primary production (Currie et al., 2021). In addition, Learman et al. (2016) found that the variability in the benthic microbial community composition along the Antarctic surface sediment is mainly driven by the quality and quantity of organic matter and the availability of nutrients. These findings agree with the results of our study that the impact of sea ice cover on organic matter fluxes is the main factor structuring the benthic microbial communities along the AP in such a way that they select the microorganisms that best respond to the given conditions.

The gradual decrease in sea ice cover along the transect of the investigated sites, accompanied by an increase in organic C-supply rates, have resulted in a distinctly different redox zonation of the underlying sediments suggesting that the different redox conditions are shaped by organic C burial rates and the activity of microorganisms with specific metabolic traits. Sediments at the heavy ice cover station were characterized by a low carbon remineralization rate of 1.1 mmol m^{-2} d^{-1} and a deeper oxygen penetration depth compared to stations with low ice cover (6.3 ± 0.7cm and 1.8 ± 0.02 to 0.5 ± 0.07cm, respectively) (Figure S2), resulting in the upper boundary of the ferruginous zone to be located below 5 cm depth (Baloza et al., 2022). However, unlike the heavy ice cover station, sediments of the low ice cover stations showed high benthic carbon remineralization rates (1.8–7.3 mmol m^{-2} d^{-1}), resulting in a more condensed redox zonation and high concentrations of dissolved Fe (> 400 µM at Shelf St4) close to the sediment surface (Figure

S2). Below the ferruginous zone, the gradual increase of H_2S concentrations below 10 cm depth was detected, marking the beginning of the sulfate reduction zone (Figure S2). In accordance with these observations, we found that the differences in microbial community composition between the high ice cover and the low ice cover stations are largely explained by dissolved O_2 and Fe concentrations in pore water (Figure 2B), which are fundamentally different in the uppermost sediment between stations with high and low ice cover (Figure 2B). This indicates that microbial communities in the surface sediments of the high ice cover station are mainly dominated by aerobes. In contrast, the variation in community composition over sediment depth at the stations with low ice cover was explained mainly by the variability of dissolved Fe concentration, S/Al, DIC, and SO_4^{2-} (Figure 2B), suggesting that iron and sulfate-reducing bacteria are the dominant players.

Microbial communities in surface sediments (i.e., 0–1 cm) of all stations are dominated by bacterial groups belonging to *Gammaproteobacteria*, *Alphaproteobacteria*, *Bacteroidota*, and *NB1-j*, which were often detected during the initial degradation of algal-derived organic matter (Bano & Hollibaugh, 2002; Teske et al., 2011; Teeling et al., 2012; Ruff et al., 2014). At the low ice cover stations, anaerobic bacterial communities of iron and sulfate reducers (31% at Shelf St4 to 41% at Shelf St7) were more abundant at these sites compared to the heavy ice cover station. The relative abundance of *Desulfobacterota* (mostly order_Sva1033, family_*Desulfocapsaceae*, phylum_*Desulfobacterota*), which harbor many species of iron reducer taxa (Roden & Lovley, 1993; Vandieken et al., 2006b; Buongiorno et al., 2019; Wunder et al., 2021) and sequences related to known sulfate reducers, such as *Desulfobacterota* (mostly *Desulfobacteria* and *Desulfobulbia*), *Myxococcota* (mostly *Polyangia*), and *Sva0485* were abundant near the sediment surface of low ice cover (> 20%) and at greater depth (14 cm depth) (> 12%). Similarly, some of those taxa have been previously observed in shallower depths in more reducing shelf sediments of the Sub-Antarctic island of South Georgia (Wunder et al., 2021) and Arctic fjords (Jørgensen et al., 2021). Unlike the low ice cover stations, the relative abundance of anaerobic microbial communities of Desulfobacterota at the heavy ice cover station increased below the oxic zone

and reached the highest relative abundance (> 10%) within the ferruginous zone, reflecting low burial rates of organic matter.

Furthermore, the high relative abundance of sulfate reducers in the ferruginous zone at the sites with low ice cover can be explained by the tight link between the biogeochemical cycles of iron and sulfur. For this reason, Fe liberation into the pore water can result either from dissimilatory iron reduction (DIR) or happen abiotically related to sulfide oxidation by Fe(III) reduction (e.g., Canfield, 1989). The tight coupling of the post-depositional iron and sulfur cycles has been demonstrated recently based on geochemical data from the Argentina continental margin (Riedinger et al., 2017), Arctic sediments (Wehrmann et al., 2017; Michaud et al., 2020) and (sub-) Antarctic sediments (Wunder et al., 2021). Wunder et al. (2021) suggested that the high relative abundance of sulfate reducers in the ferruginous zones is due to sulfate reduction masked by the reoxidation of the produced sulfide to sulfate via Fe(III) reduction supporting the persistence of sulfate reducers.

The anoxic shelf sediments have recently been considered a potential source of bioavailable Fe to Antarctic coastal waters and beyond (Monien et al., 2014). Along the sampling transect of the AP, elevated upward fluxes of DFe in the sediment were detected at the low ice cover stations (52 to 171 µmol m^{-2} d^{-1}), while a low upward flux of DFe was observed at the heavy ice cover station (17.7 µmol m^{-2} d^{-1}). The steep concentration gradients of DFe close to the sediment surface indicate that more DFe might escape from shelf sediments into the water column highlighting the importance of sediments underlying low ice cover as a potential source for limiting nutrients to the shelf waters (Baloza et al., 2022). To identify taxa potentially involved in the sedimentary biogeochemical cycling of iron, we investigated differences in bacterial community composition under different DFe fluxes.

At all sites, the distribution of *Sva1033*, a clade of Desulfuromonadia, is tightly coupled to the increase in the dissolved iron concentration showing the steepest slope in the linear regression (Figure 5). At low ice cover stations, Sva1033 increased close to surface sediment and peaked in abundance (> 7%) at several centimeter depths where iron reduction predominates. Only

sediments at the heavy ice cover station where the ferruginous zone is located at greater sediment depth, the relative abundance of *Sva1033* decreased (< 2%) near to sediment surface while it increased (> 4%) below 5 cm depth in the ferruginous zone (Figure 4). Members of this clade were detected previously in the ferruginous sediments of the (sub-) Antarctic (Wunder et al., 2021) and Arctic shelf (Ravenschlag et al., 1999; Buongiorno et al., 2019) and were suggested to be responsible for the iron reduction in these permanently cold marine sediments. Their metabolic capabilities to reduce iron have been confirmed recently by incubation experiments of Antarctic Potter Cove sediments using RNA stable isotope probing (Wunder et al., 2021). Our results provide further evidence that *Sva1033* plays an active role in the cycling of iron in Antarctic sediments.

Other putatively Fe-reducing bacterial taxa identified in this study besides Sva1033 (class *Desulfuromonadia*) are *SEEP-SRB4* (class *Desulfobulbia*), *Persicirhabdus* (class *Verrucomicrobiae*), *Halioglobus*, *order_B2M28* and *OM60 (NOR5)* clade (class *Gammaproteobacteria*), *Maribacter* and *Lutimonas* (class *Bacteroidia*) and class *Polyangia* (Figures 4 and 5). Members of these groups make up the bulk of sedimentary anaerobic communities in the ferruginous zones, and some of them were shown previously to be present in marine sediments with high dissolved iron and manganese concentrations (Santelli et al., 2008; Hubert et al., 2009; Beal et al., 2009; Li et al., 2009; Park et al., 2011; Vandieken & Thamdrup, 2013), suggesting an important role in meditating metal biogeochemical cycling. Moreover, the results of the environmental distribution for the most closely related sequences (> 99% similarity) reveal that > 70% of these taxa were detected before in permanently cold marine sediments (e.g., Antarctic and Arctic) (Ravenschlag et al., 1999; Bowman et al., 2003; Purdy et al., 2003; Li et al., 2009; Hubert et al., 2009; Park et al., 2011; Ruff et al., 2014; Wunder et al., 2021) and various deep-sea environments (Santelli et al., 2008; Beal et al., 2009; Nunoura et al., 2010; Pischedda et al., 2011; Ruff et al., 2013), indicating that most of these taxa are psychrophilic (Figure 6).

An increase in the relative sequence abundance of putatively Fe-reducing bacterial taxa in the ferruginous zone at both high ice cover and low ice cover stations (Figures 4 and 5) provides evidence that they might be involved in DIR in surface sediments of the AP or have syntrophic

partnerships and/or common metabolic preferences with iron reducers. Future work should explore the in situ metabolic activity of these potential Fe-reducing bacterial taxa, with a particular focus on Sva1033, to better understand factors that control iron bioavailability and potential efflux into the water column from Antarctic and Southern Ocean shelf sediments.

The extent of Antarctic sea ice has undergone a drastic decline since 2015, indicating increased interannual variability (Eayrs et al., 2021). Model projections further indicate a continued decline in the near future (Taylor et al., 2012). Our results show that the melting of sea ice sustains favorable light conditions and water column stratification, resulting in increased primary productivity and organic matter flux to the seafloor (Baloza et al., 2022). These changes, in turn, have an impact on the activity and composition of benthic microbial communities. Consequently, the regional (southward) shift in sea ice cover could potentially lead to an increase in benthic remineralization rates, promoting a shift in microbial communities towards anaerobic taxa and an increase in benthic iron fluxes. The latter could have positive feedback on primary production in the water column, further stimulating the overall process.

5 Conclusions

Our study reveals that sea ice cover and associated carbon burial fluxes explain up to 13% of the variability between microbial communities in the AP shelf sediments. At all stations, *Sva1033* was the dominant member of Desulfuromonadales in the ferruginous sediments, which confirms its putative role in reducing iron oxide minerals in permanently cold marine sediments. Furthermore, our approach identified for the first time other taxa that might contribute to the benthic iron cycle or have ecological relationships with the dominant iron reducers. The significant contribution of potential iron reducers (up to 15%) to microbial communities reveals the importance of sediments underlying low ice cover as a potential source of dissolved iron to shelf waters. In this regard, the findings reported here expand our knowledge about changes induced by the increase of OM load to microbial community composition in AP shelf sediments under contracting sea ice cover and stimulate future research to better elucidate the role of microbial iron reducers in the biogeochemical iron cycle.

Supplementary Materials: The following supporting information can be downloaded at: www.mdpi.com/xxx/s1, Table S1: Overview of sampled stations during RV Polarstern expedition PS118. The table consists of sampling information for each station, number of sequences in each step of the bioinformatics workflow as well as alpha diversity indices: (1) observed richness, (2) Shannon and (3) inverse Simpson, conducted using the R package 'phyloseq'. Table S2: Output PERMANOVA and distance-based redundancy analysis (dbRDA). Table S3: ASVs highly abundant in the ferruginous zone. Differential abundance of taxa between surface sediments (0–3 cm) of stations Shelf St1 and Shelf St4 samples according to the t-test based metastats analysis. Differentially abundant taxa having statistically significant differences for parametric test (glm.eBH) ($p < 0.01$) and non-parametric test (kw.ep) ($p < 0.05$) are reported for each ASV per sample. Table S4: The most closely related sequences with identity (ID) >99%, as identified with BLASTn (GeneBank nucleotide database, 12 June 2022). Figure S1: Diversity indices for bacterial communities in six different depths for five shelf stations across the eastern coast of Antarctic Peninsula. Figure S2: Representative profiles of reactive pore water compounds at the five shelf stations. Figure S3: Schematic illustration of the pore-water profiles that were typical for heavy ice cover (Shelf St1) (A) and low ice cover (Shelf St4) (B) of this study. Figure S4: Representative profiles of the depth distribution of putative Fe-reducing bacteria in relation to dissolved/pore-water iron (DFe) concentrations. Figure S5: Representative profiles of the depth distribution of putative Fe-reducing bacteria in relation to dissolved/pore-water iron (DFe) concentrations.

Author Contributions: Conceptualization, M.M., M.B., and M.H.; Fieldwork, M.B. and M.H.; molecular genetic analysis, M.B. and M.M..; geochemical analysis, M.B., M.H., S.H., and S.K..; data analysis, M.B. and M.M.; writing—original draft preparation, M.B. and M.M.; writing—review and editing, M.B., M.M., M.H., S.H., and S.K.; supervision, M.M. and M.H.; funding acquisition, M.H. All authors have read and agreed to the published version of the manuscript.

Funding: This study was funded by the AWI Grant-No. AWI_PS118_05, with open access funding enabled and organized by Project DEAL.

Institutional Review Board Statement: Not applicable.

Data Availability Statement: Sequence data for this study have been deposited in the European Nucleotide Archive (ENA) at EMBL-EBI under accession number PRJEB57442 (https://www.ebi.ac.uk/ena/data/view/PRJEB57442), using the data brokerage service of the German Federation for Biological Data GFBio, (accessed on 9 June 2023, Diepenbroek et al., 2014).

Acknowledgments: The authors thank the captain and crew members of RV POLARSTERN during the PS118 expedition as well as Jakob Barz and Swantje Rogge (HGF-MPG Joint Research Group for Deep-Sea Ecology and Technology) for technical support. The authors are also grateful to Katja Metfies for support with Illumina sequencing.

Conflicts of Interest: The authors declare no conflict of interest. The funders had no role in the design of the study; in the collection, analyses, or interpretation of data; in the writing of the manuscript; or in the decision to publish the results.

References

Abell, G. C., & Bowman, J. P. (2005). Ecological and biogeographic relationships of class Flavobacteria in the Southern Ocean. *FEMS Microbiology Ecology, 51*(2), 265-277. doi:https://doi.org/10.1016/j.femsec.2004.09.001

Aromokeye, D. A., Richter-Heitmann, T., Oni, O. E., Kulkarni, A., Yin, X., Kasten, S., et al. (2018). Temperature controls crystalline iron oxide utilization by microbial communities in methanic ferruginous marine sediment incubations. *Frontiers in microbiology, 9*, 2574. doi:https://doi.org/10.3389/fmicb.2018.02574

Aromokeye, D. A., Willis-Poratti, G., Wunder, L. C., Yin, X., Wendt, J., Richter-Heitmann, T., et al. (2021). Macroalgae degradation promotes microbial iron reduction via electron shuttling in coastal Antarctic sediments. *Environment International, 156*, 106602. doi:https://doi.org/10.1016/j.envint.2021.106602

Azam, F., & Malfatti, F. (2007). Microbial structuring of marine ecosystems. *Nature Reviews Microbiology, 5*(10), 782-791. doi:https://doi.org/10.1038/nrmicro1747

Baloza, M., Henkel, S., Geibert, W., Kasten, S., & Holtappels, M. (2022). Benthic Carbon Remineralization and Iron Cycling in Relation to Sea ice Cover Along the Eastern Continental Shelf of the Antarctic Peninsula. *Journal of Geophysical Research: Oceans, 127*(7). doi:https://doi.org/10.1029/2021JC018401

Bano, N., & Hollibaugh, J. T. (2002). Phylogenetic Composition of Bacterioplankton Assemblages from the Arctic Ocean. *Applied and Environmental Microbiology, 68*(2), 505-518. doi:doi:10.1128/AEM.68.2.505-518.2002

Beal, E. J., House, C. H., & Orphan, V. J. (2009). Manganese- and iron-dependent marine methane oxidation. *Science, 325*(5937), 184-187. doi:10.1126/science.1169984

Berner, R. A. (1980). *Early diagenesis: a theoretical approach*: Princeton University Press.

Bienhold, C., Boetius, A., & Ramette, A. (2012). The energy–diversity relationship of complex bacterial communities in Arctic deep-sea sediments. *The ISME journal, 6*(4), 724-732. doi:https://doi.org/10.1038/ismej.2011.140

Borrione, I., Aumont, O., Nielsdóttir, M., & Schlitzer, R. (2014). Sedimentary and atmospheric sources of iron around South Georgia, Southern Ocean: a modelling perspective. *Biogeosciences, 11*(7), 1981-2001. doi:https://doi.org/10.5194/bg-11-1981-2014

Bowman, J. P., McCammon, S. A., Gibson, J. A. E., Robertson, L., & Nichols, P. D. (2003). Prokaryotic Metabolic Activity and Community Structure in Antarctic Continental Shelf Sediments. *Applied and Environmental Microbiology, 69*(5), 2448-2462. doi:doi:10.1128/AEM.69.5.2448-2462.2003

Boyd, P. W., Jickells, T., Law, C., Blain, S., Boyle, E., Buesseler, K., et al. (2007). Mesoscale iron enrichment experiments 1993-2005: synthesis and future directions. *science, 315*(5812), 612-617. doi:10.1126/science.1131669

Buongiorno, J., Herbert, L. C., Wehrmann, L. M., Michaud, A. B., Laufer, K., Røy, H., et al. (2019). Complex Microbial Communities Drive Iron and Sulfur Cycling in Arctic Fjord Sediments. *Applied and Environmental Microbiology, 85*(14), e00949-00919. doi:doi:10.1128/AEM.00949-19

Burdige, D. J. (2007). Preservation of Organic Matter in Marine Sediments: Controls, Mechanisms, and an Imbalance in Sediment Organic Carbon Budgets? *Chemical Reviews, 107*(2), 467-485. doi:https://doi.org/10.1021/cr050347q

Callahan, B. J., McMurdie, P. J., Rosen, M. J., Han, A. W., Johnson, A. J. A., & Holmes, S. P. (2016). DADA2: High-resolution sample inference from Illumina amplicon data. *Nature Methods, 13*(7), 581-583. doi:10.1038/nmeth.3869

Canfield, D. E. (1989). Reactive iron in marine sediments. *Geochimica et Cosmochimica Acta, 53*(3), 619-632. doi:https://doi.org/10.1016/0016-7037(89)90005-7

Canfield, D. E. (1993). Organic matter oxidation in marine sediments. In *Interactions of C, N, P and S biogeochemical cycles and global change* (pp. 333-363): Springer.

Canfield, D. E., & Thamdrup, B. (2009). Towards a consistent classification scheme for geochemical environments, or, why we wish the term 'suboxic' would go away. *Geobiology, 7*(4), 385-392. doi:https://doi.org/10.1111/j.1472-4669.2009.00214.x

Canfield, D. E., Thamdrup, B., & Hansen, J. W. (1993). The anaerobic degradation of organic matter in Danish coastal sediments: Iron reduction, manganese reduction, and sulfate

reduction. *Geochimica et Cosmochimica Acta, 57*(16), 3867-3883. doi:https://doi.org/10.1016/0016-7037(93)90340-3

Cardman, Z., Arnosti, C., Durbin, A., Ziervogel, K., Cox, C., Steen, A. D., et al. (2014). Verrucomicrobia are candidates for polysaccharide-degrading bacterioplankton in an arctic fjord of Svalbard. *Applied and Environmental Microbiology, 80*(12), 3749-3756. doi:10.1128/aem.00899-14

Cho, H., Hwang, C. Y., Kim, J.-G., Kang, S., Knittel, K., Choi, A., et al. (2020). A Unique Benthic Microbial Community Underlying the Phaeocystis antarctica-Dominated Amundsen Sea Polynya, Antarctica: A Proxy for Assessing the Impact of Global Changes. *Frontiers in Marine Science, 6*. doi:10.3389/fmars.2019.00797

Currie, A. A., Marshall, A. J., Lohrer, A. M., Cummings, V. J., Seabrook, S., & Cary, S. C. (2021). Sea ice Dynamics Drive Benthic Microbial Communities in McMurdo Sound, Antarctica. *Frontiers in Microbiology, 12*. doi:10.3389/fmicb.2021.745915

D'Hondt, S., Jørgensen, B. B., Miller, D. J., Batzke, A., Blake, R., Cragg, B. A., et al. (2004). Distributions of microbial activities in deep subseafloor sediments. *Science, 306*(5705), 2216-2221. doi:10.1126/science.1101155

D'Hondt, S., Rutherford, S., & Spivack, A. J. (2002). Metabolic activity of subsurface life in deep-sea sediments. *Science, 295*(5562), 2067-2070. doi:10.1126/science.1064878

de Haas, H., van Weering, T. C., & de Stigter, H. (2002). Organic carbon in shelf seas: sinks or sources, processes and products. *Continental Shelf Research, 22*(5), 691-717. doi:https://doi.org/10.1016/S0278-4343(01)00093-0

Diepenbroek, M., Glöckner, F. O., Grobe, P., Güntsch, A., Huber, R., König-Ries, B., et al. (2014). *Towards an integrated biodiversity and ecological research data management and archiving platform: the German federation for the curation of biological data (GFBio).* Paper presented at the GI-Jahrestagung.

Eayrs, C., Li, X., Raphael, M. N., & Holland, D. M. (2021). Rapid decline in Antarctic sea ice in recent years hints at future change. *Nature Geoscience, 14*(7), 460-464. doi:10.1038/s41561-021-00768-3

Elderfield, H. (1985). Element cycling in bottom sediments. *Philosophical Transactions of the Royal Society of London*(A315(1531)), 19-23. Retrieved from https://www.scopus.com/inward/record.uri?eid=2-s2.0-0022243898&partnerID=40&md5=805f1ace6f01c195272239d2de931472

Falkowski, P. G., Fenchel, T., & Delong, E. F. (2008). The microbial engines that drive Earth's biogeochemical cycles. *science, 320*(5879), 1034-1039. doi:DOI: 10.1126/science.1153213

Fernandes, A., Macklaim, J., Linn, T., Reid, G., & Gloor, G. (2013). ANOVA-like differential gene expression analysis of single-organism and meta-RNA-seq. *PLoS one, 8*(7), e67019.

Fetterer, F., Knowles, K., Meier, W. N., Savoie, M., & Windnagel, A. K. (2017). Sea ice Index, Version 3. [Years 1978-2019] Sea ice Index, Version 3. [Years 1978-2019]. Boulder, Colorado USA. NSIDC: National Snow and Ice Data Center. doi:doi: https://doi.org/10.7265/N5K072F8. [last access April 2021]

Froelich, P. N., Klinkhammer, G., Bender, M. L., Luedtke, N., Heath, G. R., Cullen, D., et al. (1979). Early oxidation of organic matter in pelagic sediments of the eastern equatorial Atlantic: suboxic diagenesis. *Geochimica et Cosmochimica Acta, 43*(7), 1075-1090. doi:https://doi.org/10.1016/0016-7037(79)90095-4

Garibotti, I. A., Vernet, M., Smith, R. C., & Ferrario, M. E. (2005). Interannual variability in the distribution of the phytoplankton standing stock across the seasonal sea ice zone west of the Antarctic Peninsula. *Journal of Plankton Research, 27*(8), 825-843. doi:https://doi.org/10.1093/plankt/fbi056

Gobet, A., Boetius, A., & Ramette, A. (2014). Ecological coherence of diversity patterns derived from classical fingerprinting and N ext G eneration S equencing techniques. *Environmental Microbiology, 16*(9), 2672-2681. doi:https://doi.org/10.1111/1462-2920.12308

Hatta, M., Measures, C., Selph, K., Zhou, M., & Hiscock, W. (2013). Iron fluxes from the shelf regions near the South Shetland Islands in the Drake Passage during the austral-winter 2006. *Deep Sea Research Part II: Topical Studies in Oceanography, 90*, 89-101. doi:https://doi.org/10.1016/j.dsr2.2012.11.003

Henkel, S., Kasten, S., Hartmann, J. F., Silva-Busso, A., & Staubwasser, M. (2018). Iron cycling and stable Fe isotope fractionation in Antarctic shelf sediments, King George Island. *Geochimica et Cosmochimica Acta, 237*, 320-338. doi:https://doi.org/10.1016/j.gca.2018.06.042

Henkel, S., Kasten, S., Poulton, S. W., & Staubwasser, M. (2016). Determination of the stable iron isotopic composition of sequentially leached iron phases in marine sediments. *Chemical Geology, 421*, 93-102. doi:https://doi.org/10.1016/j.chemgeo.2015.12.003

Holmes, D. E., Nicoll, J. S., Bond, D. R., & Lovley, D. R. (2004). Potential role of a novel psychrotolerant member of the family Geobacteraceae, Geopsychrobacter electrodiphilus gen. nov., sp. nov., in electricity production by a marine sediment fuel cell. *Applied and Environmental Microbiology, 70*(10), 6023-6030. doi:https://doi.org/10.1128/AEM.70.10.6023-6030.2004

Hubert, C., Loy, A., Nickel, M., Arnosti, C., Baranyi, C., Brüchert, V., et al. (2009). A constant flux of diverse thermophilic bacteria into the cold Arctic seabed. *Science, 325*(5947), 1541-1544. doi:10.1126/science.1174012

Jørgensen, B. B., & Kasten, S. (2006). Sulfur cycling and methane oxidation. In *Marine geochemistry* (pp. 271-309): Springer.

Jørgensen, B. B., Laufer, K., Michaud, A. B., & Wehrmann, L. M. (2021). Biogeochemistry and microbiology of high Arctic marine sediment ecosystems—Case study of Svalbard fjords. *Limnology and Oceanography, 66*(S1), S273-S292. doi:https://doi.org/10.1002/lno.11551

Jørgensen, S. L., Hannisdal, B., Lanzén, A., Baumberger, T., Flesland, K., Fonseca, R., et al. (2012). Correlating microbial community profiles with geochemical data in highly stratified sediments from the Arctic Mid-Ocean Ridge. *Proceedings of the National Academy of Sciences, 109*(42), E2846-E2855. doi:https://doi.org/10.1073/pnas.1207574109

Kashefi, K., Holmes, D. E., Baross, J. A., & Lovley, D. R. (2003). Thermophily in the Geobacteraceae: Geothermobacter ehrlichii gen. nov., sp. nov., a novel thermophilic member of the Geobacteraceae from the “Bag City” hydrothermal vent. *Applied and Environmental Microbiology, 69*(5), 2985-2993. doi:https://doi.org/10.1128/AEM.69.5.2985-2993.2003

Kasten, S., Zabel, M., Heuer, V., & Hensen, C. (2003). Processes and signals of nonsteady-state diagenesis in deep-sea sediments and their pore waters. In *The South Atlantic in the late quaternary* (pp. 431-459): Springer.

Lancelot, C., de Montety, A., Goosse, H., Becquevort, S., Schoemann, V., Pasquer, B., et al. (2009). Spatial distribution of the iron supply to phytoplankton in the Southern Ocean: a model study. *Biogeosciences, 6*(12), 2861-2878. doi:10.5194/bg-6-2861-2009

Learman, D. R., Henson, M. W., Thrash, J. C., Temperton, B., Brannock, P. M., Santos, S. R., et al. (2016). Biogeochemical and Microbial Variation across 5500 km of Antarctic Surface Sediment Implicates Organic Matter as a Driver of Benthic Community Structure. *Frontiers in Microbiology, 7*. doi:10.3389/fmicb.2016.00284

Li, H., Yu, Y., Luo, W., Zeng, Y., & Chen, B. (2009). Bacterial diversity in surface sediments from the Pacific Arctic Ocean. *Extremophiles, 13*(2), 233-246. doi:https://doi.org/10.1007/s00792-009-0225-7

Lösekann, T., Knittel, K., Nadalig, T., Fuchs, B., Niemann, H., Boetius, A., et al. (2007). Diversity and abundance of aerobic and anaerobic methane oxidizers at the Haakon Mosby Mud Volcano, Barents Sea. *Applied and Environmental Microbiology, 73*(10), 3348-3362. doi:10.1128/aem.00016-07

Martin, J. H. (1990). Glacial-interglacial CO2 change: The iron hypothesis. *Paleoceanography, 5*(1), 1-13. doi: https://doi.org/10.1029/PA005i001p00001

Martin, J. H., Gordon, R. M., & Fitzwater, S. E. (1990). Iron in Antarctic waters. *Nature, 345*(6271), 156-158. doi:https://doi.org/10.1038/345156a0

Martin, M. (2011). Cutadapt removes adapter sequences from high-throughput sequencing reads. *EMBnet. journal, 17*(1), 10-12. doi:https://doi.org/10.14806/ej.17.1.200

McMurdie, P. J., & Holmes, S. (2013). phyloseq: an R package for reproducible interactive analysis and graphics of microbiome census data. *PloS one, 8*(4), e61217. doi:https://doi.org/10.1371/journal.pone.0061217

Measures, C., Brown, M., Selph, K., Apprill, A., Zhou, M., Hatta, M., et al. (2013). The influence of shelf processes in delivering dissolved iron to the HNLC waters of the Drake Passage,

Antarctica. *Deep Sea Research Part II: Topical Studies in Oceanography, 90*, 77-88. doi:https://doi.org/10.1016/j.dsr2.2012.11.004

Michaud, A. B., Laufer, K., Findlay, A., Pellerin, A., Antler, G., Turchyn, A. V., et al. (2020). Glacial influence on the iron and sulfur cycles in Arctic fjord sediments (Svalbard). *Geochimica et Cosmochimica Acta, 280*, 423-440. doi:https://doi.org/10.1016/j.gca.2019.12.033

Mitchell, B. G., & Holm-Hansen, O. (1991). Observations of modeling of the Antartic phytoplankton crop in relation to mixing depth. *Deep Sea Research Part A. Oceanographic Research Papers, 38*(8-9), 981-1007.

Molari, M., Janssen, F., Vonnahme, T. R., Wenzhöfer, F., & Boetius, A. (2020). The contribution of microbial communities in polymetallic nodules to the diversity of the deep-sea microbiome of the Peru Basin (4130–4198 m depth). *Biogeosciences, 17*(12), 3203-3222. doi:https://doi.org/10.5194/bg-17-3203-2020

Monien, P., Lettmann, K. A., Monien, D., Asendorf, S., Wölfl, A.-C., Lim, C. H., et al. (2014). Redox conditions and trace metal cycling in coastal sediments from the maritime Antarctic. *Geochimica et Cosmochimica Acta, 141*, 26-44. doi:https://doi.org/10.1016/j.gca.2014.06.003

Nielsdóttir, M. C., Bibby, T. S., Moore, C. M., Hinz, D. J., Sanders, R., Whitehouse, M., et al. (2012). Seasonal and spatial dynamics of iron availability in the Scotia Sea. *Marine Chemistry, 130-131*, 62-72. doi:https://doi.org/10.1016/j.marchem.2011.12.004

Nunoura, T., Oida, H., Nakaseama, M., Kosaka, A., Ohkubo, S. B., Kikuchi, T., et al. (2010). Archaeal diversity and distribution along thermal and geochemical gradients in hydrothermal sediments at the Yonaguni Knoll IV hydrothermal field in the Southern Okinawa trough. *Applied and Environmental Microbiology, 76*(4), 1198-1211. doi:10.1128/aem.00924-09

Oksanen, J., Blanchet, F. G., Kindt, R., Legendre, P., Minchin, P., O'hara, R., et al. (2013). Community ecology package. *R package version, 2*(0).

Oni, O., Miyatake, T., Kasten, S., Richter-Heitmann, T., Fischer, D., Wagenknecht, L., et al. (2015). Distinct microbial populations are tightly linked to the profile of dissolved iron in the methanic sediments of the Helgoland mud area, North Sea. *Frontiers in Microbiology, 6*. doi:10.3389/fmicb.2015.00365

Park, S.-J., Park, B.-J., Jung, M.-Y., Kim, S.-J., Chae, J.-C., Roh, Y., et al. (2011). Influence of Deglaciation on Microbial Communities in Marine Sediments Off the Coast of Svalbard, Arctic Circle. *Microbial Ecology, 62*(3), 537-548. doi:10.1007/s00248-011-9860-5

Pischedda, L., Militon, C., Gilbert, F., & Cuny, P. (2011). Characterization of specificity of bacterial community structure within the burrow environment of the marine polychaete Hediste (Nereis) diversicolor. *Research in Microbiology, 162*(10), 1033-1042. doi:10.1016/j.resmic.2011.07.008

Purdy, K. J., Nedwell, D. B., & Embley, T. M. (2003). Analysis of the sulfate-reducing bacterial and methanogenic archaeal populations in contrasting Antarctic sediments. *Applied and Environmental Microbiology, 69*(6), 3181-3191. doi:10.1128/aem.69.6.3181-3191.2003

Quast, C., Pruesse, E., Yilmaz, P., Gerken, J., Schweer, T., Yarza, P., et al. (2012). The SILVA ribosomal RNA gene database project: improved data processing and web-based tools. *Nucleic Acids Research, 41*(D1), D590-D596. doi:https://doi.org/10.1093/nar/gks1219

Raiswell, R., Benning, L. G., Tranter, M., & Tulaczyk, S. (2008). Bioavailable iron in the Southern Ocean: the significance of the iceberg conveyor belt. *Geochemical Transactions, 9*(1), 7. doi:10.1186/1467-4866-9-7

Raiswell, R., Hawkings, J. R., Benning, L. G., Baker, A. R., Death, R., Albani, S., et al. (2016). Potentially bioavailable iron delivery by iceberg-hosted sediments and atmospheric dust to the polar oceans. *Biogeosciences, 13*(13), 3887-3900. doi:10.5194/bg-13-3887-2016

Ravenschlag, K., Sahm, K., Knoblauch, C., Jørgensen, B. B., & Amann, R. (2000). Community structure, cellular rRNA content, and activity of sulfate-reducing bacteria in marine Arctic sediments. *Applied and Environmental Microbiology, 66*(8), 3592-3602. doi:https://doi.org/10.1128/AEM.66.8.3592-3602.2000

Ravenschlag, K., Sahm, K., Pernthaler, J., & Amann, R. (1999). High bacterial diversity in permanently cold marine sediments. *Applied and Environmental Microbiology, 65*(9), 3982-3989. doi:10.1128/AEM.65.9.3982-3989.1999

Riedinger, N., Brunner, B., Krastel, S., Arnold, G. L., Wehrmann, L. M., Formolo, M. J., et al. (2017). Sulfur cycling in an iron oxide-dominated, dynamic marine depositional system: The

Argentine continental margin. *Frontiers in Earth Science, 5*, 33. doi:https://doi.org/10.3389/feart.2017.00033

Roden, E. E., & Lovley, D. R. (1993). Dissimilatory Fe (III) reduction by the marine microorganism Desulfuromonas acetoxidans. *Applied and Environmental Microbiology, 59*(3), 734-742. doi:https://doi.org/10.1128/aem.59.3.734-742.1993

Ruff, S. E., Arnds, J., Knittel, K., Amann, R., Wegener, G., Ramette, A., et al. (2013). Microbial communities of deep-sea methane seeps at Hikurangi continental margin (New Zealand). *PLoS One, 8*(9), e72627. doi:10.1371/journal.pone.0072627

Ruff, S. E., Probandt, D., Zinkann, A.-C., Iversen, M. H., Klaas, C., Würzberg, L., et al. (2014). Indications for algae-degrading benthic microbial communities in deep-sea sediments along the Antarctic Polar Front. *Deep Sea Research Part II: Topical Studies in Oceanography, 108*, 6-16. doi:https://doi.org/10.1016/j.dsr2.2014.05.011

Sakshaug, E., Slagstad, D., & Holm-Hansen, O. (1991). Factors controlling the development of phytoplankton blooms in the Antarctic Ocean—a mathematical model. *Marine Chemistry, 35*(1-4), 259-271. doi:https://doi.org/10.1016/S0304-4203(09)90021-4

Santelli, C. M., Orcutt, B. N., Banning, E., Bach, W., Moyer, C. L., Sogin, M. L., et al. (2008). Abundance and diversity of microbial life in ocean crust. *Nature, 453*(7195), 653-656. doi:10.1038/nature06899

Savidge, G., Harbour, D., Gilpin, L., & Boyd, P. (1995). Phytoplankton distributions and production in the Bellingshausen Sea, Austral spring 1992. *Deep Sea Research Part II: Topical Studies in Oceanography, 42*(4-5), 1201-1224. doi:https://doi.org/10.1016/0967-0645(95)00062-U

Schloss, I. R., Ferreyra, G. A., & Ruiz-Pino, D. (2002). Phytoplankton biomass in Antarctic shelf zones: a conceptual model based on Potter Cove, King George Island. *Journal of Marine Systems, 36*(3-4), 129-143. doi:https://doi.org/10.1016/S0924-7963(02)00183-5

Schnakenberg, A., Aromokeye, D. A., Kulkarni, A., Maier, L., Wunder, L. C., Richter-Heitmann, T., et al. (2021). Electron Acceptor Availability Shapes Anaerobically Methane Oxidizing Archaea (ANME) Communities in South Georgia Sediments. *Frontiers in Microbiology, 12*. doi:10.3389/fmicb.2021.617280

Shaw, T. J., Gieskes, J. M., & Jahnke, R. A. (1990). Early diagenesis in differing depositional environments: The response of transition metals in pore water. *Geochimica et Cosmochimica Acta, 54*(5), 1233-1246. doi:https://doi.org/10.1016/0016-7037(90)90149-F

Smith, C. R., Mincks, S., & DeMaster, D. J. (2006). A synthesis of bentho-pelagic coupling on the Antarctic shelf: food banks, ecosystem inertia and global climate change. *Deep Sea Research Part II: Topical Studies in Oceanography, 53*(8-10), 875-894. doi:https://doi.org/10.1016/j.dsr2.2006.02.001

Smith, R. C., Baker, K. S., Dierssen, H. M., Stammerjohn, S. E., & Vernet, M. (2001). Variability of primary production in an Antarctic marine ecosystem as estimated using a multi-scale sampling strategy. *American Zoologist, 41*(1), 40-56. doi:https://doi.org/10.1093/icb/41.1.40

Sogin, M. L., Morrison, H. G., Huber, J. A., Welch, D. M., Huse, S. M., Neal, P. R., et al. (2006). Microbial diversity in the deep sea and the underexplored "rare biosphere". *Proceedings of the National Academy of Sciences, 103*(32), 12115-12120. doi:https://doi.org/10.1073/pnas.0605127103

Spreen, G., Kaleschke, L., & Heygster, G. (2008). Sea ice remote sensing using AMSR-E 89-GHz channels. *Journal of Geophysical Research: Oceans, 113*(C2). doi:https://doi.org/10.1029/2005JC003384

Stumm, W., & Morgan, J. J. (2012). *Aquatic chemistry: chemical equilibria and rates in natural waters* (Vol. 126): John Wiley & Sons.

Taylor, K. E., Stouffer, R. J., & Meehl, G. A. (2012). An overview of CMIP5 and the experiment design. *Bulletin of the American meteorological Society, 93*(4), 485-498.

Team, R. C. (2020). R: A language and environment for statistical computing. R Foundation for Statistical Computing, Vienna, Austria. URL https://www.R-project.org/.

Teeling, H., Fuchs, B. M., Becher, D., Klockow, C., Gardebrecht, A., Bennke, C. M., et al. (2012). Substrate-controlled succession of marine bacterioplankton populations induced by a phytoplankton bloom. *Science, 336*(6081), 608-611. doi:10.1126/science.1218344

Teske, A., Durbin, A., Ziervogel, K., Cox, C., & Arnosti, C. (2011). Microbial Community Composition and Function in Permanently Cold Seawater and Sediments from an Arctic Fjord of Svalbard. *Applied and Environmental Microbiology, 77*(6), 2008-2018. doi:doi:10.1128/AEM.01507-10

Thamdrup, B., Rosselló-Mora, R., & Amann, R. (2000). Microbial manganese and sulfate reduction in Black Sea shelf sediments. *Applied and Environmental Microbiology, 66*(7), 2888-2897. doi:https://doi.org/10.1128/AEM.66.7.2888-2897.2000

Van den Boogaart, K. G., & Tolosana-Delgado, R. (2013). *Analyzing compositional data with R* (Vol. 122): Springer.

Vandieken, V., Finke, N., & Jørgensen, B. B. (2006b). Pathways of carbon oxidation in an Arctic fjord sediment (Svalbard) and isolation of psychrophilic and psychrotolerant Fe (III)-reducing bacteria. *Marine Ecology Progress Series, 322*, 29-41. doi:10.3354/meps322029

Vandieken, V., Mußmann, M., Niemann, H., & Jørgensen, B. B. (2006a). Desulfuromonas svalbardensis sp. nov. and Desulfuromusa ferrireducens sp. nov., psychrophilic, Fe (III)-reducing bacteria isolated from Arctic sediments, Svalbard. *International Journal of Systematic and Evolutionary Microbiology, 56*(5), 1133-1139. doi:https://doi.org/10.1099/ijs.0.63639-0

Vandieken, V., & Thamdrup, B. (2013). Identification of acetate-oxidizing bacteria in a coastal marine surface sediment by RNA-stable isotope probing in anoxic slurries and intact cores. *FEMS Microbiology Ecology, 84*(2), 373-386. doi:10.1111/1574-6941.12069

Vaughan, D. G., Marshall, G. J., Connolley, W. M., Parkinson, C., Mulvaney, R., Hodgson, D. A., et al. (2003). Recent Rapid Regional Climate Warming on the Antarctic Peninsula. *Climatic Change, 60*(3), 243-274. doi:10.1023/A:1026021217991

Wadham, J. L., De'ath, R., Monteiro, F. M., Tranter, M., Ridgwell, A., Raiswell, R., et al. (2013). The potential role of the Antarctic Ice Sheet in global biogeochemical cycles. *Earth and Environmental Science Transactions of the Royal Society of Edinburgh, 104*(1), 55-67. doi:10.1017/S1755691013000108

Wehrmann, L. M., Riedinger, N., Brunner, B., Kamyshny, A., Hubert, C. R. J., Herbert, L. C., et al. (2017). Iron-controlled oxidative sulfur cycling recorded in the distribution and isotopic

composition of sulfur species in glacially influenced fjord sediments of west Svalbard. *Chemical Geology, 466*, 678-695. doi:https://doi.org/10.1016/j.chemgeo.2017.06.013

Wunder, L. C., Aromokeye, D. A., Yin, X., Richter-Heitmann, T., Willis-Poratti, G., Schnakenberg, A., et al. (2021). Iron and sulfate reduction structure microbial communities in (sub-) Antarctic sediments. *The ISME Journal, 15*(12), 3587-3604. doi:10.1038/s41396-021-01014-9

Zonneveld, K. A., Versteegh, G. J., Kasten, S., Eglinton, T. I., Emeis, K.-C., Huguet, C., et al. (2010). Selective preservation of organic matter in marine environments; processes and impact on the sedimentary record. *Biogeosciences, 7*(2), 483-511. doi:https://doi.org/10.5194/bg-7-483-2010

Supplementary Material

Table S1: Overview of sampled stations during RV Polarstern expedition PS118. The table consists of sampling information for each station, number of sequences in each step of the bioinformatics workflow as well as alpha diversity indices: 1) observed richness, 2) exponential Shannon and 3) inverse simpson, conducted using the R package 'Phyloseq'. This table can be downloaded from: www.mdpi.com/xxx/s1

Table S2: Output PERMANOVA and distance-based redundancy analysis (dbRDA).

		Df	SumsOfSqs	F	R^2	Pr(>F)
adonis: (data.clr [c(St1.MUC1.C3.D1, St1.MUC2.C2.D1, St1.MUC2.C3.D1, St2.MUC1.C3.D1, PS118.2.MUC2.C3.D1, PS118.2.MUC3.C2.D1, PS118.3.MUC2.C3.D1, PS118.3.MUC2.C5.D1, PS118.3.MUC4.C2.D1, PS118.4.MUC3.C3.D1, PS118.4.MUC3.C4.D1, PS118.4.MUC3.C5.D1, PS118.7.MUC1.C6.D1, PS118.7.MUC1.C7.D1, PS118.7.MUC1.C8.D1),]~ Sea_Ice_index, data = Env_data, method = 'euclidean', permutations = 9999)	Sea ice index	1	3794	1.8916	0.12702	0.0264
	Residuals	13	26074		0.87298	
	Total	14	29868		1.00000	
adonis: (data.clr ~ Sea_Ice_index/ Layer, data = Env_data, strata = Env_data$Core_ID, method = 'euclidean', permutations = 9999)	Sea ice index	1	5827	4.4165	0.04590	0.0001
	Sea ice index: layer	5	11604	1.7590	0.09141	0.0001
	Residuals	83	109509		0.86268	
	Total	89	126941		1.00000	
dbrda: data.clr ~ C/N ratio + O_2 (µmol/L) + Fe(II) (µmol/L) + Fe (III)/Al + S/Al + Sulfat (mmol/L) + DIC(µmol/L)	**ANOVA**	**Df**	**Variance**	**F**	**Pr(>F)**	**p.adjust**
	C/N ratio	1	25.98	1.8687	0.008	0.011
	O_2 (µmol/L)	1	52.19	3.7547	0.001	0.003
	Fe(II) (µmol/L)	1	51.49	3.7039	0.001	0.003
	Fe (III)/Al	1	27.93	2.0094	0.003	0.005
	S/Al	1	30.45	2.1903	0.003	0.005
	Sulfate (mmol/L)	1	13.27	0.9546	0.476	0.476
	DIC(µmol/L)	1	22.74	1.6361	0.022	0.025
	Residual	82	1139.83			

Table S3: ASVs highly abundant in the ferruginous zone. Differential abundance of taxa between surface sediments (0-3 cm) of stations **Shelf St4** and **Shelf St1** samples according to the t-test based metastats analysis. Differentially abundant taxa having statistically significant differences for parametric test (glm.eBH) ($p<0.01$) and non-parametric test (kw.ep) ($p<0.05$) are reported for each ASV per sample.

	kw.ep	glm.eBH	St4. MUC3. C5.D3	St4. MUC3 .C5.D2	St4. MUC3. C5.D1	St4. MUC3. C4.D3	St4. MUC3. C4.D2	St4. MUC3. C4.D1	St4. MUC3. C3.D3	St4. MUC3 .C3.D2	St4. MUC3. C3.D1
asv2	0.0017	0.0005	5.87	1.88	2.57	2.72	1.96	2.89	3.54	4.60	3.86
asv4	0.0003	0.0002	2.39	0.53	1.83	1.10	1.73	1.41	2.36	1.58	2.10
asv15	0.0003	0.0007	2.00	0.48	0.61	0.42	0.42	0.43	1.75	1.32	0.92
asv5	0.0003	0.0000	1.66	0.60	1.26	1.06	1.34	1.20	1.23	1.87	1.93
asv18	0.0003	0.0001	1.99	2.01	0.21	0.25	0.22	0.20	1.67	1.90	0.26
asv26	0.0003	0.0000	1.30	0.11	0.47	0.42	0.52	1.23	2.10	0.31	0.60
asv16	0.0004	0.0000	1.76	0.95	0.54	0.38	0.51	0.56	1.46	1.21	0.60
asv6	0.0015	0.0009	1.52	2.03	0.76	0.60	0.66	0.82	1.45	2.06	0.89
asv21	0.0003	0.0004	1.22	0.17	0.35	0.32	0.54	1.04	1.94	0.34	0.55
asv13	0.0003	0.0000	1.27	0.20	0.77	0.56	1.27	0.79	1.29	0.59	1.17
asv42	0.0004	0.0000	1.06	0.42	0.22	0.21	0.28	0.21	1.64	0.96	0.24
asv23	0.0004	0.0049	0.87	0.08	0.22	0.10	0.66	3.59	1.83	0.15	0.29
asv12	0.0003	0.0001	0.84	0.19	1.31	0.97	0.63	1.12	0.72	0.46	1.25
asv14	0.0044	0.0034	1.08	0.38	0.72	0.51	0.78	0.36	0.89	0.80	0.96
asv24	0.0003	0.0006	0.85	0.38	0.65	0.37	0.54	0.39	0.99	0.63	0.63
asv31	0.0003	0.0000	0.84	0.42	0.23	0.32	0.47	0.35	0.96	0.72	0.33
asv20	0.0016	0.0013	1.20	0.18	0.54	0.17	1.34	1.02	0.75	0.34	0.90
asv8	0.0006	0.0000	1.04	0.66	1.11	0.56	0.41	0.19	0.50	1.80	1.05
asv7	0.0003	0.0001	0.97	3.20	0.48	0.46	0.10	0.26	0.65	2.02	0.39
asv9	0.0003	0.0000	1.09	1.95	1.20	0.61	0.27	0.27	0.31	2.35	1.10
asv41	0.0003	0.0008	0.68	0.19	0.64	0.32	0.62	0.29	0.69	0.54	0.86
asv19	0.0020	0.0038	0.83	0.58	0.76	0.45	0.17	0.00	0.32	1.41	0.72
asv40	0.0003	0.0003	0.76	0.34	0.54	0.30	0.32	0.32	0.43	0.63	0.75
asv11	0.0005	0.0010	0.66	0.77	1.45	0.53	0.28	0.17	0.16	1.22	1.16
asv68	0.0003	0.0001	0.66	0.09	0.20	0.40	0.17	0.17	0.29	0.36	0.34
asv38	0.0003	0.0000	0.51	0.41	0.41	0.26	0.28	0.28	0.47	0.46	0.52
asv61	0.0035	0.0012	0.33	0.06	0.39	0.34	0.48	0.52	0.43	0.39	0.59
asv60	0.0037	0.0031	0.45	0.09	0.27	0.16	0.50	0.38	0.44	0.27	0.54
asv106	0.0016	0.0013	0.49	0.67	0.16	0.13	0.13	0.00	0.41	0.74	0.28
asv58	0.0004	0.0004	0.38	0.27	0.30	0.23	0.23	0.12	0.42	0.37	0.40
asv54	0.0051	0.0041	0.41	0.38	0.16	0.14	0.24	0.16	0.45	0.32	0.14
asv82	0.0003	0.0000	0.43	0.11	0.25	0.23	0.31	0.18	0.34	0.39	0.31
asv96	0.0003	0.0000	0.36	0.24	0.21	0.17	0.18	0.19	0.41	0.29	0.38

Table S3: (continued)

	kw.ep	glm.eBH	St4.MUC3.C5.D3	St4.MUC3.C5.D2	St4.MUC3.C5.D1	St4.MUC3.C4.D3	St4.MUC3.C4.D2	St4.MUC3.C4.D1	St4.MUC3.C3.D3	St4.MUC3.C3.D2	St4.MUC3.C3.D1
asv129	0.0003	0.0000	0.41	0.09	0.14	0.10	0.28	0.26	0.43	0.34	0.20
asv56	0.0037	0.0066	0.22	0.32	0.33	0.61	0.07	0.07	0.07	0.21	0.27
asv59	0.0015	0.0016	0.55	0.73	0.34	0.18	0.04	0.00	0.15	0.68	0.25
asv50	0.0019	0.0011	0.36	0.22	0.80	0.50	0.13	0.15	0.00	0.61	0.59
asv126	0.0003	0.0000	0.34	0.16	0.21	0.20	0.19	0.17	0.29	0.14	0.23
asv103	0.0016	0.0014	0.32	0.00	0.27	0.34	0.10	0.72	0.13	0.10	0.36
asv174	0.0003	0.0000	0.41	0.23	0.05	0.06	0.08	0.13	0.32	0.26	0.12
asv51	0.0005	0.0034	0.28	0.32	0.38	0.37	0.19	0.43	0.14	0.46	0.46
asv27	0.0023	0.0015	0.37	0.80	0.36	0.25	0.16	0.29	0.16	1.31	0.39
asv64	0.0003	0.0000	0.37	0.13	0.27	0.19	0.13	0.33	0.19	0.39	0.21
asv69	0.0003	0.0000	0.12	0.17	0.59	0.52	0.30	0.14	0.11	0.34	0.70
asv79	0.0003	0.0000	0.39	0.10	0.15	0.07	0.56	0.68	0.27	0.32	0.26
asv78	0.0018	0.0034	0.10	0.22	0.56	0.54	0.33	0.00	0.06	0.07	0.76
asv77	0.0003	0.0000	0.34	0.09	0.55	0.30	0.10	0.14	0.05	0.17	0.43
asv191	0.0003	0.0000	0.21	0.04	0.13	0.07	0.24	0.19	0.41	0.09	0.18
asv197	0.0003	0.0002	0.23	0.04	0.10	0.09	0.21	0.17	0.35	0.11	0.16
asv119	0.0017	0.0007	0.22	0.17	0.22	0.13	0.17	0.00	0.31	0.25	0.20

Table S3: (continued)

	kw.ep	glm.eBH	St1. MUC1. C3.D1	St1. MUC1. C3.D2	St1. MUC1. C3.D3	St1. MUC2. C2.D1	St1. MUC2. C2.D2	St1. MUC2. C2.D3	St1. MUC2. C3.D1	St1. MUC2. C3.D2	St1. MUC2. C3.D3
asv2	0.0017	0.0005	0.24	0.33	0.54	0.64	0.96	1.91	0.45	1.12	1.73
asv4	0.0003	0.0002	0.00	0.00	0.00	0.00	0.06	0.09	0.02	0.07	0.12
asv15	0.0003	0.0007	0.00	0.00	0.00	0.00	0.01	0.07	0.01	0.01	0.08
asv5	0.0003	0.0000	0.03	0.01	0.04	0.00	0.04	0.02	0.02	0.02	0.03
asv18	0.0003	0.0001	0.00	0.00	0.00	0.00	0.00	0.03	0.00	0.01	0.01
asv26	0.0003	0.0000	0.00	0.00	0.00	0.00	0.00	0.00	0.01	0.01	0.00
asv16	0.0004	0.0000	0.08	0.07	0.11	0.08	0.11	0.20	0.09	0.11	0.17
asv6	0.0015	0.0009	0.22	0.27	0.28	0.27	0.29	0.52	0.34	0.37	0.37
asv21	0.0003	0.0004	0.00	0.00	0.00	0.00	0.01	0.07	0.02	0.04	0.05
asv13	0.0003	0.0000	0.05	0.08	0.06	0.00	0.06	0.11	0.06	0.08	0.08
asv42	0.0004	0.0000	0.04	0.03	0.01	0.04	0.03	0.01	0.03	0.04	0.03
asv23	0.0004	0.0049	0.03	0.00	0.00	0.03	0.00	0.02	0.03	0.03	0.02
asv12	0.0003	0.0001	0.00	0.00	0.00	0.00	0.00	0.00	0.00	0.00	0.00
asv14	0.0044	0.0034	0.10	0.15	0.19	0.15	0.21	0.28	0.17	0.23	0.27
asv24	0.0003	0.0006	0.00	0.00	0.00	0.00	0.00	0.05	0.01	0.03	0.04
asv31	0.0003	0.0000	0.00	0.00	0.00	0.00	0.00	0.00	0.00	0.00	0.00
asv20	0.0016	0.0013	0.14	0.09	0.05	0.11	0.09	0.08	0.18	0.12	0.09
asv8	0.0006	0.0000	0.01	0.02	0.01	0.02	0.05	0.11	0.02	0.06	0.10
asv7	0.0003	0.0001	0.00	0.00	0.00	0.00	0.00	0.06	0.01	0.01	0.03
asv9	0.0003	0.0000	0.00	0.00	0.00	0.00	0.00	0.00	0.00	0.00	0.00
asv41	0.0003	0.0008	0.00	0.00	0.00	0.00	0.02	0.05	0.01	0.03	0.04
asv19	0.0020	0.0038	0.00	0.00	0.00	0.00	0.00	0.04	0.00	0.01	0.02
asv40	0.0003	0.0003	0.00	0.00	0.00	0.00	0.00	0.00	0.00	0.02	0.03
asv11	0.0005	0.0010	0.00	0.01	0.00	0.00	0.00	0.05	0.01	0.03	0.07
asv68	0.0003	0.0001	0.00	0.00	0.00	0.00	0.01	0.02	0.00	0.00	0.00
asv38	0.0003	0.0000	0.00	0.00	0.00	0.00	0.00	0.00	0.00	0.00	0.00
asv61	0.0035	0.0012	0.08	0.04	0.06	0.05	0.05	0.06	0.06	0.07	0.08
asv60	0.0037	0.0031	0.07	0.06	0.07	0.08	0.08	0.09	0.08	0.10	0.12
asv106	0.0016	0.0013	0.00	0.00	0.00	0.00	0.00	0.00	0.00	0.00	0.00
asv58	0.0004	0.0004	0.00	0.00	0.00	0.00	0.01	0.04	0.01	0.02	0.02
asv54	0.0051	0.0041	0.06	0.05	0.06	0.09	0.09	0.11	0.08	0.08	0.08
asv82	0.0003	0.0000	0.00	0.00	0.00	0.00	0.00	0.00	0.00	0.00	0.00
asv96	0.0003	0.0000	0.00	0.00	0.00	0.00	0.00	0.00	0.00	0.00	0.00
asv129	0.0003	0.0000	0.00	0.00	0.00	0.00	0.00	0.00	0.00	0.00	0.00
asv56	0.0037	0.0066	0.03	0.03	0.04	0.02	0.04	0.06	0.02	0.02	0.05
asv59	0.0015	0.0016	0.00	0.00	0.00	0.00	0.00	0.06	0.00	0.00	0.02
asv50	0.0019	0.0011	0.00	0.00	0.00	0.00	0.00	0.00	0.00	0.00	0.00
asv126	0.0003	0.0000	0.00	0.00	0.00	0.00	0.00	0.00	0.00	0.00	0.00
asv103	0.0016	0.0014	0.00	0.00	0.00	0.00	0.00	0.00	0.00	0.00	0.00
asv174	0.0003	0.0000	0.00	0.00	0.00	0.00	0.00	0.00	0.00	0.00	0.00
asv51	0.0005	0.0034	0.09	0.13	0.08	0.08	0.09	0.15	0.12	0.09	0.08
asv27	0.0023	0.0015	0.04	0.06	0.06	0.08	0.08	0.28	0.06	0.11	0.20

Table S3: (continued)

	kw.ep	glm.eBH	St1. MUC1. C3.D1	St1. MUC1 .C3.D2	St1. MUC1. C3.D3	St1. MUC2. C2.D1	St1. MUC2. C2.D2	St1. MUC2. C2.D3	St1. MUC2 .C3.D1	St1. MUC2. C3.D2	St1. MUC2. C3.D3
asv64	0.0003	0.0000	0.00	0.00	0.00	0.00	0.00	0.00	0.00	0.00	0.00
asv69	0.0003	0.0000	0.00	0.00	0.00	0.00	0.00	0.04	0.00	0.00	0.00
asv79	0.0003	0.0000	0.00	0.00	0.00	0.00	0.00	0.00	0.00	0.00	0.00
asv78	0.0018	0.0034	0.00	0.00	0.00	0.00	0.00	0.00	0.00	0.00	0.00
asv77	0.0003	0.0000	0.00	0.00	0.00	0.00	0.00	0.00	0.00	0.00	0.00
asv191	0.0003	0.0000	0.00	0.00	0.00	0.00	0.00	0.00	0.00	0.00	0.00
asv197	0.0003	0.0002	0.00	0.00	0.00	0.00	0.00	0.00	0.00	0.00	0.00
asv119	0.0017	0.0007	0.00	0.00	0.00	0.00	0.00	0.00	0.00	0.00	0.00

Table S4: The most closely related sequences with identity (ID) > 99%, as identified with BLASTn (GeneBank nucleotide database, 12 June 2022).

ASV	GeneBank ID ≥ 99% similarity	Environment(s)
asv2	FN429801.1; AF530115.1; EU287191.1; KC631541.1; GU197468.1; JQ863508.1; GQ357030.1	Antarctic cold seep sediment; Antarctic shelf sediments; Arctic surface sediment; aquaculture farm sediment; intertidal sediment; suboxic marine sediment; methane seep sediment.
asv4	EU857895.1; FN396623.1; EU362314.1; KF440288.1; KX097349.1; FJ753062.1	Antarctic marine sediment; Arctic marine surface sediment; tidal flat sediment; mud volcano; hydrothermal deposits and seafloor sediments; suboxic sediment.
asv5	KJ566283.1; JF268353.1	Arctic marine sediment; deep-sea methane seep.
asv6	KY190828.1; EU287223.1; HQ191097.1; DQ351780.1; JQ863426.1; KC463739.1; KX097752.1; KF624175.1; FM179882.1; AB305481.1; KF799091.1; AJ880527.1	Antarctic marine sediment; Arctic marine sediment; muddy intertidal sediment; Adherent bacteria in heavy metal contaminated marine sediments; anoxic marine sediment; shallow-water hydrothermal vent sediments; deep-sea sediment; oxic pyrite-particle; methane seeps; hydrothermal sediments; Ciona intestinal gut; tidal flat sediments.
asv13	FN396637.1; KX172653.1; EU491847.1; KM203427.1; JX226991.1	Arctic marine surface sediment; deep sea marine sediment; seafloor lavas; deep-sea coral; deep-sea polymetallic nodules.
asv15	AF530125.1; GU292255.1; JF767462.1; GU996528.1; AJ704698.1; HQ703820.1; FJ873360.1	Antarctic continental shelf sediments; Arctic marine sediment; salmon farm marine sediment; crude oil alkanes; marine sediment from mud volcano; marine sediment; methane-rich cold seep.
asv16	KY190870.1; FJ223335.1; KY190827.1; FN396623.1; EU362314.1; KX097349.1; HE803925.1; KJ615939.1; FJ753062.1; KC631584.1; JQ579662.1	Antarctica marine sediment; Antarctica sea-bed hypoxia and sediment; Arctic marine surface sediment; mud volcano; tidal flat sediments; deep-sea sediment; marine seabed sediments; sediment with high Fe-Mn concretions; suboxic sediment; marine finfish aquaculture farm sediment; oil-polluted subtidal sediments .

Table S4: (continued)

ASV	GeneBank ID ≥ 99% similarity	Environment(s)
asv 18	FN396617.1; MK175686.1; AB806723.1; JN621370.1; GQ246294.1; FJ873358.1; AM911597.1; FJ264600.1; KX088614.1; KX097659.1; KM356755.1; JQ036284.1; JQ863439.1;GQ357027.1; GQ261776.1; AB305506.1; MG002285.1; KF741490.1; HF922369.1; HE978803.1; JQ925095.1; JQ579936.1; DQ351760.1; KC631463.1; FJ752975.1	Arctic marine sediment; Coral microbiome; Ocean drilling core; oxide-rich marine sediments; marine sediments; methane-rich cold seep sediments; cold-water coral; methane seep sediment; Anaerobic oxidation of methane by coastal sediment; deep-sea sediment; Methane Seep Sediments; Methane Seep Carbonate Nodules; anoxic marine surface sediment; methane seep sediment; deep sea sediment; hydrothermal sediments; subsurface seawater; salt marsh sediment; high-pressure membrane capsule bioreactor; intertidal sediments; cold seep sediment; oil-polluted subtidal sediments; heavy metal contaminated marine sediments; marine finfish aquaculture farm sediment; ambient suboxic sediment.
asv21	EU050902.1; FJ223315.1; JQ197846.1; AY678530.1; AY171369.1	Arctic marine sediment; marine sediment coupling of sea-bed hypoxia; seawater next to dolphin; estuarine sediment; marine sediment.
asv23	AB598201.1; JF767423.1; KF799089.1	Sub-seafloor sediments; salmon farm marine sediment; gut microbiota.
asv26	FJ223340.1; EU287278.1; FJ659158.1; EU346635.1; MK224673.1 KX172349.1; GU584516.1; JQ200082.1; JX983867.1; GQ356980.1; AM072619.1	Antarctic marine sediment coupling of sea-bed hypoxia; Arctic surface sediment; aerobic anoxygenic photosynthesis associated with colonial ascidians; marine sponge; crustose coralline algae; seafloor sediment; marine hydrocarbon seeps; seawater; next to dolphin; biofilm; methane seep sediment; tidal-flat sediments.
asv42	KY190910.1; FJ223418.1; GU292246.1; MH929595.1;NR_152677.1; KM356330.1; KF268937.1; JQ436107.1; JQ661132.1; JQ580032.1; MW245850.1; NR042612.1; KF616716.1; FJ229466.1; DQ890444.1	Antarctic marine sediment; Antarctic sediment coupling of sea-bed hypoxia; Arctic Circle marine sediment; tundra soil; marine sediment; sediments and carbonates from the methane seep environments; marine sediment with Apatite and Chitin; seawater; soil; oil-polluted subtidal sediments; marine sponge; red algae; methane seeps; intertidal sand biofilm; mud shrimp.

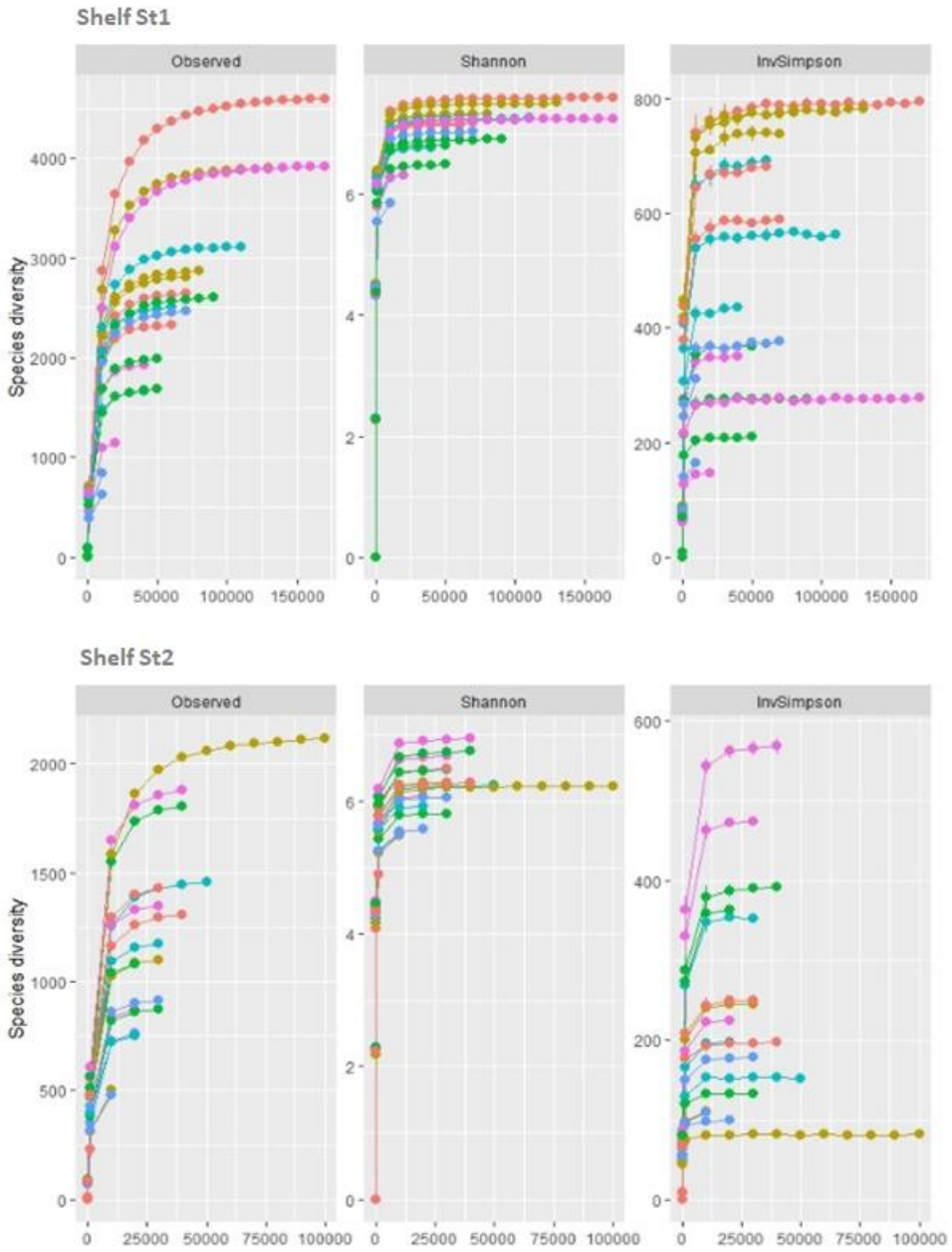

Figure S1: Diversity indices for bacterial communities in 6 different depths for 5 shelf stations across the eastern coast of Antarctic Peninsula.

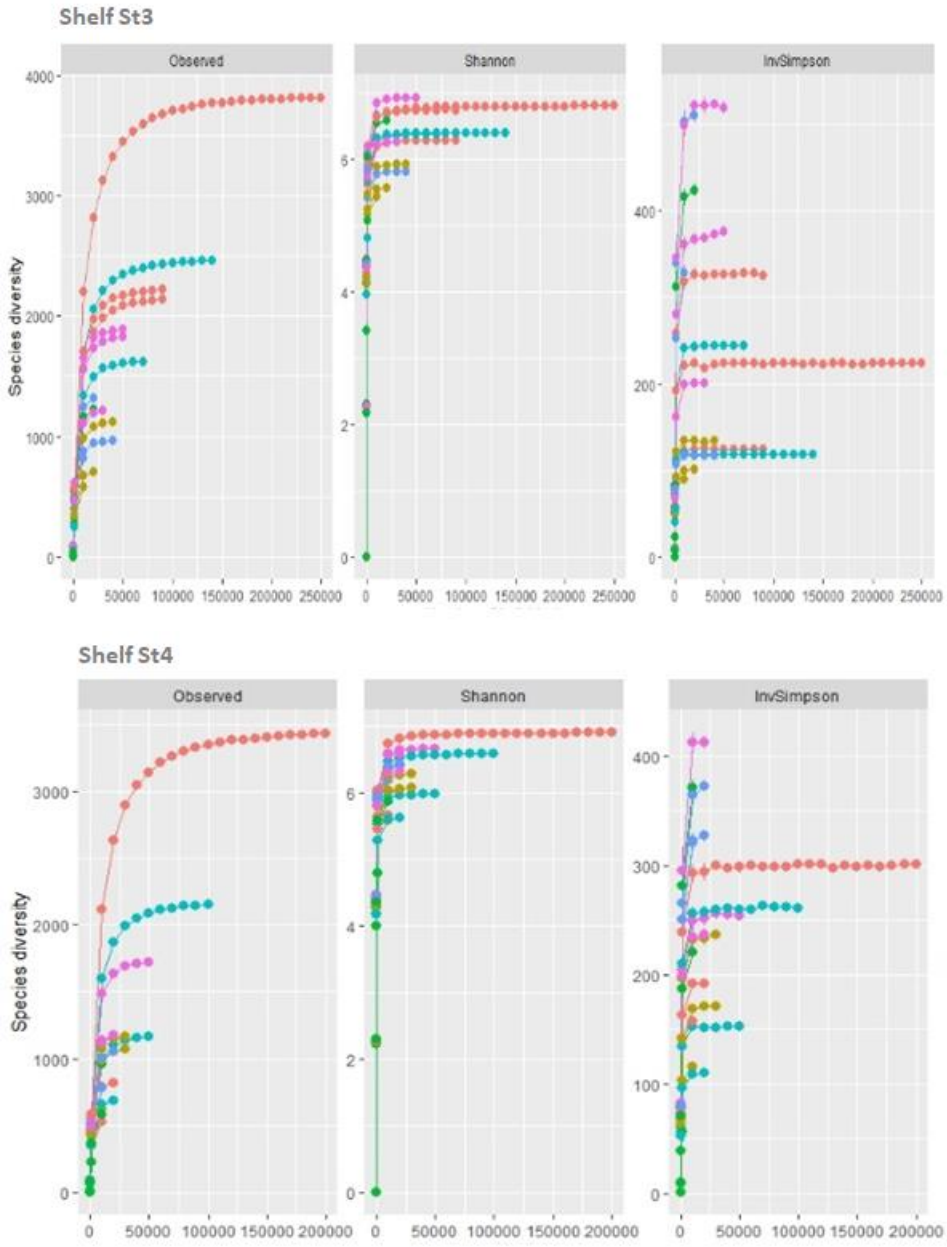

Figure S1: (continued)

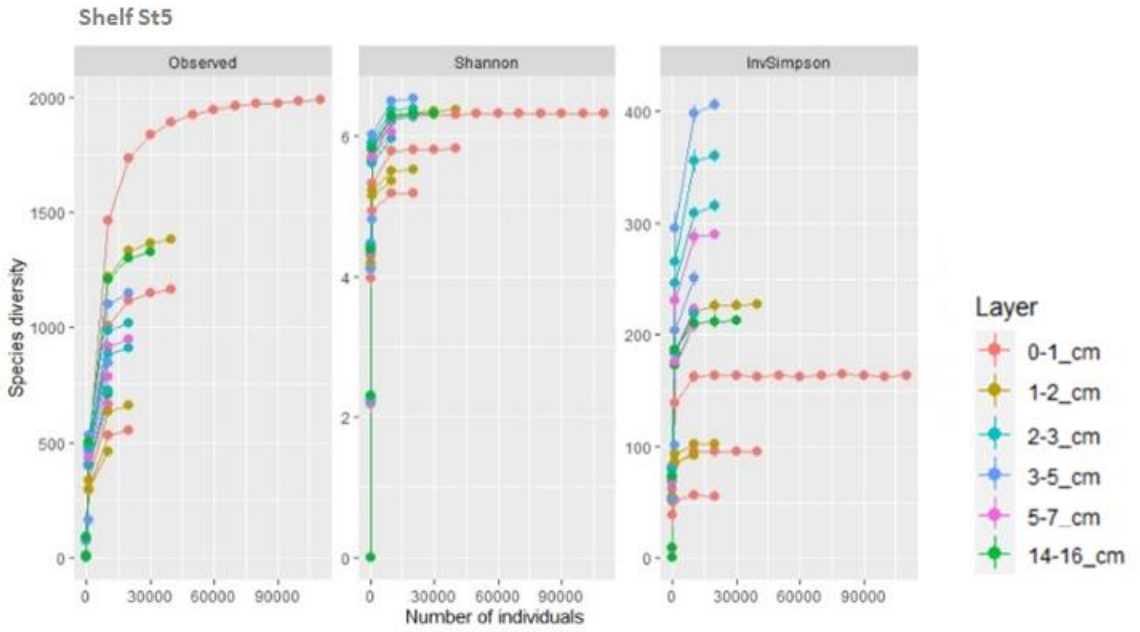

Figure S1: (continued)

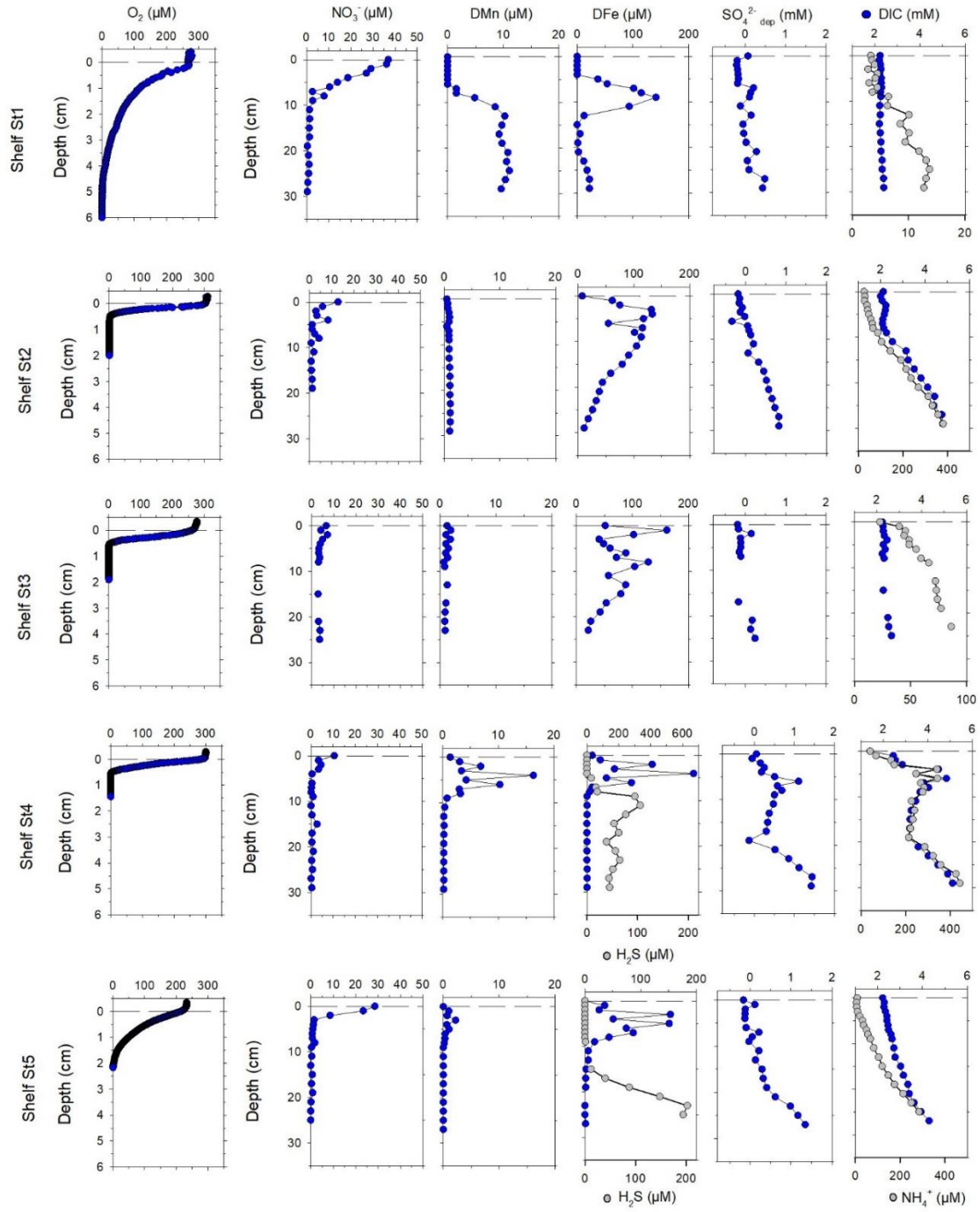

Figure S2: Representative profiles of reactive pore water compounds at the 5 shelf stations. SO_4^{2-} depletion profiles calculated based on the molar ratio of Cl^- and SO_4^{2-} of seawater (Weston et al., 2006)). Note that the scale for DFe and NH_4^+ concentrations changes between stations. Free H_2S was present only at Shelf St4 and Shelf St5. For further information: Baloza et al, (2022).

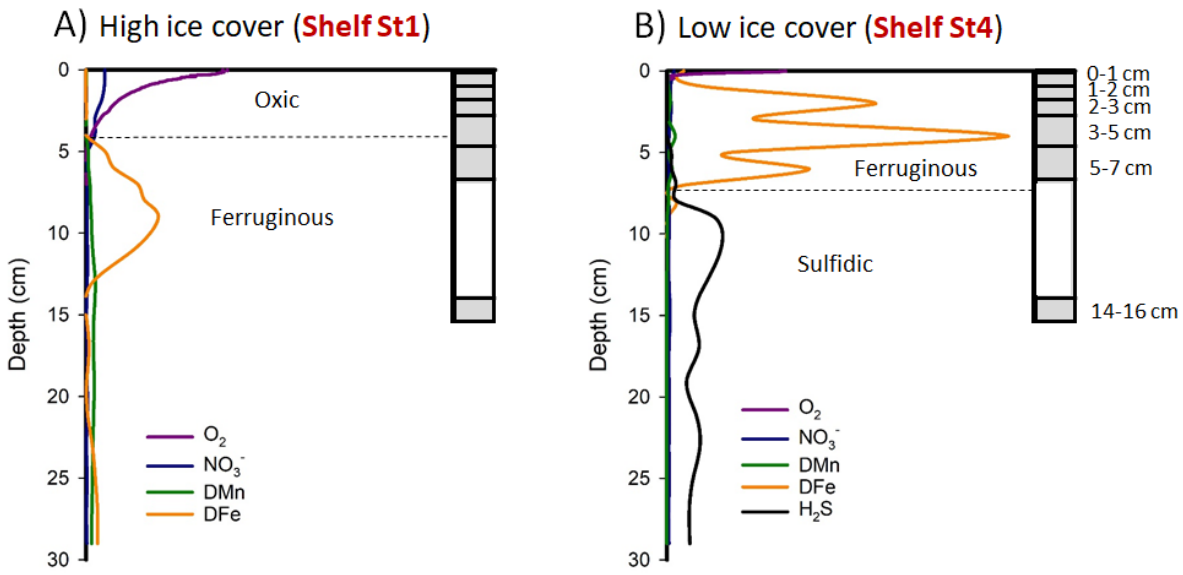

Figure S3: Schematic illustration of the porewater profiles that were typical for heavy ice cover (Shelf St1) (A) and low ice cover (Shelf St4) (B) of this study. The dashed lines mark the borders of the individual redox zones. The gray boxes to the right of each panel show the core sectioning schemes.

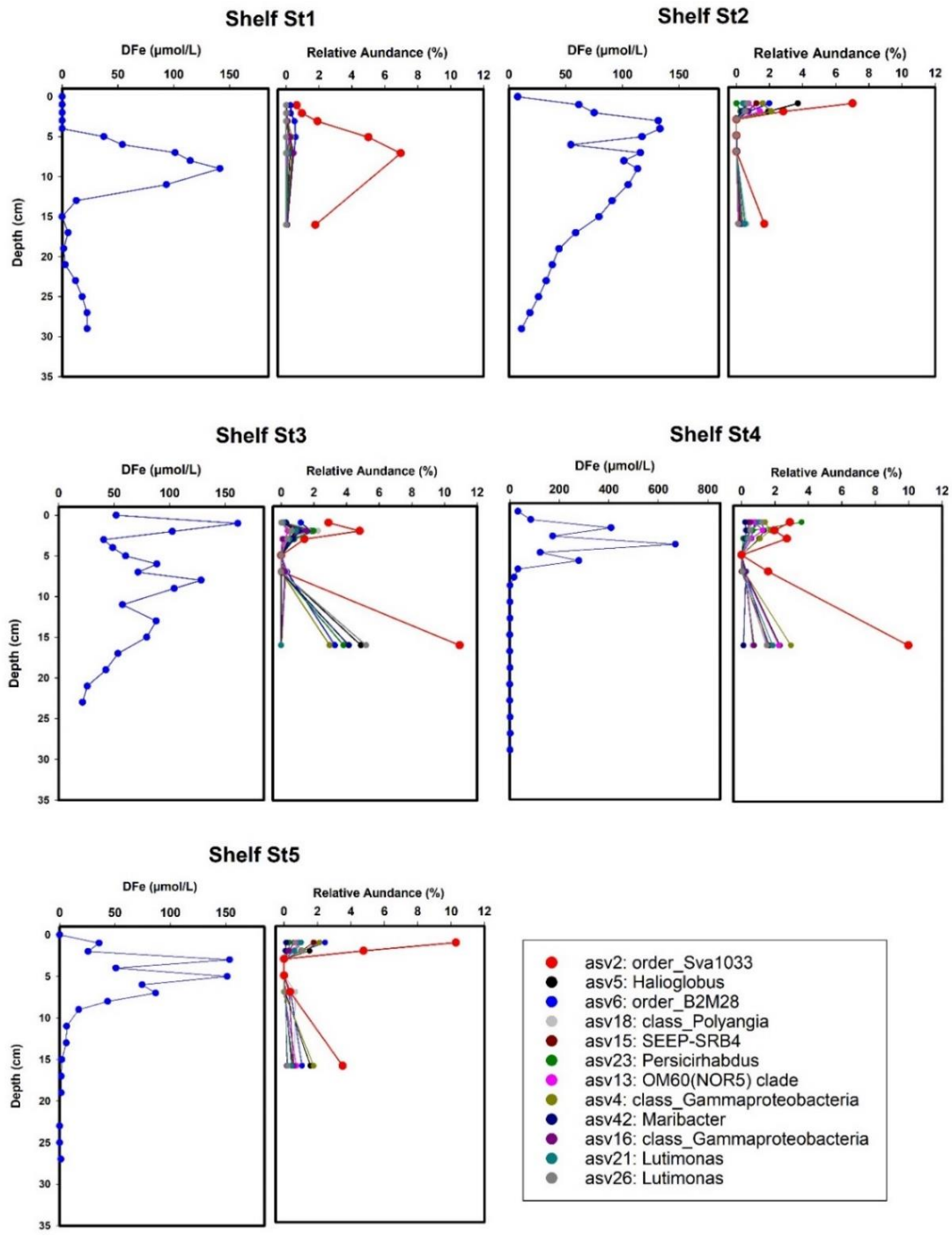

Figure S4: Representative profiles of the depth distribution of putative Fe-reducing bacteria in relation to dissolved/pore-water iron (DFe) concentrations. 12 different taxa were identified by applying differential abundance analysis. The relative abundance from one sediment core. DFe concentrations were measured in a core near (<1m) the collected microbial samples.

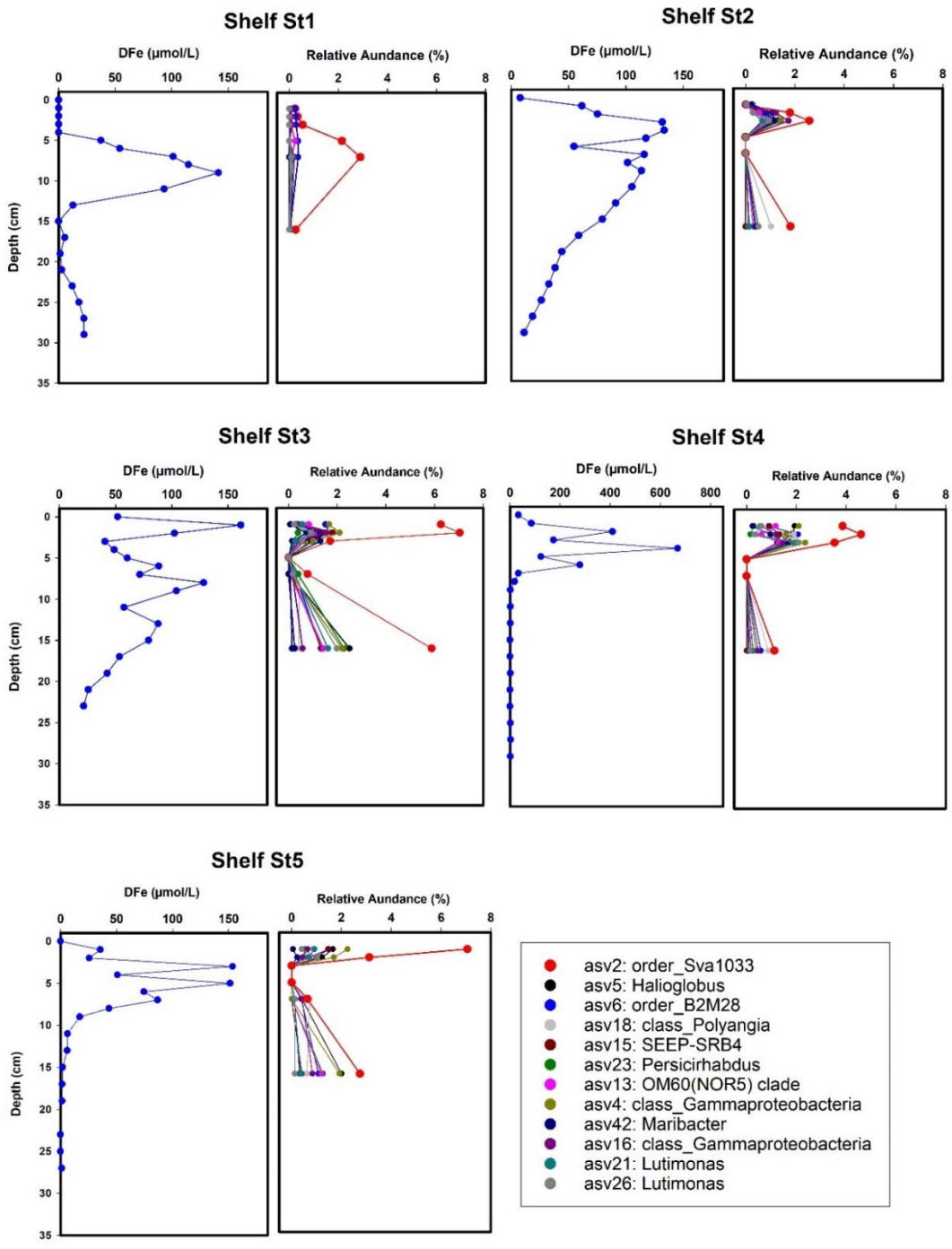

Figure S5: Representative profiles of the depth distribution of putative Fe-reducing bacteria in relation to dissolved/pore-water iron (DFe) concentrations. 12 different taxa were identified by applying differential abundance analysis. The relative abundance from one sediment core. DFe concentrations were measured in a core near (<1m) the collected microbial samples.

References

Baloza, M., Henkel, S., Geibert, W., Kasten, S., & Holtappels, M. (2022). Benthic Carbon Remineralization and Iron Cycling in Relation to Sea ice Cover Along the Eastern Continental Shelf of the Antarctic Peninsula. *Journal of Geophysical Research: Oceans, 127*(7). doi:https://doi.org/10.1029/2021JC018401

Weston, N. B., Porubsky, W. P., Samarkin, V. A., Erickson, M., Macavoy, S. E., & Joye, S. B. (2006). Porewater stoichiometry of terminal metabolic products, sulfate, and dissolved organic carbon and nitrogen in estuarine intertidal creek-bank sediments. *Biogeochemistry, 77*, 375-408.

4

Manuscript 3

Benthic carbon cycling on the southern Weddell Sea shelf

Marwa Baloza[1,2], Sandra Maier[1,3,4], Claudia Hanfland[1], Susann Henkel[1], Sabine Kasten[1,5,6], Claudio Richter[1,2], Moritz Holtappels[1,6]

[1]Alfred Wegener Institute Helmholtz Centre for Polar and Marine Research, Bremerhaven, Germany,
[2]Faculty 2 Biology /Chemistry, University Bremen, Bremen, Germany,
[3]Greenland Climate Research Centre, Greenland Institute of Natural Resources, Nuuk, Greenland,
[4]Department of Estuarine and Delta Systems, Royal Netherlands Institute for Sea Research (NIOZ-Yerseke), Yerseke, The Netherlands,
[5]Faculty of Geosciences, University Bremen, Bremen, Germany,
[6]MARUM - Center for Marine Environmental Sciences, University of Bremen, Bremen, Germany

Manuscript ready for submission to Biogeosciences

Abstract

Understanding pathways of carbon cycling on Antarctic continental shelves is critical in order to assess the potential effects of climate change on these ecosystems. Changes in primary production due to seasonal variations in sea ice cover affect the export of organic matter to the seafloor and thus control carbon cycling and burial within the sediment. Due to the remoteness of the southern Antarctic shelves, we still lack baseline knowledge about benthic carbon cycling and its main drivers in shelf sediments. In this study, we address this knowledge gap by exploring benthic oxygen uptake and sediment characteristics from 15 stations on the southern Weddell Sea shelf with heterogenous sea ice conditions and water depths, covering the Filchner Trough (794 – 932 m depth), the eastern (387 – 663 m) and the western shelf region (332 – 660 m). Rates of diffusive (DOU) and total oxygen uptake (TOU) were measured using ex-situ pore water oxygen microprofiles and sediment core incubations, respectively. In addition, pore water profiles of NO_3^-, PO_4^{3-}, NH_4^+, Mn, Fe, and SO_4^{2-} were measured as well as total organic carbon (TOC) content to characterize carbon remineralization rates and pathways. We found that O_2 penetration on the southern Weddell Sea shelf is deep (2 to >5 cm) and aerobic carbon remineralization dominates, with overall low DOU at the eastern stations (<1 mmol/m²/d) and even lower DOU at the western and Filchner Trough stations (<0.5 mmol/m²/d). DOU correlates positively with the preserved TOC contents in fine-grained sediments of Filchner Trough and western stations. In contrast, sediments of the eastern stations feature a low porosity (0.3 – 0.6), typical for coarse grained sediments, with a markedly different correlation of DOU versus TOC. Common to all stations is that dissolved Fe and Mn concentrations in pore waters are found only at greater depths (Mn at >5 cm, Fe at >10 cm or absent) suggesting that the benthic release of these nutrients in the southern Weddell Sea shelf is very low. In conclusion, we found a spatial coupling between sea ice cover and benthic carbon remineralization on the southern Weddell Sea shelf. The strikingly low benthic remineralization rates are likely due to the response of the seafloor to the long-term sea ice cover and, thereby, the organic carbon input from the upper ocean.

1 Introduction

The Southern Ocean (SO) and its shelf seas are key regions for regulating the global carbon cycle, accounting for more than 50% of the oceanic uptake of atmospheric CO_2 (Arrigo et al., 2008; Gruber et al., 2009; Takahashi et al., 2012). Deep-water exchange between the Weddell Sea and the SO, for example, is a major driver of the global thermohaline circulation, controlling both global gas exchange and the heat flux between the sea surface and the atmosphere (McNeil et al., 2001). The biological carbon pump is yet another important mechanism that facilitates the uptake of atmospheric CO_2 by the Southern Ocean, representing a potential negative feedback to climate change (e.g. Arrigo et al., 2008; Hauck et al., 2015). However, it is difficult to quantify the carbon sequestration as benthic carbon cycling on the Antarctic shelf is currently not well constrained.

Changes in primary production due to seasonal variations in sea ice cover strongly influence organic matter sedimentation and long-term sequestration. During the austral summer, Antarctic shelves are typically characterized by the occurrence of polynyas, areas of open water that form near the coast or shelf ice edge under the action of catabatic winds from the continent (Arrigo & van Dijken, 2003; Grebmeier & Barry, 2007), and by marginal ice zones (MIZ) (Grebmeier & Barry, 2007; Vernet et al., 2008). The combined effects of enhanced light conditions and water column stratification resulting from melting sea ice catalyze intensive phytoplankton blooms that usually follow the receding ice edge. MIZ and polynyas typically show the highest primary production (Savidge et al., 1995; Arrigo & van Dijken, 2003; Baloza et al., 2022), making Antarctic shelves one of the most productive high-latitude ecosystems (Arrigo et al., 2008). By contrast, where high sea ice cover persists through summer, such as in the western Weddell Sea, the low light availability limits phytoplankton growth.

On Antarctic shelves, the resulting variation in primary production is expected to lead to similar variation in the supply of organic matter (OM) to the seafloor, thus determining benthic carbon mineralization and burial. The export of OM from the upper ocean to the seafloor is controlled by the magnitude of primary production and the degree of carbon remineralization when sinking through the water column (Wassmann et al., 2004; Smith et al., 2006), which is determined by

water depth (Wenzhöfer & Glud, 2002). Thus, the large contrast in primary production between highly productive MIZs and polynyas versus heavy ice-covered areas is expected to have an imprint on the sedimentary carbon cycling, especially where water depths are shallow.

While the majority of OM produced in the surface ocean is consumed and recycled in the water column (e.g. Nelson et al., 1996), a significant fraction of OM also reaches the seafloor, where it is either remineralized or permanently buried in the sediment (e.g. Canfield, 1993; Burdige, 2007). The remineralization of OM proceeds in part through the suspension- and deposit-feeding benthic mega-, macro- and meiofauna (Smith et al., 2012; Lohrer et al., 2021), including sessile epi- and infauna, mobile forms roaming the sediment-water interface, as well as burrowing and interstitial infauna (e.g. Gutt & Starmans, 1998; Barry et al., 2003; Gutt et al., 2011). While the faunal degradation is an obligatory aerobic process with O_2 as electron acceptor, much of the OM is remineralized through a variety of microbial degradation pathways using different electron acceptors such as O_2, NO_3^-, Mn(IV), Fe(III), SO_4^{2-} and CO_2 (e.g. Elderfield, 1985; Shaw et al., 1990; Canfield et al., 1993; Jørgensen & Kasten, 2006), resulting in the production and potential efflux of nutrients. The relative importance of the various microbial metabolic pathways changes with the availability and reactivity of electron acceptors, sediment type, and OM accumulation rate (e.g. Froelich et al., 1979; Canfield et al., 1993; Kasten et al., 2004; Zonneveld et al., 2010), but generally as water depth increases, O_2 becomes more significant as oxidant driving OM mineralization. Since most of the reduced products of the other electron accepting processes (e.g. Mn^{2+}, Fe^{2+}, and HS^-) from anaerobic respiration are ultimately re-oxidized by an equivalent amount of O_2, benthic O_2 uptake is commonly used as a proxy of the total benthic carbon mineralization rate, which is a composite of aerobic and anaerobic mineralization. (e.g. Canfield et al., 1993).

This study aims to understand the impact of sea ice cover and patchy primary production on the carbon cycle and elemental fluxes in surface sediments along the eastern and western shelves of the Weddell Sea. Benthic oxygen uptake measurements and sediment characteristics were measured at 15 stations on the southern Weddell Sea shelf characterized by heterogeneous sea ice conditions and water depths, covering the Filchner Trough, the eastern and the western shelf

regions. In addition, pore water concentrations of NO_3^-, PO_4^{3-}, NH_4^+, Mn, Fe, and SO_4^{2-} were measured as well as total organic carbon (TOC) content to estimate the total carbon remineralization rate as well as the contribution of the various electron acceptors to the overall OM degradation. To develop an overall perspective of benthic carbon cycling we compare our data in the southern Weddell Sea shelf with data from other Antarctic continental shelves. Moreover, we discuss the main environmental factors driving the spatial patterns, variability, and change in benthic carbon remineralization rates in the Antarctic shelf seas.

2 Materials and Methods

2.1 Study site

The Weddell Sea plays an important role in global ocean circulation. In the Weddell Sea, the Weddell Gyre, a subpolar cyclonic circulation south of the Antarctic Circumpolar Current (ACC), diverts some of the Circumpolar Deep Water (CDW) from the ACC to the south, where it is modified to Warm Deep Water (WDW) (Figure 1) (Hellmer et al., 2016; Vernet et al., 2019). On the shelf, water masses are transformed by cooling, sea ice formation and brine injection causing increases in density. The dense water masses are exported from the shelf to the deep, contributing to the formation of Weddell Sea Bottom Water (WSBW) – a major precursor of Antarctic Bottom Water (Hellmer et al., 2016).

In this study, stations along the Filchner - Ronne Ice Shelf and the eastern Weddell Sea shelf were investigated during the research cruise PS111 with the German research vessel POLARSTERN between January and March 2018 (Schröder, 2018). During the cruise, the surface sediments of a total of 15 stations were sampled, four of which were located on the eastern Weddell Sea shelf at water depths ranging between 387 to 663 m, five in the Filchner Trough at 794 to 932 m depth, and four along the western Weddell Sea shelf at 332 to 660 m depth. Two deeper stations were sampled on the eastern Weddell Sea slope at 1405 and 1775 m water depth (Figure 1, Table 1), however only for pore water analyses.

Chlorophyll-a (Chl-a) concentrations integrated over the top 100 m of the water column were measured during the same cruise and exhibited high variabilities along the three regions, ranging

from 3.0 to 157.2 mg m^{-2} (Piontek et al., 2022), with highest values at the eastern and western shelf stations (average 82.8 mg Chl-a m^{-2}), and lowest values at Filchner Trough (average 12.3 mg Chl-a m^{-2}). Further environmental properties such as bottom water temperature, salinity, and oxygen concentration are listed in Table 1.

2.2 Calculation of Sea ice cover

The sea ice cover was calculated from satellite data using the Sea ice Index, version 3 (Fetterer et al., 2017). Daily sea ice cover of the last 30 years (1990–2019) was extracted for each station to determine the long-term mean sea ice cover (Table 1). In order to further analyze and characterize the different degrees of sea ice cover over the season, each day of the 30-year time series was classified as either *no sea ice* (<5%), *marginal sea ice* (5%–35%), *dominant sea ice* (35%–85%) and *full sea ice* (>85%) and finally weighted by the length of daylight (relative day length from sunrise to sunset). The average occurrence of each category was calculated to derive indices for the respective sea ice conditions.

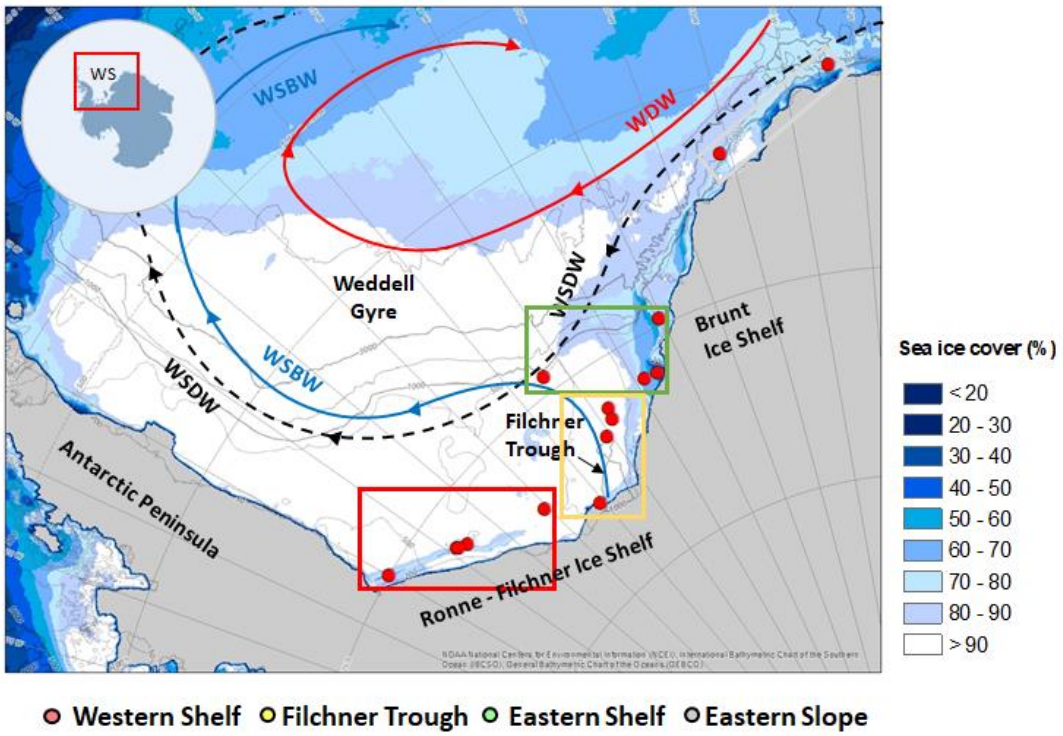

Figure 1. Map showing the Weddell Sea (location indicated by the red box in the inset) including all 15 stations (red circles) sampled during PS111 expedition and the main oceanographic features. Colors denote the percentage of sea ice concentration calculated from AMSR-E satellite estimates of daily sea ice cover (Spreen et al., 2008). Water depth is indicated by isolines. The study area was divided into the eastern slope (1405 - 1775 m depth), Filchner Trough (794 - 932 m), the eastern (387 - 663 m) and the western shelf regions (332 - 660 m). The abbreviations used in the figure are as follows: WSDW– Weddell Sea Deep Water, WDW–Warm Deep Water and WSBW –Weddell Sea Bottom Water (Orsi et al., 1995; Mathiot et al., 2011). The background bathymetry is derived from International Bathymetric Chart of the Southern Ocean (IBCSO) grid v1.0.

Table 1. Environmental settings and sediment characteristics for 15 stations collected during PS111. Bottom water temperature, salinity, and oxygen were obtained from CTD measurements. Sea ice cover is the average of the daily sea ice cover for the last 30 years (1990-2019) (Sea ice Index, version 3, Fetterer et al., 2017). The moderate sea ice index is the relative occurrence of moderate ice cover (defined as 5-35% ice cover), weighted by the length of daylight (sunrise to sunset) as described by Baloza et al. (2022). Total organic carbon (TOC) was analyzed from the surface sediment. n.a. is not analyzed.

	Station ID	Date	Lat °N	Lon °E	Water Depth	Sea ice	Mod. sea ice index	BW Temperature	BW Salinity	BW Oxygen	TOC	Mud content	Porosity
		DD/MM/YYYY			(m)	(%)		(°C)	(psu)	(µmol/l)	(wt %)	(%)	(%)
Eastern Slope	PS111_13-3	28/01/2018	-70.09	-6.85	1775	72		n.a.	n.a.	n.a.	0.333		n.a.
	PS111_15-1	01/02/2018	-71.66	-15.78	1405	78		n.a.	n.a.	n.a.	0.278		n.a.
Eastern Shelf	PS111_27-1	05/02/2018	-75.95	-29.08	425	67	0.084	-1.65	34.51	300.12	0.177	50.3	0.4
	PS111_29-3	06/02/2018	-75.97	-27.68	411	48	0.076	-1.72	34.39	306.81	0.112	23.1	0.4
	PS111_131-2	26/02/2018	-74.61	-36.93	387	93	0.024	-1.98	34.62	314.85	0.076	34.3	0.3
	PS111_139-2	01/03/2018	-74.82	-25.27	663	67	0.078	-1.68	34.37	303.24	0.250	79.0	0.6
Filchner Trough	PS111_70-2	17/02/2018	-76.11	-33.65	794	96	0.025	-1.92	34.67	313.07	0.517	94.5	0.7
	PS111_80-3	18/02/2018	-76.64	-35.42	932	98	0.011	-2.02	34.65	312.62	0.420	99.7	0.8
	PS111_98-3	20/02/2018	-77.80	-40.45	928	76	0.002	-2.20	34.63	314.41	0.390	96.1	0.7
	PS111_114-3	22/02/2018	-76.37	-33.93	839	94	0.021	-1.90	34.67	311.73	0.340	80.4	0.6
Western Shelf	PS111_40-2	10/02/2018	-76.00	-54.23	513	87	0.000	-1.78	34.40	313.51	0.453	90.1	0.7
	PS111_42-1	10/02/2018	-76.14	-53.35	493	93	0.016	-1.81	34.64	308.60	0.382	83.4	0.7
	PS111_53-3	13/02/2018	-76.02	-54.12	497	84	0.000	-1.77	34.62	305.47	0.461	86.4	0.7
	PS111_47-2	11/02/2018	-74.98	-60.00	660	65	0.002	-1.91	34.83	310.83	0.504	90.0	0.6
	PS111_60-3	14/02/2018	-77.01	-45.40	332	98	0.082	-1.89	34.67	317.09	0.181	68.1	0.6

2.3 Sample collection

Sediment cores with intact surface sediments and ambient overlying water were collected from multiple deployments of a multicorer (Oktopus GmbH, Kiel, Germany) with a core diameter of 6 cm. Immediately upon retrieval, sediment cores were transferred to the ship's cool laboratory and placed in a water bath at 0°C. Two cores were used for oxygen microprofiles and whole core oxygen consumption measurements. Another two cores were used for pore water and solid phase analyses. Prior to the sediment sampling, the water column was sampled using a Conductivity-Temperature-Depth-Probe (CTD, Seabird 911plus), equipped with an additional O_2 sensor (Sea-Bird SBE43) and a Rosette water sampler with 24 Niskin bottles of 12 L capacity.

The pore water was sampled with rhizon samplers (pore size 0.1 µm; Rhizosphere Research Products, Netherlands) within 1-2 hours after core retrieval according to procedure presented by Seeberg-Elverfeldt et al. (2005). Samples were taken at depth resolutions of 1 cm from 0-10 cm and below 10 cm with a resolution of 2 cm down to a maximum depth of 30 cm. Subsamples for cation analyses of dissolved iron (DFe) and manganese (DMn), and for nutrients such as ammonium (NH_4^+), phosphate (PO_4^{3-}), nitrate (NO_3^-), nitrite (NO_2^-) and silicate (SiO_3^{2-}) were taken. For cations, the first 1 ml of extracted pore water was discarded to ensure that the samples had not been in contact with air. Then, 1 ml of pore water was taken and filled into 2 ml polypropylene (PP) tubes prefilled with 25 µl of 2% v/v of HCl and stored at 4°C. For nutrient, sulfate (SO_4^{2-}) and chloride analyses, 4 ml of pore water were filled into 15 ml plastic tubes and stored at -20 °C. Sediments of parallel cores were sampled for porosity analyses at the same depth resolution and stored at -20 °C. Surface sediments (0–2 cm) for measuring TOC were collected and frozen at -20 °C by Lamping et al. (2021).

2.4 Diffusive oxygen uptake

Oxygen microprofiles for diffusive oxygen uptake (DOU, Table 2) were measured at 1000 µm-resolution using optodes with a tip diameter of 430 µm (Bare Fiber Oxygen Sensor, High Speed, Pyroscience). The optode bare fibers were glued into protecting needles of 15 cm length and 1 mm diameter as previously described by Ahmerkamp et al. (2017), which allows robust deep O_2 profiling with response times of < 1s. Oxygen microelectrodes were calibrated with 100% air

saturation (air-bubbled sea water) and 0% air saturation (by adding sodium dithionite) at -1.0 ± 0.3 °C and positioned by a motor-driven micromanipulator (MU1, Pyroscience). Temperature of the sediment core was recorded by a thermistor (Pyroscience) submersed into the overlying water. Profile data (depth, oxygen concentration, temperature) were recorded using a 4-channel FireSting oxygen meter (FSO2-4, Pyroscience) and processed using the "Profix" software from Pyroscience.

Oxygen microprofiles were measured in the Filchner Trough and the eastern and western shelf regions, with 2 to 3 microprofiles per station and a total of 30 microprofiles. A representative subset is shown in figure 2. For the three regions, six oxygen microprofiles were clearly disturbed by small stones that were sporadically encountered in the sediment cores. Such 'disturbed' profiles were not included in the quantification of benthic O_2 uptake rates (Table 2). Oxygen microprofiles were not measured at stations on the eastern slope. However, data for pore water profiles are presented below.

To estimate the rates of the volumetric oxygen consumption and diffusive oxygen uptake (DOU), we used the transport-reaction model PROFILE (Berg et al., 1998) for a best fit to the measured oxygen concentration profiles. The oxygen diffusion coefficient in sediments was calculated according to Berg et al. (1998) as $D_s = \varphi^2 D$ where *D* is the diffusion coefficient of O_2 in seawater at 35 PSU and 0°C, and φ is the porosity of the sediment in the specific depth layer. The boundary conditions used in PROFILE are the O_2 concentration at the top and the O_2 concentration at the bottom of the profile.

Several O_2 profiles did not reach the oxygen penetration depth (OPD). Thus, two approaches were used to test whether stations with such deep OPD (>5 cm) could introduce a bias in the estimation of the DOU rate. The first approach used the PROFILE model (Berg et al., 1998) to estimate the DOU rate by integrating the volumetric rate up to the OPD. The second approach used the uppermost gradient of the oxygen microprofile. Both approaches resulted in comparable values (see Table 2). Therefore, the DOU rate for all stations was determined using the uppermost concentration gradient.

2.5 Total oxygen uptake

Total Oxygen Uptake (TOU) rates were determined by conducting sediment core incubations. After MUC retrieval, two intact cores with overlying water column of about 10 cm were closed by rubber stoppers. The stopper was perforated with a hole to allow inserting a mini-optode (Pyroscience) from above. The overlying water in the cores was stirred by a small magnetic bar mounted in the core liners and driven by a rotating magnet outside the cores. The cores were incubated in the water bath at controlled temperatures for at least 12 hours. Oxygen concentration was measured every 5 seconds using the 4-channel FireSting oxygen meter (FSO2-4, Pyroscience) and the software Pyro Oxygen Logger. Total oxygen uptake rates (mmol m^{-2} d^{-1}) were calculated from the slope of the linear regression of the oxygen concentration change (dC) over the incubation time (dt) multiplied by the water column height, i.e. the ratio of enclosed water volume (V) and surface area of the core (A):

$$TOU = \frac{V}{A} * \frac{dC}{dt} \quad (1)$$

2.6 Fauna-mediated oxygen uptake

Fauna-mediated oxygen uptake (FOU) rate, which includes fauna respiration and bioirrigation (burrow ventilation), was determined from TOU and DOU. Since DOU mostly represents microbial respiration and TOU additionally comprises oxygen consumption by macrofauna and meiofauna activity, the difference between (TOU – DOU) can be used as a proxy for FOU rate (Glud, 2008). This approach has been suggested previously by several studies showing that FOU correlates significantly with the benthic fauna biomass (Glud et al., 1994; 1998; Wenzhöfer & Glud, 2002). In this study, we calculated FOU from the mean of DOU of each station subtracted from the mean of TOU of the same station.

$$FOU = TOU - DOU \quad (2)$$

2.7 Pore water analyses

All pore water analyses were performed at the Alfred Wegener Institute, Helmholtz Centre for Polar and Marine Research (AWI) in Bremerhaven. NH_4^+, NO_3^-, NO_2^-, and PO_4^{3-} were measured on a QuAAtro four-channel flow injection analyzer (Seal Analytical). DFe, DMn were determined

after a 10-fold dilution using Inductively Coupled Plasma Optical Emission Spectrometry (ICP-OES, Thermo iCAP7000) and yttrium was used as an internal standard to correct for differences of ionic strengths of samples. The quantification limits in two different sequences were 0.02 and 0.04 mg/l (0.4 and 0.8 µmol/l) for DFe and 0.003 and 0.007 mg/l (0.05 and 0.13 µmol/l) for DMn. Recoveries for DFe and DMn added in known concentrations to IAPSO Standard Seawater were between 97.4 and 100.4 %. Sulfate (SO_4^{2-}) and chloride samples (1:100 dilutions with ultrapure water) were analyzed by ion chromatography (Metrohm IC Net 2.3).

2.8 Solid phase analyses

Total organic carbon (TOC) contents in the surface sediment have been published by Lamping et al. (2021). Sediment porosity was determined from water content, measured as weight loss after freeze drying and assuming a solid density of 2.6 g cm $^{-3}$ as described by Burdige (2006). The grain-size properties of the samples were determined using a laser-diffraction particle size analyzer (CILAS 1180) with a range of 0.04–2500 µm. Carbonates and organic matter were removed prior to analyses by a consecutive treatment with 30% acetic acid and 12% hydrogen peroxide.

2.9 Rate measurements

The diffusive fluxes of DFe, DMn, and NO_3^- were estimated from the respective pore water concentration gradients using Fick's first law of diffusion:

$$J = -\varphi D_s \frac{dC\,(z)}{dz} \tag{3}$$

in which *J* represents the flux of the specific solute and $dC(z)/dz$ represents the concentration gradient of the solute in a specific depth interval calculated by linear regression. Rates of denitrification in the sediment were estimated as the diffusive downward flux of NO_3^- in the pore water below the NO_3^- maximum, i.e. below the nitrification zone (J_{NO3-}, Eq. 3). The nitrification rates were calculated from the sum of both upward and downward fluxes of NO_3^-.

3 Results

3.1 Sea ice conditions and bottom water characteristics

Long-term sea ice cover (Table 1) was lower at the eastern shelf (48 – 93%) compared to the western shelf (65 – 98%) and Filchner Trough (76 – 98%). Consequently, the moderate sea ice index at the eastern shelf was higher (0.024 – 0.084) than at the western shelf (0.000 – 0.082) and Filchner Trough (0.002 – 0.025). Bottom water temperatures of -1.98 to -1.65 °C were recorded along the eastern and western shelf stations whereas at the Filchner Trough stations temperatures ranged from -2.20 to -1.90 °C. The average bottom water salinity in all stations was 34.37 to 34.83 PSU. Bottom-water oxygen concentrations were between 300 and 317 µmol/l at all stations.

3.2 General sediment characteristics

TOC contents in the surface sediments in the three regions along the southern Weddell Sea shelf range between 0.076 and 0.517 wt% (Table1). TOC in the eastern shelf (0.076 – 0.250 wt%) was approximately half of that in the Filchner Trough (0.340 – 0.517 wt%) and the western shelf regions (0.181 – 0.504 wt%). Higher TOC contents were observed in fine-grained sediments of the Filchner Trough and at western shelf stations with a mud content of 68.1 – 99.7% and a high porosity of 0.6 – 0.8 (Table 1). However, mud content and porosity at the eastern shelf stations were lower (23.1 – 79.0% mud, 0.3 – 0.6 porosity, Table 1). As a result, a significant positive correlation between TOC content (wt%) and porosity (R^2=0.697, p=0.0004) was found (Figure 3 A+C). Interestingly, another positive correlation was found between TOC content and water depth (R^2=0.347, p=0.0340) for the three regions (Figure 3 D).

3.3 Oxygen uptake rates

Oxygen microprofiles in the eastern shelf exhibited steeper O_2 gradients and shallower O_2 penetration depths (OPD) (1.9 – 4.7cm) compare to the Filchner Trough and the western shelf regions where the OPD exceeded the maximum measuring depth of 5 cm. Oxygen concentration at the sediment–water interface ranged from 300 to 315 µM equivalent to 79.6 – 82.8% air saturation (Figure 2; Table 1). Diffusive oxygen uptake rates (DOU) in the eastern shelf (0.35 to 0.95 mmol O_2 m^{-2} d^{-1}) were approximately 3 times higher than in the western shelf (0.21 $\pm$ 0.01

to 0.34 ± 0.01 mmol O_2 m^{-2} d^{-1}) and Filchner Trough (0.13 to 0.44 ± 0.11 mmol O_2 m^{-2} d^{-1}) (Table 2). The volumetric O_2 consumption rates close to the sediment surface were lower at the western and Filchner Trough stations (5 – 60 nmol cm^{-3} d^{-1}) compared to the eastern shelf stations (40 – 65 nmol cm^{-3} d^{-1}). At all stations, total oxygen uptake rates (TOU) ranged from 0.26 ± 0.17 to 1.45 ± 0.36 mmol O_2 m^{-2} day^{-1} showing little spatial variation. Fauna mediated oxygen uptake rates (FOU) showed a greater contribution than DOU at Filchner Trough compared to the other shelf stations (Table 2).

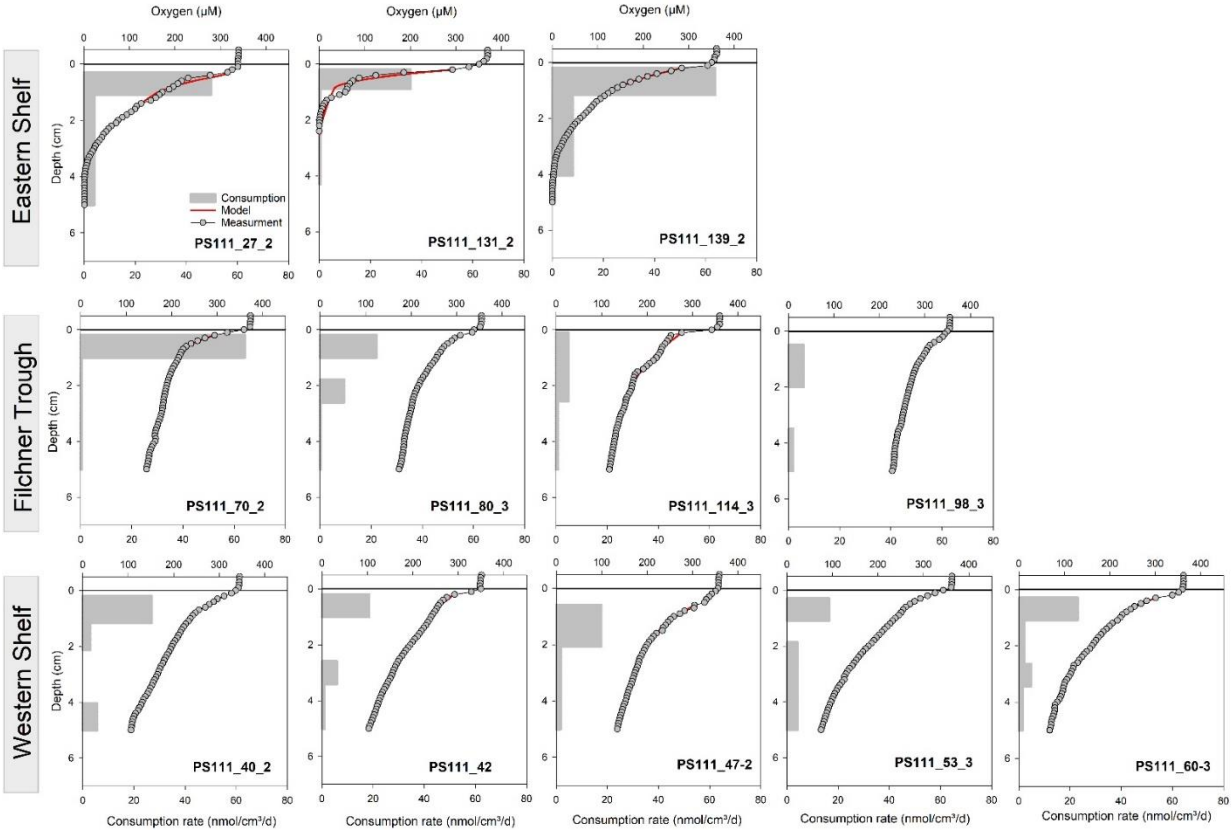

Figure 2. Representative O_2 profiles measured with optical microsensors for Filchner Trough, eastern and western shelves of the Weddell Sea. The horizontal lines indicate the sediment surface. Grey circles mark measured O_2 profiles. Red lines are the modeled oxygen profiles and grey shaded boxes show the modeled consumption rate for specific depth intervals, both

calculated using the transport-reaction model PROFILE (Berg et al., 1998). Note the different scales for the consumption rates

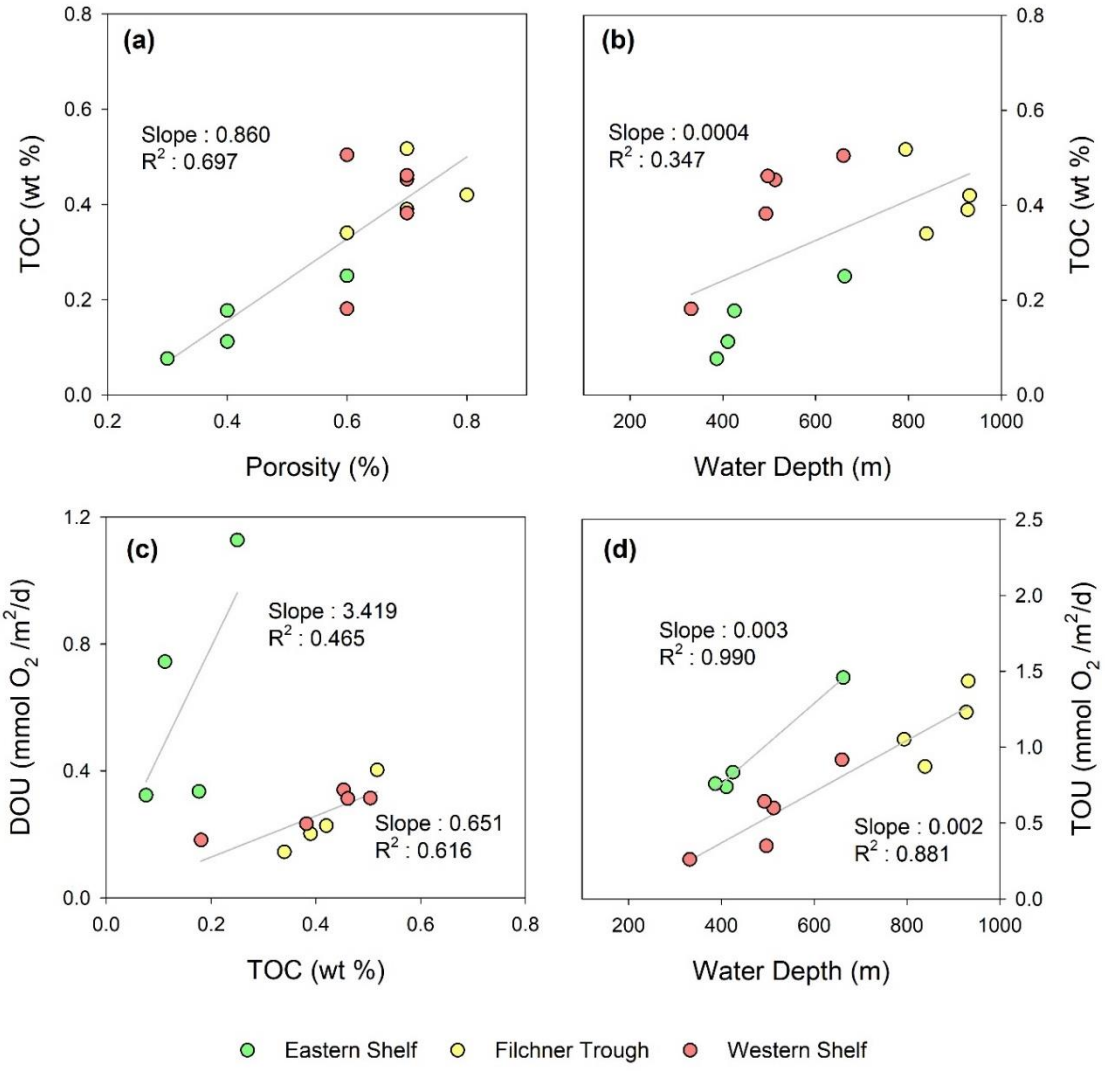

Figure 3. Correlations between characteristic variables of sampled stations: **(a)** significant linear relationship between the TOC contents (wt%) and porosity values (RSE of slopes < 19.8%, p=0.0004). **(b)** Significant increase of TOC contents with water depth (RSE of slopes < 41.3%, p=0.0340). **(c)** Significant linear relationship between TOC contents and diffusive oxygen uptake (DOU) rates for Filchner Trough and western shelf (RSE of slopes < 7.1%, p<0.0001) however, stations at the eastern shelf is not significant (RSE of slopes < 42.9%, p=0.2581). **(d)** Significant correlation between sediment oxygen uptakes (TOU) in different water depths (332–932 m) for

both the eastern shelf (RSE of slopes < 6.4%, p=0.005) and Filchner Trough and western shelf (RSE of slopes < 11.7%, p=0.0002).

3.4 Pore water chemistry

Pore water profiles obtained at the eastern shelf stations show a more condensed redox zonation compared to the western shelf and Filchner Trough stations (Figure 4). Nitrate concentrations decreased within the uppermost 5 cm indicating denitrification just below the oxygen penetration depth. The nitrate reduction zone is followed by a steady downward increase of DMn and DFe concentrations below 4.5 cm depth. Maximum concentrations of DMn (61 µM) and DFe (105 µM) were found at deepest sampling depths of 23 cm. Pore water SO_4^{2-} concentrations were constant (27 mM) over depth at all stations.

In the sediments at Filchner Trough and the western shelf, pore water concentrations of NO_3^- exhibited a maximum at 5 cm depth marking the nitrification zone. At the western shelf, NO_3^- decreased to zero at ~25 cm depth, whereas the decrease was less pronounced at Filchner Trough (Figure 4). Below the denitrification zone, the Mn-reduction starts deeper in the Filchner Trough sediments where DMn concentrations are generally lower (4 µM at 33 cm depth) compared to the western shelf where DMn concentrations are 63 µM at 35 cm depth. Concentrations of DFe in pore water were below the detection limit at all stations in both regions, except at station PS111_53_3, where DFe increased below 30 cm depth. Concentrations of NH_4^+ were very low at all stations (Figure 4). On the other hand, PO_4^{3-} concentrations were low near the surface sediment and slightly increased at 2 cm depth (<15 µM). The deep and rather moderate increase of DFe is in line with a rather slow increase in NH_4^+ and PO_4^{3-} concentrations with depth (<5 µM NH_4^+ and <15 µM PO_4^{3-}).

Pore water profiles obtained at the eastern slope show similar patterns as the western shelf and Filchner Trough (Figure 4). Although measurements of oxygen concentration profiles at the eastern slope are lacking, we assume that the maximum oxygen penetration should lie at a depth between 3 to 4 cm indicated by the nitrate peak marking the nitrification zone. A rather deep and broad nitrate reduction zones is in accordance with the absence of DMn, DFe, and the absence of net SO_4^{2-} reduction at the upper 20 cm sediment depth.

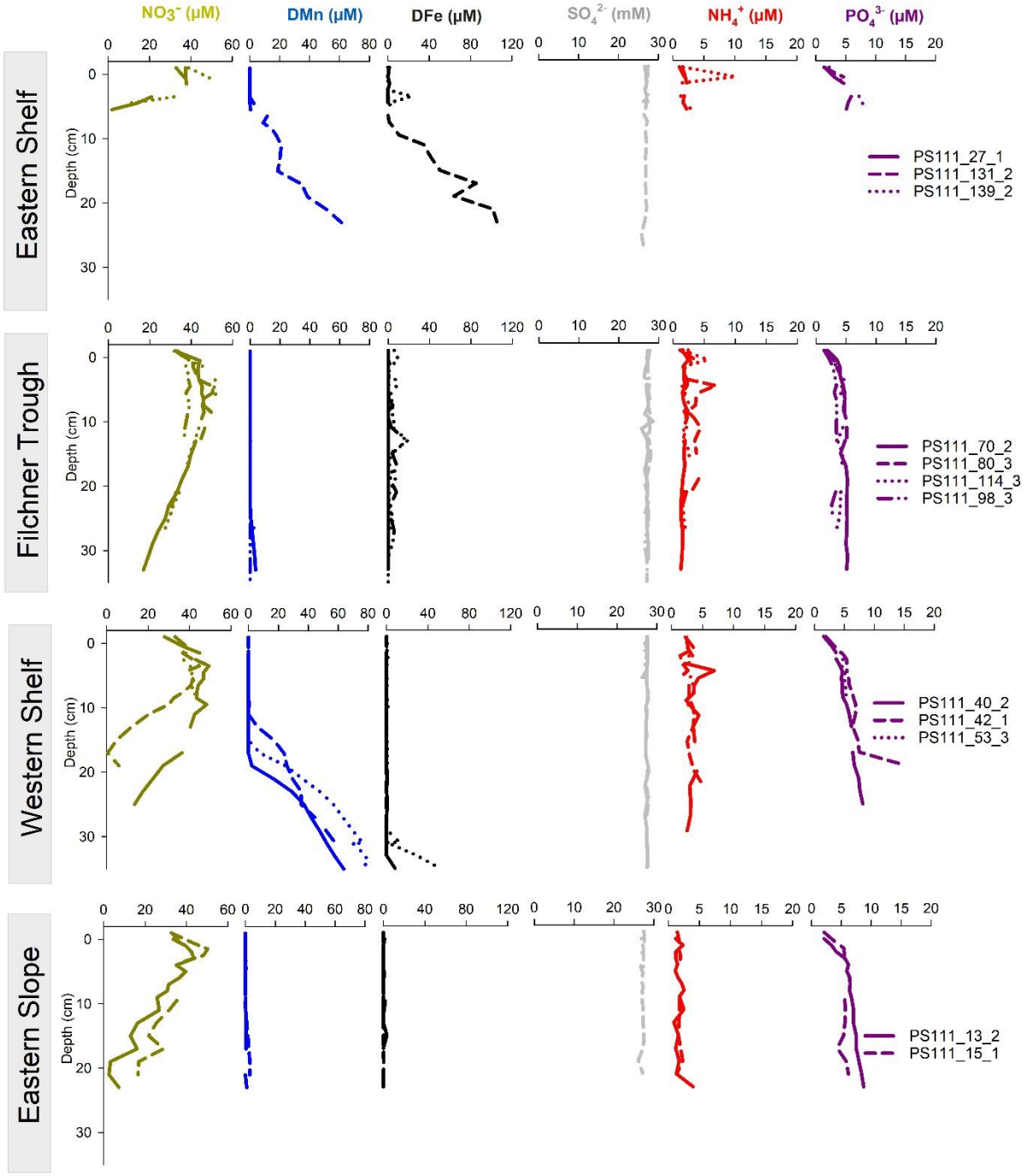

Figure 4. Representative profiles of reactive pore water compounds at eastern slope, Filchner Trough, eastern and western shelves of the Weddell Sea. Note that the scale for DMn and DFe concentrations changes between stations.

Table 2. DOU, diffusive oxygen uptake; TOU, total oxygen uptake; FOU, Fauna mediated oxygen uptake; DOU/TOU, is the relative contribution of diffusive oxygen (expressed as a percentage); n.a.: not analyzed. Data are presented as average ± SD with the number of profile measurements in parentheses. Only one pore water profile was measured for NO_3^- and DFe. Diffusive fluxes of denitrification and DFe were estimated from pore water concentration gradients. DOU (gradient) is estimated from the uppermost gradient of the oxygen microprofile while DOU (rate integration) is estimated using the PROFILE model (Berg et al., 1998) and integrating the volumetric rate up to the OPD.

	Station ID	OPD	DOU (gradient)	DOU (rate integration)	TOU	FOU	(DOU/TOU)	Denitrification	DFe flux
		cm	mmol/m²/d	mmol/m²/d	mmol/m²/d	mmol/m²/d	%	mmol/m²/d	µmol/m²/d
Eastern Shelf	PS111_27-1	4.7	0.34±0.01(3)	0.47±0.06 (3)	0.83 ±0.12 (2)	0.35	56.95	0.011	0.00
	PS111_29-3	n.a.	n.a.	n.a.	0.73	n.a.	n.a.	n.a.	n.a.
	PS111_131-2	1.9	0.32±0.18(3)	0.35±0.19 (3)	0.75 ±0.03 (2)	0.40	46.16	0.000	3.42
	PS111_139-2	4.55 ±0.35(2)	1.13±0.47(2)	0.95±0.14 (2)	1.45 ±0.36 (2)	0.50	65.46	0.022	16.10
Filchner Trough	PS111_70-2	n.a.	0.40±0.05(2)	0.44 ±0.11 (2)	1.05 ±0.05(2)	0.60	42.37	0.004	0.00
	PS111_80-3	n.a.	0.23±0.11(2)	0.26 ±0.17 (2)	1.43 ±0.36(2)	1.17	18.17	0.004	0.00
	PS111_98-3	n.a.	0.20±0.20(3)	0.21 ±0.20 (3)	1.15 ±0.18 (2)	0.94	18.36	0.001	0.00
	PS111_114-3	n.a.	0.14	0.13	0.87 ±0.11(2)	0.73	15.67	0.002	0.00
Western Shelf	PS111_40-2	n.a.	0.34±0.00(2)	0.34 ±0.01 (2)	0.59 ±0.15 (2)	0.25	58.13	0.005	3.88
	PS111_42-1	n.a.	0.23±0.02(2)	0.21 ±0.01 (2)	0.64 ±0.22 (2)	0.42	33.13	0.010	0.00
	PS111_53-3	n.a.	0.31±0.03(2)	0.31 ±0.03 (2)	0.34 ±0.26 (2)	0.03	88.88	0.004	8.50
	PS111_47-2	n.a.	0.31±0.03(2)	0.26 ±0.07 (2)	0.91 ±0.11 (2)	0.65	28.65	n.a.	n.a.
	PS111_60-3	n.a.	0.18±0.00(3)	0.21 ±0.04 (3)	0.26 ±0.17 (2)	0.04	82.61	n.a.	n.a.

4 Discussion

4.1 Benthic carbon remineralisation rates on the southern Weddell Sea shelf

The main focus of this paper is to quantify and discuss benthic carbon cycling in the permanently cold sediment of the southern Weddell Sea shelf; however, the data also offer the opportunity to compare different regions of the Antarctic shelf that are characterized by variable sea ice cover and water depth.

Our results suggest that benthic oxygen uptake rates on the southern Weddell Sea shelf are coupled to spatial variations in sea ice cover. In areas of high sea ice cover in summer (Filchner Trough and western shelf), deep oxygen penetration (>5 cm) and very low DOU (<0.5 mmol O2 /m²/d) show low metabolic activity of the sediment microbial and faunal community. In contrast, sediment on the eastern shelf with less sea ice cover in summer (48 – 98 %), had a shallow OPD (2 – 4 cm) and a relatively high DOU (0.35 – 0.95 mmol O_2 /m²/d), suggesting an enhanced metabolic activity, possibly facilitated by increased primary production and organic carbon export to the seafloor (Sachs et al., 2009; Glud et al., 2021).

Although DOU was highest at the eastern shelf stations, TOC content was the lowest here. This apparent mismatch between DOU and TOC can be attributed in part to differences in sediment grain size (Guo et al., 2021) and porosity (Liao et al., 2018). If sediment samples with a large sand content and low porosity have an OC content per volume sediment that is similar to fine sediment samples, then, the common presentation of TOC as per weight percent would result in systematic lower TOC values for these low-porosity sediments. Consequently, DOU correlates positively with TOC only in the fine-grained sediment cluster of the Filchner Trough and western shelf stations (Figure 4c), whereas sediments of the eastern shelf stations feature a low porosity (0.3– 0.6) and tend to cluster separately, with a steep slope but a weaker linear regression between DOU and TOC (Figure 3c). Interestingly, a positive correlation between total oxygen uptake (TOU) rates and water depth was observed. These results suggest that at greater water depths the accumulation of fine sediments and hence high TOU is induced by reduced bottom water currents, whereas at shallower water depths coarser sediments are indicative of higher current intensity (e.g. Sval'nov & Alekseeva, 2006; Jørgensen et al., 2022).

The organic carbon supply to the sediments is one of the major controls on sedimentary redox processes (e.g. Seiter et al., 2005; Freitas et al., 2021). As organic carbon supply rates decrease, aerobic respiration becomes the major carbon remineralization pathway (e.g. Betzer et al., 1984; Glud, 2008). The low organic carbon content (0.076 – 0.51 wt%) along the southern Weddell Sea shelf increases the relative importance of aerobic respiration, while the other electron acceptors are of minor importance. Accordingly, denitrification and metal reduction only contributed <9 % to the total carbon remineralization in all three regions. The low contribution of nitrate reduction (1 – 20 µmol C /m²/d) in the southern Weddell Sea shelf is comparable to a study of Hulth et al. (1997) who measured 5 to 70 µmol C /m²/d near the Filchner-Ronne Ice Shelf relative to a carbon supply of 0.50 to 1.94 mmol C /m²/d. Similar low denitrification rates (<3 µmol C /m²/d) and metal reduction rates (<0.2 and <0.03 µmol C /m²/d for Mn and Fe, respectively) are reported for example for deep-sea sediments of the eastern Pacific between 3116 – 3225 m water depth with a low carbon supply (0.032 – 0.035 mmol C /m²/d) (Bender & Heggie, 1984). In summary, oxic respiration is by far the dominant carbon remineralization pathway contributing >90 % to the total carbon remineralization in the southern Weddell Sea shelf and indicating an overall low carbon flux and a strong food limitation for the benthic communities.

Accordingly, pore water fluxes of dissolved micronutrients, which are controlled primarily by the amount of organic carbon remineralization in the sediment (Jørgensen, 1983; Monien et al., 2014; Dale et al., 2015; Baloza et al., 2022), were detected only at greater depths (DMn at >5 cm, DFe at >20 cm or absent), especially on the eastern and western shelves. The maximum values of DFe found in these sediments are significantly lower (< 110 µM and < 50 µM, respectively), compared to shelf sediment of the Antarctic Peninsula (AP) (670 µM at 5 cm depth, Baloza et al., 2022). Likewise, estimated upward DFe flux were lower in the study area (eastern shelf: 3.42 to 31.06 µmol Fe /m^2/d , western shelf: 3.88 to 8.50 µmol Fe /m^2/d) compared to the eastern coast of the AP (51.90 to 170.63 µmol Fe /m^2/d, (Baloza et al., 2022). In general, measurements of DFe porewater fluxes from the Antarctic shelf are very limited (Monien et al., 2014; Henkel et al., 2018; Schnakenberg et al., 2021; Wunder et al., 2021; Baloza et al., 2022; Burdige & Christensen, 2022). A comparison of our data with the available literature shows that the estimated total DFe fluxes on the southern Weddell Sea shelf are remarkably low. The deep ferruginous zone and the

low flux of dissolved iron within the sediments suggest a very limited efflux of DFe back to the water column.

4.2 Factors controlling benthic carbon remineralization in Antarctic shelf sediments

The Antarctic shelf is large, comprising about 11% of the global shelf area, and deep (500-1000 m) (Smith et al., 2006). It is characterized by extreme seasonality in sea ice cover and primary production (Clarke & Johnston, 2003; Smith et al., 2006). These properties affect the export of organic matter to the seafloor and microbial activity in the seabed thus controlling carbon cycling and burial within the sediment. (e.g. Baloza et al., 2022; 2023).

Annual extent and duration of the sea ice cover heavily influence the light availability as well as water-column stratification and, thus, the amount of annual primary and export production (e.g. Savidge et al., 1995; Vernet et al., 2019). Sea ice cover, derived from 30 years of satellite observations, is high on the southern Weddell Sea shelf (48–98%), Amundsen Sea (57–71%), and Ross Sea (69–77%) while low on the eastern shelf of the Antarctic Peninsula (AP) (33– 49%) and in the Bransfield Strait (26–40%) (Table 3).

To understand the effect of sea ice cover on benthic carbon cycling along the Antarctic shelf seas, data on benthic carbon remineralization and carbon supply rates were compiled from this study and the literature (see Table 3). The lowest carbon supply and remineralization rates occur at the heavy ice-covered regions of the southern Weddell Sea shelf (average 0.65 mmol C /m^2 /d), Amundsen Sea (average 1.67 mmol C /m^2 /d), and Ross Sea (average 1.86 mmol C /m^2 /d) (Table 3) while the moderate sea ice cover regions of the eastern shelf of the AP and Bransfield Strait exhibit high carbon supply and remineralization rates of 3.93 and 2.24 mmol C/m^2/d, respectively. This suggests that the occurrence of moderate sea ice cover supports surface primary production and an increased organic carbon flux, which finally fuels benthic carbon cycling. Our findings are consistent with a recent study by Baloza et al. (2022) who found that the rates of carbon supply and remineralization along the shelf of the AP increased exponentially with the occurrence of moderate sea ice cover (ice cover of 5%–35%), indicating favorable light conditions and water column stratification to enhance surface primary production (Figure 5a+b). Accordingly, the moderate sea ice index we found for the southern Weddell Sea (0.000– 0.084)

was relatively low compared to the values reported for the AP (0.038-0.174) (Figure 5). In conclusion, the large differences in benthic C-remineralization between shelf regions in Antarctica are largely caused by the long-term imprint of sea ice cover which affects primary production and the organic carbon input from the upper ocean.

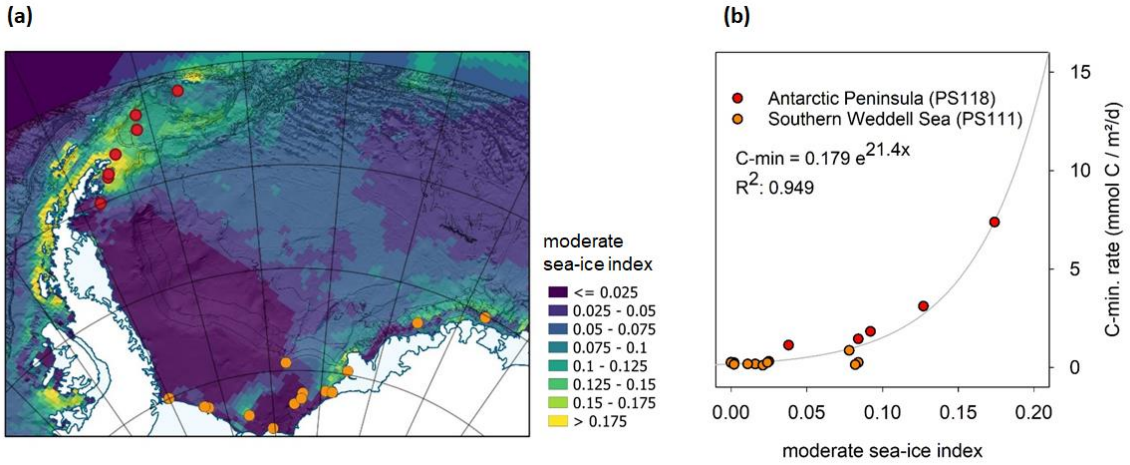

Figure 5. (a) Map of moderate sea ice index, defined as relative occurrence of marginal sea ice cover (5-35%), weighted by the length of daylight (sunrise to sunset) modified from Baloza et al. (2022). Values were derived from satellite data of daily sea ice cover from 1990 to 2019 at 25 km resolution (Fetterer, 2017). Isolines denote water depths. **(b)** The estimated carbon remineralisation rates as function of the moderate sea ice index. The relationship is best explained by an exponential growth function with a growth constant of 21 (RSE < 4.1%, $p<0.0001$). The assumption for applying a growth function is that increasing periods of favorable sea ice conditions lead to over-proportional primary production and, subsequently, over-proportional organic carbon supply of the sediments. Sampling stations in this study are shown as orange dots compiled with sampled stations along Antarctic Peninsula from PS118 expedition as red dots (Baloza et al., 2022).

Besides sea ice cover as controlling factor for primary production (Vernet et al., 2008), it is of interest to investigate if direct measurements of primary production can also explain the variability in the benthic carbon remineralization and carbon supply rates. Primary production on the continental shelf has been measured by von Bröckel (1985), von Bodungen et al.(1986), Smith et al. (1996) and Lee et al. (2017) (Table 3). Overall, primary productivity on the Antarctic continental shelf is patchy, with variable production within polynyas and marginal ice zones (Arrigo et al., 2008; Westwood et al., 2010; Deppeler et al., 2018). Rates of primary production can reach >110 mmol C /m^2 /d in the Amundsen Sea polynya (Lee et al., 2017), presently considered to be the most productive Antarctic polynya (Arrigo & van Dijken, 2003). Primary production within the southern Weddell Sea polynyas is 50 – 139 mmol C /m^2 /d (von Bröckel, 1985), which is comparable to the tip of the AP (34 – 149 mmol C /m^2 /d) (von Bodungen et al., 1986). Primary production reported in the Ross Sea polynya ranged from 25 to 108 mmol C /m^2 /d (Smith et al., 1996).

Because the Antarctic continental shelf is deep (on average 600 m), the recycling of organic matter while sinking through the water column attenuates the carbon flux to the seafloor and, subsequently, the benthic carbon turnover (e.g. Suess, 1980). The equation from Berger (1987) is used to estimate the fraction of primary production (Table 3) reaching the sea floor:

$$J_{Corg} = 17\ \mathrm{PP/z} + \mathrm{PP}/100$$

where J_{Corg} is the deposition flux of organic carbon (in mmol C m^{-2} day^{-1}) at water depth z (in meters) and PP is the primary production (in mmol C /m^2 /d).

The calculated C supply (flux to the seafloor) exceeds the measured carbon supply by a factor of up to 15 (see Table 3, Figure 6). The large discrepancy between calculated and measured benthic carbon supply rates point towards the fact that PP rates from field measurements only provide a temporal snapshot of seasonal production, which is highly variable due to the strong seasonality at these latitudes (Bélanger et al., 2007). While the accumulation of benthic carbon represents a long-term integrated measure of the OC flux (Seiter et al., 2005; Smith et al., 2006), PP

measurements during field campaigns usually reflect the summer situation when the region is accessible for research vessels. Even satellite-based remote measurements of PP, which can be conducted throughout the year, have their shortcomings in these latitudes, because the presence of sea ice, even at low ice concentrations, impedes the measurements of ocean color from remote sensing (Bélanger et al., 2007). Instead, the significant correlation between benthic carbon remineralization rates and the moderate sea ice index (Figure 5b), as a proxy for favorable algal growth conditions, suggests that long-term sea ice cover may be a good predictor of the benthic carbon remineralization rate. As the exponential relation in figure 5 holds for stations of similar water depth only, the flux attenuation due to water depth should be considered in future studies.

Table 3. Compiled data of sea ice cover, surface primary production, benthic carbon remineralization rates, and carbon supply rates from different regions in the Antarctic shelf.

Region		Sea ice cover	Mod. Sea ice index	Water Depth	Primary Production	C remin rate	Measured C supply rate	Calculated C supply rate	Measured C supply rate/ Calculated C supply rate	Sed. rate	Citation
		(%)		(m)		mmol C /m^2 /d			%	cm/yr	
Weddell Sea	Halley bay Polynya	48-93	0.024-0.084	387-663	63- 99	0.57-1.12	1.06	2.9-4.4	13.3-15.8	-	This study, (1), (2), (3)
	Ronne Polynya	65-98	0.000-0.082	332-660	50.8-139.1	0.20-0.70	0.69-1.36	3.4-5.3	6.4-20.7	-	This study, (1). (2), (3)
	Flincher Ice shelf	76-98	0.002-0.025	794-932	37– 47	0.67-1.10	0.28-1.80	1.2-1.3	52.6-92.9	-	This study, (1), (2),
	Antarctic Peninsula Shelf	33-49	0.084-0.174	415-455	34.4-149.6	3.08-5.52	3.20-12.97	3.3-5.1	89.9-108.5	0.22-0.76	(3), (4)
Bellingshausen Sea	Bransfield Strait	26-40	0.066-0.078	550-625	17 – 150	2.04-2.39	0.685	3.2-3.3	60.8-73.8	0.06-0.16	(5), (6), (7), (13)
Amundsen Sea	Polynya	57-61	0.194-0.207	730-825	110	1.87-2.39	0.15-0.29	3.4-3.7	55.7-65.2	0.18-0.20	(8), (9)
	Ice shelf and marginal ice zone	69-71	0.087-0.127	530-1064	110	1.21	-	2.9-4.6	26.1-42.5	0.12-0.13	(8), (9)
Ross Sea	Western polynya	69-77	0.042-0.071	300 - 800	25-108	1.17-2.55	0.228-1.83	2.9	39.9-87.2	0.06-0.27	(10), (11), (12), (13)

Note. The ice cover (30 year average of daily sea ice concentration) was calculated from historic satellite data Sea ice Index, version 3, (Fetterer, 2017). The moderate sea ice index is the relative occurrence of moderate ice cover (defined as 5-35% ice cover), weighted by the length of daylight (sunrise to sunset) as described by Baloza et al. (2022). Organic carbon flux was calculated using Berger et al. (1987) equation. References: (1) (von Bröckel, 1985), (2) (Hulth et al., 1997), (3) (von Bodungen et al., 1986), (4) (Baloza et al., 2022), (5) (Masqué et al., 2002), (6) (Figueiras et al., 1998), (7) (Hartnett et al., 2008), (8) (Kim et al., 2016), (9) (Lee et al., 2017), (10) (Barry et al., 2003), (11) (Grebmeier et al., 2003), (12) (Ledford-Hoffman et al., 1986), (13) (DeMaster et al., 1991).

5 Conclusions and Outlook

Benthic oxygen uptake rates on the southern Weddell Sea shelf are coupled to spatial variations in sea ice cover, with deep oxygen penetration and very low DOU in the heavily sea ice covered Filchner Trough and on the western shelf, and shallow oxygen penetration and relatively high DOU on the eastern shelf. DOU is positively correlated with preserved TOC in fine-grained sediments of the Filchner Trough and western stations. In contrast, sediments from the eastern stations have low porosity (0.3-0.6), typical of coarse-grained sediments, with a markedly different correlation of DOU with TOC. For both sediment provinces, TOU appears to increase with water depth, with elevated rates of up to 1.5 mmol/m²/d in the Filchner Trough and near the shelf break in the east. These results suggest that at greater water depths the accumulation of fine sediments and hence high TOU is induced by reduced bottom water currents, whereas at shallower water depths coarser sediments are indicative of higher current intensity. Common to all stations is that dissolved Fe and Mn concentrations in pore water are only found at greater depths (Mn at >5 cm, Fe at >10 cm or absent), suggesting very limited release of these nutrients back into the water column.

This study highlights the pivotal role of sea ice cover in driving benthic carbon cycling in different regions of the Antarctic shelf. A critical avenue for advancing our understanding of benthic carbon cycling in future research is to simultaneously consider the effects of both sea ice cover and water depth on organic matter fluxes. A comprehensive assessment of the current benthic carbon cycle on the Antarctic continental shelf is essential to anticipate the effects of continued global warming and expected reductions in sea ice extent.

Acknowledgements

We would like to express our sincere gratitude to the captain and crew of R/V POLARSTERN for their help and efforts during expedition PS111. Special thanks to Dr. Lasse Sander (AWI Sylt) for the grain size analyses of the sediments. I would like to express my deep appreciation to Nele Lamping and Juliane Müller for providing us with the TOC data. We also thank Ingrid Stimac and Ingrid Dohrmann (AWI Bremerhaven) for the pore water analyses. This study was funded by the

Helmholtz research program “Changing Earth – Sustaining our Future” and Grant-No. AWI_PS111_00. Open Access funding was facilitated and organized by the DEAL project.

References

Ahmerkamp, S., Winter, C., Krämer, K., Beer, D. d., Janssen, F., Friedrich, J., et al. (2017). Regulation of benthic oxygen fluxes in permeable sediments of the coastal ocean. Limnology and Oceanography, 62(5), 1935-1954. doi:https://doi.org/10.1002/lno.10544

Arrigo, K. R., van Dijken, G., & Long, M. (2008). Coastal Southern Ocean: A strong anthropogenic CO_2 sink. *Geophysical Research Letters, 35*(21). doi:https://doi.org/10.1029/2008GL035624

Arrigo, K. R., & van Dijken, G. L. (2003). Phytoplankton dynamics within 37 Antarctic coastal polynya systems. *Journal of Geophysical Research: Oceans, 108*(C8).

Baloza, M., Henkel, S., Geibert, W., Kasten, S., & Holtappels, M. (2022). Benthic Carbon Remineralization and Iron Cycling in Relation to Sea ice Cover Along the Eastern Continental Shelf of the Antarctic Peninsula. *Journal of Geophysical Research-Oceans, 127*(7), e2021JC018401. doi:ARTN e2021JC01840110.1029/2021JC018401

Baloza, M., Henkel, S., Kasten, S., Holtappels, M., & Molari, M. (2023). The Impact of Sea ice Cover on Microbial Communities in Antarctic Shelf Sediments. *Microorganisms, 11*(6), 1572. doi:10.3390/microorganisms11061572

Barry, J. P., Grebmeier, J. M., Smith, J., & Dunbar, R. B. (2003). Oceanographic versus seafloor-habitat control of benthic megafaunal communities in the S.W. Ross Sea, Antarctica. *Antarctic Research Series, 78*, 327-354. Retrieved from https://www.scopus.com/inward/record.uri?eid=2-s2.0-33745689977&partnerID=40&md5=e754807f8ef312d252c0f35b6ee3d014

Bélanger, S., Ehn, J. K., & Babin, M. (2007). Impact of sea ice on the retrieval of water-leaving reflectance, chlorophyll a concentration and inherent optical properties from satellite ocean color data. *Remote Sensing of Environment, 111*(1), 51-68. doi:https://doi.org/10.1016/j.rse.2007.03.013

Bender, M. L., & Heggie, D. T. (1984). Fate of organic carbon reaching the deep sea floor: a status report. *Geochimica et Cosmochimica Acta, 48*(5), 977-986. doi:https://doi.org/10.1016/0016-7037(84)90189-3

Berg, P., Risgaard-Petersen, N., & Rysgaard, S. (1998). Interpretation of measured concentration profiles in sediment pore water. *Limnology and Oceanography, 43*(7), 1500-1510. doi:https://doi.org/10.4319/lo.1998.43.7.1500

Berger, W. (1987). Overview and maps of primary production and export production. Productivity and organic carbon flux. Part I.

Betzer, P. R., Showers, W. J., Laws, E. A., Winn, C. D., DiTullio, G. R., & Kroopnick, P. M. (1984). Primary productivity and particle fluxes on a transect of the equator at 153 W in the Pacific Ocean. Deep Sea Research Part A. *Oceanographic Research Papers, 31*(1), 1-11.

Burdige, D. J. (2006). Geochemistry of marine sediments: Princeton University Press.

Burdige, D. J. (2007). Preservation of Organic Matter in Marine Sediments: Controls, Mechanisms, and an Imbalance in Sediment Organic Carbon Budgets? *Chemical Reviews, 107*(2), 467-485. doi:https://doi.org/10.1021/cr050347q

Burdige, D. J., & Christensen, J. P. (2022). Iron biogeochemistry in sediments on the western continental shelf of the Antarctic Peninsula. *Geochimica et Cosmochimica Acta, 326*, 288-312. doi:https://doi.org/10.1016/j.gca.2022.03.013

Canfield, D. E. (1993). Organic matter oxidation in marine sediments. In Interactions of C, N, P and S biogeochemical cycles and global change (pp. 333-363): Springer.

Canfield, D. E., Jørgensen, B. B., Fossing, H., Glud, R., Gundersen, J., Ramsing, N. B., et al. (1993). Pathways of organic carbon oxidation in three continental margin sediments. *Marine Geology, 113*(1-2), 27-40.

Clarke, A., & Johnston, N. M. (2003). Antarctic marine benthic diversity. *In Oceanography and Marine Biology, An Annual Review, Volume 41* (pp. 55-57): CRC Press.

Dale, A. W., Nickelsen, L., Scholz, F., Hensen, C., Oschlies, A., & Wallmann, K. (2015). A revised global estimate of dissolved iron fluxes from marine sediments. *Global Biogeochemical Cycles, 29*(5), 691-707. doi:https://doi.org/10.1002/2014GB005017

DeMaster, D. J., Nelson, T. M., Harden, S. L., & Nittrouer, C. A. (1991). The cycling and accumulation of biogenic silica and organic carbon in Antarctic deep-sea and continental margin environments. *Marine Chemistry, 35*(1), 489-502. doi:https://doi.org/10.1016/S0304-4203(09)90039-1

Deppeler, S., Petrou, K., Schulz, K. G., Westwood, K., Pearce, I., McKinlay, J., et al. (2018). <? xmltex\vspace* 5mm?> Ocean acidification of a coastal Antarctic marine microbial community reveals a critical threshold for CO_2 tolerance in phytoplankton productivity. *Biogeosciences, 15*(1), 209-231.

Elderfield, H. (1985). Element cycling in bottom sediments. *Philosophical Transactions of the Royal Society of London. Series A, Mathematical and Physical Sciences, 315*(1531), 19-23.

Fetterer, F., Knowles, K., Meier, W. N., Savoie, M., & Windnagel, A. K. . (2017). Sea ice index, version 3. [Years 1978-2019]. NSIDC: National Snow and Ice Data Center. doi:https://doi.org/10.7265/N5K072F8

Figueiras, F., Estrada, M., López, O., & Arbones, B. (1998). Photosynthetic parameters and primary production in the Bransfield Strait: relationships with mesoscale hydrographic structures. *Journal of Marine Systems, 17*(1-4), 129-141.

Freitas, F. S., Pika, P. A., Kasten, S., Jørgensen, B. B., Rassmann, J., Rabouille, C., et al. (2021). New insights into large-scale trends of apparent organic matter reactivity in marine sediments and patterns of benthic carbon transformation. *Biogeosciences, 18*(15), 4651-4679. doi:10.5194/bg-18-4651-2021

Froelich, P. N., Klinkhammer, G. P., Bender, M. L., Luedtke, N. A., Heath, G. R., Cullen, D., et al. (1979). Early oxidation of organic matter in pelagic sediments of the eastern equatorial Atlantic: suboxic diagenesis. *Geochimica et Cosmochimica Acta, 43*(7), 1075-1090. doi:https://doi.org/10.1016/0016-7037(79)90095-4

Glud, R., Gundersen, J. K., Barker Jørgensen, B., Revsbech, N. P., & Schulz, H. D. (1994). Diffusive and total oxygen uptake of deep-sea sediments in the eastern South Atlantic Ocean:in situ and laboratory measurements. *Deep Sea Research Part I: Oceanographic Research Papers, 41*(11), 1767-1788. doi:https://doi.org/10.1016/0967-0637(94)90072-8

Glud, R. N. (2008). Oxygen dynamics of marine sediments. *Marine Biology Research, 4*(4), 243-289. doi:10.1080/17451000801888726

Glud, R. N., Berg, P., Thamdrup, B., Larsen, M., Stewart, H. A., Jamieson, A. J., et al. (2021). Hadal trenches are dynamic hotspots for early diagenesis in the deep sea. *Communications Earth & Environment, 2*(1), 21. doi:10.1038/s43247-020-00087-2

Glud, R. N., Holby, O., Hoffmann, F., & Canfield, D. E. (1998). Benthic mineralization and exchange in Arctic sediments (Svalbard, Norway). *Marine Ecology Progress Series, 173*, 237-251.

Grebmeier, J., & Barry, J. (2007). Benthic processes in polynyas. *Elsevier Oceanography Series, 74*, 363-390.

Grebmeier, J. M., Ditullio, G. R., Barry, J. P., & Cooper, L. W. (2003). Benthic carbon cycling in the Ross Sea Polynya, Antarctica: Benthic community metabolism and sediment tracers. *Antarctic Research Series, 78*, 313-326.

Gruber, N., Gloor, M., Mikaloff Fletcher, S. E., Doney, S. C., Dutkiewicz, S., Follows, M. J., et al. (2009). Oceanic sources, sinks, and transport of atmospheric CO_2. *Global Biogeochemical Cycles, 23*(1). doi:https://doi.org/10.1029/2008GB003349

Guo, J., Yuan, H., Song, J., Li, X., Duan, L., Li, N., et al. (2021). Evaluation of Sedimentary Organic Carbon Reactivity and Burial in the Eastern China Marginal Seas. *Journal of Geophysical Research: Oceans, 126*(4), e2021JC017207. doi:https://doi.org/10.1029/2021JC017207

Gutt, J., Barratt, I., Domack, E., d'Acoz, C. d. U., Dimmler, W., Grémare, A., et al. (2011). Biodiversity change after climate-induced ice-shelf collapse in the Antarctic. *Deep Sea Research Part II: Topical Studies in Oceanography, 58*(1-2), 74-83.

Gutt, J., & Starmans, A. (1998). Structure and biodiversity of megabenthos in the Weddell and Lazarev Seas (Antarctica): ecological role of physical parameters and biological interactions. *Polar Biology, 20*, 229-247.

Hartnett, H., Boehme, S., Thomas, C., DeMaster, D., & Smith, C. (2008). Benthic oxygen fluxes and denitrification rates from high-resolution porewater profiles from the Western Antarctic Peninsula continental shelf. *Deep Sea Research Part II: Topical Studies in Oceanography, 55*(22), 2415-2424. doi:https://doi.org/10.1016/j.dsr2.2008.06.002

Hauck, J., Völker, C., Wolf-Gladrow, D. A., Laufkötter, C., Vogt, M., Aumont, O., et al. (2015). On the Southern Ocean CO_2 uptake and the role of the biological carbon pump in the 21st century. *Global Biogeochemical Cycles, 29*(9), 1451-1470.

Hellmer, H. H., Rhein, M., Heinemann, G., Abalichin, J., Abouchami, W., Baars, O., et al. (2016). Meteorology and oceanography of the Atlantic sector of the Southern Ocean—a review of German achievements from the last decade. *Ocean Dynamics, 66*(11), 1379-1413.

Henkel, S., Kasten, S., Hartmann, J. F., Silva-Busso, A., & Staubwasser, M. (2018). Iron cycling and stable Fe isotope fractionation in Antarctic shelf sediments, King George Island. *Geochimica et Cosmochimica Acta, 237*, 320-338. doi:https://doi.org/10.1016/j.gca.2018.06.042

Hulth, S., Tengberg, A., Landén, A., & Hall, P. O. (1997). Mineralization and burial of organic carbon in sediments of the southern Weddell Sea (Antarctica). *Deep Sea Research Part I: Oceanographic Research Papers, 44*(6), 955-981.

Jørgensen, B. (1983). Processes at the sediment-water interface. œ In: BOLIN, B. & COOK, RB (Hrsg.): *The major biogeochemical cycles and their interaction*. Chapter 18: 477-509. In: Wiley, Chichester.

Jørgensen, B. B., & Kasten, S. (2006). Sulfur cycling and methane oxidation. *Marine geochemistry,* 271-309.

Jørgensen, B. B., Wenzhöfer, F., Egger, M., & Glud, R. N. (2022). Sediment oxygen consumption: Role in the global marine carbon cycle. *Earth-Science Reviews, 228*, 103987. doi:https://doi.org/10.1016/j.earscirev.2022.103987

Kasten, S., Zabel, M., Heuer, V., & Hensen, C. (2004). Processes and signals of nonsteady-state diagenesis in deep-sea sediments and their pore waters. *The South Atlantic in the Late Quaternary: Reconstruction of Material Budgets and Current Systems*, 431-459.

Kim, S.-H., Choi, A., Yang, E. J., Lee, S., & Hyun, J.-H. (2016). Low benthic respiration and nutrient flux at the highly productive Amundsen Sea Polynya, Antarctica. *Deep Sea Research Part II: Topical Studies in Oceanography, 123*, 92-101.

Lamping, N., Müller, J., Hefter, J., Mollenhauer, G., Haas, C., Shi, X., et al. (2021). Evaluation of lipid biomarkers as proxies for sea ice and ocean temperatures along the Antarctic continental margin. *Climate Past, 17*(5), 2305-2326. doi:10.5194/cp-17-2305-2021

Ledford-Hoffman, P. A., DeMaster, D., & Nittrouer, C. (1986). Biogenic-silica accumulation in the Ross Sea and the importance of Antarctic continental-shelf deposits in the marine silica budget. *Geochimica et Cosmochimica Acta, 50*(9), 2099-2110.

Lee, S., Hwang, J., Ducklow, H. W., Hahm, D., Lee, S. H., Kim, D., et al. (2017). Evidence of minimal carbon sequestration in the productive Amundsen Sea polynya. *Geophysical Research Letters, 44*(15), 7892-7899. doi:https://doi.org/10.1002/2017GL074646

Liao, W., Hu, J., & Peng, P. a. (2018). Burial of Organic Carbon in the Taiwan Strait. *Journal of Geophysical Research: Oceans, 123*(9), 6639-6652. doi:https://doi.org/10.1029/2018JC014285

Lohrer, A. M., Norkko, A. M., Thrush, S. F., & Cummings, V. J. (2021). Climate cascades affect coastal Antarctic seafloor ecosystem functioning. *Global Change Biology, 27*(23), 6181-6191.

Masqué, P., Isla, E., Sanchez-Cabeza, J. A., Palanques, A., Bruach, J. M., Puig, P., et al. (2002). Sediment accumulation rates and carbon fluxes to bottom sediments at the Western Bransfield Strait (Antarctica). *Deep Sea Research Part II: Topical Studies in Oceanography, 49*(4-5), 921-933.

Mathiot, P., Goosse, H., Fichefet, T., Barnier, B., & Gallée, H. (2011). Modelling the seasonal variability of the Antarctic Slope Current. *Ocean Science, 7*(4), 455-470. doi:10.5194/os-7-455-2011

McNeil, B. I., Tilbrook, B., & Matear, R. J. (2001). Accumulation and uptake of anthropogenic CO2 in the Southern Ocean, south of Australia between 1968 and 1996. *Journal of Geophysical Research: Oceans, 106*(C12), 31431-31445. doi:https://doi.org/10.1029/2000JC000331

Monien, P., Lettmann, K. A., Monien, D., Asendorf, S., Wölfl, A.-C., Lim, C. H., et al. (2014). Redox conditions and trace metal cycling in coastal sediments from the maritime Antarctic. *Geochimica et Cosmochimica Acta, 141*, 26-44. doi:https://doi.org/10.1016/j.gca.2014.06.003

Nelson, D. M., DeMaster, D. J., Dunbar, R. B., & Smith Jr, W. O. (1996). Cycling of organic carbon and biogenic silica in the Southern Ocean: Estimates of water-column and sedimentary fluxes on the Ross Sea continental shelf. *Journal of Geophysical Research: Oceans, 101*(C8), 18519-18532.

Orsi, A. H., Whitworth III, T., & Nowlin Jr, W. D. (1995). On the meridional extent and fronts of the Antarctic Circumpolar Current. *Deep Sea Research Part I: Oceanographic Research Papers, 42*(5), 641-673.

Piontek, J., Meeske, C., Hassenrück, C., Engel, A., & Jürgens, K. (2022). Organic matter availability drives the spatial variation in the community composition and activity of Antarctic marine bacterioplankton. *Environmental Microbiology, 24*(9), 4030-4048. doi:https://doi.org/10.1111/1462-2920.16087

Sachs, O., Sauter, E. J., Schlüter, M., van der Loeff, M. M. R., Jerosch, K., & Holby, O. (2009). Benthic organic carbon flux and oxygen penetration reflect different plankton provinces in the Southern Ocean. *Deep Sea Research Part I: Oceanographic Research Papers, 56*(8), 1319-1335.

Savidge, G., Harbour, D., Gilpin, L. C., & Boyd, P. W. (1995). Phytoplankton distributions and production in the Bellingshausen sea, Austral spring 1992. *Deep Sea Research Part II: Topical Studies in Oceanography, 42*(4), 1201-1224. doi:https://doi.org/10.1016/0967-0645(95)00062-U

Schnakenberg, A., Aromokeye, D. A., Kulkarni, A., Maier, L., Wunder, L. C., Richter-Heitmann, T., et al. (2021). Electron Acceptor Availability Shapes Anaerobically Methane Oxidizing Archaea (ANME) Communities in South Georgia Sediments. *Frontiers in Microbiology, 12*. doi:10.3389/fmicb.2021.617280

Schröder, M. (2018). The expedition PS111 of the research vessel POLARSTERN to the southern Weddell Sea in 2018. . *In Berichte zur Polar- und Meeresforschung = Reports on Polar and Marine Research, 718*, 1 - 161. doi:https://doi.org/10.2312/BzPM_0718_2018

Seeberg-Elverfeldt, J., Schlüter, M., Feseker, T., & Kölling, M. (2005). Rhizon sampling of porewaters near the sediment-water interface of aquatic systems. *Limnology and Oceanography: Methods, 3*(8), 361-371. doi:https://doi.org/10.4319/lom.2005.3.361

Seiter, K., Hensen, C., & Zabel, M. (2005). Benthic carbon mineralization on a global scale. *Global Biogeochemical Cycles, 19*(1). doi:https://doi.org/10.1029/2004GB002225

Shaw, T. J., Gieskes, J. M., & Jahnke, R. A. (1990). Early diagenesis in differing depositional environments: the response of transition metals in pore water. *Geochimica et Cosmochimica Acta, 54*(5), 1233-1246.

Smith, C. R., DeMaster, D. J., Thomas, C., Sršen, P., Grange, L., Evrard, V., et al. (2012). Pelagic-benthic coupling, food banks, and climate change on the West Antarctic Peninsula Shelf. *Oceanography, 25*(3), 188-201.

Smith, C. R., Mincks, S., & DeMaster, D. J. (2006). A synthesis of bentho-pelagic coupling on the Antarctic shelf: food banks, ecosystem inertia and global climate change. *Deep Sea Research Part II: Topical Studies in Oceanography, 53*(8-10), 875-894.

Smith, W. O., Nelson, D. M., DiTullio, G. R., & Leventer, A. R. (1996). Temporal and spatial patterns in the Ross Sea: phytoplankton biomass, elemental composition, productivity and growth rates. *Journal of Geophysical Research: Oceans, 101*(C8), 18455-18465.

Spreen, G., Kaleschke, L., & Heygster, G. (2008). Sea ice remote sensing using AMSR-E 89-GHz channels. *Journal of Geophysical Research: Oceans, 113*(C2). doi:https://doi.org/10.1029/2005JC003384

Suess, E. (1980). Particulate organic carbon flux in the oceans—surface productivity and oxygen utilization. *Nature, 288*(5788), 260-263.

Sval'nov, V. N., & Alekseeva, T. N. (2006). Characteristics of the grain-size composition of deep-water oceanic sediments. *Lithology and Mineral Resources, 41*(3), 201-214. doi:10.1134/S0024490206030011

Takahashi, T., Sweeney, C., Hales, B., Chipman, D. W., Newberger, T., Goddard, J. G., et al. (2012). The changing carbon cycle in the Southern Ocean. *Oceanography, 25*(3), 26-37.

Vernet, M., Geibert, W., Hoppema, M., Brown, P. J., Haas, C., Hellmer, H., et al. (2019). The Weddell Gyre, Southern Ocean: present knowledge and future challenges. *Reviews of Geophysics, 57*(3), 623-708.

Vernet, M., Martinson, D., Iannuzzi, R., Stammerjohn, S., Kozlowski, W., Sines, K., et al. (2008). Primary production within the sea ice zone west of the Antarctic Peninsula: I—Sea ice,

summer mixed layer, and irradiance. *Deep Sea Research Part II: Topical Studies in Oceanography, 55*(18), 2068-2085. doi:https://doi.org/10.1016/j.dsr2.2008.05.021

von Bodungen, B., Smetacek, V. S., Tilzer, M. M., & Zeitzschel, B. (1986). Primary production and sedimentation during spring in the Antarctic Peninsula region. Deep Sea Research Part A. *Oceanographic Research Papers, 33*(2), 177-194.

von Bröckel, K. (1985). Primary production data from the south-eastern Weddell Sea. *Polar Biology, 4*, 75-80.

Wassmann, P., et al. (2004). Particulate Organic Carbon Flux to the Arctic Ocean Sea Floor. In R. Stein & R. W. MacDonald (Eds.), *The Organic Carbon Cycle in the Arctic Ocean* (pp. 73-87). Springer, Berlin, Heidelberg. https://doi.org/10.1007/978-3-642-18912-8_5

Wenzhöfer, F., & Glud, R. N. (2002). Benthic carbon mineralization in the Atlantic: a synthesis based on in situ data from the last decade. *Deep Sea Research Part I: Oceanographic Research Papers, 49*(7), 1255-1279. doi:https://doi.org/10.1016/S0967-0637(02)00025-0

Westwood, K. J., Griffiths, F. B., Meiners, K. M., & Williams, G. D. (2010). Primary productivity off the Antarctic coast from 30–80 E; BROKE-West survey, 2006. *Deep Sea Research Part II: Topical Studies in Oceanography, 57*(9-10), 794-814.

Wunder, L. C., Aromokeye, D. A., Yin, X., Richter-Heitmann, T., Willis-Poratti, G., Schnakenberg, A., et al. (2021). Iron and sulfate reduction structure microbial communities in (sub-) Antarctic sediments. *The ISME Journal, 15*(12), 3587-3604. doi:10.1038/s41396-021-01014-9

Zonneveld, K. A., Versteegh, G. J., Kasten, S., Eglinton, T. I., Emeis, K.-C., Huguet, C., et al. (2010). Selective preservation of organic matter in marine environments; processes and impact on the sedimentary record. *Biogeosciences, 7*(2), 483-511.

5

Manuscript 4

The Imprint of Sea ice on the Biological Carbon Pump in the Southern Ocean

Moritz Holtappels[1,3] and **Marwa Baloza**[1,2]

[1]Alfred Wegener Institute Helmholtz Centre for Polar and Marine Research, Am Handelshafen 12, 27570 Bremerhaven, Germany
[2]Faculty 2 Biology / Chemistry, University Bremen, Leobener Str., 28359 Bremen, Germany
[3] MARUM - Center for Marine Environmental Sciences, University of Bremen, 28359 Bremen, Germany

Corresponding author: Moritz Holtappels (moritz.holtappels@awi.de)

Manuscript ready for submission to Nature Geoscience

Abstract

The Seasonal Ice Zone (SIZ) around Antarctica covers an area of 16 million km^2 and is considered the largest biogeochemical province in the Southern Ocean. Despite a well-documented control of sea ice on primary production, its large-scale effect on the biological carbon pump, i.e. the sinking of organic carbon into deep waters and ultimately to the sediments, remains poorly constrained. Here we demonstrate that the degree of sea ice cover during the growth season is a strong predictor for carbon remineralization rates in underlying sediments. We compiled the available benthic rate measurements for the SIZ and found that 83 % of the variability can be explained by only two environmental factors: long-term occurrence of moderate sea ice cover, and water depth. The empirical model was used to estimate the benthic carbon remineralization for the entire SIZ, resulting in 46 Tg C yr^{-1}, of which 71 % can be assigned to shelf sediments of less than 1000 m water depth. Applying an empirical function, the burial rate and the total organic carbon supply to the sediments were estimated to be 6 and 52 Tg C yr^{-1}, respectively, and the carbon export from the euphotic zone (<133 m) was calculated to be ~300 Tg C yr^{-1}.

1 Introduction

The sea ice in the Southern Ocean covers an area of approx. 19 million km^2, shaping physical parameters of the ocean surface, in particular gas and heat exchange, light availability and water column stratification, of which the latter are crucial for algal growth (Gupta et al., 2020). The pronounced seasonality of day length and heat input at these latitudes results in a seasonal variation of sea ice cover of 16 million km^2, making the seasonal ice zone (SIZ) one of the largest biogeochemical provinces where local growth conditions change over the sea ice season from light limitation beneath the dense ice cover, to a more favorable light regime and shallow mixed layer in the marginal ice zone (MIZ), to a less favorable deep mixed layer in the ice-free waters (Sakshaug et al., 1991; Vernet et al., 2008; Baloza et al., 2022).

During several field studies it has been observed that MIZ-conditions, especially during a retreating ice-edge, promote algae blooms (Mitchell & Holm-Hansen, 1991; Sakshaug et al., 1991; Garibotti et al., 2005). On the other hand, estimates from remote sensing of Chlorophyll-a suggest only minor increases in primary production per area in the MIZ compare to those in open waters (Arrigo et al., 2008). However, these rates are likely conservative because the presence of sea ice, even at low ice concentrations, impedes the measurements of ocean color from remote sensing (Bélanger et al., 2007). Model results indicate that the most important driver of MIZ blooms is enhanced light penetration into a shallow mixed layer, rather than nutrient availability (Taylor et al., 2013).

These effects of sea ice on the primary production in the Antarctic ocean are of particular interest, because it regulates the biological carbon pump (BCP) in a region where the most prominent bottom waters are formed (Jacobs, 2004). Especially on the continental shelf, particulate organic carbon (POC) sinking out of the euphotic layer enters denser water masses below, many of them precursors of Antarctic bottom waters, so that the associated organic and inorganic carbon pool is efficiently sequestered (Arrigo et al., 2008). A thorough assessment of the current BCP is required to anticipate effects of ongoing global warming and expected decline in sea ice extent.

A way to assess the BCP is to survey the ocean sediments as a final trap for the sinking POC. Several empirical functions have been established relating benthic carbon cycling, water depth and surface ocean productivity (Middleburg et al., 1997; Egger et al., 2018; Jørgensen et al., 2022). Important concepts have been introduced to estimate (i) net primary production (NPP) from remote sensing of chlorophyll-a and sea surface temperature (Falkowski et al., 1988), (ii) the ratio between NPP and the export production (pe-ratio), i.e. the fraction sinking out of the euphotic zone (Dunne et al., 2005), (iii) the flux attenuation with water depth due to the mineralization of sinking POC (Martin et al., 1987), and (iv) the fraction of organic carbon supply to the sea floor and its mineralization and burial (Dunne et al., 2007). In lack of ocean colour data for sea ice covered regions, we establish a new empirical relation based on the occurrence of moderate sea ice cover as a proxy for favourable growth conditions, which can be derived from several decades of daily sea ice observations from remote sensing. Further, the empirical relation considers the flux attenuation due to water depth (Martin et al., 1987) to finally estimate benthic carbon mineralization rates.

2 Results and Discussion

2.1 The moderate ice cover index (MICI)

Assuming favorable conditions for algae blooms in the MIZ, the duration of MIZ-like conditions for a specific location should determine to some degree the overall productivity and the carbon export. Although the MIZ moves with the ice edge over the course of the season, the occurrence of moderate sea ice conditions can be very different across the regions. For example, the positions of the monthly mean ice edge (Figure 1a) indicate a fast-moving ice edge in the middle of the Weddell gyre where the distance between monthly ice edge positions is large, and a slow-moving ice edge at the tip of the Antarctic Peninsula where the ice edge positions converge. We take a closer look at two example locations, which are positioned in both regions but at similar latitudes (dots shown in Figure 1a). The classification of the sea ice conditions into no ice cover (<5 % ice cover), moderate ice cover (5-35 %) and dominant ice cover (35-100 %) shows very different durations of moderate sea ice cover (Figure 1b). In the central Weddell Gyre, the duration of moderate ice cover in the summer season is often less than a week, while at the tip of the Antarctic Peninsula these conditions persist for up to several weeks.

To express these regional differences, we use a “moderate ice cover index” (MICI), which has been established by Baloza et al. (2022) in a previous study. We used 30 years of daily sea ice observations from the National Snow and Ice Data Centre (1990-2019, Sea Ice Index, version 3, Fetterer et al., 2017) with a spatial resolution of 25x25 km. For each day and location, the occurrence of moderate ice cover was determined and weighted by the relative day length (sunrise to sunset for the respective latitude and day of year). Finally, MICI represents a 30-year average of these values, which can vary between 0 and 1 (no or permanent moderate ice cover during the daylight period). A map with MICI values for the entire seasonal ice zone is shown in Figure 2. Interestingly, some bathymetric features, such as the South Sandwich Trench and the Kerguelen Plateau show pronounced MICI values, suggesting a strong impact of topography on ocean currents and sea ice drift for these regions (compare Figures 1a & 2).

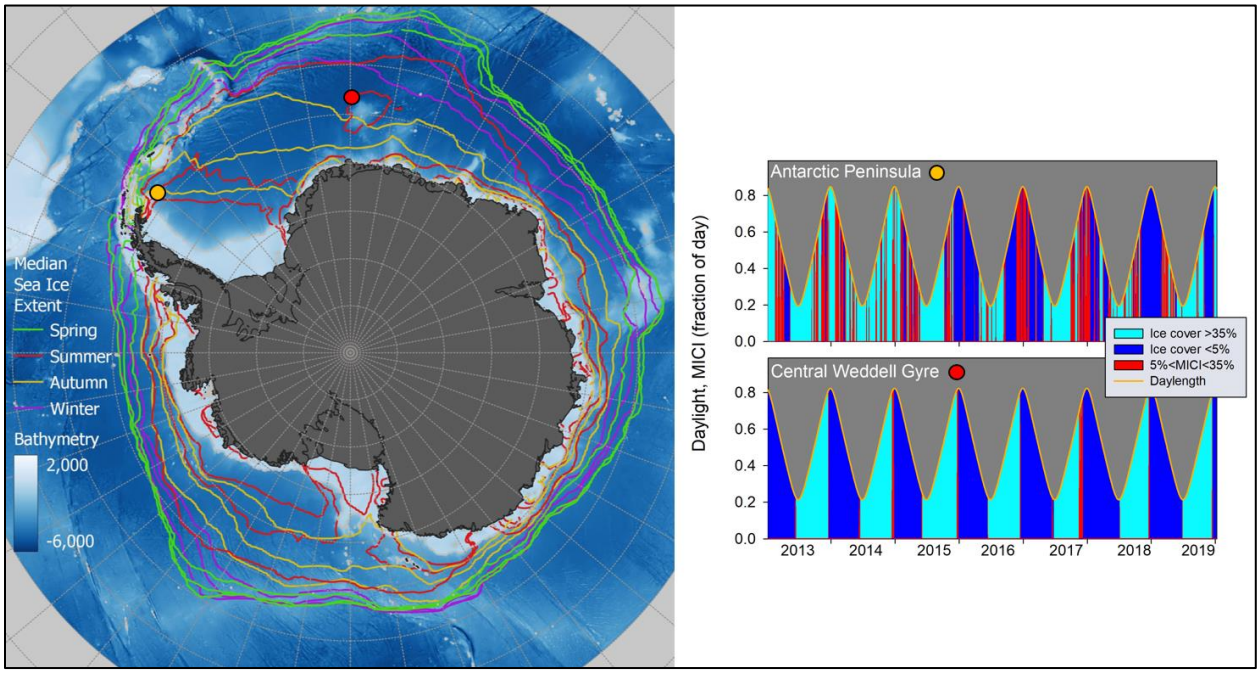

Figure 1. Seasonal position of the ice edge and occurrence of different sea ice conditions for two example locations. a, International Bathymetric Chart of the Southern Ocean (IBCSO, version 2) and positions of median sea ice extent for the months of the different seasons in green (spring: Oct, Nov, Dec) red (summer: Jan, Feb, Mar), yellow (autumn: Apr, May, Jun) and purple (winter: Jul, Aug, Sept). Two stations (red and yellow dots) represent contrasting regions at similar latitude. **b**, for the two representative stations, the day length and the daily ice cover are

indicated by the color code over seven years. Regions where the ice edge positions in the map concentrate indicate a slow change of seasonal ice conditions with moderate sea ice cover persisting several weeks. Regions with a large spread ice edge positions indicate a rapid change of ice conditions with moderate sea ice cover of less than a week.

2.2 The MICI-Benthos model, a new empirical relation for benthic carbon mineralization in the SIZ

Baloza et al. (2022) proposed the following exponential function, which relates the occurrence of moderate sea ice cover (MICI) and the benthic carbon re-mineralization rates (in mmol C m^{-2} d^{-1}) of five stations on the continental shelf of the eastern Antarctic Peninsula: $C_{min} = m * \exp(b * MICI)$, with m = 0.56 and b = 14.7. The stations were at similar water depths (400 m ± 50 m), so that the function did not include water depth as an independent variable. Here we expand the equation by including a term for the flux attenuation due to water depth (z):

$$C_{min} = a * \exp(b * MICI) * (z/100)^c \quad (1)$$

The last term $(z/100)^c$ introduces the power law proposed by Martin et al (1987), with water depth z and the exponent c = -0.86. The MICI exponent remains at b = 14.7, so that the factor a is simply calculated by equating equation (1) with Baloza's expression and solving for $a = m/(z/100)^c$. Inserting m = 0.56 and z = 400m from Baloza et al. (2022) results in a = 1.85.

To validate the MICI-benthos model (equation 1), we compiled all available benthic rate measurements within the seasonal ice zone (Figure 2). We considered rates that are based on diffusive oxygen uptake measurements derived from oxygen micro-profiles. At low benthic rates, this method is much less prone to errors than whole core or chamber incubations (see methods for more details). We compiled 62 stations from Sachs et al. (2009) representing also data from Holby et al. (1994, 1996) and Schlueter et al. (1990, 1991), from Baloza et al. (2022) we compiled 7 stations and from a recent expedition we added unpublished data for 11 stations (Figure 3a).

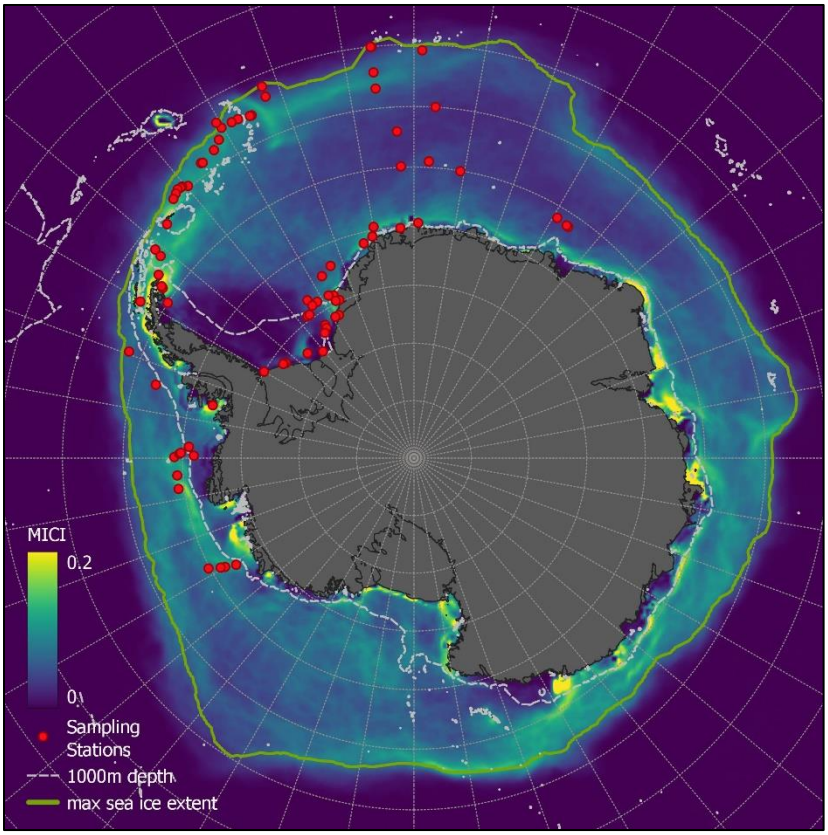

Figure 2. The distribution of the moderate ice cover index (MICI) within the seasonal ice zone. The MICI reflects the occurrence of moderate sea ice cover weighted by day length and averaged over 30 years of daily sea ice observations (1990-2019). High MICI values indicate favorable conditions for algae growth due to a prolonged moderate ice cover. Locations (N=80) with available rates of benthic carbon re-mineralization are marked by red dots. Shelf areas are marked by the 1000 m depth contour. The boundary of the seasonal ice zone is marked by the average maximum sea ice extent.

MICI values of the 80 stations varied from 0.002 to 0.2 and water depths varied from 330 m to 5300 m (Figure 3b). To our surprise, the 'a priori' parameterization of the model could already explain 79 % of the variability in measured benthic carbon re-mineralization (Table 1). A least square fit increased the coefficient of determination for measured versus modelled rates to R^2 = 0.83 (Figure 3) with slightly different constants for the final model (Table 1).

Constant	for C_{min}		for C_{supply}
	a priori	best fit	best fit
a	1.84	1.16 (0.26)	1.16 (0.27)
b	14.7	15.6 (0.99)	16.5 (1.04)
c	-0.86	-0.84 (0.08)	-0.84 (0.08)
R^2	0.785	0.832	0.836

Table 1. Values for the constants of equation (1), standard error in brackets. The "a priori" values were derived using the combined equations from Baloza et al. (2022) and Martin et al. (1987) (see text). Constraints for the best fit of the carbon supply: values should be equal or larger than those used for the best fit of the carbon mineralization.

In addition to the organic carbon that is mineralized in the sediments, a small amount of organic carbon is buried and both fractions add to the carbon supply rate received by the sediments: $C_{supply} = C_{min} + C_{burial}$. Dunne et al. (2007) compiled data for the burial efficiency and found the following equation relating C_{supply} and C_{burial} for sediments: $C_{burial} = C_{supply} * (0.013 + 0.53 * \mathrm{C}_{supply}{}^2/(7 + \mathrm{C}_{supply})^2$. Applying these relations, equation (1) was fitted to the carbon supply rate of the compiled stations (R^2 = 0.83). The constants used to model the carbon supply are shown in table 1.

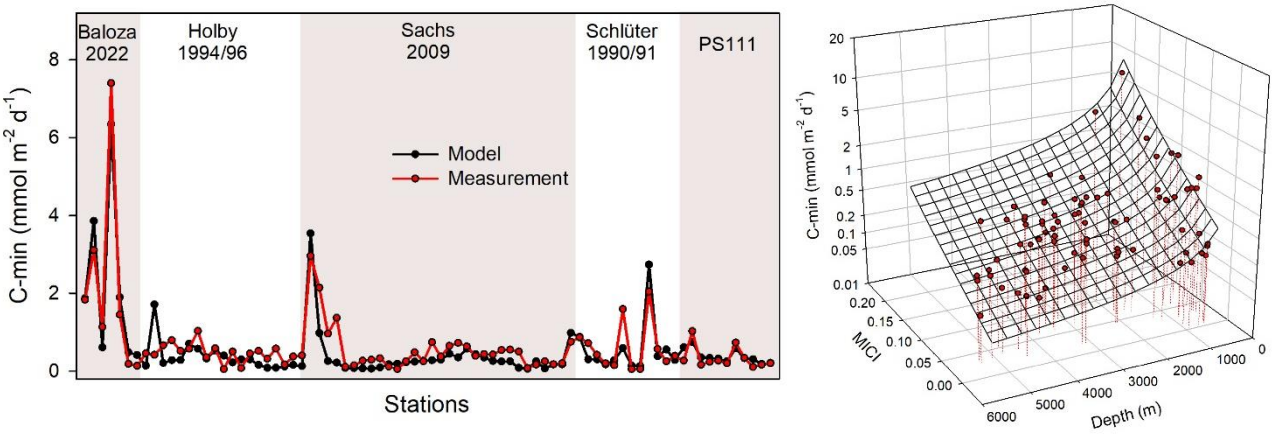

Figure 3. Comparison of measured and modelled rates of benthic carbon re-mineralization. **a,** list of all stations sorted by data source. **b**, measured values (dots) and modelled values (mesh) in a 3-dimensional space, showing the distribution of independent variables (water depth and MICI) across the scales. The modelled values in **a** are calculated from equation (1) with the constants: a = 1.16 (±0.26), b = 15.6 (±0.99), c = -0.84 (±0.082) derived from a least square fit ($p<0.0001$, $R^2=0.832$).

2.3 Organic carbon fluxes in the SIZ

In the following, the MICI-Benthos model (equation 1) was used with the respective constants in table 1 to extrapolate benthic supply and re-mineralization rates of organic carbon to the entire area of the SIZ. Values for water depth were taken from International Bathymetric Chart of the Southern Ocean (IBCSO, version 2, see Figure 1a) and MICI values were interpolated to IBCSO resolution (500 m x 500 m) before applying the MICI-Benthos model. The distribution of estimated remineralization rates is shown in Figure 4. Elevated rates are indicated for the continental shelf, especially at the Antarctic Peninsula and the Amundsen Sea in West Antarctica, and the D'Urville Sea, Davis Sea and Prydz Bay in East Antarctica. In the deep sea, elevated rates are indicated east of the tip of the Antarctic Peninsula, spanning from the Powell Basin to the South Shetland Islands and beyond. For the total SIZ, carbon mineralization amounts to 46 Tg C yr^{-1}, of which 33 Tg C yr^{-1} are mineralized on the continental shelf at below 1000 m water depth (Figure 5a). The shelf area covers 15 % of the SIZ area but is responsible for 71 % of the benthic carbon mineralization. The benthic carbon burial is estimated to 6 Tg C yr^{-1} so that the benthic carbon supply amounts to 52 Tg C yr^{-1} with a shelf contribution of 75 %. On the continental shelf,

the depth range between 200-350 m contributes most to the rates, although water depths at around 500 m are most abundant (Figure 5b). The export flux of organic carbon out of the euphotic zone was calculated assuming an average depth of the mixed layer of 133 m, comparable to Schlitzer (2002). Within the SIZ the export flux amounts to 305 Tg C yr^{-1} with an average flux of 16 g C m^{-2} yr^{-1}.

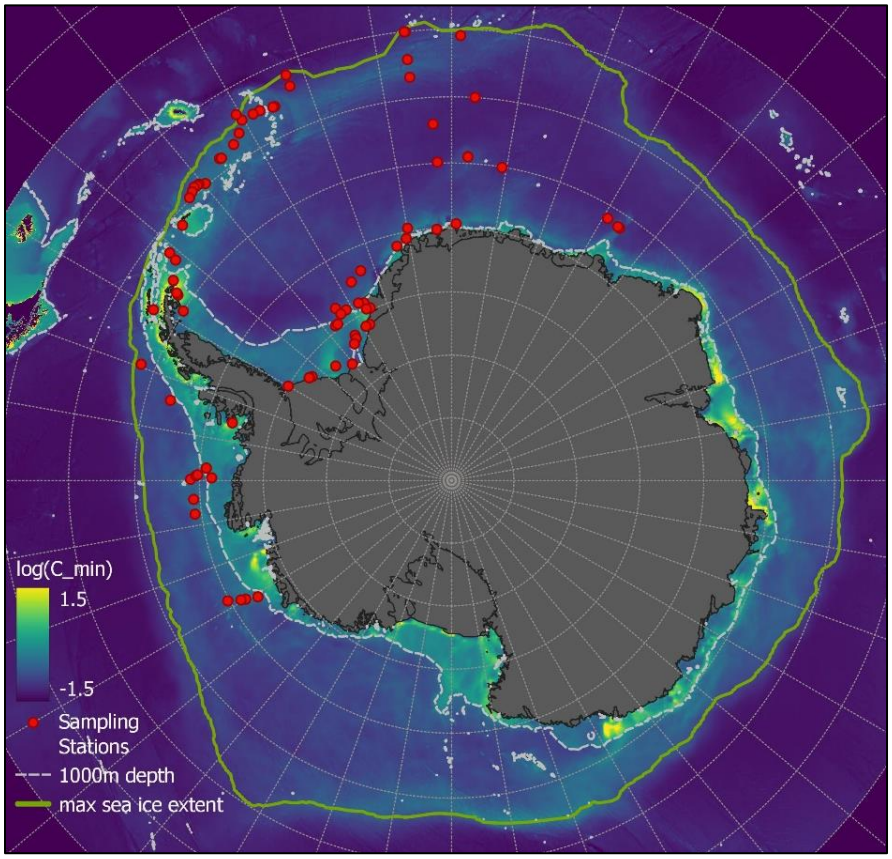

Figure 4. Distribution of benthic remineralization rate of organic carbon. Rates (in mmol C m^{-2} d^{-1}) are shown on a logarithmic scale. The empirical model is applicable only with the seasonal ice zone (SIZ). The boundary of SIZ the is marked by the average maximum sea ice extent. Locations (N=80) with available measured rates of benthic carbon re-mineralization are marked by red dots. Shelf areas are marked by the 1000 m depth contour.

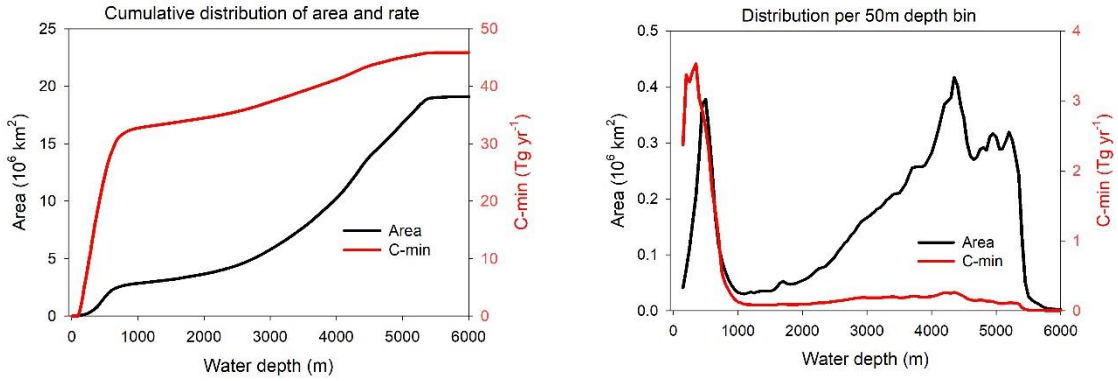

Figure 5. Distribution of seabed area and total rate of organic carbon mineralization over water depth. **a**, cumulative rate and area for water depths of 100-6000 m. The continental shelf contributes 33 Tg C yr^{-1} (~70 %) to the overall carbon mineralization rate of 46 Tg C yr^{-1}. **b**, distribution of rate and area for 50m depth bins. The most abundant water depth on the continental shelf is at around 500m. Prominent deep-sea areas are between 3000-5500 m water depth. Carbon mineralization rates peak between 200-350 m water depth.

To assess the validity of the model for POC fluxes in the upper and mid-water column, we compared the export at specific water depths with those of two studies, Schlitzer (2002) and Nissen et al. (2022). Schlitzer combined global ocean circulation and biogeochemical models with large sets of hydrographic, oxygen, nutrient and carbon data to estimate the export fluxes of POC for the entire Southern Ocean. Values between 5 and 30 g C m^{-2} yr^{-1} were estimated for the seasonal ice zone (compare Figure 5 in Schlitzer 2002), which agrees well with the average flux of 16 g C m^{-2} yr^{-1} estimated by our MICI-Benthos model. Nissen et al. (2022) combined the Finite Element Sea Ice Ocean Model (FESOM) with the Regulated Ecosystem Model (REcoM) to estimate the carbon sequestration to below 2000 m water depth in the southern Weddell Sea basin. The carbon flux from sedimentation of POC ranges between 1.4 and 2.0 Tg C yr^{-1} depending on climate forcing. For the same area and depth our model predicts a POC flux of 1.1 Tg C yr^{-1}. In summary, the comparison shows that POC fluxes at different depths can be reproduced quite well by the MICI-Benthos model. However, further validation is recommended using the POC fluxes derived from sediment traps.

2.4 Mechanisms explaining the MICI-impact on the Biological Carbon Pump

The simplicity of the MICI-Benthos model, which incorporates only the combination of moderate ice cover and day length as a proxy for export production, indicates a strong control of sea ice on the productivity. As is usual with empirical models, we can only speculate about the mechanisms that cause the correlations. Compared to the moderate ice cover index, we found that the number of ice-free days does not correlate with benthic rates, although studies suggest that algae growth is significantly elevated at ice-free days compared to days with full ice cover (compare Arrigo et al. (2008) for pelagic production and Arrigo et al. (1997) for sea ice production). Studies of direct measurements of chlorophyll-a content at the marginal ice zone (Smith et al., 1987; Bruyant et al., 2022) suggest that strong blooms are caused by the interplay of increased light availability and a shallowing mixed layer depth upon sea ice melt. As reported for temperate regions (Townsend & Cammen, 1988; Griffiths et al., 2017), we hypothesize that these blooms make an above average contribution to the benthic carbon supply, because the initially exponential growth exceeds that of planktonic consumers and thus increases the efficiency of the export and downward transport of organic carbon from the mixed layer to the deep. Indeed, preliminary results from a mooring deployed in the central Weddell gyre (Hellmer & Holtappels, 2021) show increased chlorophyll-a concentrations in the mixed layer associated with sea ice melt in spring, but interestingly also upon freeze up in autumn. The autumn bloom is likely caused by a pycnocline deepening and gradual erosion associated to surface water cooling, which effectively injects new nutrients into the mixed layer. In summary, we hypothesize that both processes are at work and that the exponential growth during spring and autumn blooms cause the strong correlation between the moderate ice cover index (MICI) and the benthic carbon supply.

2.5 Impact of anticipated changes in sea ice cover

Climate change in the Southern Ocean has significantly influenced sea ice dynamics, as evidenced by recent observations indicating a substantial reduction in sea ice extent around Antarctica. The winter maximum extent has reached a historic low with a reduction of one million square kilometers in the annual maximum sea ice extent (Parkinson, 2019; Melsheimer et al., 2023). This continued decline is part of a persistent trend in Antarctic sea ice since 2015 (Eayrs et al., 2021),

suggesting further reductions in the near future. The effect of climate change on the Southern Ocean productivity has been reviewed by Petrou et al. (2016) and Deppeler & Davidson (2017) who amongst others also discuss the effect of changing sea ice extent. Changes in sea ice extent are expected to result in notable changes in physical conditions, particularly water column stratification and light availability. However, the changes in extent and duration of marginal ice zones is assumed to be of minor importance because the yearly averaged production is reported to be comparable to that in the open ocean (Arrigo et al. 2008). In contrast, our results indicate an above-average contribution of primary production under moderate ice cover to the export of organic carbon, which calls for a more thorough investigation of possible changes in sea ice dynamics, in particular possible shifts in the area and duration of moderate ice cover. In general, a reduction in sea ice extent, for example a loss of 1 Mio km^2 of maximum sea ice, means a loss of area in which growth dynamics upon ice melting and freezing can take effect, and thus suggests a potential reduction in organic carbon export for the affected area. In addition, any change in the duration of favorable growth conditions under moderate ice cover is assumed to affect the carbon export. For example, the almost year-round marginal ice zone at the tip of the Antarctic peninsula (Figure 1+2) may shift southward in summer, so that open water conditions and decreased carbon export would be expected on the shelf. However, in this region such unfavorable development may be counteracted by increased nutrient input form glacial melt water runoff. In general, the mechanisms relating sea ice melt and freeze up with carbon export dynamics need more in-depth investigation to better assess the anticipated change in sea ice extend for the future BCP.

3 Methods

3.1 Moderate ice cover index

The moderate ice cover index (MICI) is a new proxy proposed by Baloza et al. (2022), which indicates favorable light conditions and water column stratification for phytoplankton blooms. The MICI was extracted from 30 years of daily sea ice observations from the National Snow and Ice Data Centre (1990-2019, Sea Ice Index, version 3, Fetterer et al., 2017) with a spatial resolution of 25x25km. For each day and location, the occurrence of moderate ice cover (5-35%)

was determined and weighted by the relative day length (sunrise to sunset for the respective latitude and day of year). The MICI thus represents a 30-year average of these values, which can vary between 0 and 1 (no or permanent moderate ice cover during the daylight period). All calculations were carried out with the software matlab.

3.2 Bathymetry

Bathymetric data was taken from the International Bathymetric Chart of the Southern Ocean Version 2 (IBCSO v2) (Dorschel et al., 2022). The spatial resolution is 500 m x 500 m. The bathymetry data was downloaded from https://doi.pangaea.de/10.1594/PANGAEA.937574.

3.3 Benthic carbon mineralization rates.

We considered rates based on diffusive oxygen uptake measurements derived from oxygen-depth profiles. These measurements, especially at low benthic rates, are much less prone to inaccuracies than rates derived from long-term incubations of sediment cores, because (i) they can be performed multiple times immediately upon sediment retrieval, (ii) they are rather insensitive to poor sensor accuracy (profiles range from near 100% to zero), and (iii) they increase in sensitivity at low rates due to non-linear increase of the O_2 penetration depth with decreasing oxygen uptake. Data were compiled from the literature, including 62 stations as reported by Sachs et al. (Sachs et al., 2009), which also represents data from studies by Bathmann et al. (1994), Miller & Grobe (1996), Smetacek et al. (1997), and Schlüter (1990, 1991). In addition, we compiled data from Baloza et al. (2022), which included 7 stations, and unpublished data from 11 stations collected during the PS111 expedition. Table S1 lists the data used in this paper. It includes the diffusive oxygen uptake data that form the basis of this analysis, together with the moderate ice cover index and the corresponding water depth dataset. Similar to Sachs et al. (2009), all diffusive oxygen uptake data were transformed to organic carbon fluxes using the modified Redfield ratio of O_2/Corg = 170/117 from Anderson and Sarmiento (1994).

3.4 The MICI-Benthos model and extrapolation of organic carbon fluxes.

The MICI-Benthos model is explained in the main text. Equation 1 together with the respective constants (Table 1) was used to calculate respective benthic rates of C-mineralization and C-supply for the entire SIZ. The calculations were performed within the open-source GIS software

QGIS using the raster calculator and employing raster data for bathymetry and MICI on a 500 x 500x grid. Raster layer statistics in QGIS were used to sum up the areal rates for defined depth ranges and to finally sum up rates for shelf and deep-sea regions. Fixed depths of 133m and 2000m were implemented in equation 1 to calculate the POC fluxes at these water depths.

References

Anderson, L. A., & Sarmiento, J. L. (1994). Redfield ratios of remineralization determined by nutrient data analysis. *Global Biogeochemical Cycles, 8*(1), 65-80. doi:https://doi.org/10.1029/93GB03318

Arrigo, K. R., van Dijken, G. L., & Bushinsky, S. (2008). Primary production in the Southern Ocean, 1997–2006. *Journal of Geophysical Research: Oceans, 113*(C8). doi:https://doi.org/10.1029/2007JC004551

Arrigo, K. R., Worthen, D. L., Lizotte, M. P., Dixon, P., & Dieckmann, G. (1997). Primary Production in Antarctic Sea Ice. *Science, 276*(5311), 394-397. doi:doi:10.1126/science.276.5311.394

Baloza, M., Henkel, S., Geibert, W., Kasten, S., & Holtappels, M. (2022). Benthic carbon remineralization and iron cycling in relation to sea ice cover along the eastern continental shelf of the Antarctic Peninsula. *Journal of Geophysical Research: Oceans, 127*(7), e2021JC018401.

Bathmann, U., Fütterer, D., & De Baar, H. (1994). Die Expeditionen ANTARKTIS X/6-8 des Forschungsschiffes" POLARSTERN" 1992/93= The expeditions ANTARKTIS X/6-8 of the research vessel" POLARSTERN" in 1992/93. *Berichte zur Polarforschung (Reports on Polar Research), 135*.

Bélanger, S., Ehn, J. K., & Babin, M. (2007). Impact of sea ice on the retrieval of water-leaving reflectance, chlorophyll a concentration and inherent optical properties from satellite ocean color data. *Remote Sensing of Environment, 111*(1), 51-68.

Bruyant, F., Amiraux, R., Amyot, M. P., Archambault, P., Artigue, L., Barbedo de Freitas, L., et al. (2022). The Green Edge cruise: investigating the marginal ice zone processes during late spring and early summer to understand the fate of the Arctic phytoplankton bloom. *Earth Syst. Sci. Data, 14*(10), 4607-4642. doi:10.5194/essd-14-4607-2022

Deppeler, S. L., & Davidson, A. T. (2017). Southern Ocean phytoplankton in a changing climate. *Frontiers in Marine Science, 4*, 40.

Dorschel, B., Hehemann, L., Viquerat, S., Warnke, F., Dreutter, S., Tenberge, Y. S., et al. (2022). The International Bathymetric Chart of the Southern Ocean Version 2. *Scientific Data, 9*(1), 275. doi:10.1038/s41597-022-01366-7

Dunne, J. P., Armstrong, R. A., Gnanadesikan, A., & Sarmiento, J. L. (2005). Empirical and mechanistic models for the particle export ratio. *Global Biogeochemical Cycles, 19*(4). doi:https://doi.org/10.1029/2004GB002390

Dunne, J. P., Sarmiento, J. L., & Gnanadesikan, A. (2007). A synthesis of global particle export from the surface ocean and cycling through the ocean interior and on the seafloor. *Global Biogeochemical Cycles, 21*(4). doi:10.1029/2006GB002907

Eayrs, C., Li, X., Raphael, M. N., & Holland, D. M. (2021). Rapid decline in Antarctic sea ice in recent years hints at future change. *Nature Geoscience, 14*(7), 460-464. doi:10.1038/s41561-021-00768-3

Egger, M., Riedinger, N., Mogollón, J. M., & Jørgensen, B. B. (2018). Global diffusive fluxes of methane in marine sediments. *Nature Geoscience, 11*(6), 421-425.

Falkowski, P. G., Flagg, C. N., Rowe, G. T., Smith, S. L., Whitledge, T. E., & Wirick, C. D. (1988). The fate of a spring phytoplankton bloom: export or oxidation? *Continental Shelf Research, 8*(5-7), 457-484.

Fetterer, F., Knowles, K., Meier, W. N., Savoie, M., & Windnagel, A. K. (2017). Sea ice index, version 3. [Years 1978-2019]. NSIDC: National Snow and Ice Data Center. doi:https://doi.org/10.7265/N5K072F8

Garibotti, I. A., Vernet, M., Smith, R. C., & Ferrario, M. E. (2005). Interannual variability in the distribution of the phytoplankton standing stock across the seasonal sea-ice zone west of the Antarctic Peninsula. *Journal of Plankton Research, 27*(8), 825-843. doi:10.1093/plankt/fbi056

Griffiths, J. R., Kadin, M., Nascimento, F. J., Tamelander, T., Törnroos, A., Bonaglia, S., et al. (2017). The importance of benthic–pelagic coupling for marine ecosystem functioning in a changing world. *Global Change Biology, 23*(6), 2179-2196.

Gupta, M., Follows, M. J., & Lauderdale, J. M. (2020). The effect of Antarctic sea ice on Southern Ocean carbon outgassing: Capping versus light attenuation. *Global Biogeochemical Cycles, 34*(8), e2019GB006489.

Hellmer, H. H., & Holtappels, M. (2021). The Expedition PS124 of the Research Vessel POLARSTERN to the southern Weddell Sea in 2021. *Berichte zur Polar-und Meeresforschung= Reports on polar and marine research, 755*.

Jacobs, S. S. (2004). Bottom water production and its links with the thermohaline circulation. *Antarctic Science, 16*(4), 427-437.

Jørgensen, B. B., Wenzhöfer, F., Egger, M., & Glud, R. N. (2022). Sediment oxygen consumption: Role in the global marine carbon cycle. *Earth-science reviews, 228*, 103987.

Martin, J. H., Knauer, G. A., Karl, D. M., & Broenkow, W. W. (1987). VERTEX: carbon cycling in the northeast Pacific. *Deep Sea Research Part A. Oceanographic Research Papers, 34*(2), 267-285.

Melsheimer, C., Spreen, G., Ye, Y., & Shokr, M. (2023). First results of Antarctic sea ice type retrieval from active and passive microwave remote sensing data. *The Cryosphere, 17*(1), 105-126. doi:10.5194/tc-17-105-2023

Middleburg, J., Soetaert, K., & Herman, P. (1997). Empirical relationships for use in global diagenetic models. *Oceanographic Literature Review, 7*(44), 698.

Miller, H., & Grobe, H. (1996). Die Expedition ANTARKTIS-XI/3 mit FS" Polarstern" 1994= The expedition ANTARKTIS-XI/3 of RV" Polarstern" in 1994. *Berichte zur Polarforschung (Reports on Polar Research), 188*.

Mitchell, B. G., & Holm-Hansen, O. (1991). Observations of modeling of the Antartic phytoplankton crop in relation to mixing depth. *Deep Sea Research Part A. Oceanographic Research Papers, 38*(8-9), 981-1007.

Nissen, C., Timmermann, R., Hoppema, M., Gürses, Ö., & Hauck, J. (2022). Abruptly attenuated carbon sequestration with Weddell Sea dense waters by 2100. *Nature Communications, 13*(1), 3402. doi:10.1038/s41467-022-30671-3

Parkinson, C. L. (2019). A 40-y record reveals gradual Antarctic sea ice increases followed by decreases at rates far exceeding the rates seen in the Arctic. *Proceedings of the National Academy of Sciences, 116*(29), 14414-14423.

Petrou, K., Kranz, S. A., Trimborn, S., Hassler, C. S., Ameijeiras, S. B., Sackett, O., et al. (2016). Southern Ocean phytoplankton physiology in a changing climate. *Journal of Plant Physiology, 203*, 135-150. doi:https://doi.org/10.1016/j.jplph.2016.05.004

Sachs, O., Sauter, E. J., Schlüter, M., Rutgers van der Loeff, M. M., Jerosch, K., & Holby, O. (2009). Benthic organic carbon flux and oxygen penetration reflect different plankton provinces in the Southern Ocean. *Deep Sea Research Part I: Oceanographic Research Papers, 56*(8), 1319-1335. doi:https://doi.org/10.1016/j.dsr.2009.02.003

Sakshaug, E., Slagstad, D., & Holm-Hansen, O. (1991). Factors controlling the development of phytoplankton blooms in the Antarctic Ocean—a mathematical model. *Marine Chemistry, 35*(1-4), 259-271.

Schlitzer, R. (2002). Carbon export fluxes in the Southern Ocean: results from inverse modeling and comparison with satellite-based estimates. *Deep Sea Research Part II: Topical Studies in Oceanography, 49*(9-10), 1623-1644.

Schlüter, M. (1990). Zur Frühdiagenese von organischem Kohlenstoff und Opal in Sedimenten des südlichen und östlichen Weddellmeeres: geochemische Analyse und Modellierung= Early diagenesis of organic carbon and opal in sediments of the southern and eastern Weddell Sea: geochemical analysis and modelling. *Berichte zur Polarforschung (Reports on Polar Research), 73*.

Schlüter, M. (1991). Organic carbon flux and oxygen penetration into sediments of the Weddell Sea: indicators for regional differences in export production. *Marine chemistry, 35*(1-4), 569-579.

Smetacek, V., De Baar, H., Bathmann, U., Lochte, K., & Van Der Loeff, M. R. (1997). Ecology and biogeochemistry of the Antarctic Circumpolar Current during austral spring: a summary of Southern Ocean JGOFS cruise ANT X/6 of RV Polarstern. *Deep Sea Research Part II: Topical Studies in Oceanography, 44*(1-2), 1-21.

Smith, W. O., Baumann, M. E. M., Wilson, D. L., & Aletsee, L. (1987). Phytoplankton biomass and productivity in the marginal ice zone of the Fram Strait during summer 1984. *Journal of Geophysical Research: Oceans, 92*(C7), 6777-6786. doi:https://doi.org/10.1029/JC092iC07p06777

Taylor, M. H., Losch, M., & Bracher, A. (2013). On the drivers of phytoplankton blooms in the Antarctic marginal ice zone: A modeling approach. *Journal of Geophysical Research: Oceans, 118*(1), 63-75.

Townsend, D. W., & Cammen, L. M. (1988). Potential importance of the timing of spring plankton blooms to benthic-pelagic coupling and recruitment of juvenile demersal fishes. *Biological Oceanography, 5*(3), 215-228.

van der Loeff, M. M. R., & Berger, G. W. (1991). Scavenging and particle flux: seasonal and regional variations in the Southern Ocean (Atlantic sector). *Marine chemistry, 35*(1-4), 553-567.

Vernet, M., Martinson, D., Iannuzzi, R., Stammerjohn, S., Kozlowski, W., Sines, K., et al. (2008). Primary production within the sea-ice zone west of the Antarctic Peninsula: I—Sea ice, summer mixed layer, and irradiance. *Deep Sea Research Part II: Topical Studies in Oceanography, 55*(18), 2068-2085. doi:https://doi.org/10.1016/j.dsr2.2008.05.021

Supplementary Materials

Table S1. Geographical location and characteristics of the stations. DOU is the diffusive oxygen uptake, MICI is the moderate ice cover index, which is the relative occurrence of moderate ice cover (defined as 5-35% ice cover), weighted by the length of daylight (sunrise to sunset) as described by Baloza et al. (2022).

Station	Sampling Date	Lat.	Long.	Water Depth [m]	Season	DOU (mmol/m²/d)	MICI	Ref data
PS118_7	28/03/2019	-60.93	-46.56	329	summer	1.98	0.09312	Baloza et al. (2022)
PS118_2	11/03/2019	-63.97	-55.91	415	summer	3.54	0.15231	Baloza et al. (2022)
PS118_1	04/03/2019	-64.98	-57.75	428	summer	1.40	0.03641	Baloza et al. (2022)
PS118_4	17/03/2019	-63.05	-54.33	447	summer	6.87	0.18810	Baloza et al. (2022)
PS118_3	14/03/2019	-63.81	-55.74	455	summer	1.75	0.11206	Baloza et al. (2022)
PS118_6	26/03/2019	-61.57	-51.13	2908	summer	0.24	0.12750	Baloza et al. (2022)
PS118_5	20/03/2019	-62.26	-51.43	3295	summer	0.18	0.12492	Baloza et al. (2022)
PS111_131-2	26/02/2018	-74.61	-36.94	387	summer	0.35	0.03107	PS111 expedition
PS111_29-3	06/02/2018	-75.97	-27.68	411	summer	1.33	0.04694	PS111 expedition
PS111_42-1	10/02/2018	-76.15	-53.36	493	summer	0.21	0.00940	PS111 expedition
PS111_53-3	13/02/2018	-76.03	-54.12	497	summer	0.31	0.00716	PS111 expedition
PS111_40-2	10/02/2018	-76.00	-54.24	513	summer	0.35	0.00544	PS111 expedition
PS111_47-2	11/02/2018	-74.98	-60.00	660	summer	0.26	0.00398	PS111 expedition
PS111_139-2	01/03/2018	-74.82	-25.28	663	summer	0.95	0.05836	PS111 expedition
PS111_70-2	17/02/2018	-76.11	-33.65	794	summer	0.45	0.03174	PS111 expedition
PS111_114-3	22/02/2018	-76.38	-33.93	839	summer	0.14	0.02917	PS111 expedition
PS111_98-3	20/02/2018	-77.80	-40.45	928	summer	0.21	0.00196	PS111 expedition
PS111_80-3	18/02/2018	-76.64	-35.43	932	summer	0.26	0.01223	PS111 expedition
PS1549-1	16/11/1987	-62.99	-60.22	1002	spring	4.30	0.19574	Sachs et al. (2009)
PS1565-3	05/12/1987	-63.90	-69.50	462	summer	3.11	0.07065	Sachs et al. (2009)
PS1596-2	21/01/1988	-74.26	-26.29	2494	summer	1.26	0.15765	Schlüter (1990, 1991)

Table S1: (continued)

Station	Sampling Date	Lat.	Long.	Water Depth [m]	Season	DOU (mmol/m²/d)	MICI	Ref data
PS1599-2	22/01/1988	-74.07	-27.72	2482	summer	1.04	0.06755	Schlüter (1990, 1991)
PS1605-2	25/01/1988	-74.06	-31.76	1674	summer	0.61	0.05859	Schlüter (1990, 1991)
PS1606-2	25/01/1988	-73.50	-34.03	2932	summer	0.29	0.13414	Schlüter (1990, 1991)
PS1607-2	26/01/1988	-74.10	-33.67	1598	summer	0.22	0.10129	Schlüter (1990, 1991)
PS1611-4	27/01/1988	-74.62	-36.10	422	summer	2.31	0.10238	Schlüter (1990, 1991)
PS1635-3	15/02/1988	-71.86	-23.46	3958	summer	0.07	0.07049	Schlüter (1990, 1991)
PS1636-2	16/02/1988	-72.34	-26.82	3764	summer	0.07	0.06245	Schlüter (1990, 1991)
PS1637-2	18/02/1988	-74.76	-26.44	444	summer	2.97	0.03573	Schlüter (1990, 1991)
PS1638-2	24/02/1988	-69.73	-9.91	2365	summer	0.82	0.03519	Schlüter (1990, 1991)
PS1639-2	25/02/1988	-70.50	-10.63	1566	summer	0.36	0.03772	Schlüter (1990, 1991)
PS1645-2	29/02/1988	-70.93	-13.16	1905	summer	0.57	0.03745	Schlüter (1990, 1991)
PS1772-6	13/11/1989	-55.46	1.17	4136	spring	0.58	0.03388	van der Loeff and Berger (1991)
PS1811-1	23/03/1990	-66.09	33.70	1146	autumn	1.39	0.02125	Sachs et al. (2009)
PS1812-1	26/03/1990	-66.06	33.28	1358	autumn	1.99	0.05184	Sachs et al. (2009)
PS1823-5	05/04/1990	-65.94	30.83	4442	autumn	0.16	0.07836	Sachs et al. (2009)
PS1826-6	13/04/1990	-65.03	9.19	4783	autumn	0.22	0.07568	Sachs et al. (2009)
PS1832-4	17/04/1990	-64.91	-2.55	5060	autumn	0.39	0.08370	Sachs et al. (2009)
PS2278-5	25/08/1992	-55.97	-22.25	4414	winter	0.42	0.09194	Sachs et al. (2009)
PS2280-1	26/08/1992	-56.83	-22.33	4747	winter	0.47	0.09821	Sachs et al. (2009)
PS2288-1	03/09/1992	-57.76	-25.34	3880	spring	0.17	0.10806	Sachs et al. (2009)
PS2290-1	04/09/1992	-57.73	-25.63	3449	spring	0.07	0.10250	Sachs et al. (2009)
PS2292-1	04/09/1992	-57.54	-27.46	3164	spring	0.36	0.10146	Sachs et al. (2009)
PS2293-1	05/09/1992	-57.52	-28.50	3355	spring	0.70	0.09977	Sachs et al. (2009)
PS2299-1	07/09/1992	-57.51	-30.23	3378	spring	0.36	0.10797	Sachs et al. (2009)
PS2304-2	09/09/1992	-58.23	-31.51	3824	spring	1.08	0.10902	Sachs et al. (2009)
PS2305-1	09/09/1992	-58.73	-33.01	3241	spring	0.55	0.10726	Sachs et al. (2009)
PS2306-1	10/09/1992	-59.00	-35.84	1979	spring	0.94	0.10039	Sachs et al. (2009)
PS2307-2	10/09/1992	-59.06	-35.58	2528	spring	1.05	0.10339	Sachs et al. (2009)
PS2312-1	12/09/1992	-59.83	-39.71	1666	spring	0.92	0.11046	Sachs et al. (2009)
PS2314-1	12/09/1992	-59.55	-40.51	2333	spring	0.57	0.06755	Sachs et al. (2009)
PS2315-1	12/09/1992	-59.54	-40.82	2911	spring	0.63	0.05859	Sachs et al. (2009)
PS2316-1	12/09/1992	-59.48	-41.34	3639	spring	0.62	0.13414	Sachs et al. (2009)
PS2317-1	13/09/1992	-59.64	-41.99	4035	spring	0.79	0.10129	Sachs et al. (2009)
PS2318-1	13/09/1992	-59.84	-42.88	4546	spring	0.80	0.10238	Sachs et al. (2009)

Table S1: (continued)

Station	Sampling Date	Lat.	Long.	Water Depth [m]	Season	DOU (mmol/m²/d)	MICI	Ref data
PS2357-2	05/10/1992	-56.94	-30.53	3374	spring	0.75	0.06536	Bathmann et al. (1994) and Smetacek et al. (1997)
PS2361-1	14/10/1992	-55.02	-5.91	3194	spring	0.46	0.02031	Bathmann et al. (1994) and Smetacek et al. (1997)
PS2365-1	25/10/1992	-55.02	-6.02	3117	spring	0.73	0.02022	Sachs et al. (2009)
PS2365-2	25/10/1992	-55.02	-6.02	3117	spring	0.84	0.02022	Bathmann et al. (1994) and Smetacek et al. (1997)
PS2370-4	05/11/1992	-58.38	-5.93	5039	spring	0.24	0.06774	Bathmann et al. (1994) and Smetacek et al. (1997)
PS2371-1	12/11/1992	-57.07	-5.99	3660	spring	0.55	0.06879	Bathmann et al. (1994) and Smetacek et al. (1997)
PS2522-1	28/01/1994	-66.89	-74.12	3436	summer	0.67	0.05659	Bathmann et al. (1994) and Sachs et al. (2009)
PS2528-1	06/02/1994	-71.99	-75.28	446	summer	0.61	0.10445	Bathmann et al. (1994) and Sachs et al. (2009)
PS2537-1	16/02/1994	-69.31	-89.74	3781	summer	0.96	0.08782	Bathmann et al. (1994) and Sachs et al. (2009)
PS2538-1	17/02/1994	-69.73	-88.92	3236	summer	1.15	0.09881	Bathmann et al. (1994) and Sachs et al. (2009)
PS2539-2	17/02/1994	-69.86	-88.71	2646	summer	0.75	0.08844	Bathmann et al. (1994) and Sachs et al. (2009)
PS2542-1	18/02/1994	-70.52	-87.10	677	summer	0.84	0.07082	Bathmann et al. (1994) and Sachs et al. (2009)
PS2543-3	18/02/1994	-70.95	-89.36	537	summer	1.50	0.04491	Bathmann et al. (1994) and Sachs et al. (2009)
PS2546-1	02/03/1994	-72.05	-120.93	2384	autumn	0.51	0.09057	Bathmann et al. (1994) and Sachs et al. (2009)
PS2547-2	02/03/1994	-71.15	-119.92	2092	autumn	0.85	0.11507	Bathmann et al. (1994) and Sachs et al. (2009)
PS2548-2	02/03/1994	-70.79	-119.51	2642	autumn	0.07	0.11002	Bathmann et al. (1994) and Sachs et al. (2009)
PS2550-1	03/03/1994	-69.86	-118.22	3108	autumn	0.73	0.08134	Bathmann et al. (1994) and Sachs et al. (2009)

Table S1: (continued)

Station	Sampling Date	Lat.	Long.	Water Depth [m]	Season	DOU (mmol/m²/d)	MICI	Ref data
PS2553-2	05/03/1994	-69.50	-97.44	4299	autumn	0.11	0.11965	Bathmann et al. (1994) and Sachs et al. (2009)
PS2556-1	08/03/1994	-69.50	-94.17	3586	autumn	0.65	0.10916	Bathmann et al. (1994) and Sachs et al. (2009)
PS65/701-2	27/04/2004	-59.99	3.52	5341	autumn	0.11	0.02827	Sachs et al. (2009)
PS71/017-12	22/12/2007	-70.08	-3.38	1927	summer	0.24	0.06301	Sachs et al. (2009)
PS71/033-19	31/12/2007	-62.01	-2.98	5338	summer	0.36	0.03344	Sachs et al. (2009)
PS71/039-10	03/01/2008	-64.48	2.87	2151	summer	0.25	0.04444	Sachs et al. (2009)
PS71/039-4	03/01/2008	-64.50	2.88	2125	summer	0.29	0.04386	Sachs et al. (2009)
PS71/047-1	07/01/2008	-69.67	1.04	1843	summer	1.09	0.14779	Sachs et al. (2009)

References

Baloza, M., Henkel, S., Geibert, W., Kasten, S., & Holtappels, M. (2022). Benthic carbon remineralization and iron cycling in relation to sea ice cover along the eastern continental shelf of the Antarctic Peninsula. *Journal of Geophysical Research: Oceans, 127*(7), e2021JC018401.

Bathmann, U., Fütterer, D., & De Baar, H. (1994). Die Expeditionen ANTARKTIS X/6-8 des Forschungsschiffes" POLARSTERN" 1992/93= The expeditions ANTARKTIS X/6-8 of the research vessel" POLARSTERN" in 1992/93. *Berichte zur Polarforschung (Reports on Polar Research), 135*.

Sachs, O., Sauter, E. J., Schlüter, M., Rutgers van der Loeff, M. M., Jerosch, K., & Holby, O. (2009). Benthic organic carbon flux and oxygen penetration reflect different plankton provinces in the Southern Ocean. *Deep Sea Research Part I: Oceanographic Research Papers, 56*(8), 1319-1335. doi:https://doi.org/10.1016/j.dsr.2009.02.003

Schlüter, M. (1990). Zur Frühdiagenese von organischem Kohlenstoff und Opal in Sedimenten des südlichen und östlichen Weddellmeeres: geochemische Analyse und Modellierung= Early diagenesis of organic carbon and opal in sediments of the southern and eastern Weddell Sea: geochemical analysis and modelling. *Berichte zur Polarforschung (Reports on Polar Research), 73*.

Schlüter, M. (1991). Organic carbon flux and oxygen penetration into sediments of the Weddell Sea: indicators for regional differences in export production. *Marine chemistry, 35*(1-4), 569-579.

Smetacek, V., De Baar, H., Bathmann, U., Lochte, K., & Van Der Loeff, M. R. (1997). Ecology and biogeochemistry of the Antarctic Circumpolar Current during austral spring: a summary of Southern Ocean JGOFS cruise ANT X/6 of RV Polarstern. *Deep Sea Research Part II: Topical Studies in Oceanography, 44*(1-2), 1-21.

van der Loeff, M. M. R., & Berger, G. W. (1991). Scavenging and particle flux: seasonal and regional variations in the Southern Ocean (Atlantic sector). *Marine chemistry, 35*(1-4), 553-567.

6

Synthesis

The paradigm of tight pelagic-benthic coupling on the Antarctic shelf suggests that current and future changes in sea ice and primary production resulting from global climate change will have major impacts on benthic carbon cycling (Smetacek & Nicol, 2005; Smith et al., 2006; Barnes, 2015; Barnes et al., 2018; Rogers et al., 2020; Pineda-Metz, 2020). Understanding the pathways of carbon cycling on Antarctic continental shelf is critical in order to assess the potential effects of climate change on these systems. Changes in primary production due to seasonal variations in sea ice cover affect the export of organic matter to the seafloor, thereby controlling carbon cycling and burial in the sediment (Barnes, 2015; Isla, 2016; Barnes et al., 2018). Due to the remoteness of the Antarctic shelf, we still lack baseline knowledge about benthic carbon cycling and its main drivers in shelf sediments.

The highly contrasting sea ice conditions on the Antarctic shelf provide a natural laboratory to compare the imprints of sea ice versus open-water conditions on primary production, carbon export, and finally on the benthic carbon supply and remineralization rates. In this work, I first studied the geochemistry of shelf sediments along the Antarctic Peninsula, in particular the fluxes of carbon and iron in the sediment, and between water column and sediments. The results were interpreted in the context of sea ice cover, revealing a positive correlation between moderate

sea ice cover and increased carbon fluxes to the sediment **(manuscript 1)**. Furthermore, microbial communities were examined and their different composition highlighted with respect to the detected element fluxes, especially of iron **(manuscript 2)**. The investigation was then extended towards the strongly sea ice covered southern shelf of the Weddell Sea, where benthic measurements revealed a dependence of carbon fluxes also on sediment grain size and water depth **(manuscript 3)**. Finally, the strong dependencies of the carbon fluxes on sea ice cover and water depth were combined to derive a simple empirical model that allows the extrapolation and budgeting of benthic carbon fluxes for the entire sea ice zone **(manuscript 4)**. In the following, I provide a brief overview of how the results of this cumulative work contribute to answering the original research questions in **chapter 1**.

6.1 How are benthic remineralization rates affected by long-term sea ice cover?

The effects of sea ice cover on benthic carbon cycling was investigated in different regions of the Weddell Sea shelf. On the eastern shelf of the Antarctic Peninsula (AP), five stations were sampled along a 400-mile transect at comparable water depths of 330–450 m to avoid the influence of water depth on the benthic carbon supply rates **(see Table 1, manuscript 1)**. Furthermore, fifteen stations were sampled along the southern Weddell Sea shelf with heterogenous sea ice conditions and water depths **(see Table 1, manuscript 3)**. Long-term sea ice cover varied along the transect **(manuscript 1)**, with heavily ice-covered station in the south (81%) and progressively moderate sea ice cover (47% - 34%) to less ice cover towards the north (28%). In contrast, the southern Weddell Sea shelf stations remained consistently covered by heavy sea ice (98% - 48%) **(manuscript 3)**.

The findings revealed a distinct pattern in benthic carbon supply and remineralisation rates: heavily ice-covered stations with low light availability and strong summer stratification, or ice-free station with high light availability and low stratification, had low carbon supply rates. Conversely, stations with moderate sea ice cover had high carbon supply rates, suggesting that primary and export production thrived under conditions where there was both sufficient light and shallow stratification to support a mixing depth far above the critical depth (as depicted in Figure 1). A moderate sea ice cover index (MICI) was established from 30 years of daily satellite

observations, measuring the occurrence of moderate (5% to 35%) sea ice cover. MICI was used as a long-term integrating measure of favorable algal growth conditions and compared to the benthic carbon remineralization, a long-term integrating measure of benthic carbon supply. A positive correlation was found between MICI and measured carbon supply and remineralisation rates, and the relationship was best described by an exponential equation. The results suggest that moderate sea ice cover promotes primary production and that the temporal duration of such conditions affect the production in an exponential way, indicating the growth characteristics of a phytoplankton bloom. It can be speculated that in addition to a favorable light regime and water column stratification, the constant supply of meltwater maintains a constant supply of nutrients, particularly iron, which further enhances primary production (Schloss et al., 2002). These findings align with previous studies conducted in the coastal waters of the West Antarctic Peninsula, which have attributed high biomass (e.g., chlorophyll a) to factors such as light availability and shallow mixed-layer depths (Sakshaug et al., 1991; Mitchell & Holm-Hansen, 1991; Schloss et al., 2002).

Conversely, the ice-free station displayed a lower carbon supply and remineralisation rates and was subject to wind-driven mixing of the water column. This mixing can deepen the mixed layer depth below the critical depth, leading to reduced surface production (Savidge et al., 1995). Stations with heavy sea ice cover as described in manuscript 1 and 3 also showed reduced carbon supply and remineralisation rates and were subject to reduced light availability, which suppressed primary production (Arrigo et al., 2008; Bourgeois et al., 2017). In conclusion, sea ice cover was a main variable explaining the large range of benthic carbon remineralization rates between 0.5 and 7.4 mmol C m^{-2} d^{-1} found at comparable water depths in both study regions, along the AP **(manuscript 1)** and at the southern Weddell Sea shelf **(manuscript 3)**. Indeed, the imprint of sea ice on the benthic carbon supply was so evident that a large number of benthic rates from the literature could be predicted by a simple empirical model based on only two environmental variables, MICI and water depth **(manuscript 4)**. The explanatory power of the model highlights sea ice as a meaningful proxy variable, which is easily observed from space and part of many physical models of the Ocean.

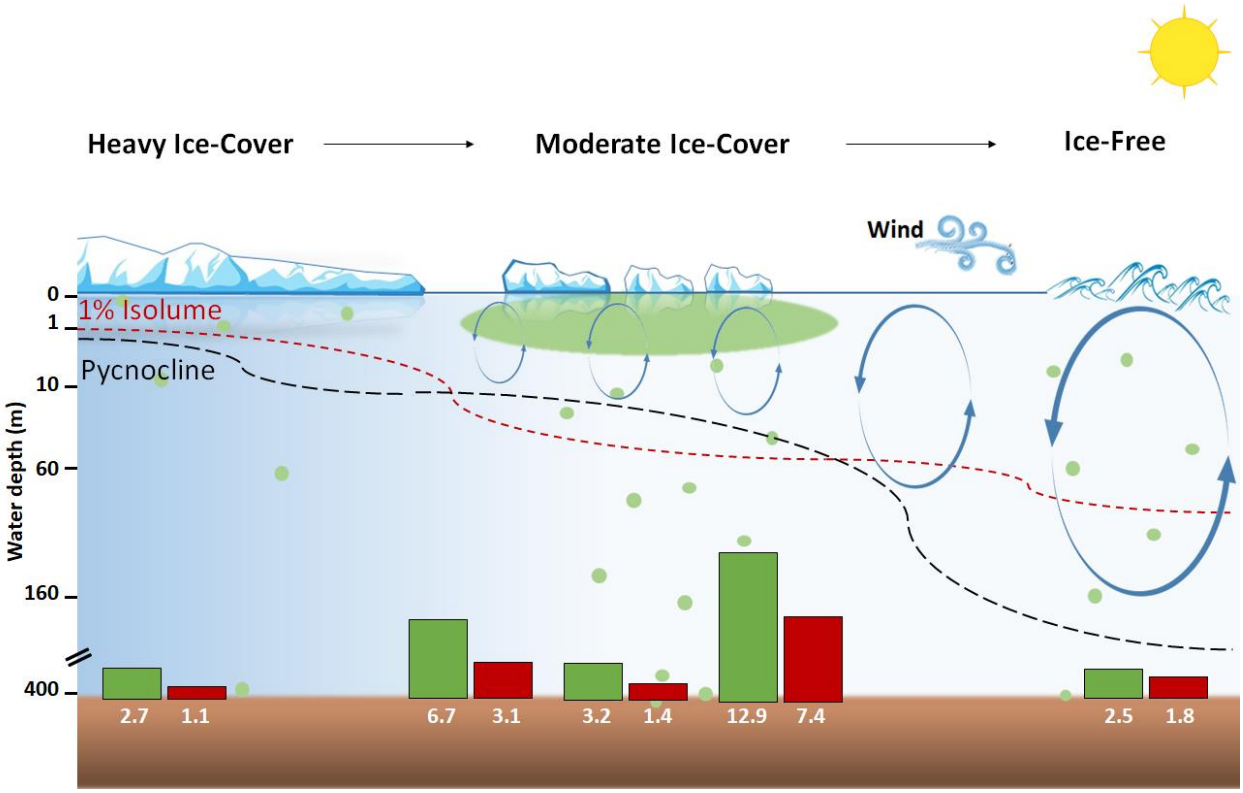

Figure 1. Schematic representation of the physical constraints on surface primary production, and the pattern of carbon supply and carbon remineralization rates in the sediments under heavy ice cover, moderate ice cover, and ice-free areas, modified from Deppeler & Davidson (2017). The blue ovals and arrows represent the depth of wind-driven mixing. The black dashed line denotes the location of the pycnocline, and the red dashed line shows the approximate depth at 1% surface irradiance. The bar chart shows the carbon supply (green bars) and remineralization rates (red bars) in mmol C m^{-2} d^{-1} at 5 stations along the retrieved 400-mile transect as described in manuscript 1.

6.2 What are the major degradation pathways of organic matter in Antarctic shelf sediments under varying sea ice conditions?

The gradual decrease in sea ice cover along the investigated transect, accompanied by an increase in carbon supply rates, has led to marked shifts in organic carbon degradation pathways. This highlights the critical role of carbon supply in controlling sediment redox processes. As sea ice decreases, the main pathways of organic carbon degradation shift towards anaerobic iron and sulfate reduction.

In stations characterized by heavy ice cover and relatively modest total organic carbon (TOC) contents of 0.71 wt%, aerobic pathways of carbon remineralization are the dominant degradation pathway, accounting for more than 94% of the total carbon remineralization **(manuscript 1)**. Similarly, heavy ice cover along the southern Weddell Sea, where TOC contents range from 0.076 to 0.51 wt%, aerobic respiration dominates carbon remineralization, contributing more than 94% of the total carbon remineralization **(manuscript 3)**. In these areas, denitrification and metal reduction exhibit notably low rates, contributing less than 9% to the total carbon remineralization process. These results are consistent with data from the Filchner-Ronne Ice Shelf, which also reports limited denitrification rates (Hulth et al., 1997).

Conversely, dissimilatory iron reduction (DIR) becomes a more prominent anaerobic carbon remineralization process at stations with moderate sea ice cover and intermediate TOC levels of 0.19 and 1.02 wt%, contributing about 4% to 14%. However, it should be noted that the contribution of DIR may be overestimated, as dissolved iron can also result from sulfide oxidation via iron reduction (Poulton et al., 2004; Wehrmann et al., 2017). In certain cases, sulfate-reducing organoclastic reactions may occur without being detected in the sulfate profile due to short diffusion paths and rapid sulfate replenishment in the upper sediment layers. This phenomenon has also been observed in Arctic fjord sediments, where high levels of reducible iron oxides combined with low amounts of fresh organic matter led to a prevalence of dissimilatory iron reduction (Wehrmann et al., 2014). As the TOC content increases from about 1.2 wt%, sulfate reduction becomes the dominant anaerobic carbon remineralization pathway, overtaking other processes such as iron reduction, which typically contributes a maximum of 3% to total carbon remineralization. In this case, sulfate reduction accounts for over 30% of total carbon

remineralization. This observation is consistent with previous research in the northern Barents Sea, where ice-free conditions supported higher rates of sulfate reduction compared to ice-covered stations with lower carbon export to the sediment (Nickel et al., 2008). Overall, the dominant pathways of carbon remineralization in the Antarctic shelf show significant variation, with anaerobic sulfate reduction dominating in areas of higher TOC along the east coast of the AP, and aerobic respiration dominating in areas of lower TOC along the southern Weddell Sea shelf.

6.3 What is the contribution of Antarctic shelf sediments to benthic remineralization in the Southern Ocean?

The contribution of Antarctic shelf sediments to benthic remineralization in the Southern Ocean was estimated by combining field measurements (**manuscript 4**) of benthic remineralization rates and empirical relationships. Analysis of the data obtained has shown that a significant proportion, 83%, of the variability in remineralization rates can be explained by two environmental variables: the long-term occurrence of moderate sea ice cover and water depth. The empirical model derived from this analysis was then applied to estimate benthic carbon remineralization for the entire Seasonal Ice Zone (SIZ), yielding a total of 46 Tg C yr^{-1}. Remarkably, a significant proportion of this, 33 Tg C yr^{-1}, is accounted for by shelf sediments with depths of up to 1000 m. Although the continental shelf represents only 15% of the SIZ, it contributes a significant 71% of the benthic carbon remineralization in the entire zone.

Furthermore, by applying an empirical function to estimate burial rates, the study estimated the total organic carbon supply to the sediments to be approximately 52 Tg C yr^{-1}, with the shelf sediments contributing significantly at 75%. In summary, Antarctic shelf sediments make a remarkable contribution to benthic remineralization in the Southern Ocean indicating a high carbon sequestration throughout the entire Southern Ocean.

6.4 How is iron cycling affected by organic carbon accumulation and how much iron is recycled back into the water column?

Pore water profiles of shelf sediments with the highest carbon supply rate show a rapid depletion of oxygen and nitrate in the uppermost sediment layer, followed by a distinct zone of elevated dissolved iron (DFe) concentrations at depths of 3-7 cm **(manuscript 1, see Figure 3)**. Sites with

moderate carbon supply rates show a broad ferruginous zone that dominates the upper 20 cm of the sediment. In contrast, the heavy ice cover site shows deeper occurrences of elevated DFe concentrations at depths of 25 to 30 cm, corresponding to a lower carbon supply rate. Furthermore, pore water profiles indicate that DFe concentrations at heavy ice cover stations along the southern Weddell Sea shelf are either found at considerable depths (>20 cm) or are absent **(manuscript 3, see Figure 4)**, which is consistent with previous findings by Hulth et al. (1997) reporting low carbon inputs near the Filchner-Ronne Ice Shelf.

A tight coupling of the iron- and phosphate cycles was also found. The presence of phosphate (PO_4^{3-}) plays a crucial role in the formation of iron minerals and consequently influences the rate of microbial iron reduction (O'loughlin et al., 2021) (shown in Figure 2). As organic matter remineralizes, PO_4^{3-} is released into the pore water and subsequently diffuses upwards, which can either be released into the bottom waters or adsorbed onto primary and secondary iron oxide minerals (Paytan & McLaughlin, 2007) (shown in Figure 2A). During sediment accumulation, reactive iron oxides and adsorbed or co-precipitated PO_4^{3-} are gradually buried until they reach the iron reduction zone. Within this zone, the iron oxides undergo reductive dissolution, resulting in the release of both DFe and PO_4^{3-} into the pore water (Canfield et al., 1993; Holmkvist et al., 2010; Küster-Heins et al., 2010; März et al., 2018) (shown in Figure 2B). The intricate iron cycling, involving transitions between oxidized and reduced states exerts predominant control over the flux of PO_4^{3-}. In addition, this process can favor the formation of secondary, poorly crystalline iron (oxyhydr) oxide minerals at the iron redox boundary. These minerals are characterized by their large surface area and enhanced reactivity (Canfield et al., 2006), which makes them capable of adsorbing substantial amounts of PO_4^{3-}.

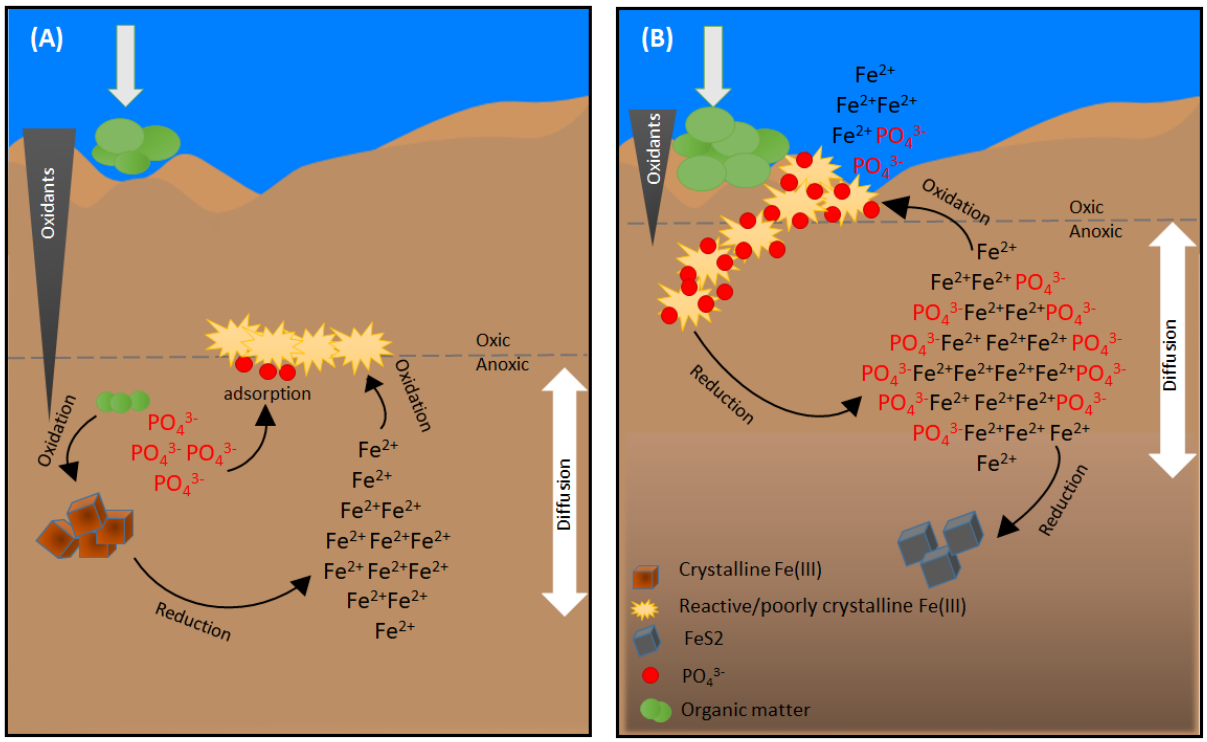

Figure 2. The schematic diagram shows the coupled cycles of iron and phosphorus in the Antarctic shelf sediments. (A) During organic matter remineralization, PO_4^{3-} is released into the pore water and subsequently diffuses upwards, where it can either be released into the bottom waters or adsorbed onto primary and secondary iron oxide minerals. (B) In sediments with high carbon supply rates, reactive iron oxides and adsorbed or co-precipitated PO_4^{3-} are gradually buried until they reach the iron reduction zone. Within this zone, the iron oxides undergo reductive dissolution, resulting in the release of both DFe and PO_4^{3-} into the pore water.

A tight coupling between carbon remineralization and DFe flux rates was found, meaning that the iron release into the pore water is driven by organic matter degradation. This finding is consistent with the results of Elrod et al. (2004), who emphasized the importance of benthic carbon remineralization rates as a key factor in predicting DFe fluxes. Estimates of total DFe fluxes derived from porewater profiles along the eastern coast of the AP revealed a range of from 32 to 316 µmol DFe m^{-2} d^{-1} (see Table 2, **manuscript 1**). This range is remarkably consistent with previously reported DFe fluxes in Potter Cove sediments, which ranged from 11 to 424 µmol DFe m^{-2} d^{-1} (Monien, 2014). However, the estimated benthic DFe release to the water column was

modeled to range from 0.62 to 4.54 µmol DFe m^{-2} d^{-1}, a substantial reduction that is 30-70 times lower than the upward DFe fluxes (Figure 3A+B), which accounts for the reoxidation and precipitation of DFe within the thin oxic layer. The ratio of DFe release to carbon remineralized is approximately 10^{-3}, which is 1-2 orders of magnitude higher than the Fe:C ratios of sinking particles (10^{-5} to 10^{-4}) (Boyd et al., 2007). These high DFe fluxes highlight the importance of the sediments underlying the moderate ice cover as a source of limiting nutrients for the adjacent shelf waters. On the other hand, the estimated DFe fluxes in the southern Weddell Sea shelf regions were significantly (10 to 100 times) lower than the DFe fluxes observed along the east coast of the AP, suggesting a limited release of micronutrients into the water column **(manuscript 3)**. In summary, this link between carbon remineralization and DFe efflux, coupled with the previously established correlation between sea ice conditions and organic matter export, highlights the influence of sea ice cover on the potential release of DFe and PO_4^{3-} from the seafloor.

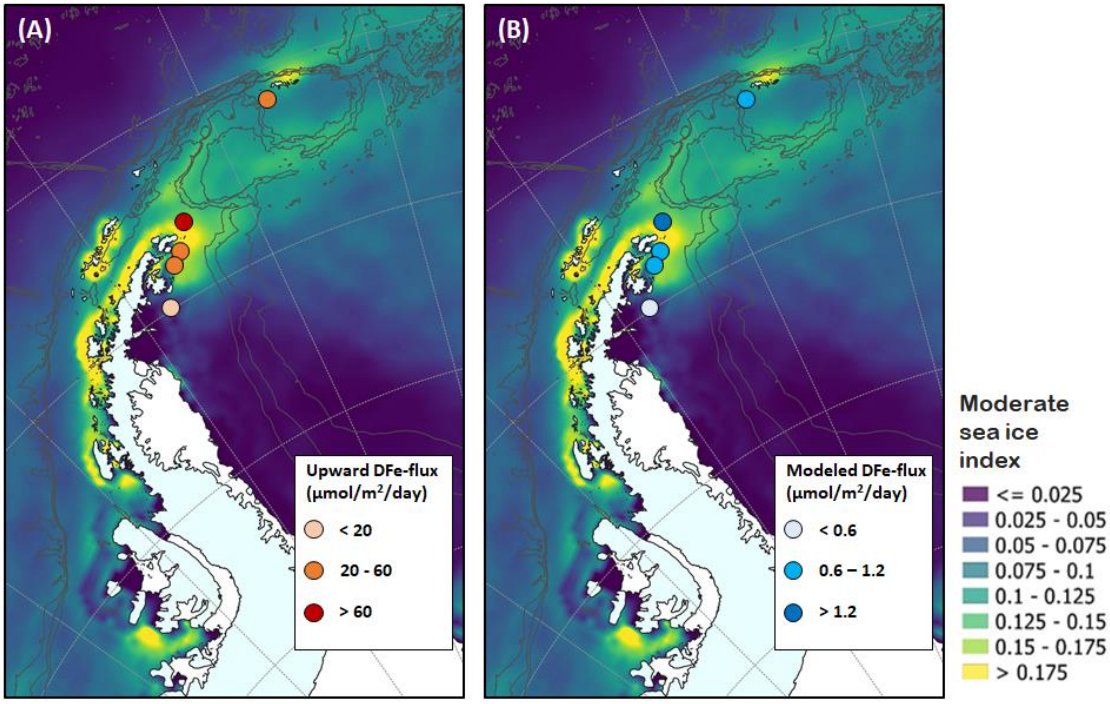

Figure 3. Map of sampling stations along a gradient of sea ice cover from the AP (manuscript 1) showing DFe flux. (A) Upward DFe flux within the sediments as inferred from pore water profiles and (B) modeled DFe efflux to bottom waters was estimated from an empirical model Dale et al. (2015).

6.5 What is the impact of sea ice cover on the benthic microbial community?

The impact of sea ice cover on benthic microbial communities was investigated in surface sediments collected along the AP transect using 16S ribosomal RNA (rRNA) gene sequencing **(manuscript 2)**. The findings indicated that sea ice cover and the associated carbon burial fluxes accounted for up to 13% of the variation observed in microbial communities in the AP shelf sediments **(see Table S2, manuscript 2)**. Furthermore, the result of the similarity test (ANOSIM) revealed significant differences in the bacterial communities between the heavy ice cover and low ice cover stations (ANOSIM, $r > 0.53$, $p < 0.001$).

The gradual decrease in sea ice cover along the transect of the investigated sites, accompanied by an increase in carbon supply rates, has resulted in a distinctly different redox zonation of the underlying sediments suggesting that the different redox conditions are shaped by organic carbon burial rates and the activity of microorganisms with specific metabolic traits. As sea ice decreases, the benthic microbial community shifts towards anaerobic bacterial communities of iron and sulfate reducers. These communities were more abundant at the low ice cover stations than at the heavy ice cover station **(Figure 3, manuscript 2)**. Despite the comparable carbon supply rates at both the ice-free and heavy ice-covered stations, there is a discernible increase in the benthic carbon remineralization rate at the ice-free station. This observation is attributed to a notable 2°C increase in bottom water temperature, which causes an increase in carbon remineralization rate and a concomitant decrease in carbon burial rate **(see Tables 1 and 3, manuscript 1)**, thus resulting in a different microbial community composition.

Notably, the relative abundance of Desulfobacterota, which includes many iron-reducing bacterial species, as well as sequences related to known sulfate reducers, was prominent in the sediments with low ice cover. Similarly, this bacterial phylum has been observed in high abundance at shallower depths in the more reducing shelf sediments of the sub-Antarctic island of South Georgia (Wunder et al., 2021) and Arctic fjords (Jørgensen et al., 2021). Overall, this study expands our knowledge of the pivotal role of sea ice cover and its effect on organic carbon fluxes in driving changes in microbial communities in Antarctic shelf sediments.

6.6 How do microbial communities change in the ferruginous zone?

Microbial communities along the transect change significantly in the ferruginous zone. Differential abundance analysis revealed that 791 ASVs (amplicon sequence variants) differed significantly between the upper 3 cm of the low ice cover sediment and the upper 3 cm of the heavy ice cover sediment ($p < 0.05$; **Table S3, manuscript 2**). Among these taxa, 12 ASVs contributed individually to more than 1 % of the total community in the ferruginous zone and together accounted for up to 20% at the low ice cover stations in contrast to only <6 % at the heavy ice cover station of bacteria community in the ferruginous zone. The major bacterial groups present were identified as members of *Desulfuromonadia*, *Desulfobulbia*, *Verrucomicrobiae*, *Gammaproteobacteria*, *Bacteroidia* and *Polyangia* **(Figure 4, manuscript 2)**.

Sva1033, a clade of *Desulfuromonadia*, showed a tight coupling with increasing DFe concentration, with the steepest slope in the linear regression **(Figures 5 and 6, manuscript 2)**. At low ice cover stations, Sva1033 increased near the surface sediment and peaked in abundance (>7 %) at several centimeter depths where iron reduction prevails. In sediments at the heavy ice cover station, where the ferruginous zone is located at greater sediment depths, the relative abundance of Sva1033 decreases (<2 %) near the sediment surface, while increasing (>4 %) below 5 cm depth in the ferruginous zone **(Figure 4, manuscript 2)**. Members of this clade have previously been detected in the ferruginous sediments of the (sub-) Antarctic (Wunder et al., 2021) and the Arctic shelf (Buongiorno et al., 2019; Jørgensen et al., 2021), and have been suggested to be responsible for the iron reduction in these marine sediments. Their metabolic capabilities to reduce iron was recently confirmed by incubation experiments of Antarctic Potter Cove sediments using RNA stable isotope probing (Wunder et al., 2021). Our results provide further evidence that Sva1033 plays an active role in iron cycling in Antarctic sediments.

Besides Sva1033, the other putatively iron reducing bacterial taxa make up the majority of sedimentary anaerobic communities in the ferruginous zones and some of them have previously been found in marine sediments with high dissolved iron and manganese concentrations (Santelli et al., 2008; Li et al., 2009; Hubert et al., 2009; Beal et al., 2009; Park et al., 2011; Vandieken & Thamdrup, 2013), suggesting their role in meditating metal cycling. Furthermore, the results for

the most closely related sequences (>99 % similarity) indicate that >70 % of these taxa have been detected in permanently cold marine sediments (e.g., Antarctic and Arctic) (Ravenschlag et al., 1999; Purdy et al., 2003; Bowman et al., 2003; Li et al., 2009; Hubert et al., 2009; Park et al., 2011; Ruff et al., 2014; Wunder et al., 2021), indicating that most of these taxa are psychrophilic **(Figure 6, manuscript 2)**. In summary, the increase in the relative abundance of Sva1033 and other putatively iron reducing bacterial taxa in the ferruginous zones of both high ice cover and low ice cover stations supports the potential role of Sva1033 in DIR in surface sediments of the AP and identifies other unknown taxa that may be involved in DIR or have syntrophic partnerships and/or common metabolic preferences with iron reducers.

Outlook

The thesis has highlighted the pivotal role of sea ice cover in driving the benthic carbon cycle along the Antarctic continental shelf **(manuscripts 1, 2, 3, and 4)**. The relation between long-term sea ice conditions and benthic carbon supply and remineralization rates has been concluded from correlating data sets and empirical relations. An important next step is to improve the mechanistic understanding of the cause and effects that result in such strong imprint of sea ice cover, focusing on seasonal dynamics of primary and export production. One problem is that measuring export production, which is the main driver of carbon sequestration, has not been reliably measured across the entire Antarctic continental shelf. It is also unclear how much of the organic carbon is ultimately recycled and how much is sequestered. Therefore, a detailed analysis of primary production and export production, and their control by water column structure (mixing depth), nutrient supply (iron), phytoplankton species composition, and grazing (zooplankton) is needed to gain more insight.

To achieve this, the use of moored instruments can provide year-round water column data, even in the presence of winter pack ice cover. Sediments, acting as historical records of environmental

conditions, can shed light on water column processes when studied. Establishing a connection between water column fluxes, as measured by traps, and sediment deposition and accumulation on the seafloor can provide a better understanding of the relative importance of particle sinking processes and the factors influencing particle transport. In addition, laboratory experiments with multiple stressors (e.g., CO_2, iron, temperature) are essential to assess taxon-specific aggregation capacities in the presence or absence of grazers, such as copepods. Furthermore, tracking the pathways of sub-thermocline and bottom waters and establishing robust estimates of deep water production are further important to study, because they may provide, in combination with the biological carbon pump, an efficient shortcut of carbon sequestration to the deep ocean.

Furthermore, a better understanding of the effect of sea ice cover on sediment geochemistry is needed for many other regions of Antarctica. For example, regions in East Antarctica have not yet been investigated. Despite the comprehensive focus of this thesis on different geochemical aspects **(manuscripts 1, 2, and 3)**, there are still some open questions that require further investigation. Knowledge of biogeochemical processes and metal cycling in surface sediments of the Antarctic shelf may be important to shed more light on the importance of local shelf sediments as a source of essential nutrients such as iron. In particular, it has been estimated that the increase in iron-induced productivity may have contributed about 30% of the 80 ppm decrease in atmospheric CO_2 observed during the glacial maximum by enhancing the biological carbon pump of the ocean (Sigman & Boyle, 2000). However, further research, including water column iron data, is essential to better estimate the iron flux to the Southern Ocean in a warming world. In addition, **manuscript 2** highlighted the importance of putative iron reducing bacterial taxa in the ferruginous zone, providing evidence that they may be involved in DIR in surface sediments of the AP, or have syntrophic partnerships and/or common metabolic preferences with iron reducers. Future work should investigate the in situ metabolic activity of these potential iron reducing bacterial taxa, with a particular focus on Sva1033, to better understand the factors controlling iron bioavailability and potential efflux to the water column from Southern Ocean and Antarctic shelf sediments.

References

Arrigo, K. R., van Dijken, G. L., & Bushinsky, S. (2008). Primary production in the Southern Ocean, 1997–2006. *Journal of Geophysical Research: Oceans*, *113*(C8). doi:https://doi.org/10.1029/2007JC004551

Barnes, D. (2015). Antarctic sea ice losses drive gains in benthic carbon drawdown. *Current Biology*, *25*(18), R789-R790.

Barnes, D. K., Fleming, A., Sands, C. J., Quartino, M. L., & Deregibus, D. (2018). Icebergs, sea ice, blue carbon and Antarctic climate feedbacks. *Philosophical Transactions of the Royal Society A: Mathematical, Physical and Engineering Sciences, 376*(2122), 20170176.

Beal, E. J., House, C. H., & Orphan, V. J. (2009). Manganese- and iron-dependent marine methane oxidation. *Science, 325*(5937), 184-187. doi:10.1126/science.1169984

Bourgeois, S., Archambault, P., & Witte, U. (2017). Organic matter remineralization in marine sediments: A Pan-Arctic synthesis. *Global Biogeochemical Cycles, 31*(1), 190-213.

Bowman, J. P., McCammon, S. A., Gibson, J. A. E., Robertson, L., & Nichols, P. D. (2003). Prokaryotic Metabolic Activity and Community Structure in Antarctic Continental Shelf Sediments. *Applied and Environmental Microbiology, 69*(5), 2448-2462. doi:doi:10.1128/AEM.69.5.2448-2462.2003

Boyd, P. W., Jickells, T., Law, C., Blain, S., Boyle, E., Buesseler, K., et al. (2007). Mesoscale iron enrichment experiments 1993-2005: synthesis and future directions. *Science, 315*(5812), 612-617.

Buongiorno, J., Herbert, L. C., Wehrmann, L. M., Michaud, A. B., Laufer, K., Røy, H., et al. (2019). Complex Microbial Communities Drive Iron and Sulfur Cycling in Arctic Fjord Sediments. *Applied and Environmental Microbiology, 85*(14), e00949-00919. doi:doi:10.1128/AEM.00949-19

Canfield, D. E., Rosing, M. T., & Bjerrum, C. (2006). Early anaerobic metabolisms. *Philosophical Transactions of the Royal Society B: Biological Sciences, 361*(1474), 1819-1836.

Canfield, D. E., Thamdrup, B., & Hansen, J. W. (1993). The anaerobic degradation of organic matter in Danish coastal sediments: iron reduction, manganese reduction, and sulfate reduction. *Geochimica et Cosmochimica Acta, 57*(16), 3867-3883.

Dale, A. W., Nickelsen, L., Scholz, F., Hensen, C., Oschlies, A., & Wallmann, K. (2015). A revised global estimate of dissolved iron fluxes from marine sediments. *Global Biogeochemical Cycles, 29*(5), 691-707. doi:https://doi.org/10.1002/2014GB005017

Deppeler, S. L., & Davidson, A. T. (2017). Southern Ocean phytoplankton in a changing climate. *Frontiers in Marine Science, 4*, 40.

Elrod, V. A., Berelson, W. M., Coale, K. H., & Johnson, K. S. (2004). The flux of iron from continental shelf sediments: A missing source for global budgets. *Geophysical Research Letters, 31*(12).

Holmkvist, L., Arning, E. T., Küster-Heins, K., Vandieken, V., Peckmann, J., Zabel, M., et al. (2010). Phosphate geochemistry, mineralization processes, and Thioploca distribution in shelf sediments off central Chile. *Marine geology, 277*(1-4), 61-72.

Hubert, C., Loy, A., Nickel, M., Arnosti, C., Baranyi, C., Brüchert, V., et al. (2009). A constant flux of diverse thermophilic bacteria into the cold Arctic seabed. *Science, 325*(5947), 1541-1544. doi:10.1126/science.1174012

Hulth, S., Tengberg, A., Landén, A., & Hall, P. O. (1997). Mineralization and burial of organic carbon in sediments of the southern Weddell Sea (Antarctica). *Deep Sea Research Part I: Oceanographic Research Papers, 44*(6), 955-981.

Isla, E. (2016). Environmental controls on sediment composition and particle fluxes over the Antarctic continental shelf. In A. Beylich, J. Dixon, & Z. Zwoliński (Eds.), Source-to-sink fluxes in undisturbed cold environments (pp. 199–212). Cambridge University Press, Cambridge. https://doi.org/10.1017/CBO9781107705791.017

Jørgensen, B. B., Laufer, K., Michaud, A. B., & Wehrmann, L. M. (2021). Biogeochemistry and microbiology of high Arctic marine sediment ecosystems—Case study of Svalbard fjords. *Limnology and Oceanography, 66*(S1), S273-S292. doi:https://doi.org/10.1002/lno.11551

Küster-Heins, K., Steinmetz, E., De Lange, G. J., & Zabel, M. (2010). Phosphorus cycling in marine sediments from the continental margin off Namibia. *Marine geology, 274*(1-4), 95-106.

Li, H., Yu, Y., Luo, W., Zeng, Y., & Chen, B. (2009). Bacterial diversity in surface sediments from the Pacific Arctic Ocean. *Extremophiles, 13*(2), 233-246. doi:https://doi.org/10.1007/s00792-009-0225-7

März, C., Riedinger, N., Sena, C., & Kasten, S. (2018). Phosphorus dynamics around the sulphate-methane transition in continental margin sediments: Authigenic apatite and Fe (II) phosphates. *Marine geology, 404*, 84-96.

Mitchell, B. G., & Holm-Hansen, O. (1991). Observations of modeling of the Antartic phytoplankton crop in relation to mixing depth. Deep Sea Research Part A. *Oceanographic Research Papers, 38*(8-9), 981-1007.

Monien, P. (2014). *The geochemical response of sedimentary archives to rapid recent glacier retreat at the western Antarctic Peninsula (WAP): from source to sink.* Universität Oldenburg.

Nickel, M., Vandieken, V., Bruechert, V., & Jørgensen, B. B. (2008). Microbial Mn (IV) and Fe (III) reduction in northern Barents Sea sediments under different conditions of ice cover and organic carbon deposition. *Deep Sea Research Part II: Topical Studies in Oceanography, 55*(20-21), 2390-2398.

O'loughlin, E. J., Boyanov, M. I., Gorski, C. A., Scherer, M. M., & Kemner, K. M. (2021). Effects of Fe (III) oxide mineralogy and phosphate on Fe (II) secondary mineral formation during microbial iron reduction. *Minerals, 11*(2), 149.

Park, S.-J., Park, B.-J., Jung, M.-Y., Kim, S.-J., Chae, J.-C., Roh, Y., et al. (2011). Influence of Deglaciation on Microbial Communities in Marine Sediments Off the Coast of Svalbard, Arctic Circle. *Microbial Ecology, 62*(3), 537-548. doi:10.1007/s00248-011-9860-5

Paytan, A., & McLaughlin, K. (2007). The oceanic phosphorus cycle. *Chemical Reviews, 107*(2), 563-576.

Pineda-Metz, S. E. A. (2020). Benthos-pelagos interconnectivity: Antarctic shelf examples. In S. Jungblut, V. Liebich, & M. Bode-Dalby (Eds.), YOUMARES 9 – The Oceans: Our Research, Our Future. Proceedings of the 2018 Conference for YOUng MArine RESearchers in Oldenburg, Germany (pp. 211-223). Springer, Cham. https://doi.org/10.1007/978-3-030-20389-4_11

Poulton, S. W., Krom, M. D., & Raiswell, R. (2004). A revised scheme for the reactivity of iron (oxyhydr) oxide minerals towards dissolved sulfide. *Geochimica et Cosmochimica Acta, 68*(18), 3703-3715.

Purdy, K. J., Nedwell, D. B., & Embley, T. M. (2003). Analysis of the sulfate-reducing bacterial and methanogenic archaeal populations in contrasting Antarctic sediments. *Applied and Environmental Microbiology, 69*(6), 3181-3191. doi:10.1128/aem.69.6.3181-3191.2003

Ravenschlag, K., Sahm, K., Pernthaler, J., & Amann, R. (1999). High bacterial diversity in permanently cold marine sediments. *Applied and Environmental Microbiology, 65*(9), 3982-3989. doi:10.1128/AEM.65.9.3982-3989.1999

Rogers, A., Frinault, B., Barnes, D., Bindoff, N., Downie, R., Ducklow, H., et al. (2020). Antarctic futures: an assessment of climate-driven changes in ecosystem structure, function, and service provisioning in the Southern Ocean. *Annual Review of Marine Science, 12*, 87-120.

Ruff, S. E., Probandt, D., Zinkann, A.-C., Iversen, M. H., Klaas, C., Würzberg, L., et al. (2014). Indications for algae-degrading benthic microbial communities in deep-sea sediments along the Antarctic Polar Front. *Deep Sea Research Part II: Topical Studies in Oceanography, 108*, 6-16. doi:https://doi.org/10.1016/j.dsr2.2014.05.011

Sakshaug, E., Slagstad, D., & Holm-Hansen, O. (1991). Factors controlling the development of phytoplankton blooms in the Antarctic Ocean—a mathematical model. *Marine Chemistry, 35*(1-4), 259-271.

Santelli, C. M., Orcutt, B. N., Banning, E., Bach, W., Moyer, C. L., Sogin, M. L., et al. (2008). Abundance and diversity of microbial life in ocean crust. *Nature, 453*(7195), 653-656. doi:10.1038/nature06899

Savidge, G., Harbour, D., Gilpin, L. C., & Boyd, P. W. (1995). Phytoplankton distributions and production in the Bellingshausen sea, Austral spring 1992. *Deep Sea Research Part II: Topical Studies in Oceanography, 42*(4), 1201-1224. doi:https://doi.org/10.1016/0967-0645(95)00062-U

Schloss, I. R., Ferreyra, G. A., & Ruiz-Pino, D. (2002). Phytoplankton biomass in Antarctic shelf zones: a conceptual model based on Potter Cove, King George Island. *Journal of Marine Systems, 36*(3-4), 129-143.

Sigman, D. M., & Boyle, E. A. (2000). Glacial/interglacial variations in atmospheric carbon dioxide. *Nature, 407*(6806), 859-869.

Smetacek, V., & Nicol, S. (2005). Polar ocean ecosystems in a changing world. *Nature, 437*(7057), 362-368.

Smith, C. R., Mincks, S., & DeMaster, D. J. (2006). A synthesis of bentho-pelagic coupling on the Antarctic shelf: food banks, ecosystem inertia and global climate change. *Deep Sea Research Part II: Topical Studies in Oceanography, 53*(8-10), 875-894.

Vandieken, V., & Thamdrup, B. (2013). Identification of acetate-oxidizing bacteria in a coastal marine surface sediment by RNA-stable isotope probing in anoxic slurries and intact cores. *FEMS Microbiology Ecology, 84*(2), 373-386. doi:10.1111/1574-6941.12069

Wehrmann, L. M., Formolo, M. J., Owens, J. D., Raiswell, R., Ferdelman, T. G., Riedinger, N., et al. (2014). Iron and manganese speciation and cycling in glacially influenced high-latitude fjord sediments (West Spitsbergen, Svalbard): Evidence for a benthic recycling-transport mechanism. *Geochimica et Cosmochimica Acta, 141*, 628-655. doi:https://doi.org/10.1016/j.gca.2014.06.007

Wehrmann, L. M., Riedinger, N., Brunner, B., Kamyshny Jr, A., Hubert, C. R., Herbert, L. C., et al. (2017). Iron-controlled oxidative sulfur cycling recorded in the distribution and isotopic composition of sulfur species in glacially influenced fjord sediments of west Svalbard. *Chemical Geology, 466*, 678-695.

Wunder, L. C., Aromokeye, D. A., Yin, X., Richter-Heitmann, T., Willis-Poratti, G., Schnakenberg, A., et al. (2021). Iron and sulfate reduction structure microbial communities in (sub-) Antarctic sediments. *The ISME Journal, 15*(12), 3587-3604. doi:10.1038/s41396-021-01014-9

Acknowledgments

So here, I am at the very last chapter of my PhD. Looking back on the past five years, my stay at the Alfred Wegener Institute has been a tremendous journey of excitement, passion, success, stress, moments of uncertainty, and fulfillment. Being the only enthusiastic student of geochemistry and molecular microbiology in the Bentho-Pelagic Processes group has posed its challenges. Nevertheless, I am grateful to have led and participated in a 'collective' endeavor of an 'ensemble' of many brilliant scientists.

First and foremost, I would like to praise Allah, the Almighty, the Merciful, and the Compassionate for the blessings Allah has bestowed upon me during my study and the completion of this thesis. May Allah's blessings be upon His final Prophet Muhammad (peace be upon him), his family, and his companions.

Indeed, this thesis is the result of the hard work and collaboration of many people, and I acknowledge their tireless contributions to the body of work for my thesis.

Dear Moritz Holtappels, I am deeply grateful for your invaluable supervision and mentoring! This opportunity has been a turning point in my academic and professional journey, and I am deeply appreciative of the trust and confidence you have placed in me. Thank you for all your amazing ideas, your proactive nature and your constructive feedback!

Dear Massimiliano Molari, thank you for your enduring support throughout my PhD journey. Your encouragement and constructive feedback have not only refined my research skills but have also inspired me to delve deeper into the complexities of microbes.

I would also like to thank Sabine Kasten and Claudio Richter for their contribution to this thesis as members of my thesis advisory committee and for the fruitful discussions and advice during the TAC meeting. Dear Sabine, I will always cherish the inspiring words you shared with me during our last meeting – "Chapeau Madame!" These words not only affirmed my efforts but also served as a motivating force.

Special thanks go to all listed coauthors for their dedicated support in revising the manuscripts included in this thesis.

Dear Ingrid Stimac, Ingrid Dohrmann, Jakob Barz, Swantje Rogge, and Valéa Schumacher, I greatly appreciated your support in the lab and with various instruments and measurements. Special thanks to Susann Henkel, Lasse Sander, Juliane Müller and Katja Metfies for their help in obtaining some of the data for the thesis and for allowing access to their laboratories.

Dear Bentho-Pelagic Processes fellows Krissi, Marie, Anna, Bingbing, Felix, Thomas, Susana, and Ulrike it was a great pleasure to share this PhD experience with you – the good and the bad times! Thanks for all the joint lunch breaks. I also thank all members of the Bentho Pelagic Processes working group at AWI for your administrative and scientific support.

Thank you also to Sandra Maier, Andreas Rogge, and Santiago Pineda Metz for your valuable comments on the introduction chapter of the thesis.

I would also like to thank Jon Hawkings for reviewing this thesis and Tilmann Harder, Gabriel Akoko Juma, and Olivia Kohler for being part of my examination committee.

A big thank you to Joan Kobori for your invaluable support and belief in my academic journey. I am deeply grateful for all these transformative opportunities. Dear NF-POGO family, thank you so much for all the opportunities you have given me. Dear Eva-Maria Brodte and Bärbel Wichmann, thank you so much for all your support and encouragement.

Dear Yasmine, Marwa, Mariam, and Chimaa your encouragement, shared laughter, and understanding during the highs and lows of this endeavor have been a constant source of strength. Thank you Dr. Abu Al-khair and Mrs. Umamah for being my second family and great support in Germany. Dear Rojin, Berfin, and Jan thank you so much for all the time we spent at the Spielplatz!

Dear friends of Microbial Diversity 2023 course, thank you for an amazing time in Woods Hole - it was the best possible end to my PhD journey. Thank you Mache, Nada, Ligia, Nicole, Alex, and Yakshi.

Last but not least, my dear family in Egypt and everywhere, from the oldest to the youngest. I am grateful for your presence in my life, your sacrifices, your love, and your encouragement.

Dear Mum, I am incredibly grateful to you for always supporting me to achieve my dreams, for allowing me to make my own way, and for always having my back! In loving memory of my dear father, whose unwavering support and encouragement have left an indelible mark on my life. I dedicate my achievements to your memory and am grateful for the foundation you provided and the invaluable lessons you taught me. Thank you, Dad, for being my guiding light even in your absence. My dearest Samah, thank you for your encouragement, understanding, and continued belief in my abilities, which has been a constant source of strength. Thank you for being my rock and source of inspiration. Dear Bassem and Ahmed, thank you for your love and support.

Contribution to multi-author article/manuscript

Declaration on the contribution of the candidate to a multi-author article/manuscript which is included as a chapter in the submitted doctoral thesis

<u>Manuscript 1:</u> Benthic Carbon Remineralization and Iron Cycling in Relation to Sea ice Cover Along the Eastern Continental Shelf of the Antarctic Peninsula

Contribution of the candidate in % of the total work load (up to 100% for each of the following categories):

Study concept and design:	ca. 30 %
Fieldwork:	ca. 75 %
Lab work and/or acquisition of data:	ca. 90 %
Data analysis and interpretation:	ca. 75 %
Preparation of figures and tables:	ca. 75 %
Drafting of the manuscript:	ca. 80 %

<u>Manuscript 2:</u> The Impact of Sea ice Cover on Microbial Communities in Antarctic Shelf Sediments

Contribution of the candidate in % of the total work load (up to 100% for each of the following categories):

Study concept and design:	ca. 60 %
Fieldwork:	ca. 75 %
Lab work and/or acquisition of data:	ca. 100 %
Data analysis and interpretation:	ca. 85 %
Preparation of figures and tables:	ca. 100 %
Drafting of the manuscript:	ca. 85 %

<u>Manuscript 3:</u> Benthic Carbon Cycling on the Southern Weddell Sea Shelf

Contribution of the candidate in % of the total work load (up to 100% for each of the following categories):

Study concept and design:	ca. 60 %
Fieldwork:	ca. 0 %
Lab work and/or acquisition of data:	ca. 50 %
Data analysis and interpretation:	ca. 90 %
Preparation of figures and tables:	ca. 100 %
Drafting of the manuscript:	ca. 90 %

<u>Manuscript 4:</u> The Imprint of Sea ice on the Biological Carbon Pump in the Southern Ocean

Contribution of the candidate in % of the total work load (up to 100% for each of the following categories):

Study concept and design:	ca. 20 %
Data analysis and interpretation:	ca. 20 %
Preparation of figures and tables:	ca. 10 %
Drafting of the manuscript:	ca. 30 %

Date:

Signature:

Versicherung an Eides Statt

Ich, Marwa Baloza,

versichere an Eides Statt durch meine Unterschrift, dass ich die vorstehende Arbeit selbständig und ohne fremde Hilfe angefertigt und alle Stellen, die ich wörtlich dem Sinne nach aus Veröffentlichungen entnommen habe, als solche kenntlich gemacht habe, mich auch keiner anderen als der angegebenen Literatur oder sonstiger Hilfsmittel bedient habe.

Ich versichere an Eides Statt, dass ich die vorgenannten Angaben nach bestem Wissen und Gewissen gemacht habe und dass die Angaben der Wahrheit entsprechen und ich nichts verschwiegen habe.

Die Strafbarkeit einer falschen eidesstattlichen Versicherung ist mir bekannt, namentlich die Strafandrohung gemäß § 156 StGB bis zu drei Jahren Freiheitsstrafe oder Geldstrafe bei vorsätzlicher Begehung der Tat bzw. gemäß § 161 Abs. 1 StGB bis zu einem Jahr Freiheitsstrafe oder Geldstrafe bei fahrlässiger Begehung.

_____ _____

Ort, Datum Unterschrift